8-1-2014

Synthesis and Characterization of Novel Platinum(II) and Platinum(IV) Complexes Containing 4,4'--Disubstituted--2,2'--bipyridine Ligands for the Treatment of Cancer

Van Vo
University of Nevada, Las Vegas, vanv0683@yahoo.com

SYNTHESIS AND CHARACTERIZATION OF NOVEL PLATINUM(II) and PLATINUM(IV) COMPLEXES CONTAINING 4,4′-DISUBSTITUTED-2,2′-BIPYRIDINE LIGANDS FOR THE TREATMENT OF CANCER

by

Van Vo

Bachelor of Science in Biochemistry
University of Nevada, Las Vegas
2005

Master of Science in Biochemistry
University of Nevada, Las Vegas
2007

A dissertation submitted in partial fulfillment
of the requirements for the

Doctor of Philosophy - Chemistry

Department of Chemistry
College of Sciences
The Graduate College

University of Nevada, Las Vegas
August 2014

UNIVERSITY OF NEVADA LAS VEGAS

THE GRADUATE COLLEGE

We recommend the dissertation prepared under our supervision by

Van Vo

entitled

Synthesis and Characterization of Novel Platinum(II) and Platinum(IV) Complexes Containing 4,4′-Disubstituted-2,2′-bipyridine Ligands for the Treatment of Cancer

is approved in partial fulfillment of the requirements for the degree of

Doctor of Philosophy - Chemistry

Department of Chemistry

Bryan L. Spangelo, Ph.D., Committee Co-Chair

Pradip K. Bhowmik, Ph.D., Committee Co-Chair

Ronald K. Gary, Ph.D., Committee Member

Vernon Hodge, Ph.D., Committee Member

Steen Madsen, Ph.D., Graduate College Representative

Kathryn Hausbeck Korgan, Ph.D., Interim Dean of the Graduate College

August 2014

ABSTRACT

Synthesis and Characterization of Novel Platinum(II) and Platinum(IV) Complexes Containing 4,4′-Disubstituted-2,2′-bipyridine Ligands for the Treatment of Cancer

By

Van Vo

Dr. Pradip K. Bhowmik, Examination Committee Co-Chair

Dr. Bryan L. Spangelo, Examination Committee Co-Chair

Department of Chemistry

University of Nevada, Las Vegas

Three series of platinum(II) and platinum(IV) complexes containing 4,4′-disubstituted-2,2′-bipyridine ligands have been synthesized and characterized by ^{1}H NMR, ^{13}C NMR spectroscopy, elemental analysis, mass spectroscopy, and differential scanning calorimetry measurements. The MTS cell proliferation assay was used to examine the *in vitro* anti-proliferative activities of these complexes in various human breast, lung, and prostate cancer cells. The cell's response to the complexes varies between different cell lines; however, the low EC_{50} values determined from the MTS data indicate that several of the complexes are much more potent than cisplatin.

Flow cytometric analysis of selected compounds revealed induction of apoptosis and some necrosis. One of the complexes, **Pt(II)-4C**, was further studied by examining its interaction with DNA and its effect on mitogen-activated protein kinase (MAPK) signaling. Data from UV-Vis analysis with calf thymus DNA, gel electrophoresis with plasmid pBR322 DNA, and inductively coupled plasma-atomic emission spectrometry (ICP-AES) indicate that **Pt(II)-4C** is able to bind to DNA, cause unwinding of the circular plasmid DNA, as well as covalently modify cellular DNA. Results from western

blotting, flow cytometric immunofluorescence, and immunofluorescence microscopy indicate activation of JNK, ERK, and p38. Cells treated with **Pt(II)-4C** in the presence of JNK and p38 inhibitors had increased cell viability compared to cells treated with **Pt(II)-4C** alone indicating that JNK and p38 are involved in **Pt(II)-4C** induced cell death.

These results demonstrate the potential utilization of these novel complexes for the treatment of cancer.

ACKNOWLEDGEMENTS

The successful completion of this dissertation was possible due to the contribution of several people. First, I would like to express my deepest gratitude to my co-advisors, Drs. Pradip K. Bhowmik and Bryan L. Spangelo, for the support and guidance that they have given me. Their confidence in my ability has given me various opportunities for self-improvements and to build my resume. I would also like to express my appreciation to my committee members, Drs. Ronald Gary, Vernon Hodge, and Steen Madsen, for their time and suggestions to improve my dissertation.

I am very grateful to Dr. Haesook Han for initiating my involvement in the synthesis of the compounds. Additionally, her training in organic reactions and advices are much appreciated. I would like to thank the Chemistry Department's faculty and staff members, especially, Dr. Dennis Lindle, Dr. David Hatchett, Dr. Kathleen Robins, Dr. Spencer Steinberg, Deborah Masters, Mark Miyamoto, Dennis Stevens, and Carolyn Hatchett, for the advices and assistance that they have provided.

I am appreciative of the sponsors of the Donna Weistrop and David B Shaffer and the Patricia Sastaunak Scholarships for their generosity. Additionally, my dissertation was completed in part by the support of the UNLV Graduate and Professional Student Association and the American Chemical Society Southern Nevada Section.

I am thankful to Shirley Shen, Sophie Choe, and Casey Hall-Wheeler for their technical assistance, my dissertation is better because of the data obtained with their help. I would like to express my appreciation to Ontida Tanthmanatham for her assistance with the synthesis of some of the compounds, and Michael Main, Keon Pierre, and Izua Alaniz

for their help with the DNA binding studies. I would like to thank my friends and colleagues (Jung Jae Koh, Tae Soo Jo, Alexi Nedeltchev, Becky Hess, Daniella Sandoval, Ata ur Rahman Mohammed Abdul, and Priyatham Gorjala) for their assistance and advices.

Finally, my family has been immensely supportive through all these academic years; my gratitude towards them could not be express in words. Additionally, Luis Morales was an indispensable source of encouragement; I could not thank him enough.

DEDICATION

This dissertation work is dedicated to my former graduate advisor, Professor Stephen W. Carper. May he rest in peace.

TABLE OF CONTENTS

LIST OF TABLES

LIST OF FIGURES

LIST OF SCHEMES

CHAPTER 1

INTRODUCTION

1.1 General statement

This dissertation has been organized as manuscripts (Chapters 2–5). Chapter 2 corresponds to the contents of a published paper[1] with the format modified to fit the formatting requirements. Chapters 3–5 are manuscripts in preparation.

1.2 Background and Significance

1.2.1 Cancer and current treatment options

Currently, about 25% of the deaths in the United States are due to cancer, making it the second leading cause of death. In 2014, an estimated 1.7 million new cancer cases (855,000 males and 810,000 females) and 586,000 cancer deaths (310,000 males and 276,000 females) are projected to occur.[2] Prostate and lung cancers are the top two leading cancer types in males; whereas, breast and lung cancers are the top two leading cancers in females.

Not only is cancer a leading cause of death in the U.S., but it is also a leading cause of death worldwide. In 2012, there were an estimated 14.1 million new cases of cancer and 8.2 million cancer-related deaths worldwide.[3] With an estimated 1.7 million new cancer cases diagnosed in 2012 (25% of all cancers), breast cancer is the most frequent cancer among women and is the second most common cancer in the world. Overall, with 522,000 deaths, breast cancer ranks as the fifth cause of death from cancer. Lung cancer remains as the most commonly diagnosed and cause of cancer-related death

in the world with an estimated 1.8 million new cases and 1.6 million deaths in 2012. In 2012, there were an estimated 1.1 million new cases of prostate cancer worldwide, making it the second most common cancer in men and the fourth common cancer overall. Additionally, it is the fifth leading cause of cancer-related death (307,000 deaths) in men.[3]

If the trends for the global cancer rates remain the same, it is projected that the number of new cases of cancer will increase to 22.2 million and the number of cancer-related deaths will increase to 13.2 million by the year 2030.[4] These are an increase of about 60% compared to the estimates from 2012, which is a cause for concern.

Cancer treatment varies depending on the type of cancer and its stage. The three classical approaches to cancer treatment are surgery, radiotherapy, and chemotherapy. If the cancer is localized, surgery is usually the first approach; however, if surgery cannot be performed or does not successfully remove all of the diseased cells, then radiotherapy, chemotherapy, or a combination of the three is used. For certain breast and prostate cancers, hormonal therapy is an alternative treatment option. Additionally, with the recent technological advances and a better understanding of cancer cell biology, more selective treatment options such as targeted therapy and immunotherapy are now available.[5,6]

1.2.2 Platinum (Pt)-based chemotherapy

1.2.2.1 Cisplatin and related compounds

Many new innovative methods of cancer treatment are continuously being introduced; however, chemotherapy remains a standard treatment option. A chemotherapeutic drug that is commonly prescribed for the treatment of many cancers is

cisplatin (CDDP), a square-planar Pt(II) compound coordinated to two ammonia and two chloride ligands in *cis* configuration (Figure 1-1). Cisplatin was first synthesized by Peyrone in 1844 and Rosenberg accidentally discovered its antitumoral property in 1965, which sparked an interest in the development of platinum complexes as chemotherapeutic drugs in the 1960s.[7–11] Cisplatin gained approval for clinical treatment by the U.S. Food and Drug Administration (FDA) in the late 1970s and is now widely used in the treatment of many malignancies, including glioblastoma multiforme, cancers of the bladder, lung,

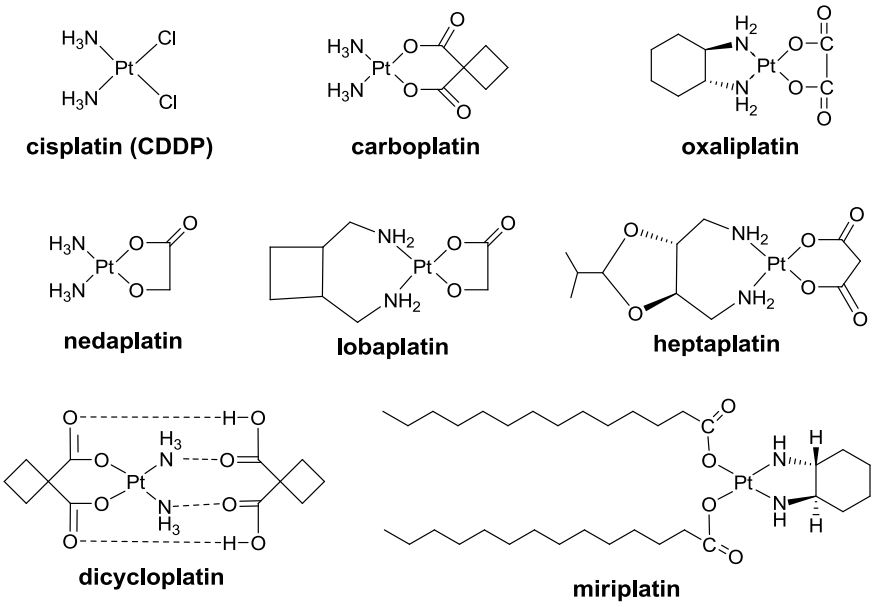

Figure 1 – 1. Structures of cisplatin and platinum(II) complexes in clinical use.

breast, uterus and cervix, and testicular cancer.[11,12] Research on platinum drugs has resulted in the synthesis of thousands of platinum complexes; however, only a few have been approved for clinical use. Along with cisplatin, two other Pt(II) complexes, carboplatin and oxaliplatin, are approved for use worldwide (Figure 1-1). Additionally, five other Pt(II) complexes are used in selected countries; lobaplatin and dicycloplatin in China, nedaplatin and miriplatin in Japan, and heptaplatin in Korea.[9–11,13–16]

Figure 1 – 2. General structure of Pt(II) and Pt(IV) complexes.

As many researchers remain focused on improving Pt(II) complexes, some are expanding into the development of Pt(IV) complexes. Unlike Pt(II) complexes which have four coordinating ligands attached to the Pt center (giving it a +2 oxidation state), Pt(IV) complexes have six coordinating ligands (giving it a +4 oxidation state) (Figure 1-2). These complexes are generally prepared by oxidation of Pt(II) compounds with Cl_2 or H_2O_2 and further modified by reactions with various reagents to produce the desired axial ligands.[13,17,18] They are described as prodrugs because these compounds require activation through intracellular enzymatic reduction to Pt(II). The use of Pt(IV) complexes as prodrugs is of interest due to advantages of the Pt(IV) structure over Pt(II). They have a low-spin d^6 octahedral geometry, which make these compounds more inert to substitution reactions than its Pt(II) counterparts. The decreased reactivity leads to a reduction in side effects and the potential for oral administration. The added coordination of the axial ligands of Pt(IV) complexes allow for greater flexibility in strategies that improve solubility and target selectivity.[13,19] Along with cisplatin, several Pt(IV) complexes (cis-$[Pt(NH_3)_2Cl_4]$, trans-$[Pt(NH_3)_2Cl_4]$ and $[Pt(en)Cl_4]$) were described by Rosenberg *et al.*; however, they were less effective than cisplatin.[20] Since then, Iproplatin, tetraplatin, and satraplatin are several other Pt(IV) complexes which have entered clinical trials (Figure 1-3). Tetraplatin was abandoned in Phase I clinical trials

due to severe neurotoxicity. Iproplatin was abandoned because it was less effective than cisplatin and carboplatin. Satraplatin can be administered orally and is less toxic than cisplatin, but there is no improvement in overall survival benefit. It is still undergoing clinical trials in combination with other chemotherapeutic agents.[13,19–21]

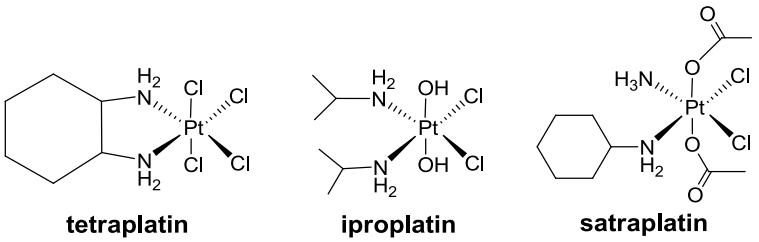

Figure 1 – 3. Structures of some platinum(IV) complexes that have entered clinical trials.

Presently, about 50% of cancer chemotherapeutic regimens consist of platinum (Pt)-based drugs; however, treatment with platinum drugs is accompanied by severe side effects such as nephrotoxicity, neuropathy, ototoxicity, and myelosuppression. Additionally, other drawbacks such as intrinsic or acquired resistance and limited activity against some major types of cancer have impeded the clinical utility of these drugs.[9,10,13,20,21] To circumvent these drawbacks, the quest for improved platinum drugs continues with the goal of discovering compounds with greater efficacy and reduced toxicity.

1.2.2.2 Cellular response to platinum drugs

The cytotoxic effect of cisplatin is mainly due to the formation of DNA adducts even though only a small percentage (5–10%) of the intracellular cisplatin concentration is found in the nucleus.[22] When administered into the body, cisplatin is kept inactivated by the high chloride ion concentration in the extracellular space. Once inside the cell where the chloride ion concentration is low, cisplatin is activated by substitution of the

labile chloride ligands with water molecules and then undergoes nucleophilic attack of the N7 position of guanine (and adenine to a lesser extent) to form irreversible cisplatin-DNA cross-links.[7,8,12,13,22] Although the overall structure of the DNA double helix stays the same, the arrangement of several bases are disrupted because of unwinding and a high degree of bending toward the major groove.[13,23,24] Cisplatin-induced DNA damage elicits various cellular responses such as cell cycle arrest, activation of repair mechanisms, stress response, and cell death pathways. The two pathways that are of interest for this dissertation are the p53 and the mitogen-activated protein kinases (MAPK).

The p53 protein is a tumor suppressor that is involved in many processes including activation of DNA repair, cell cycle arrest, and initiation of apoptosis.[25] During normal cellular conditions, p53 has a short half-life and is kept at a low level by the Mdm2 ubiquitin ligase. However, the interaction of p53 with Mdm2 decreases when stimulated by stress signals, which allows for the accumulation and phosphorylation of p53.[25,26] Activated p53 can then interact with other proteins such as p21 (cell cycle protein) or Bax (apoptotic protein).[26] Current data from the literature indicate that the role of p53 in cisplatin treated cells varies depending on the cell line and duration of treatment. In some reports, cisplatin-induced apoptosis is described as requiring functional p53; however, the opposite is reported by some authors indicating that cells with wild-type p53 are resistant to cisplatin treatment and sensitivity is achieved by inhibition of its expression.[22,26]

The MAPKs are proteins that are activated by various stimuli to regulate cellular processes such as proliferation, differentiation, movement, survival, and programmed death.[22,26] Three major MAPK members are extracellular signal-regulated kinases (ERK),

c-Jun N-terminal kinases (JNK), and p38 kinases. Generally, ERK has a role in cell proliferation and development; however, JNK and p38 have roles in apoptotic signaling, inflammatory responses, and protective responses.[22] These proteins are activated through phosphorylation by upstream kinases and, in turn, phosphorylate downstream targets to activate them. ERK, JNK, and p38 have all been demonstrated to be activated by cisplatin; however, similar to p53, their roles also vary between different cell lines and duration of treatment. In some studies, in accordance with their roles, ERK activation protects cells from apoptosis, whereas, activation of JNK and p38 leads to apoptotic cell death; on the other hand, some studies demonstrated the opposite.[22,26–28]

1.3 Research objectives

Described herein is a multidisciplinary dissertation project involving various fields of science including synthetic organic chemistry, inorganic chemistry, analytical chemistry, and cancer biochemistry, for the development of novel chemotherapeutic agents.

The nitrogen containing 2,2′-bipyridine compounds are attractive ligands to use for the synthesis of platinum drugs because of their high redox stability and ease of functionalization.[29,30] Various metal complexes containing 2,2′-bipyridine have been reported to have antitumor activity,[31–39] but these compounds have drawbacks such as requiring special glassware or reaction conditions, and having lower activity than cisplatin. These drawbacks contributed to the motivation to develop platinum complexes containing the 2,2′-bipyridyl moiety with improved efficacy.

The goals of this project are to synthesize and characterize novel Pt(II) and Pt(IV) cisplatin analogues containing 4,4′-disubstituted-2,2′-bipyridine, examine the cytotoxicity

of the synthesized compounds using a variety of human cancer cell lines, and characterize the mechanism of action of the novel platinum complexes on selected human cancer cells. These goals are accomplished with the following aims:

- Aim I: Synthesis and characterization of novel Pt(II) and Pt(IV) cisplatin analogues

  Rationale. Although platinum-based drugs are used in about 50% of cancer chemotherapeutic regimens, drawbacks such as cellular resistance, toxic side effects, and the narrow spectrum of activity warrant the need for development of platinum drugs with superior characteristics. Additionally, the National Cancer Institute has reported a shortage of chemotherapeutic drugs for several years. Synthesis of new drugs will not only alleviate this shortage problem and circumvent the drawbacks of current platinum drugs, but also allow patients to have access to alternative treatment options.

  - Study 1: Synthesis of new platinum compounds containing 4,4′-disubstituted-2,2′-bipyridine using various organic reactions and purification methods (i.e., recrystallization, extraction, and column chromatography).
  - Study 2: Characterize the chemical structures and confirm the purity of the compounds using elemental analysis, ^{1}H and ^{13}C NMR (nuclear magnetic resonance spectroscopy), and DSC (differential scanning calorimetry).
- Aim II: Assessment of the cytotoxicity of the synthesized compounds in multiple human cancer cell lines and determination of the cell death pathway (apoptosis *vs.* necrosis) induced by the active platinum complexes.

Rationale. Often a chemotherapeutic drug such as cisplatin is effective for some type of cancers, but ineffective in others. Thus, it is necessary to examine the cytotoxicity of the compounds in various cancer cells to determine the potency and potential application of these compounds.

- Study 1: Determine the cytotoxicity profiles of the synthesized platinum compounds in various human cancer cell lines using the MTS colorimetric cell proliferation assay.
- Study 2: Detect changes in the cell cycle and cell death pathways (apoptosis or necrosis) activated by the platinum complexes using DNA laddering assay, flow cytometry, and fluorescence microscopy.

- Aim III: Characterization of the mechanism of action of the novel cisplatin analogues on selected human cancer cells

  Rationale. Understanding the cellular effect of a drug is important when developing treatment strategies and predicting possible side effects. There is still much to be explored about the biological effects of cisplatin; however, it is known that cisplatin binds to DNA and forms adducts that damage the DNA and activates the apoptotic pathway. The synthesized platinum(II) complexes have a platinum center that is similar to cisplatin [Pt(IV) complexes are expected to be intracellularly reduced to Pt(II)] and may bind to DNA to cause damage in a mechanism analogous to cisplatin.

  - Study 1: Analyze the interaction of the novel platinum complexes with DNA using UV-Vis spectroscopy with calf thymus DNA and gel electrophoresis with plasmid pBR322 DNA.

- Study 2: Determine the uptake of the novel platinum compounds and the level of DNA binding in select human cancer cell lines using inductively coupled plasma-atomic emission spectrometry (ICP-AES)
- Study 3: Identify the proteins mediating cell death responses activated by the novel platinum compounds in select human cancer cell lines using western blotting analysis, flow cytometry, and immunofluorescence microscopy.

Chapters 2–5 describe the synthesis of three novel Pt(II) and Pt(IV) complexes and the structural characterization of these complexes by ^{1}H NMR, ^{13}C NMR spectroscopy, elemental analysis, mass spectroscopy, and differential scanning calorimetry (DSC) measurements. The anti-proliferative activities of these compounds against a panel of human cancer cell lines are also described and compared to that of cisplatin and carboplatin. Additionally, the structure-activity relationship is explored to provide a rational basis for the discovery of novel platinum compounds with increased effectiveness and low toxic side effects. Furthermore, data from various experimental techniques (UV-Vis spectroscopy and gel electrophoresis to study interactions with DNA; ICP-AES for the detection of platinum uptake by cells and binding to DNA; western blotting, immunofluorescence, and flow cytometry for analysis of changes in protein expression) are presented to describe the interactions of these complexes with biological molecules and gain insight into the mechanism of action, which will further aid in the development of promising chemotherapeutic agents.

1.4 References

1. Vo, V.; Tanthmanatham, O.; Han, H.; Bhowmik, P. K.; Spangelo, B. L. Synthesis of [$PtCl_2$(4,4′-dialkoxy-2,2′-bipyridine)] complexes and their in vitro anticancer properties. *Metallomics* **2013,** *5,* 973-987.
2. Siegel, R.; Ma, J.; Zou, Z.; Jemal, A. Cancer statistics, 2014. *CA Cancer J. Clin.* **2014,** *64,* 9–29.
3. Ferlay, J.; Soerjomataram, I.; Ervik, M.; Dikshit, R.; Eser, S.; Mathers, C.; Rebelo, M.; Parkin, D. M.; Forman, D.; Bray, F. GLOBOCAN 2012 v1.0, Cancer Incidence and Mortality Worldwide: IARC CancerBase No. 11 [Internet]. Lyon, France: International Agency for Research on Cancer; 2013. http://globocan.iarc.fr (accessed March 9, 2014).
4. Bray, F.; Jemal, A.; Grey, N.; Ferlay, J.; Forman, D. Global cancer transitions according to the Human Development Index (2008–2030): a population-based study. *Lancet Oncol.* **2012,** *13,* 790-801.
5. Biemar, F.; Foti, M. Global progress against cancer—challenges and opportunities. *Cancer Biol. Med.* **2013,** *10,* 183-186.
6. Urruticoechea, A.; Alemany, R.; Balart, J.; Villanueva, A.; Viñals, F.; Capellá, G. Recent advances in cancer therapy: an overview. *Curr. Pharm. Des.* **2010,** *16,* 3-10.
7. Liedert, B.; Pluim, D.; Schellens, J.; Thomale, J. Adduct-specific monoclonal antibodies for the measurement of cisplatin-induced DNA lesions in individual cell nuclei. *Nucleic Acids Res.* **2006,** *34: e47,* 1-12.
8. Wozniak, K.; Blasiak, J. Recognition and repair of DNA-cisplatin adducts. *Acta Biochim. Pol.* **2002,** *49,* 583–596.
9. Harper, B. W.; Krause-Heuer, A. M.; Grant, M. P.; Manohar, M.; Garbutcheon-Singh, K. B.; Aldrich-Wright, J. R. Advances in Platinum Chemotherapeutic. *Chem. Eur. J.* **2010,** *16,* 7064-7077.
10. Casini, A.; Reedijk, J. Interactions of anticancer Pt compounds with proteins: an overlooked topic in medicinal inorganic chemistry? *Chem. Sci.* **2012,** *3,* 3135–3144.

11. Florea, A. M.; Büsselberg, D. Cisplatin as an Anti-Tumor Drug: Cellular Mechanisms of Activity, Drug Resistance and Induced Side Effects. *Cancers* **2011,** *3,* 1351-1371.

12. Jamieson, E.; Lippard, S. Structure, recognition, and processing of cisplatin-DNA adducts. *Chem. Rev.* **1999,** *99,* 2467-2498.

13. Wexselblatt, E.; Gibson, D. What do we know about the reduction of Pt(IV) pro-drugs? *J. Inorg. Biochem.* **2012,** *117,* 220-229.

14. Wang, X.; Guo, Z. Targeting and delivery of platinum-based anticancer drugs. *Chem. Soc. Rev.* **2013,** *42,* 202–224.

15. Kamimura, K.; Suda, T.; Tamura, Y.; Takamura, M.; Yokoo, T.; Igarashi, M.; Kawai, H.; Yamagiwa, S.; Nomoto, M.; Aoyagi, Y. Phase I study of miriplatin combined with transarterial chemotherapy using CDDP powder in patients with hepatocellular carcinoma. *BMC Gastroenterology* **2012,** *12,* 127.

16. Li, G.-q.; Chen, X.-g.; Wu, X.-p.; Xie, J.-d.; Liang, Y.-j.; Zhao, X.-q. C. W.-q.; Fu, L.-w. Effect of Dicycloplatin, a Novel Platinum Chemotherapeutical Drug, on Inhibiting Cell Growth and Inducing Cell Apoptosis. *PLoS ONE* **2012,** *7,* e48994.

17. Lee, Y.-A.; Yoo, K. H.; Jung, O.-S. Oxidation of Pt(II) to Pt(IV) complex with hydrogen peroxide in glycols. *Inorg. Chem. Commun.* **2003,** *6,* 249-251.

18. Alderden, R. A.; Hall, M. D.; Hambley, T. W. The Discovery and Development of Cisplatin. *J. Chem. Educ.* **2006,** *83,* 728-734.

19. Muhammad, N.; Guo, Z. Metal-based anticancer chemotherapeutic agents. *Curr. Opin. Chem. Biol.* **2014,** *19,* 144-153.

20. Wong, D. Y. Q.; Ang, W. H. Development of Platinum(IV) Complexes as Anticancer Prodrugs: The Story so Far. *COSMO* **2012,** *8,* 121-134.

21. Marques, M. P. M. Platinum and Palladium Polyamine Complexes as Anticancer Agents: The Structural Factor. *ISRN Spectroscopy* **2013,** *2013,* 1-29.

22. Gómez-Ruiz, S.; Maksimović-Ivanić, D.; Mijatović, S.; Kaluđerović, G. N. On the discovery, biological effects, and use of Cisplatin and metallocenes in anticancer chemotherapy. *Bioinorg. Chem. Appl.* **2012,** *2012,* 140284.

23. Huang, H.; Woo, J.; Ally, S.; Hopkins, P. DNA-DNA interstrand cross-linking by cis-diamminedichloroplatinum(II): N7(dG)-to-N7(dG) cross-linking at 5′d(GC) in synthetic oligonucleotides. *Bioorg. Med. Chem.* **1995,** *3,* 659-669.

24. Takahara, P. M.; Frederik, C. A.; Lippard, S. J. Crystal Structure of the Anticancer Drug Cisplatin Bound to Duplex DNA. *J. Am. Chem. Soc.* **1996,** *118,* 12309-12321.

25. Gudkov, A. V.; Komarova, E. A. Dangerous habits of a security guard: the two faces of p53 as a drug target. *Hum. Mol. Genet.* **2007,** *16,* 67-72.

26. Basu, A.; Krishnamurthy, S. Cellular Responses to Cisplatin-Induced DNA Damage. *J. Nucleic Acids* **2010,** *2010,* 201367.

27. Germain, C. S.; Niknejad, N.; Ma, L.; Garbuio, K. . H. T.; Dimitroulakos, J. Cisplatin Induces Cytotoxicity through the Mitogen-Activated Protein Kinase Pathways and Activating Transcription Factor 3. *Neoplasia* **2010,** *12,* 527-538.

28. Guégan, J.-P.; Ezan, F.; Théret, N.; Langouët, S.; Baffet, G. MAPK signaling in cisplatin-induced death: predominant role of ERK1 over ERK2 in human hepatocellular carcinoma cells. *Carcinogenesis* **2013,** *34,* 38-47.

29. Kaes, C.; Katz, A.; Hosseini, M. W. Bipyridine: The Most Widely Used Ligand. A Review of Molecules Comprising at Least Two 2,2′-Bipyridine Units. *Chem. Rev.* **2000,** *100,* 3553-3590.

30. Jones, N. A.; Antoon, J. W.; Bowie, A. L.; Borak, J. B.; Stevens, E. P. Synthesis of 2,2′-Bipyridyl-Type Compounds via the Suzuki-Miyaura Cross-Coupling Reaction. *J. Heterocycl. Chem.* **2007,** *44,* 363-368.

31. Puthraya, K. H.; Srivastava, T. S.; Amonka, A. J.; Adwankar, M. K.; Chitnis, M. P. Some Mixed-Ligand Palladium(II) Complexes of 2,2′-Bipyridine and Amino Acids as Potential Anticancer Agents. *J. Inorg. Biochem.* **1985,** *25,* 207-215.

32. Puthraya, K. H.; Srivastava, T. S.; Amonka, A. J.; Adwankar, M. K.; Chitnis, M. P. Some Potential Anticancer Palladium(II) Complexes of 2,2′-Bipyridine and Amino Acids. *J. Inorg. Biochem.* **1986,** *265,* 45-54.

33. Cristalli, G.; Franchetti, P.; Nasini, E.; Vittori, S.; Grifantini, M.; Barzi, A.; Pepri, E.; Ripa, S. Metal(II) complexes of 2,2′-bipyridyl-6-carbothioamide as anti-tumor and anti-fungal agents. *Eur. J. Med. Chem.* **1988,** *23,* 301-305.

34. Garelli, N.; Vierling, P.; Fischel, J. L.; Milano, G. E. Cytotoxic activity of new amphiphilic perfluoroalkylated bipyridine platinum and palladium complexes incorporated into liposomes. *J. Med. Chem.* **1993,** *28,* 235-242.

35. Elwell, K. E.; Hall, C.; Tharkar, S.; Giraud, Y.; Bennet, B. L.; Bae, C.; Carper, S. W. A fluorine containing bipyridine cisplatin analog is more effective than cisplatin at inducing apoptosis in cancer cell lines. *Bioorg. Med. Chem.* **2006,** *14,* 8692-8700.

36. Mansouri-Torshizi, H.; I-Moghaddam, M.; Divsalar, A.; Saboury, A. -A. 2,2′-Bipyridinebutyldithiocarbamatoplatinum(II) and palladium(II) complexes: synthesis, characterization, cytotoxicity, and rich DNA-binding studies. *Bioorg. Med. Chem.* **2008,** *16,* 9616-9625.

37. Vo, V.; Kabuloglu-Karayusuf, Z. G.; Carper, S. W.; Bennett, B. L.; Evilia, C. Novel 4,4′-diether-2,2′-bipyridine cisplatin analogues are more effective than cisplatin at inducing apoptosis in cancer cell lines. *Bioorg. Med. Chem.* **2010,** *18,* 1163-1170.

38. Chang, T. T.; More, S. V.; Lu, N.; Jhuo, J.-W.; Chen, Y.-C.; Jao, S. C.; Li, W.-S. Polyfluorinated bipyridine cisplatins manipulate cytotoxicity through the induction of S-G2/M arrest and partial intercalation mechanism. *Bioorg. Med. Chem.* **2011,** *19,* 4887-4894.

39. Mansouri-Torshizi, H.; Eslami-Moghadam, M.; Divsalar, A.; Saboury, A.-A. DNA-Binding Studies of Some Potential Antitumor 2,2′-bipyridine Pt(II)/Pd(II) Complexes of piperidinedithiocarbamate. Their Synthesis, Spectroscopy and Cytotoxicity. *Acta Chim. Slov.* **2011,** *58,* 811-822.

CHAPTER 2

SYNTHESIS OF [PTCL$_2$(4,4′-DIALKOXY-2,2′-BIPYRIDINE)] COMPLEXES AND THEIR *IN VITRO* ANTICANCER PROPERTIES*

2.1 Abstract

A series of [Pt(II)Cl$_2$(4,4′-dialkoxy-2,2′-bipyridine)] complexes of the general formula of [Pt(II)Cl$_2$(4,4′-bis(RO)-2,2′-bipyridine)] (where R = –(CH$_2$)$_{n-1}$CH$_3$, n = 2–6, 8) were synthesized and characterized using ^{1}H NMR, ^{13}C NMR spectroscopy, elemental analysis, mass spectroscopy, and differential scanning calorimetry measurements. The *in vitro* anti-proliferative activities of these compounds were evaluated against human cancer cell lines A549 (lung adenocarcinoma), DU145 (prostate carcinoma), MCF-7 (breast adenocarcinoma), and MDA-MB-435 (melanoma) using the MTS cell proliferation assay. Several Pt(II) coordination compounds were found to have greatly enhanced activity compared to cisplatin after a one hour treatment in all cell lines tested. A structure-activity relationship was observed, that is, the activity increases as the carbon chain length of the alkyl group increases. The activity was maximum when the carbon chain length reached four or five carbons and decreased with the longer carbon chain length. Fluorescence microscopy and flow cytometry data indicate that the main mode of cell death is through apoptosis with some necrotic responses.

---

* This chapter corresponds to the content of the published paper:

Vo V, Tanthmanatham O, Han H, Bhowmik PK, Spangelo BL. Synthesis of [PtCl$_2$(4,4′-dialkoxy-2,2′-bipyridine)] complexes and their *in vitro* anticancer properties. *Metallomics,* 2013, 5, 973-987.

2.2 Introduction

Cisplatin (CDDP) is a relatively small coordination compound of platinum (Pt) that was approved by the US FDA in 1978 for the clinical treatment of various cancers.[1–3] Thirty-five years since its FDA approval cisplatin has remained one of the most commonly prescribed chemotherapeutic drugs. However, the clinical application of cisplatin is limited due to toxic side effects, such as kidney damage and cellular resistance (either intrinsic or acquired).[3–7] Due to these issues, numerous cisplatin analogues have been synthesized and investigated with varying anti-neoplastic activity. Currently, only two cisplatin analogues have been approved by the US FDA. The first was carboplatin, which was approved in 1989, for the treatment of lung and ovarian cancer. The second was oxaliplatin, approved in 2002, for the treatment of colorectal cancer.[1,6] Although these drugs have less toxic side effects than cisplatin, they are only as effective or in some cases less effective than cisplatin. Additionally, side effects such as myelosuppression have limited their usefulness.[1,8]

The first report for the synthesis of 2,2′-bipyridine dates back to 1888 by Fritz Blau[9] and then by Newkome *et al.*[10] and it is now one of the most extensively studied chelating agents. The 2,2′-bipyridine compounds are commonly used as bidentate transition metal ligands because various functional groups can easily be attached and they have high redox stability.[11,12] These compounds are used in electron-transfer processes, luminescent devices, and nanomaterials. Additionally, they have applications in areas such as photonics and electrochemistry.[10,11] Various metal complexes containing 2,2′-bipyridine have been reported to have antitumor activity,[13–21] some of the representative Pt-complexes (**1–10**) are depicted in Fig. 2-1.

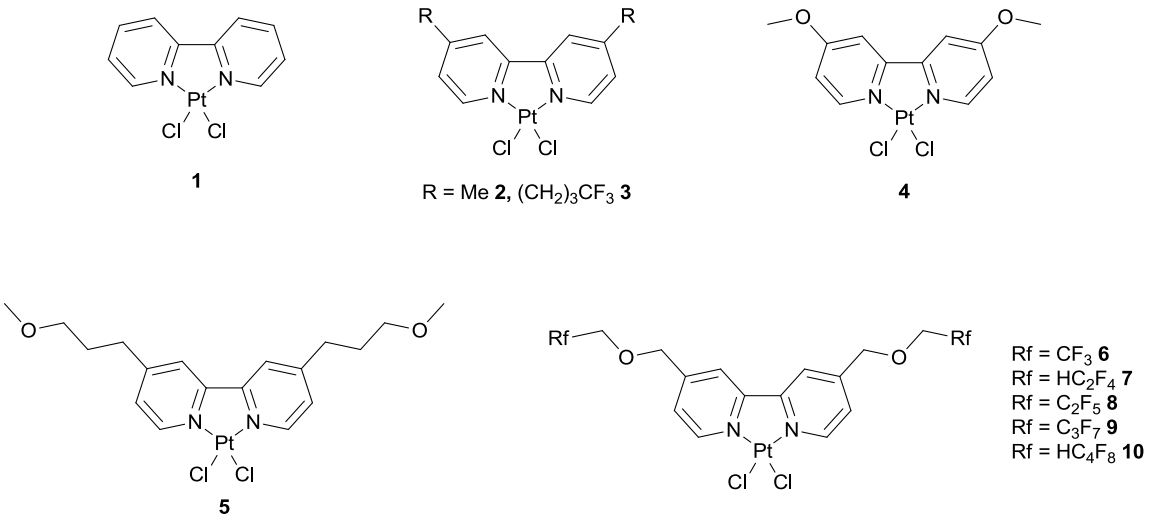

Figure 2 – 1. Some representative chemical structures of known [Pt(II)Cl_2(4,4′-disubstituted-2,2′-bipyridine)] complexes.

Complex **1** was reported to have some activity against NCI-H460 lung cancer cells, but was less active than cisplatin (determined by MTT assay with a 48 h treatment).[22] Complexes **2** and **3** were reported to be at least 100 times more lethal than cisplatin as determined in clonogenic survival assays of MDA-MB-231 human breast cancer cells and its two engineered derivatives treated for 1 h with the complexes. It was also demonstrated that **3** was more lethal than cisplatin in human prostate (DU145) and lung (A549) cancer cells.[17] Complexes **4** and **5** were shown to be more lethal than cisplatin in A549, DU145, and MDA-MB-435 (now classified as a melanoma cell line) when tested using a clonogenic survival assay with a 1 h treatment duration.[19] The activity of complexes **6-10** has been tested in MCF-7 (breast cancer), MDA-MB-231, and A549 cells.[20] Complexes **6-8** exhibited anti-proliferative activity against MDA-MB-231, but no significant activity against MCF-7 and A549 cells. Complexes **9** and **10** did not have significant activity against any of the cell lines tested.

Although complexes **2-5** were demonstrated to be effective, the synthesis of the ligands for the more active complexes (**3** and **5**) involved the use of the strong base lithium diisopropylamide (LDA) to deprotonate the starting 4,4′-dimethyl-2,2′-bipyridine compound.[19,23] This strong base is inconvenient to use, since it reacts violently with water; thus, the reaction must be performed in a specialized glassware under argon or nitrogen. Additionally, other properties *(e.g.,* corrosivity and pyrophoricity) make this base quite difficult to use.[24] Synthesis of the ligands for complexes **6-10** require fluorinated alcohols that are quite expensive. Additionally, the synthetic reaction has a step that produces moisture-sensitive alkoxide as an intermediate.[20,25] Working with the moisture-sensitive compounds requires the additional step of drying all glassware and reagents before use.

In an effort to find a more suitable replacement for current anticancer Pt compounds, an improved method for a two-step synthesis of a series of [Pt(II)Cl_2(4,4′-dialkoxy-2,2′-bipyridine)] complexes of the general formula of [Pt(II)Cl_2(4,4′-bis(RO)-2,2′-bipyridine)] (where R = –$(CH_2)_{n-1}CH_3$, n = 2–6, 8) was developed. This method does not require the use of strong bases and gives high yields, resulting in cost-effective preparation of prospective antitumor drugs. Platinum complexes of these novel chemical structures have not, to our knowledge, been previously reported. Herein, we describe their synthesis and characterization by ^{1}H NMR, ^{13}C NMR spectroscopy, elemental analysis, mass spectroscopy, and differential scanning calorimetry (DSC) measurements. The anti-proliferative activities of these compounds against a panel of human cancer cell lines are described and compared to that of cisplatin—a gold standard for cancer therapy.

2.3 Experimental

2.3.1 General

All starting materials including 4,4′-dimethoxy-2,2′-bipyridine and reagents for the synthetic procedures were purchased from the commercial vendors (Sigma-Aldrich, TCI, Alfa-Aesar, or Acros) unless otherwise noted. They were of high purity and were used without further purification unless noted in the procedure. Minimum essential medium (MEM), fetal bovine serum (FBS), phosphate buffered saline (PBS), trypsin-EDTA, and penicillin-streptomycin were purchased from Life Technologies (Carlsbad, CA). The RPMI 1640 medium was purchased from ATCC (Manassas, VA) and HEPES, crystal violet, CDDP and dimethyl sulfoxide (DMSO) were purchased from Sigma-Aldrich. All reagents and enzymes used for flow cytometry were of analytical grade qualities and were purchased from Sigma-Aldrich, unless otherwise noted.

2.3.2 Chemical characterization instrumentation

All of the NMR spectra were obtained utilizing a Varian spectrometer at 298 K or the indicated temperature using deuterated dimethyl sulfoxide (DMSO-d_6) or chloroform ($CDCl_3$) as the solvents: ^{1}H NMR, 400 MHz; and ^{13}C NMR, 100 MHz. Either residual solvent or tetramethylsilane (TMS) were used as the internal chemical shift reference. Thermal transitions were determined by using a TA Instruments DSC 2010 differential scanning calorimeter in nitrogen at heating and cooling rates of 10 °C min^{-1}. The temperature axis of the DSC thermogram was calibrated with reference standards of high purity indium and tin before use. An amount of 2–3 mg of compound was used in this measurement. The T_{onset} and T_{max} temperatures of a melting endotherm of a compound were recorded from the DSC thermogram as Mp (T_{onset}–T_{max}). Elemental analysis was

determined by NuMega Resonance Labs Inc. (San Diego, CA) by using a Perkin Elmer PE2400-Series II with a CHNS/O analyzer. Mass analysis was also determined by NuMega Resonance Labs Inc. by using a Perkin Elmer PE-SCIEX API-150.

2.3.3 Preparation of 2,2′-bipyridine-4,4′-diol

The 2,2′-bipyridine-4,4′-diol was synthesized according to a previously published procedure with a slight modification of the reaction condition.[26] Briefly, 48 wt% HBr in H_2O (15.5 equiv.) was slowly added to a solution of 4,4′-dimethoxy-2,2′-bipyridine (1.0 equiv.) in glacial acetic acid and the resulting mixture was heated to reflux for a period of 72 h. The solvents were removed under vacuum resulting in the product residue that was dissolved in H_2O. Insoluble material was removed by filtration and the pH of the filtrate was adjusted to neutral using NH_4OH. The colourless solid product precipitated out and was collected by vacuum filtration. It was then washed with plenty of H_2O and dried at 80 °C *in vacuo.* The compound was then used without further purification in the next step.

2.3.4 Preparation of 4,4′-dialkoxy-2,2′-bipyridine

The appropriate alkyl halide (2.2 equiv.) was slowly added to a mixture of 2,2′-bipyridine-4,4′-diol (1 equiv.) and Cs_2CO_3 or K_2CO_3 (2.2 equiv.) in DMF at *ca.* 60 °C. The suspension was heated to reflux for 48 h then allowed to cool to room temperature. The salt was removed by vacuum filtration and washed with DMF. Rotary evaporator was used to remove the solvent from the solution resulting in the solid residue that was washed with water and collected by vacuum filtration. Recrystallization from acetone-H_2O afforded the pure product as shiny, colourless crystals.

4,4′-Diethoxy-2,2′-bipyridine (L-2C). Yield: 86%, white crystals. Mp 122–124 °C.[27,28] ^{1}H NMR (298 K, 400 MHz, DMSO-d_6): δ (ppm) = 8.46 (d, 1H, J = 5.7 Hz), 7.90 (d, 1H, J = 2.5 Hz), 6.99 (dd, 1H, J = 5.7, 2.6 Hz), 4.20 (q, 2H, J = 7.0 Hz), 1.37 (t, 3H, J = 7.0 Hz). ^{13}C NMR (298 K, 100 MHz, DMSO-d_6): δ (ppm) = 165.9, 157.3, 150.9, 111.5, 106.8, 64.0, 14.8. ESI-MS: m/z 245.40 $[M + H]^+$.

4,4′-Dipropoxy-2,2′-bipyridine (L-3C). Yield: 93%, white crystals. Mp 97–99 °C. ^{1}H NMR (342 K, 400 MHz, DMSO-d_6): δ (ppm) = 8.45 (d, 1H, J = 5.6 Hz), 7.90 (d, 1H, J = 2.5 Hz), 6.97 (dd, 1H, J = 5.6, 2.6 Hz), 4.11 (t, 2H, J = 6.5 Hz), 1.83–1.74 (m, 2H), 1.01 (t, 3H, J = 7.4 Hz). ^{13}C NMR (302 K, 100 MHz, DMSO-d_6): δ (ppm) = 165.5, 156.8, 150.4, 110.9, 106.3, 69.1, 21.7, 10.2. Anal. Calcd for $C_{16}H_{20}N_2O_2$ (272.34 g mol^{-1}): C, 70.56; H, 7.40; N, 10.29%; found: C, 70.70; H, 7.80; N, 10.56%; ESI-MS: m/z 273.30 $[M + H]^+$.

4,4′-Dibutoxy-2,2′-bipyridine (L-4C). Yield: 86%, white crystals. Mp 99–101 °C.[29] ^{1}H NMR (332 K, 400 MHz, DMSO-d_6): δ (ppm) = 8.46 (d, 1H, J = 5.6 Hz), 7.90 (d, 1H, J = 2.5 Hz), 6.98 (dd, 1H, J = 5.6, 2.6 Hz), 4.15 (t, 2H, J = 6.5 Hz), 1.78–1.71 (m, 2H), 1.51–1.42 (m, 2H), 0.95 (t, 3H, J = 7.4 Hz). ^{13}C NMR (332 K, 100 MHz, DMSO-d_6): δ (ppm) = 166.1, 157.5, 150.9, 111.4, 107.1, 68.0, 30.9, 19.0, 14.0. Anal. Calcd for $C_{18}H_{24}N_2O_2$ (300.40 g mol^{-1}): C, 71.97; H, 8.05; N, 9.33%; found: C, 72.56; H, 7.81; N, 9.45%; ESI-MS: m/z 301.30 $[M + H]^+$.

4,4′-Dipentyloxy-2,2′-bipyridine (L-5C). Yield: 78%, white crystals. Mp 85–86 °C. ^{1}H NMR (298 K, 400 MHz, $CDCl_3$): δ (ppm) = 8.45 (d, 1H, J = 5.6 Hz), 7.95 (d, 1H, J = 2.5 Hz), 6.82 (dd, 1H, J = 5.7, 2.6 Hz), 4.12 (t, 2H, J = 6.5 Hz), 1.86–1.79 (m, 2H), 1.50–1.35 (m, 4H), 0.94 (t, 3H, J = 7.1 Hz). ^{13}C NMR (298 K, 100 MHz, $CDCl_3$): δ

(ppm) = 166.2, 157.9, 150.1, 111.3, 106.7, 68.1, 28.6, 28.1, 22.4, 14.0. Anal. Calcd for $C_{20}H_{28}N_2O_2$ (328.45 g mol^{-1}): C, 73.14; H, 8.59; N, 8.53%; found: C, 72.89; H, 8.90; N, 8.61%; ESI-MS: m/z 329.60 $[M + H]^+$.

4,4′-Dihexyloxy-2,2′-bipyridine (L-6C). Yield: 65%, white crystals. Mp 95–96 °C. ^{1}H NMR (298 K, 400 MHz, $CDCl_3$): δ (ppm) = 8.45 (d, 1H, *J* = 5.7 Hz), 7.95 (d, 1H, *J* = 2.5 Hz), 6.82 (dd, 1H, *J* = 5.7, 2.6 Hz), 4.12 (t, 2H, *J* = 6.5 Hz), 1.85–1.77 (m, 2H), 1.51–1.44 (m, 2H), 1.39–1.30 (m, 4H), 0.91 (t, 3H, *J* = 7.0 Hz). ^{13}C NMR (298 K, 100 MHz, $CDCl_3$): δ (ppm) = 166.2, 157.9, 150.1, 111.3, 106.7, 68.1, 31.5, 28.9, 25.6, 22.6, 14.0. Anal. Calcd for $C_{22}H_{32}N_2O_2$ (356.50 g mol^{-1}): C, 74.12; H, 9.05; N, 8.98%; found: C, 74.71; H, 8.83; N, 7.80%; ESI-MS: *m/z* 357.70 $[M + H]^+$.

4,4′-Dioctyloxy-2,2′-bipyridine (L-8C). Yield: 79%, white crystals. Mp 91–93 °C. ^{1}H NMR (298 K, 400 MHz, $CDCl_3$): δ (ppm) = 8.45 (d, 1H, *J* = 5.7 Hz), 7.95 (d, 1H, *J* = 2.6 Hz), 6.81 (dd, 1H, *J* = 5.7, 2.6 Hz), 4.12 (t, 2H, *J* = 6.5 Hz), 1.85–1.78 (m, 2H), 1.50–1.43 (m, 2H), 1.38–1.26 (m, 8H), 0.89 (t, 3H, *J* = 7.0 Hz). ^{13}C NMR (298 K, 100 MHz, $CDCl_3$): δ (ppm) = 166.2, 157.9, 150.1, 111.3, 106.7, 68.0, 31.8, 29.3, 29.2, 29.0, 26.0, 22.7, 14.1. Anal. Calcd for $C_{26}H_{40}N_2O_2$ (412.61 g mol^{-1}): C, 75.68; H, 9.77; N, 6.79%; found: C, 75.63; H, 10.12; N, 6.90%; ESI-MS: m/z 413.9 $[M + H]^+$.

2.3.5 Preparation of [Pt(II)Cl_2(4,4′-dialkoxy-2,2′-bipyridine)] complexes

The salt $K_2[PtCl_4]$ (1.2 equiv.) was dissolved in 1–2 mL of H_2O and then added to a solution of 4,4′-dialkoxy-2,2′-bipyridine (1.0 equiv.) in acetone. The mixture was heated to reflux for 24 h. The product (yellow solid) precipitated out either in hot condition or upon cooling. Water was added to ensure the complete precipitation of the product. The crude product was separated by vacuum filtration. The pure product was

obtained by first washing with cold water and then hot hexane, unless otherwise noted.

[$PtCl_2$(4,4′-dimethoxy-2,2′-bipyridine)] (Pt-1C). Yield: 92%, bright yellow powder (by washing with hot methanol). Mp 311–316 °C. ^{1}H NMR (298 K, 400 MHz, DMSO-d_6): δ (ppm) = 9.13 (d, 1H, J =6.8 Hz), 8.19 (d, 1H, J =2.8 Hz), 7.40 (dd, 1H, J = 6.9, 2.8 Hz), 4.05 (s, 3H). ^{13}C NMR (298 K, 100 MHz, DMSO-d_6): δ (ppm) = 168.2, 158.4, 149.5, 113.2, 111.1, 57.6. Anal. Calcd for $C_{12}H_{12}Cl_2N_2O_2Pt$ (482.23 g mol^{-1}): C, 29.89; H, 2.51; N, 5.81%; found: C, 30.04; H, 2.75; N, 5.77%.

[$PtCl_2$(4,4′-diethoxy-2,2′-bipyridine)] (Pt-2C). Yield: 97%, bright yellow powder (by washing with hot acetone). Mp 318–322 °C. ^{1}H NMR (332 K, 400 MHz, DMSO-d_6): δ (ppm) = 9.15 (d, 1H, J = 6.8 Hz), 8.14 (d, 1H, J = 2.8 Hz), 7.35 (dd, 1H, J = 6.8, 2.7 Hz), 4.36 (q, 2H, J = 7.0 Hz), 1.41 (t, 3H, J = 7.0 Hz). ^{13}C NMR (332 K, 100 MHz, DMSO-d_6): δ (ppm) = 167.5, 158.6, 149.6, 113.4, 111.3, 66.1, 14.5. Anal. Calcd for $C_{14}H_{16}Cl_2N_2O_2Pt$ (510.28 g mol^{-1}): C, 32.95; H, 3.16; N, 5.49%; found: C, 33.30; H, 2.84; N, 5.80%; ESI-MS: m/z 548.80 $[M + K]^+$.

[$PtCl_2$(4,4′-dipropoxy-2,2′-bipyridine)] (Pt-3C). Yield: 95%, bright yellow powder. Mp 269–272 °C. ^{1}H NMR (342 K, 400 MHz, DMSO-d_6): δ (ppm) = 9.15 (d, 1H, J = 6.8 Hz), 8.13 (d, 1H, J = 2.8 Hz), 7.34 (dd, 1H, J = 6.8, 2.8 Hz), 4.27 (t, 2H, J = 6.5 Hz), 1.87–1.78 (m, 2H), 1.03 (t, 3H, J = 7.4 Hz). ^{13}C NMR (302 K, 100 MHz, DMSO-d_6): δ (ppm) = 167.7, 158.5, 149.6, 113.4, 111.3, 71.6, 22.0, 10.5. Anal. Calcd for $C_{16}H_{20}Cl_2N_2O_2Pt$ (538.33 g mol^{-1}): C, 35.70; H, 3.74; N, 5.20%; found: C, 35.41; H, 3.89; N, 5.27%; ESI-MS: m/z 560.20 $[M + Na]^+$.

[$PtCl_2$(4,4′-dibutoxy-2,2′-bipyridine)] (Pt-4C). Yield: 93%, bright yellow powder. Mp 229–230 °C. ^{1}H NMR (298 K, 400 MHz, DMSO-d_6): δ (ppm) = 9.13 (d, 1H,

J = 6.9 Hz), 8.20 (d, 1H, *J* = 2.8 Hz), 7.40 (dd, 1H, *J* = 6.9, 2.8 Hz), 4.30 (t, 2H, *J* = 6.5 Hz), 1.83–1.76 (m, 2H), 1.53–1.44 (m, 2H), 0.97 (t, 3H, *J* = 7.3 Hz). ^{13}C NMR (298 K, 100 MHz, DMSO-d_6): δ (ppm) = 167.6, 158.5, 149.5, 113.4, 111.3, 69.9, 30.6, 19.0, 14.0. Anal. Calcd for $C_{18}H_{24}Cl_2N_2O_2Pt$ (566.39 g mol^{-1}): C, 38.17; H, 4.27; N, 4.95%; found: C, 38.18; H, 4.61; N, 4.99%; ESI-MS: *m/z* 588.40 $[M + Na]^+$.

[$PtCl_2$(4,4′-dipentoxy-2,2′-bipyridine)] (Pt-5C). Yield: 92%, bright yellow powder. Mp 173–175 °C. ^{1}H NMR (298 K, 400 MHz, $CDCl_3$): δ (ppm) = 8.81 (d, 1H, *J* = 6.8 Hz), 7.47 (d, 1H, *J* = 2.7 Hz), 6.73 (dd, 1H, *J* = 6.8, 2.7 Hz), 4.29 (t, 2H, *J* = 6.4 Hz), 1.92–1.85 (m, 2H), 1.54–1.38 (m, 4H), 0.97 (t, 3H, *J* = 7.2 Hz). ^{13}C NMR (298 K, 100 MHz, $CDCl_3$): δ (ppm) = 167.0, 158.0, 148.9, 112.7, 110.2, 70.1, 28.4, 27.9, 22.4, 14.0. Anal. Calcd for $C_{20}H_{28}Cl_2N_2O_2Pt$ (594.44 g mol^{-1}): C, 40.41; H, 4.75; N, 4.71%; found: C, 40.46; H, 5.00; N, 4.58%; ESI-MS: *m/z* 616.80 [M + Na]+.

[$PtCl_2$(4,4′-dihexyloxy-2,2′-bipyridine)] (Pt-6C). Yield: 61%, bright yellow powder. Mp 176–179 °C. ^{1}H NMR (298 K, 400 MHz, $CDCl_3$): δ (ppm) = 8.78 (d, 1H, *J* = 6.8 Hz), 7.47 (d, 1H, *J* = 2.7 Hz), 6.71 (dd, 1H, *J* = 6.8, 2.7 Hz), 4.29 (t, 2H, *J* = 6.4 Hz), 1.91–1.84 (m, 2H), 1.56–1.48 (m, 2H), 1.41–1.33 (m, 4H), 0.93 (t, 3H, *J* = 7.0 Hz). ^{13}C NMR (298 K, 100 MHz, $CDCl_3$): δ (ppm) = 167.0, 158.0, 148.8, 112.7, 110.2, 70.2, 31.5, 28.7, 25.5, 22.6, 14.1. Anal. Calcd for $C_{22}H_{32}Cl_2N_2O_2Pt$ (622.49 g mol^{-1}): C, 42.45; H, 5.18; N, 4.50%; found: C, 42.53; H, 5.40; N, 4.68%; ESI-MS: m/z 644.40 $[M + Na]^+$.

[$PtCl_2$(4,4′-dioctyloxy-2,2′-bipyridine)] (Pt-8C). Yield: 61%, bright yellow powder (recrystallized from $CHCl_3$-CH_3OH). Mp 169–172 °C. ^{1}H NMR (298 K, 400 MHz, $CDCl_3$): δ (ppm) = 8.83 (d, 1H, *J* = 6.8 Hz), 7.47 (d, 1H, *J* = 2.8 Hz), 6.74 (dd, 1H, *J* = 6.8, 2.7 Hz), 4.30 (t, 2H, *J* = 6.4 Hz), 1.92–1.85 (m, 2H), 1.56–1.48 (m, 2H), 1.41–

1.28 (m, 8H), 0.91 (t, 3H, J = 7.0 Hz). ^{13}C NMR (298 K, 100 MHz, $CDCl_3$): δ (ppm) = 167.1, 158.0, 148.9, 112.7, 110.2, 70.2, 31.8, 29.3, 29.2, 28.8, 25.9, 22.7, 14.1. Anal. Calcd for $C_{26}H_{40}Cl_2N_2O_2Pt$ (678.60 g mol^{-1}): C, 46.02; H, 5.94; N, 4.13%; found: C, 46.26; H, 6.04; N, 4.29%; ESI-MS: m/z 701.20 $[M + Na]^+$.

2.3.6 Cell culture

Human cancer cell lines A549 (lung adenocarcinoma), DU145 (prostate carcinoma), MCF-7 (breast adenocarcinoma), and MDA-MB-435 (melanoma) were obtained from American Culture Type Collection (ATCC). The A549, MCF-7, and MDA-MB-435 cells were grown in MEM supplemented with 10% FBS, 25 mM HEPES buffer (pH 7.4), penicillin (100 U mL^{-1}) and streptomycin (100 µg mL^{-1}). The DU145 cell line was grown in RPMI 1640 supplemented with 10% FBS, 25 mM HEPES buffer (pH 7.4), penicillin (100 U mL^{-1}) and streptomycin (100 µg mL^{-1}). All cell lines were maintained at 37 °C in a humidified, 5% CO_2 atmosphere.

2.3.7 Preparation of stock solutions

CDDP stock was dissolved in 0.15 M NaCl, carboplatin stock was dissolved in 5% glucose, ligands and synthesized Pt-complexes were dissolved in DMSO.

2.3.8 Cell viability assay

Cells were cultured at a density of 2 x 10^3 cells per well in flat bottomed 96-well plates in 100 µL of complete growth medium and incubated for 2 d to reach ~ 50% confluence. The cells were then treated with solvent or the appropriate drugs for 1 h, washed thrice with 100 µL PBS, and incubated in 100 µL of fresh medium. After 2 d, the medium was replaced with 120 µL of medium containing CellTiter 96® Aq_{ueous} One Solution Reagent (MTS reagent) (Promega, Madison, WI). After 4 h in culture the cell

viability was determined by measuring the absorbance at 490 nm using a Tecan Infinite M1000 microplate reader. The 48 h treatment was done in a similar method, except the cells were not washed after treatment and the MTS reagent was immediately added. Viability of treated groups was calculated as a percent of control and graphed with GraphPad Prism.

2.3.9 Flow cytometry

2.3.9.1 Propidium iodide (PI) staining

Cells (~50% confluent) were incubated at 37 °C in a humidified, 5% CO_2 atmosphere for 1 h with the indicated concentration of **Pt-4C**. After 1 h, cells were washed with 5 mL PBS and fresh medium added. Cells were incubated at 37 °C in a humidified, 5% CO_2 atmosphere for 12, 24, and 48 h, at which point cells were harvested, counted and centrifuged at 500 x g for 5 min. Cells were then washed two times with 5 mL PBS, fixed by resuspending in 0.1 mL PBS and 1 mL of cold 95% ethanol with gentle vortexing. Fixed cells were stored at 4 °C until analysis. For analysis, fixed cells were washed once with 1-2 mL PBS and centrifuged at 500 × g for 5 minutes. Cells were resuspended in 100 µL of 1.0% Triton X-100 buffer solution. The RNAse solution (100 µL of a 1.0 mg mL^{-1}) was added and allowed to stand at room temperature for 10-15 min. While in the dark, 200 µL of a 100 µg mL^{-1} PI stain was added to make a final concentration of 50 µg mL^{-1} and gently vortexed. Cell mixture was incubated at room temperature for 30 min. Cytometry acquisition was done on Becton Dickinson FACS Calibur with the argon laser set at 488 nm on the linear Flow Channel 2 (FL-2) with Doublet Discriminatory Module (DDM) and threshold set on FL-2.

2.3.9.2 Annexin V-FITC/PI staining

Cells (40-50% confluent) were incubated at 37 °C in a humidified, 5% CO_2 atmosphere for 1 h with the indicated concentration of **Pt-4C**. After 1 h, cells were washed with 5 mL PBS and fresh medium was added. Cells were incubated at 37 °C in a humidified, 5% CO2 atmosphere for 12, 24, and 48 h, at which point cells were harvested and counted. Next, the cells were centrifuged at 500 × g for 5 min and washed once with 5 mL Ca^{2+} and Mg^{2+} free PBS. Pellets were then washed in 2.0 mL 1X Annexin-V Binding buffer (BD Bioscience, San Jose, CA) and centrifuged at 500 × g for 5 min. The pellets were treated with Annexin-V-FITC conjugate (BD Bioscience, San Jose, CA) and incubated in the dark for 15 min. Just before acquisition, the volume of cells-conjugate mixture was adjusted by addition of 1X Annexin-V binding buffer. Acquisition to discriminate between apoptotic and necrotic cells was done by staining the cell-conjugate mixture with 10 μL of PI (50 μg mL^{-1}) solution (BD Bioscience, San Jose, CA). Acquisitions were done on FACS Calibur Cytometer on the FL1 (Annexin) and FL3 (PI) channels with threshold and Duplet Discriminating Module (DDM) set at FL1. The level of shift in events distribution in the Annexin-V only and Annexin-V-PI populations in comparison to control is indicative of degree of effectiveness of the treatment agents. A quantitative measure of these event shifts was accomplished by gating.

2.3.10 Fluorescence microscopy

A number of 5000 or 10 000 cells per well were seeded in a 4 well chamber slide with a final volume of 0.5 mL. Cells were incubated at 37 °C for ~72 h and then treated with EC_{50} concentration of **Pt-4C** for 1 h at 37 °C. Cells were washed twice with 0.5 mL PBS and fresh medium (0.5 mL) was added. Cells were incubated at 37 °C for 2 h. While

in the dark, medium was removed, cells were washed with 0.5 mL PBS, and then 0.5 mL of 2 μg mL^{-1} Hoechst 33342 and 10 μg mL^{-1} PI stain (in PBS) was added for a final concentration of 1 μg mL^{-1} Hoechst 33342 and 5 μg mL^{-1} PI. Cells were incubated for 15 min at room temperature. Images were acquired within 5 min with a Nikon Eclipse microscope, model TE2000-U. Three random areas on each slide were imaged for bright field, cells stained with Hoechst, and cells stained with PI (9 images were obtained for each slide: 3 for bright field, 3 for Hoechst staining, and 3 for PI staining).

2.3.11 DNA laddering

Cells (~50% confluent) were treated with 10-35 μM **Pt-4C** for 1 h. 24 h post treatment, cells were collected, washed with PBS, and the pellet resuspended in 500 μL of lysis buffer (100 mM Tris-HCl pH 8.0, 5 mM EDTA, 1% SDS, 0.5% Triton X-100, 200 mM NaCl, 100 μg mL^{-1} proteinase K). After 2 h of incubation at 56 °C, 500 μL of 2-propanol was added, mixed by inversion, and DNA was precipitated overnight at -20 °C. The DNA was pelleted by centrifugation at 16 000 × g for 15 min at 4 °C. The pellet was washed once with 70% ethanol and air dried by inverting the tube on a tissue for 10 min. The DNA was dissolved in 20 μL of TE Buffer (10 mM Tris, 1 mM EDTA) containing 0.2 mg mL^{-1} RNAse A and incubated at 37 °C for 1 h. The DNA concentration was determined with the NanoDrop ND-1000 Spectrophotometer and 2 μg of DNA was analyzed on a 2% agarose gel in TBE buffer (2 mM EDTA, pH 8.0; 89 mM Tris; 89 mM boric acid). The gel was stained with 1 μg mL^{-1} ethidium bromide for 30 min, rinsed with water, and exposed to UV light.

2.3.12 Statistical analysis

GraphPad Prism 4 was used to graph viability curves. ModFit version 3.0 was used for the flow cytometry analysis. Microsoft Office Excel was used to run Student's t-test; values with $p < 0.05$ were considered significant. Student's t-tests were used to verify significant differences among the EC_{50} values.

2.4 Results and discussion

2.4.1 Synthesis and characterization

Except for 4,4′-dimethoxy-2,2′-bipyridine (henceforth referred to as **L-1C**), which was purchased from a commercial vendor, all ligands were synthesized by reacting a respective primary alkyl halide with a mixture of 2,2′-bipyridine-4,4′-diol and Cs_2CO_3 or K_2CO_3 in DMF on heating to reflux for 48 h. For the synthesis of **L-2C**—**L-4C** with high yields, Cs_2CO_3 was used instead of the usual K_2CO_3 because the latter base gave relatively low yields. However, the synthesis of **L-5C**, **L-6C** and **L-8C** with K_2CO_3 gave respectable yields. The platinum complexes were formed by adding an aqueous solution of $K_2[PtCl_4]$ to a solution of the ligand in acetone and on heating to reflux for 24 h (Scheme 2-1). All ligands are white and produce a colourless solution when dissolved in

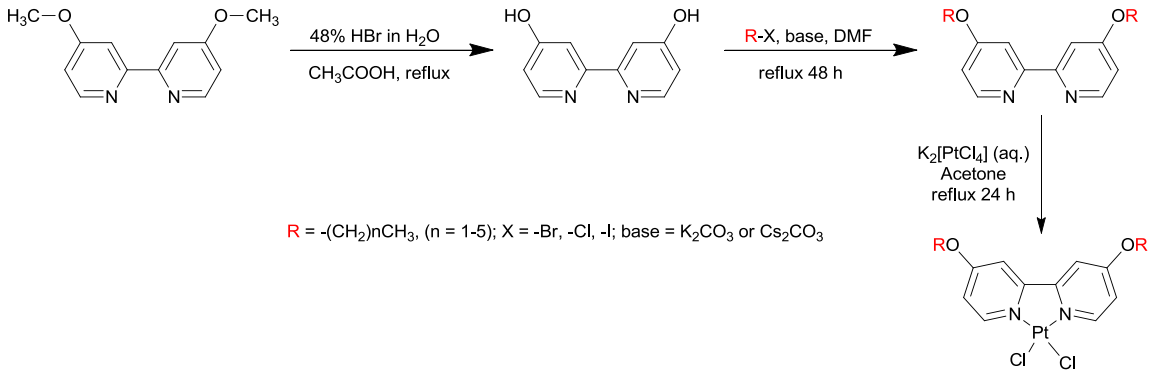

Scheme 2 – 1. Scheme for the synthesis of Pt(II)-complexes (**Pt-2C**—**Pt-6C**, **Pt-8C**).

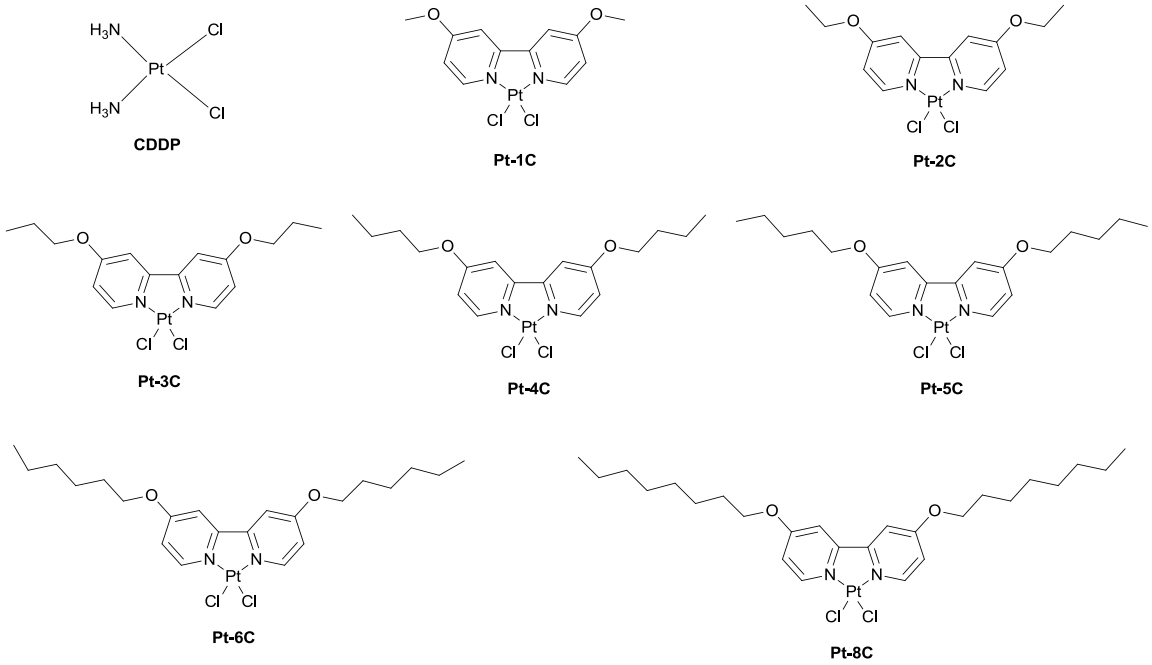

Figure 2 – 2. Chemical structures of CDDP and the synthesized [Pt(II)Cl_2(4,4′-dialkoxy-2,2′-bipyridine)] complexes.

organic solvents; however, all the platinum complexes are yellow solids and generate a yellow solution when dissolved in organic solvents. Thus, the progress of the reaction was monitored visually by the appearance of a yellow solution or precipitate. The chemical structures of cisplatin and the synthesized platinum complexes are shown in Fig. 2-2. **L-2C**[27,28] and **L-4C**[29] were previously synthesized using an alternative method with longer synthetic steps and produces a dinitro intermediate that is potentially explosive. The synthesis and the *in vitro* cytotoxicity of the platinum complex **Pt-1C** have been reported previously.[19] The synthesis of **Pt-2C** has also been previously reported for its electrochemical and electronic properties;[30] however, no literature on activity against cancer cells is available to date. The Pt-complexes, **Pt-3C**—**Pt-6C** and **Pt-8C**, have not been reported in the literature.

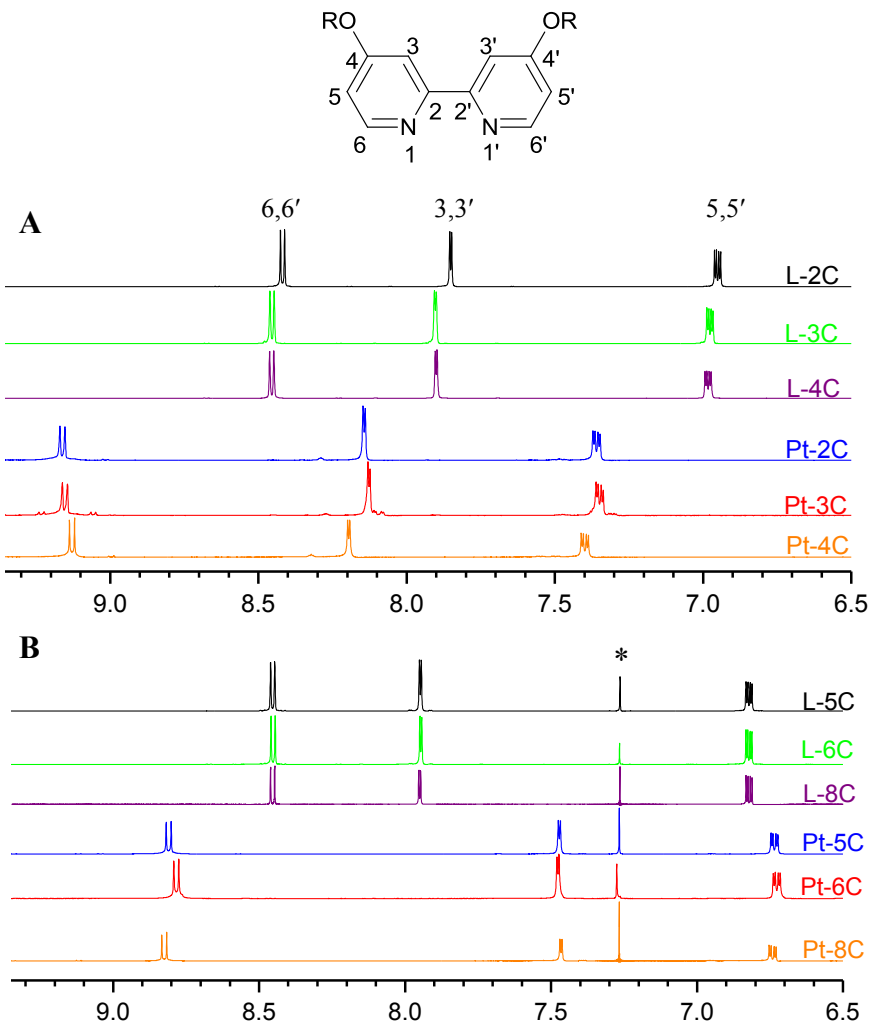

Figure 2 – 3. The aromatic region of ligands and platinum(II)-complexes from ^{1}H NMR spectra. Spectra were recorded in DMSO-d_6 and $CDCl_3$ at the temperatures indicated in the Experimental section (* solvent peak).

All of the compounds were characterized by ^{1}H and ^{13}C NMR spectroscopy, elemental analysis, mass spectrometry, and DSC measurements. Elemental and mass spectrometry analyses of the complexes were in excellent agreement (within 0.5% for elemental analyses and 5 ppm for mass spectrometry) with the expected values; thus, validating the molecular formulae of these compounds. The ^{1}H and ^{13}C NMR spectra of the compounds **L-2C**—**L-4C**, and **Pt-2C**—**Pt-4C** were recorded in DMSO-d_6, whereas

those of the compounds **L-5C—L-8C**, and **Pt-5C—Pt-8C** were recorded in $CDCl_3$. The spectra of all of the compounds displayed the expected proton and carbon resonances. The ^1H NMR chemical shifts of the aromatic region of the ligands and platinum complexes are depicted in Fig. 2-3 and summarized in Table 2-1. The chemical shifts of the protons at the 6,6′ positions are the most downfield, protons at the 5,5′ positions are the most upfield and protons at the 3,3′ positions are in between. When 4,4′-dialkoxy-2,2′-bipyridine was coordinated to platinum(II), all aromatic proton peaks of the complexes in DMSO-d_6 are shifted downfield compared to the ligand while only the peak corresponding to the protons at the 6,6′ positions of complexes recorded in $CDCl_3$ are shifted downfield, and peaks corresponding to the 5,5′ and 3,3′ positions are shifted upfield. Similarly, the carbon signals at the 5,5′ positions, those of 3,3′ position and methylene carbon signal next to the oxygen in both the deuterated solvents were shifted downfield to varying degrees, but the carbon signals at 6,6′ positions in these solvents were slightly shifted to upfield (Fig. 2S-1, Appendix 1). The difference in the direction of the chemical shifts is due to differences in the interaction of the compounds with the organic solvents of varying polarity used (Table 2-1).

Table 2 – 1. Chemical shifts (ppm) in the aromatic region of ligands and platinum(II)Cl_2 complexes from ^{1}H NMR spectra recorded in DMSO-d_6 and $CDCl_3$ at the temperatures indicated in the Experimental section

Compound	Solvent	$\delta_{H\text{-}6,6'}$ (ppm)	$\delta_{H\text{-}5,5'}$ (ppm)	$\delta_{H\text{-}3,3'}$ (ppm)
L-2C (**Pt-2C**)	DMSO-d_6	8.46 (9.15)	6.99 (7.35)	7.90 (8.14)
L-3C (**Pt-3C**)	DMSO-d_6	8.45 (9.15)	6.97 (7.34)	7.90 (8.13)
L-4C (**Pt-4C**)	DMSO-d_6	8.46 (9.13)	6.98 (7.40)	7.90 (8.20)
L-5C (**Pt-5C**)	$CDCl_3$	8.45 (8.81)	6.82 (6.73)	7.95 (7.47)
L-6C (**Pt-6C**)	$CDCl_3$	8.45 (8.78)	6.82 (6.71)	7.95 (7.47)
L-8C (**Pt-8C**)	$CDCl_3$	8.45 (8.83)	6.81 (6.74)	7.95 (7.47)

Thermal transitions of the synthesized compounds were determined by DSC measurements. Each of the DSC thermograms for ligands **L-2C**—**L-8C** displayed a single endotherm in the first heating cycle and a single exotherm in the first cooling cycle corresponding to its melting and crystallization transitions, respectively. Correspondingly, there were a melting endotherm in the second heating cycle and a crystallization exotherm in the second cooling cycle. **L-2C** had the highest melting at 124 °C and **L-5C** had the lowest at 86 °C. **L-3C**, **L-4C**, **L-6C**, and **L-8C** had melting points ranging between 93-100 °C with no apparent trends. Platinum complexes had varying DSC thermograms. The DSC thermograms of Pt(II) complexes produced rather complex thermal properties. For example, **Pt-2C** and **Pt-3C** showed a single endotherm in the first heating cycle (Fig. 2S-2, Appendix 1), but no exotherm in the first cooling cycle. Correspondingly, there was no melting endotherm in the second heating cycle and no exotherm in the second cooling cycle. These complexes once melted could not crystallize and, therefore, formed amorphous phases. **Pt-4C** showed a sharp single endotherm (melting) in the first heating cycle, but showed a broad, exotherm in the first cooling cycle. Correspondingly, it showed a slightly broad endotherm at a lower temperature

when compared with that in the first heating cycle, but showed a broad exotherm in the second cooling cycle (not shown). **Pt-5C** showed two sharp endotherms in the first heating cycle and two broad exotherms in the first cooling cycle. Correspondingly, it showed two endotherms in the second heating cycle and two broad exotherms in the second cooling cycle. The first low- temperature endotherm was related to the crystal-to-crystal transition and the high-temperature one was related to its melting transition (Fig. 2S-2, Appendix 1). **Pt-6C** showed three endotherms in the first heating cycle, but no exotherms in the first cooling cycle. During the second heating cycle, once it traversed through the glass transition temperature, it showed a cold crystallization exotherm and three endotherms. Again, there were no exotherms in the second cooling cycle. The two low-temperature endotherms were related to the crystal-to-crystal transitions and the highest-temperature endotherm was related to its melting transition. The observed crystal-crystal transitions of these two Pt(II)-complexes are in excellent agreement with those of other Pt(II)-complexes.[31] **Pt-8C** showed a sharp melting endotherm in the first heating cycle and a sharp exotherm in the first cooling cycle. Correspondingly, it showed a sharp melting transition in the second heating cycle and a sharp crystallization exotherm in the second cooling cycle (Fig. 2S-2, Appendix 1). It was found that the melting transitions of the Pt(II)-complexes were much higher than those of the ligands and decrease as the carbon number of the alkoxy group increases in the series examined.

2.4.2 Biological properties

2.4.2.1 *In vitro* cytotoxic activity

Lung cancer is one of the leading causes of cancer death not only in the U.S., but also worldwide; thus, the activity of the ligands and Pt compounds were first tested in the

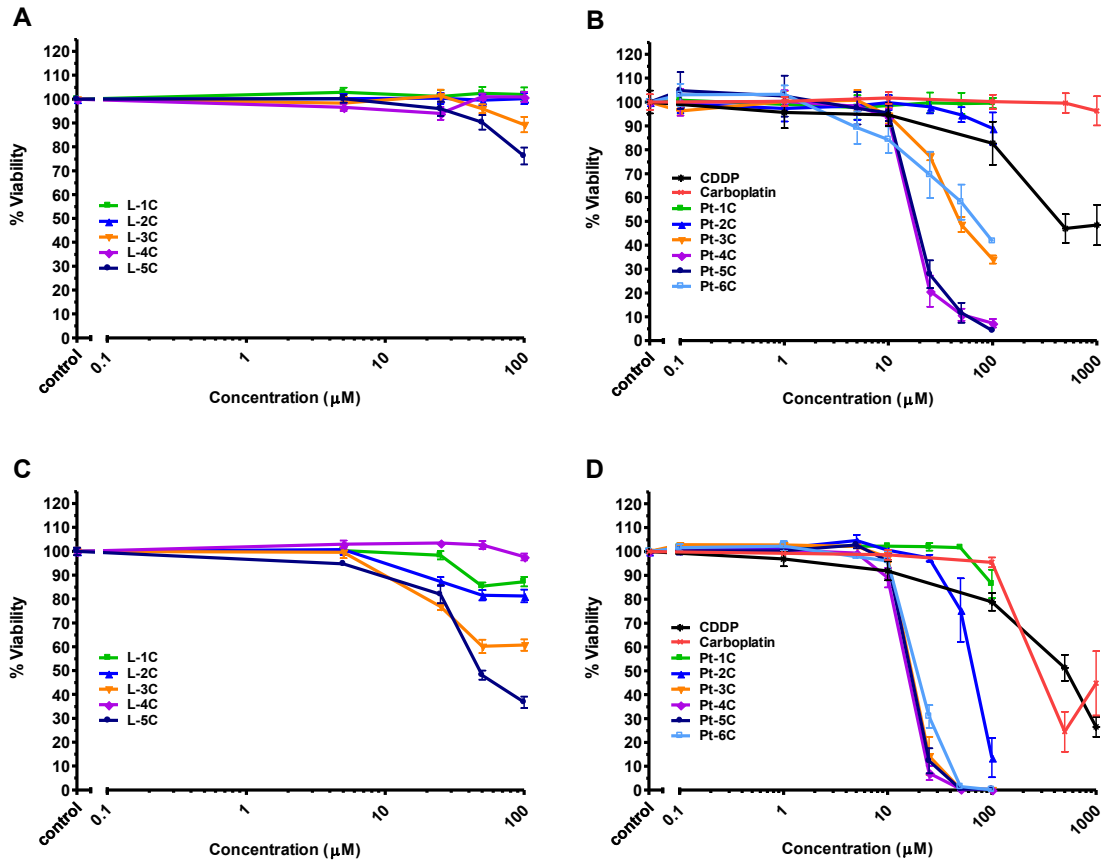

Figure 2 – 4. Cytotoxic activity of the synthesized ligands and Pt(II)Cl_2 complexes vs. CDDP and carboplatin against A549 human lung cancer cells. Cells were treated with the ligands, CDDP, or the platinum analogs at various concentrations for (A, B) 1 h or (C, D) 48 h and the viability was determined using the MTS assay. Data points represent mean ± SD of at least three independent experiments done in quadruplicates.

human lung cancer cell line A549 and compared to cisplatin and carboplatin using an MTS colorimetric assay to determine cell viability. For a 1 h treatment, **L-1C—L-5C** had little to no effect on A549 cell viability (Fig. 2-4 A). Carboplatin also did not have any effect on the cells when treated for 1 h (Fig. 2-4 B). Cisplatin caused a concentration-dependent decreased in A549 cell viability with a reduction of about 50% at 1000 μM.

Similar to carboplatin, the analogues containing 1 (**Pt-1C**) or 2 (**Pt-2C**) carbon chain length had no effect on the cells. When the carbon chain length was increased to three (**Pt-3C**), the cell viability decreased with increasing concentrations. The analogues containing four (**Pt-4C**) and five (**Pt-5C**) carbon chain lengths had similar activities and caused further decrease in cell viability compared to the **Pt-3C**. When the chain length was increased to 6 carbons (**Pt-6C**), the activity was reversed compared to **Pt-4C** and **Pt-5C** and was similar to **Pt-3C** (Fig. 2-4 B). A549 cells remained unaffected by **L-1C**, **L-2C**, and **L-4C** when the treatment was extended to 48 h; however, **L-3C** and **L-5C** decreased cell viability by 40% and 60%, respectively, at 100 μM (Fig. 2-4 C). The **Pt-1C** analogue was still without effect when treatment was extended to 48 h; however, **Pt-2C** was very effective and caused almost complete reduction of cell viability at 100 μM (Fig. 2-4 D). The activities of **Pt-4C** and **Pt-5C** were comparable to the 1 h treatment. Interestingly, the activities of **Pt-3C** and **Pt-6C** were now increased to levels similar to **Pt-4C** and **Pt-5C**. The activities of CDDP and carboplatin were also increased in the 48 h treatment compared to the 1 h treatment; however, both drugs were still less effective than **Pt-2C—Pt-6C**. The effective concentrations that result in 50% cell viability (EC_{50}) for the complexes are given in Table 2-2. As shown, the EC_{50} of CDDP and carboplatin are much higher than **Pt-2C—Pt-6C**. **L-6C**, **L-8C**, and **Pt-8C** were not tested due to poor solubility in common solvents used for *in vitro* testing.

Table 2 – 2 Effective concentrations that gives 50% cell death (EC_{50}) determined from A549 MTS assay data of at least three independent experiments

Compound	EC_{50} (μM) for 1 h	EC_{50} (μM) for 48 h
CDDP	1000 ± 0	500 ± 100
Carboplatin	> 1000	300 ± 30[a]
Pt-1C	>100	>100
Pt-2C	>100	66 ± 7 [a]
Pt-3C	48 ± 3 [a]	17 ± 1 [a]
Pt-4C	17 ± 1 [a]	15.4 ± 0.5 [a]
Pt-5C	18 ± 1 [a]	16.5 ± 0.5 [a]
Pt-6C	66 ± 16 [a]	19.1 ± 0.8 [a]
Pt-8C	ND	ND

Data represent mean ± SD from three independent experiments done in quadruplicates.

[a] $P<0.05$ compared to CDDP.

The MTS cell viability results demonstrated a concentration and time-dependent effect of complexes of CDDP, carboplatin, and **Pt-2C—Pt-6C** against human A549 lung cancer cells. It is apparent that most of these complexes have higher activity than cisplatin and carboplatin. The trend of the activity of the complexes at 1 h exposure in A549 cells is **Pt-4C** ≈ **Pt-5C** > **Pt-3C** ≈ **Pt-6C** > CDDP > **Pt-2C** ≈ carboplatin ≈ **Pt-1C**. The activity of the complexes increases as the carbon number on the alkoxy group increases, which peaked with the complexes having four (**Pt-4C**) and five carbon chains (**Pt-5C**) and then decreased with the complex having a six carbon chain (**Pt-6C**). It is interesting to note that a difference of one carbon number caused the activity to increase or decrease by 3 or 4 times. This may be attributed to changes in molecular weight and lipophilicity, which could affect cellular uptake of the compounds.[32,33]

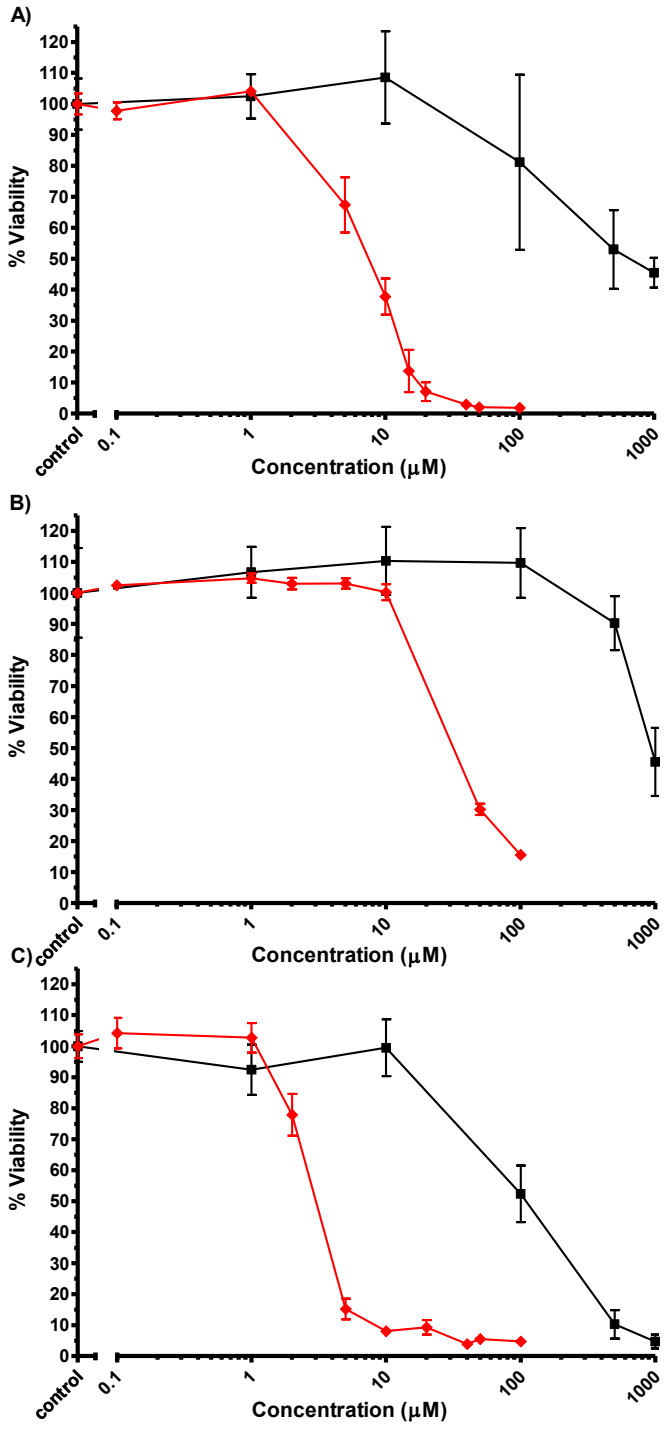

Figure 2 – 5. Cytotoxicity of various human cancer cells (A) DU145, (B) MCF-7, and (C) MDA-MB-435 treated for 1 h with CDDP (■) or **Pt-4C** (♦). Data points represent mean ± SD of at least two independent experiments done in quadruplicates.

Based on the results of A549 cells, one of the highly effective compounds, **Pt-4C**, was used for further testing. To determine if **Pt-4C** has a broad spectrum of activity against other types of oncogenic cells, the activity of this complex was tested against a prostate cancer cell line (DU145), a melanoma cell line (MDA-MB-435), and a breast cancer cell line (MCF-7). Similar to A549, **Pt-4C** also had a concentration-dependent effect against all cell lines tested in a 1 h treatment (Fig. 2-5). The EC_{50} varied slightly among the different cell lines (Table 2-3); the EC_{50} of **Pt-4C** was in the low micromolar range, whereas, the EC_{50} of cisplatin was 25–63 times higher depending on the cell line. The MDA-MB-435 cell line was the most sensitive to **Pt-4C** treatment, followed by DU145. The MCF-7 cell line had the highest EC_{50} and was the least sensitive to **Pt-4C**. These results indicate that this compound is much more potent compared to cisplatin and has a broad spectrum of activity.

Table 2 – 3 EC_{50} (μM) values of **Pt-4C** determined from MTS assay data of at least two independent experiments done in quadruplicates

Cell line	Cancer type	CDDP	**Pt-4C**
A549	lung	1000 ± 0	17 ± 1 [a]
DU145	prostate	500 ± 200	8 ± 2 [a]
MCF-7	breast	910 ± 90	32 ± 5 [a]
MDA-MB-435	melanoma	110 ± 40	4 ± 1 [a]

Data represent mean ± SD from three independent experiments done in quadruplicates. [a] $P<0.05$ compared to CDDP.

2.4.2.2 Evaluation of apoptosis

2.4.2.2.1 Cell cycle analysis by flow cytometry.

The MTS data indicate that these Pt-complexes induce cell death in various human cancer cells. There are two major forms of cell death: apoptosis and necrosis.

Apoptosis is a genetically-driven programmed cell death characterized by features such as cell shrinkage and chromatin condensation and fragmentation.[34] Necrosis results from physical injuries and may result from exposure to chemotherapeutic drugs. Necrotic cells swell up and lyse, releasing cellular contents and cause inflammatory responses. Apoptosis is the main mode of cell death in cells treated with cisplatin (human ovarian cancer cell line A2780,[35] human cervix carcinoma cell line HeLa,[36] ovarian cancer cells OV2008[37]). We hypothesized that the **Pt-4C** complex would also induce apoptosis; thus, **Pt-4C** treated cells were analyzed by flow cytometry using propidium iodide (PI) and Annexin V/PI double staining to detect apoptotic features.

The effect of **Pt-4C** on the cell cycle distribution of A549, DU145, and MCF-7 cells was examined by flow cytometry with PI staining (Fig. 2- 6). Cells were treated for 1 h with EC_{50} concentration of **Pt-4C** and harvested 24 and 48 h after treatment. The cells were fixed, stained with PI and analyzed with a flow cytometer which measures the PI fluorescence. In A549 (Fig. 2-6 A), **Pt-4C** treatment did not induce any cell cycle arrest. However, it caused a decrease in all stages of the cell cycle and an increase in the sub-G1 population. The effects of **Pt-4C** on the cell cycle distribution of DU145 cells (Fig. 2-6 B) and MCF-7 cells (Fig. 2-6 C) were similar to A549 cells. Both MCF-7 and DU145 had a higher percentage of cells in sub-G1 after 48 h compared to 24 h.

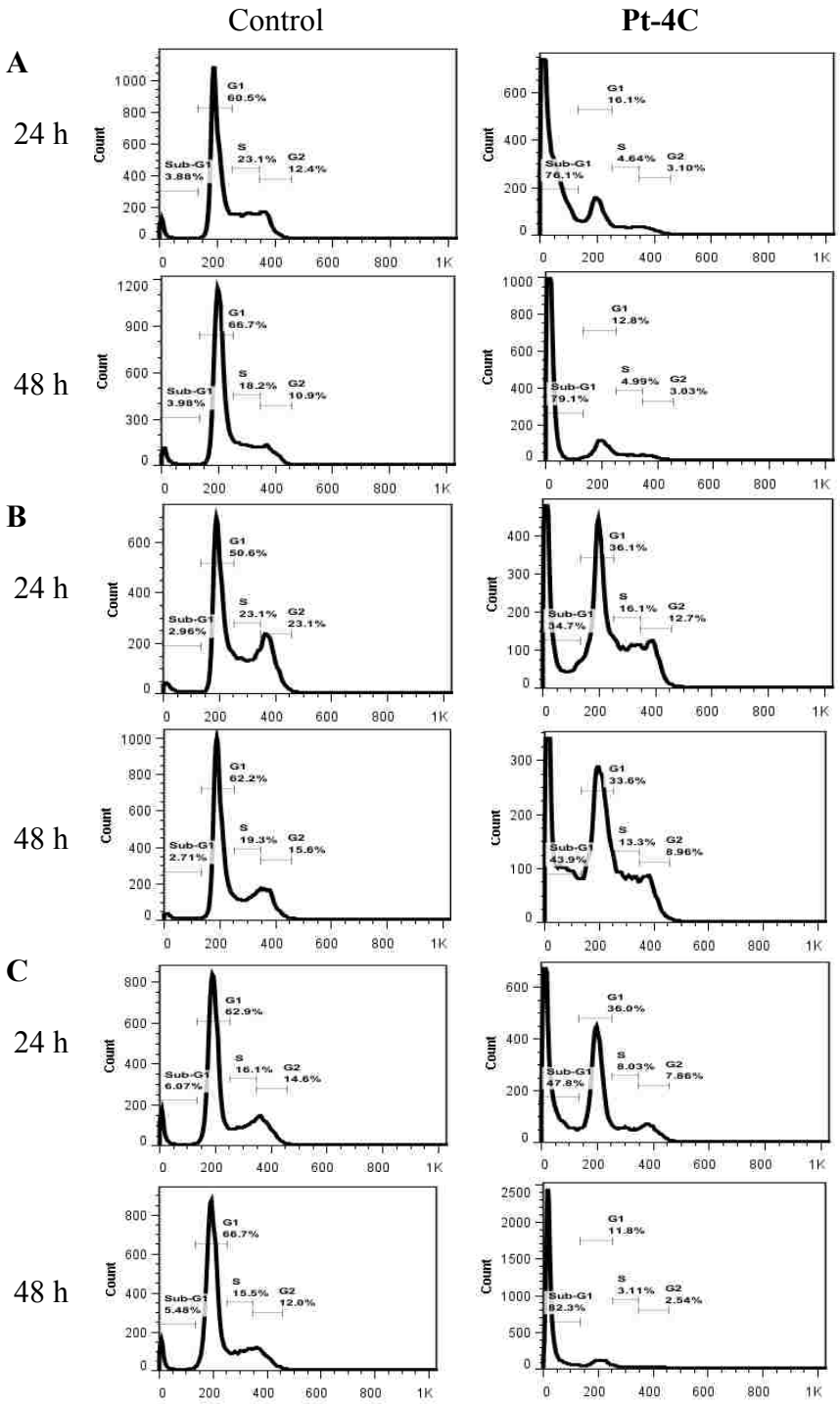

Figure 2 – 6. Flow cytometry with PI staining (A) A549, (B) DU145, and (C) MCF7. Cells were treated with EC_{50} **Pt-4C** for 1 h then harvested 24 and 48 h after treatment. Cells were fixed, stained with PI and analyzed with a flow cytometer. Data are representative plots of three independent experiments.

2.4.2.2.2 Detection of membrane changes by flow cytometry

Analysis of the PI staining of **Pt-4C** treated cells demonstrate that the EC_{50} concentration of **Pt-4C** did not induce cell cycle arrest in A549, DU145, and MCF-7 cells, but caused a time-dependent increase in the sub-G1 population. The PI fluorescence intensity is proportional to DNA content; the sub-G1 peak represents cells with less DNA content than the cells in the G1 phase and are usually described as apoptotic cells.[20] However, cells undergoing necrosis have membrane damage and DNA content can leak out causing them to have less DNA than cells in G1 phase. Thus, it is unclear if the sub-G1 peak represents cells undergoing apoptosis or necrosis. Consequently, Annexin V/PI staining was used to determine apoptotic vs. necrotic cell death.

An event that happens in early apoptosis is flipping of phosphatidylserine to the membrane surface which is recognized by Annexin V. The effect of **Pt-4C** in A549, DU145, and MCF-7 cells was analyzed by flow cytometry with Annexin V to detect early apoptosis and PI staining to detect late apoptosis or necrosis. Cells were treated with EC_{50} concentration of **Pt-4C** for 1 h then harvested 12, 24, and 48 h post treatment. Cells were stained with Annexin V and PI and analyzed with a flow cytometer. For all time points, A549 cells treated with **Pt-4C** were decreased in quadrant four (Q4) and increased in both quadrant two (Q2) and quadrant three (Q3) populations, indicating an increase in early apoptotic and late apoptotic/necrotic cells with a corresponding decrease in live cells (Fig. 2-7). The 24 h group had higher percentages of early apoptotic and late apoptotic/ necrotic cells (cells in Q2 and Q3) than the 12 h group; however, the 48 h group had lower percentages than 24 h. Similar to A549, DU145 cells treated with **Pt-4C** were also decreased in Q4 and increased in both Q2 and Q3 compared to control,

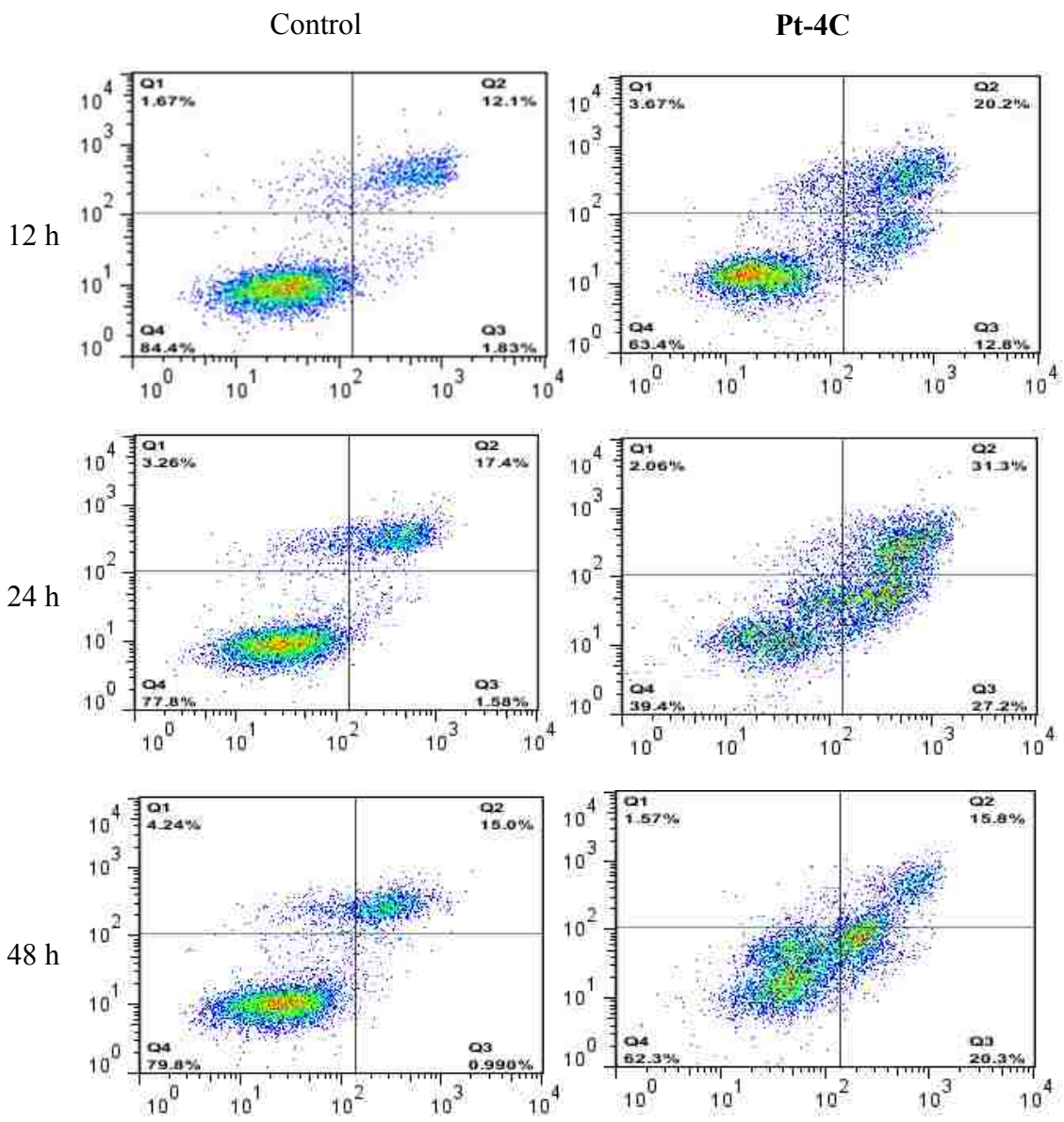

Figure 2 – 7. A549 Flow with Annexin V/PI staining. A549 cells were treated with EC_{50} **Pt-4C** for 1 h then harvested 12, 24, and 48 h after treatment. Cells were stained with Annexin V and PI and analyzed with a flow cytometer. Q1 is PI positive representing necrotic cells, Q2 is Annexin V/PI positive representing late apoptotic/necrotic cells, Q3 is Annexin V positive and PI negative representing early apoptotic cells, and Q4 is Annexin V/PI negative representing live cells. Data are representative of three independent experiments.

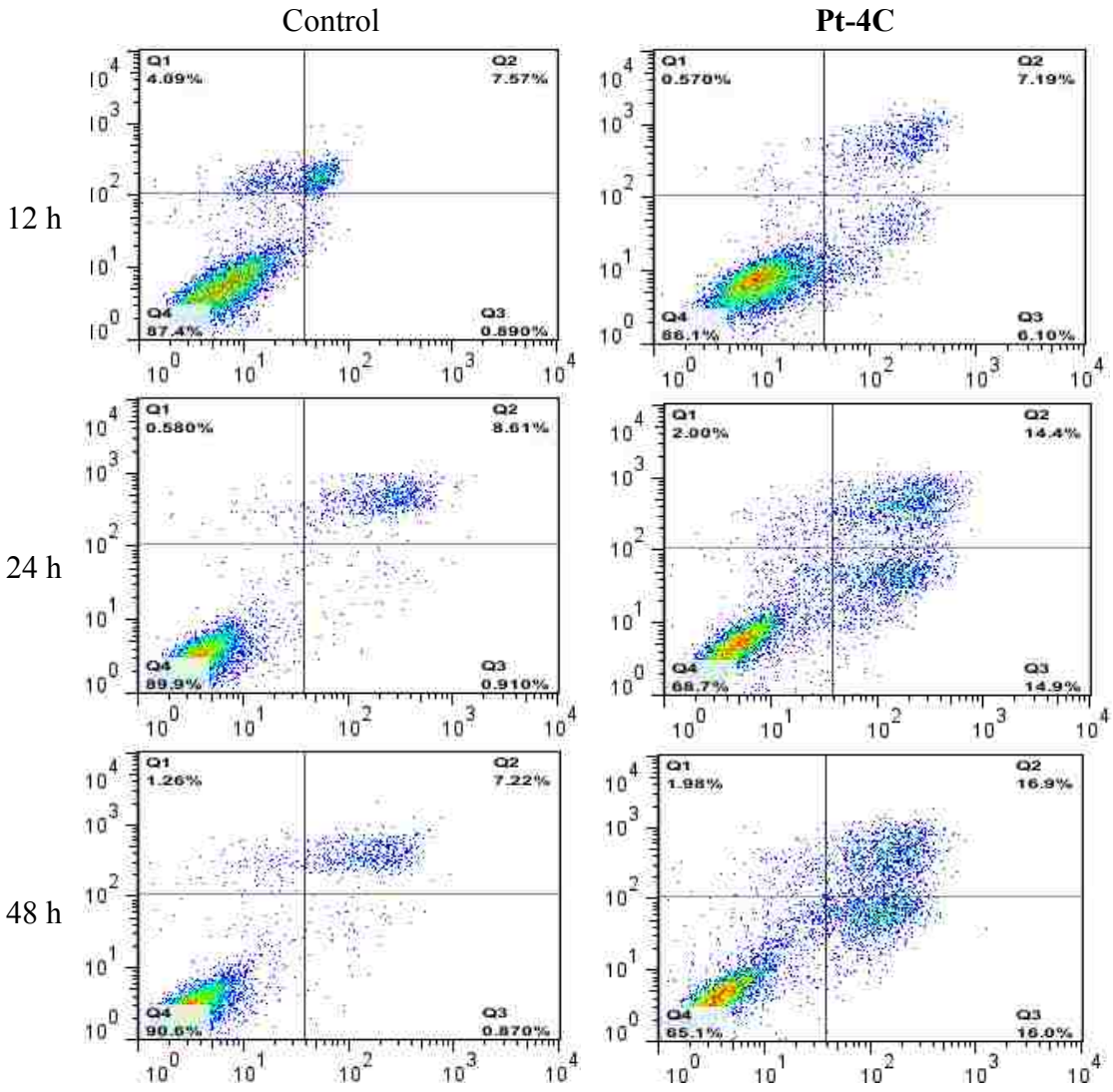

Figure 2 – 8. DU145 Flow with Annexin V/PI staining. Cells were treated with EC_{50} **Pt-4C** for 1 h then harvested 12, 24, and 48 h after treatment. Cells were stained with Annexin V and PI and analyzed with a flow cytometer. Q1 is PI positive representing necrotic cells, Q2 is Annexin V/PI positive representing late apoptotic/necrotic cells, Q3 is Annexin V positive and PI negative representing early apoptotic cells, and Q4 is Annexin V/PI negative representing live cells. Data are representative plots of three independent experiments.

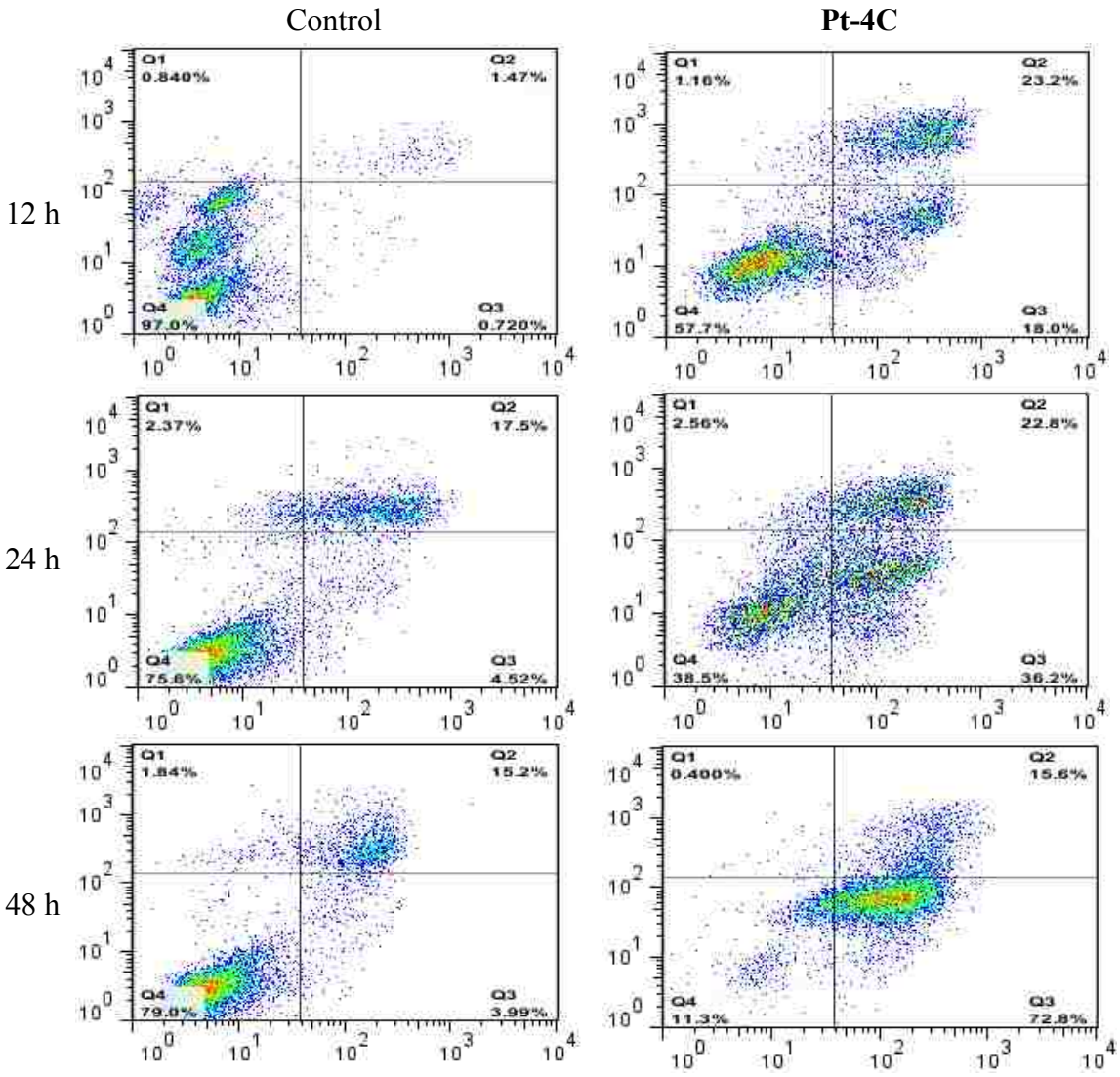

Figure 2 – 9. MCF-7 Flow with Annexin V/PI staining. Cells were treated with EC_{50} **Pt-4C** for 1 h then harvested 12, 24, and 48 h after treatment. Cells were stained with Annexin V and PI and analyzed with a flow cytometer. Q1 is PI positive representing necrotic cells, Q2 is Annexin V/PI positive representing late apoptotic/necrotic cells, Q3 is Annexin V positive and PI negative representing early apoptotic cells, and Q4 is Annexin V/PI negative representing live cells. Data are representative plots of three independent experiments.

indicating a decrease in live cells and an increased in early apoptotic and late apoptotic/necrotic cells (Fig. 2-8). The percentages of cells in Q2 and Q3 (early apoptotic and late apoptotic/necrotic cells) were higher in the 24 h group than the 12 h group and the 48 h group had values similar to the 24 h group. MCF-7 cells treated with **Pt-4C** had increased early apoptotic and late apoptotic/necrotic cells (Q2 and Q3) in the 12 and 24 h groups, but only increased early apoptotic (Q3) cells in the 48 h group (Fig. 2-9). The increase in early apoptotic and late apoptotic/necrotic cells (Q2 and Q3 populations) was accompanied by a corresponding decrease in live cells (the Q4 population). These results demonstrate that **Pt-4C** induces apoptosis in these cell lines and some necrotic responses were also observed.

2.4.2.2.3 Analysis of morphological changes by fluorescence microscopy and DNA laddering

The effect of **Pt-4C** in A549 cells was examined further by DNA laddering and fluorescence microscopy. One of the features of apoptosis is cleavage of DNA into fragments with increments of 180–200 bp which can be detected as a DNA ladder when separated on an agarose gel. To observe this phenomenon, A549 cells were treated with 10–35 μM **Pt-4C** for 1 h and the DNA was extracted 24 h post treatment. The DNA was separated on an agarose gel to detect a ladder pattern. The DNA of control cells did not have the typical ladder pattern of apoptotic cells, whereas, the DNA of cells treated with **Pt-4C** at concentrations ranging from 10–35 μM shows the laddering pattern (Fig. 2-10). For analysis of cells using fluorescence microscopy, the cells were treated with the EC_{50} concentration of **Pt-4C** for 1 h and then stained with Hoechst (Ho) and PI. PI is

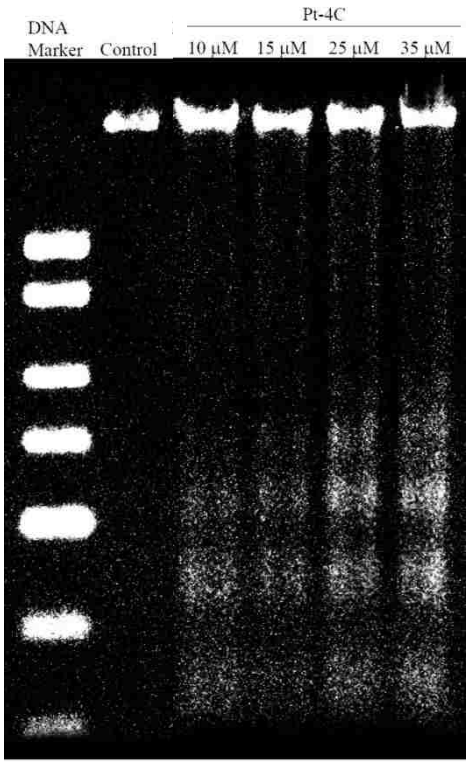

Figure 2 – 10. A549 apoptotic DNA laddering. Cells were treated for 1 h with varying concentrations of **Pt-4C** and DNA was extracted 24 h post treatment.

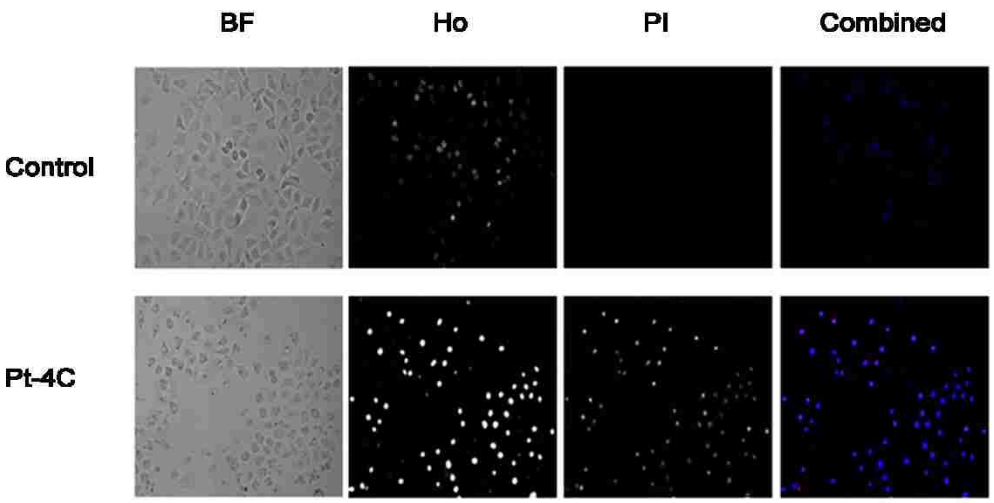

Figure 2 – 11. A549 fluorescence microscopy. Cells were stained with Hoechst (Ho) and propidium iodide (PI) 2 h post treatment with EC_{50} concentration of the **Pt-4C** for 1 h. Bright fluorescence indicates positive staining. PI stains necrotic cells and Ho stains live and apoptotic cells, with intense bright fluorescence indicating apoptotic cells. Images are representative of at least two independent experiments.

membrane impermeable and only stains cells with membrane damage. Ho is membrane permeable and can stain both live cells and cells undergoing apoptosis; cells with intense bright fluorescence indicate apoptotic cells. To determine the effect of **Pt-4C** in A549, the cells were treated with the EC_{50} concentration of **Pt-4C** for 1 h, and then 2 h post treatment the cells were stained with Ho and PI. Control cells show some positive Ho staining, but no positive staining (Fig. 2-11). Cells treated with **Pt-4C** had more Ho and PI positive staining than control; many Ho positive cells were also PI positive. Additionally, bright field (BF) images showed altered cell morphology (shrunken and rounding up) in **Pt-4C** treated cells compared to control. These results confirm that **Pt-4C** induces apoptosis in A549 cells and are consistent with the mode of cell death induced by other Pt(II) complexes reported in the literature.[17,19,20]

2.4.2.3 *In vivo* toxicity

Pt-4C was sent to Molecular Diagnostic Services Laboratory (San Diego, CA) for *in vivo* toxicity testing in *C57BL/6* female mice. The animals were divided into three groups: group one had three animals and received one intraperitoneal (IP) injection of **Pt-4C** at a dose of 12.5 mg kg^{-1} d^{-1}; group two had three animals and received a dose of 12.5 mg kg^{-1} d^{-1} for three days; group three had one animal and was the vehicle control. One animal from group two exhibited slight lethargy after the first injection, but quickly recovered 2 h after the injection. All animals survived during the study period of 7 d post injection and no abnormal observations were noted indicating that this compound is not toxic in an animal model.

2.5 Conclusions

A series of platinum(II) complexes containing 2,2′-bipyridyl with alkoxy substituents of increasing carbon chain length at the 4,4′ positions were successfully synthesized. The direct two step procedure generally gave moderate to high yields and did not require expensive fluorinated reagents or the use of a potentially dangerous strong base. These complexes were demonstrated to have a concentration and time-dependent effect on various cancer cells. Furthermore, a structure-activity relationship was also observed. Various methods employed indicate that one of the complexes, **Pt-4C**, induced apoptosis in A549, DU145, and MCF-7 cells. It is likely that the other Pt-complexes synthesized also induce cell death through apoptosis due to their similar chemical structures. All of these exciting results demonstrate the potential utilization of our platinum complexes as chemotherapeutic drugs in the treatment of a broad range of cancers. However, further studies are needed to evaluate the prospective translation of these compounds into clinical use.

Understanding the cellular effects of a drug is important when developing treatment strategies and predicting possible side effects. There is still much to be explored about the biological effects of cisplatin; however, it is known that cisplatin binds to DNA and forms adducts that damage the DNA and activates the apoptotic pathway.[1,2,38–40] The newly synthesized Pt(II) complexes have a platinum center that is similar to cisplatin and may bind to DNA to cause damage in a mechanism analogous to cisplatin. Differences in cellular uptake and DNA binding may underlie the pronounced improvement of the **Pt-4C** cytotoxicity profile compared to cisplatin.

Determination of the mechanism of action requires an examination of the signaling events that occur. Since **Pt-4C** induces apoptosis in A549, DU145 and MCF-7 cells, it is necessary to investigate the involvement of proteins in the apoptotic pathway. A protein that is of interest is p53, a tumor suppressor protein that is involved in many processes including activation of DNA repair, cell cycle arrest, and initiation of apoptosis.[41] The role of p53 in CDDP treated cells varies depending on the cell line and duration of treatment.[42–45] Thus, it is likely that p53 expression is affected by treatment with **Pt-4C** and the other Pt-complexes. Interestingly, we have found that **Pt-4C** caused a transient dose-dependent induction of p53 expression in A549 cells, which is currently under investigation in our laboratory. Additionally, mitogen-activated protein kinases (ERK, JNK, p38) are involved in signaling for cell survival and apoptosis.[42] Generally, ERK has a role in cell proliferation and development, whereas JNK and p38 have roles in apoptotic signaling. These proteins have been associated with CDDP treatment; however, similar to p53, their roles also vary depending on the cell line and duration of treatment.[42,45–47] Thus, it will be interesting to examine the roles of these proteins in response to treatment with **Pt-4C**.

2.6 Acknowledgements

This project was supported by grants from the National Center for Research Resources (5P20RR016464-11) and the National Institute of General Medical Sciences (8P20GM103440-11). B.L.S. acknowledges National Institute of Health grant number R15NS051198-01A1S1. P.K.B. acknowledges the University of Nevada Las Vegas (UNLV) for New Investigation Award (NIA), Planning Initiative Award (PIA), and Applied Research Initiative (ARI) grants, and the donors of the Petroleum Research Fund

(PRF# 35903-B7), administered by the American Chemical Society, and an award (CCSA# CC5589) from Research Corporation for the support of this research. This project was also supported in part by the University of Nevada Las Vegas Graduate and Professional Student Association and the College of Sciences.

2.7 References

1. F. Arnesano and G. Natile. Mechanistic insight into the cellular uptake and processing of cisplatin 30 years after its approval by FDA. *Coord. Chem. Rev.* **2009**, *253*, 2070-2081.
2. R. C. Todd and S. J. Lippard. Inhibition of transcription by platinum antitumor compounds. *Metallomics* **2009**, *1*, 280-291.
3. A. M. Florea and D. Busselberg. Cisplatin as an Anti-Tumor Drug: Cellular Mechanisms of Activity, Drug Resistance and Induced Side Effects. *Cancers* **2011**, *3*,1351-1371.
4. Y.-P. Ho, S. C. F. Au-Yeung and K. K. W. To. Platinum-based anticancer agents: Innovative design strategies and biological perspectives. *Med. Res. Rev.* **2003**, *23*, 633-655.
5. A. S. Abu-Surrah and M. Kettunen. Platinum group antitumor chemistry: design and development of new anticancer drugs complementary to cisplatin. *Curr. Med. Chem.* **2006**, *13*, 1337-1357.
6. I. Kostova. Platinum complexes as anticancer agents. *Recent Pat. Anti-Cancer Drug Discovery* **2006**, *1*, 1-22.
7. X. Wang and Z. Guo. Targeting and delivery of platinum-based anticancer drugs. *Chem. Soc. Rev*. **2013***, 42,* 202-224.
8. C. A. Rabik and M. E. Dolan. Molecular mechanisms of resistance and toxicity associated with platinating agents. *Cancer Treat. Rev.* **2007**, *33*, 9-23.
9. F. Blau. Die destillation pyridinmonocarbonsaurer salze. *Ber. Dtsch. Chem. Ges.* **1888**, *21*, 1077-1088.
10. G. R. Newkome, A. K. Patri, E. Holder and U. S. Schubert. Synthesis of 2,2′-Bipyridines: Versatile Building Blocks for Sexy Architectures and Functional Nanomaterials. *Eur. J. Org. Chem.* **2004**, *2004*, 235-254.
11. C. Kaes, A. Katz and M. W. Hosseini. Bipyridine: the most widely used ligand. A review of molecules comprising at least two 2,2′-bipyridine units. *Chem. Rev.* **2000**, *100*, 3553-3590.

12. N. A. Jones, J. W. Antoon, A. L. Bowie, J. B. Borak and E. P. Stevens. Synthesis of 2,2′-Bipyridyl-Type Compounds via the Suzuki-Miyaura Cross-Coupling Reaction. *J. Heterocycl. Chem.* **2007**, *44*, 363-368.
13. K. H. Puthraya, T. S. Srivastava, A. J. Amonka, M. K. Adwankar and M. P. Chitnis. Some mixed-ligand palladium(II) complexes of 2,2′-bipyridine and amino acids as potential anticancer agents. *J. Inorg. Biochem.* **1985**, *25*, 207-215.
14. K. H. Puthraya, T. S. Srivastava, A. J. Amonka, M. K. Adwankar and M. P. Chitnis. Some potential anticancer palladium(II) complexes of 2,2′-bipyridine and amino acids. *J. Inorg. Biochem.* **1986**, *265*, 45-54.
15. G. Cristalli, P. Franchetti, E. Nasini, S. Vittori, M. Grifantini, A. Barzi, E. Pepri and S. Ripa. Metal(II) complexes of 2,2′-bipyridyl-6-carbothioamide as anti-tumor and anti-fungal agents. *Eur. J. Med. Chem.* **1988**, *23*, 301-305.
16. N. Garelli, P. Vierling, J. L. Fischel and G. Milano. Cytotoxic activity of new amphiphilic perfluoroalkylated bipyridine platinum and palladium complexes incorporated into liposomes. *Eur. J. Med. Chem.* **1993**, *28*, 235-242.
17. K. E. Elwell, C. Hall, S. Tharkar, Y. Giraud, B. L. Bennet, C. Bae and S. W. Carper. A fluorine containing bipyridine cisplatin analog is more effective than cisplatin at inducing apoptosis in cancer cell lines. *Bioorg. Med. Chem.* **2006**, *14*, 8692-8700.
18. H. Mansouri-Torshizi, M. I-Moghaddam, A. Divsalar and A.-A. Saboury. 2,2′-Bipyridinebutyldithiocarbamatoplatinum(II) and palladium(II) complexes: synthesis, characterization, cytotoxicity, and rich DNA-binding studies. *Bioorg. Med. Chem.* **2008**, *16*, 9616-9625.
19. V. Vo, Z. G. Kabuloglu-Karayusuf, S. W. Carper, B. L. Bennett and C. Evilia. Novel 4,4′-diether-2,2′-bipyridine cisplatin analogues are more effective than cisplatin at inducing apoptosis in cancer cell lines. *Bioorg. Med. Chem.* **2010**, *18*, 1163-1170.
20. T. T. Chang, S. V. More, N. Lu, J. W. Jhuo, Y. C. Chen, S. C. Jao and W. S. Li. Polyfluorinated bipyridine cisplatins manipulate cytotoxicity through the induction of S-G2/M arrest and partial intercalation mechanism. *Bioorg. Med. Chem.* **2011**, *19*, 4887-4894.

21. H. Mansouri-Torshizi, M. Eslami-Moghadam, A. Divsalar and A.-A. Saboury. DNA-Binding studies of some potential antitumor 2,2′–bipyridine Pt(II)/Pd(II) complexes of piperidinedithiocarbamate. Their synthesis, spectroscopy and cytotoxicity. *Acta Chim. Slov.* **2011**, *58*, 811-822.
22. N. Ferri, S. Cazzaniga, L. Mazzarella, G. Curigliano, G. Lucchini, D. Zerla, R. Gandolfi, G. Facchetti, M. Pellizzoni and I. Rimoldi. Cytotoxic effect of (1-methyl-1H-imidazol-2-yl)-methanamine and its derivatives in Pt^{II} complexes on human carcinoma cell lines: a comparative study with cisplatin. *Bioorg. Med. Chem.* **2013**, *21*, 2379-2386.
23. B. L. Bennett, K. A. Robins, R. Tennant, K. Elwell, F. Ferri, I. Bashta and G. Aguinaldo. Fluorous modification of 2,2′-bipyridine. *J. Fluorine Chem.* **2006**, *127*, 140-145.
24. J. A. Schwindeman, C. J. Woltermann and R. J. Letchford. Safe handling of organolithium compounds in the laboratory. *Chem. Health Saf.* **2002**, *9*, 7-11.
25. N. Lu, Y.-C. Lin, J.-Y. Chen, T.-C. Chen, S.-C. Chen, Y.-S. Wen and L.-K. Liu. Synthesis, structure and reactivity of novel palladiumdichloride-2,2′-bipyridine with 4,4′-bis(fluorous-ponytail). *Polyhedron* **2007**, *26*, 3045-3053.
26. Y.-R. Hong and C. B. Gorman. Synthetic Approaches to an Isostructural Series of Redox-Active, Metal Tris(bipyridine) Core Dendrimers. *J. Org. Chem.* **2003**, *68*, 9019-9025.
27. G. Maerker and F. H. Case. The Synthesis of Some 4,4′-Disubstituted 2,2′-Bipyridines. *J. Am. Chem. Soc.* **1958**, *80*, 2745-2748.
28. Y.-J. Kwark. Alkoxy bipyridine ligands for ATRP of styrene and methyl methacrylate. *Macromol. Res.* **2009**, *17*, 218-220.
29. J. Skarzewski and J. Mlochowski. New Complexing Surfactants. Syntheses of 4-Alkoxypyridines and Bipyridines. *Heterocycles* **1979**, *12*, 1403-1406.
30. E. J. L. McInnes, R. D. Farley, C. C. Rowlands, A. J. Welch, L. Rovatti and L. J. Yellowlees. On the electronic structure of $[Pt(4,4'\text{-}X_2\text{-bipy})Cl_2]^{0/-/2-}$: An electrochemical and spectroscopic (UV/Vis, EPR, ENDOR) study. *J. Chem. Soc., Dalton Trans.* **1999**, 4203-4208.

31. R. J. Allenbaugh, C. K. Schauer, A. Josey, J. D. Martin, D. V. Anokhin and D. A. Ivanov. Effect of Axial Interactions on the Formation of Mesophases: Comparison of the Phase Behavior of Dialkyl 2,2′-bipyridyl-4,4′-dicarboxylate Complexes of Pt(II), Pt(IV), and Pt(II)/Pt(IV) Molecular Alloys. *Chem. Mater.* **2012**, *24*, 4517-4530.
32. M. D. Hall, S. Amjadi, M. Zhang, P. J. Beale and T. W. Hambley. The mechanism of action of platinum(IV) complexes in ovarian cancer cell lines. *J. Inorg. Biochem.* **2004**, *98*, 1614-1624.
33. S. P. Oldfield, M. D. Hall and J. A. Platts. Calculation of lipophilicity of a large, diverse dataset of anticancer platinum complexes and the relation to cellular uptake. *J. Med. Chem.* **2007**, *50*, 5227-5237.
34. S. Elmore. Apoptosis: A Review of Programmed Cell Death. *Toxicol. Pathol.* **2007**, *35*, 495-516.
35. K. M. Henkels and J. J. Turchi. Cisplatin-induced apoptosis proceeds by caspase-3-dependent and -independent pathways in cisplatin-resistant and -sensitive human ovarian cancer cell lines. *Cancer Res.* **1999**, *59*, 3077-3083.
36. X. Wang, J. L. Martindale and N. J. Holbrook. Requirement for ERK activation in cisplatin-induced apoptosis. *J. Biol. Chem.* **2000**, *275*, 39435-39443.
37. S. Al-Bahlani, M. Fraser, A. Y. C. Wong, B. S. Sayan, R. Bergeron, G. Melino and B. K. Tsang. P73 regulates cisplatin-induced apoptosis in ovarian cancer cells via a calcium/calpain-dependent mechanism. *Oncogene* **2011**, *30*, 4219-4230.
38. H. Huang, J. Woo, S. Ally and P. Hopkins. DNA-DNA interstrand cross-linking by cis-diamminedichloroplatinum(II): N7(dG)-to-N7(dG) cross-linking at 5′d(GC) in synthetic oligonucleotides. *Bioorg. Med. Chem.* **1995**, *3*, 659-669.
39. E. R. Jamieson and S. J. Lippard. Structure, recognition, and processing of cisplatin-DNA adducts. *Chem. Rev.* **1999**, *99*, 2467-2498.
40. J. Goodisman, D. Hagrman, K. A. Tacka and A. K. Souid. Analysis of cytotoxicities of platinum compounds. *Cancer Chemother. Pharmacol.* **2006**, *57*, 257-267.
41. A. V. Gudkov and E. A. Komarova. Dangerous habits of a security guard: the two faces of p53 as a drug target. *Hum. Mol. Genet.* **2007**, *16*, 67-72.
42. A. Basu and S. Krishnamurthy. Cellular Responses to Cisplatin-Induced DNA Damage. *J. Nucleic Acids* **2010**, *2010*, 201367.

43. M. L. Duarte, E. de Moraes, E. Pontes, L. Schluckebier, J. L. de Moraes, P. Hainaut and C. G. Ferreira. Role of p53 in the induction of cyclooxygenase-2 by cisplatin or paclitaxel in non-small cell lung cancer cell lines. *Cancer Lett.* **2009**, *279*, 57-64.
44. E. G. Konstantakou, G. E. Voutsinas, P. K. Karkoulis, G. Aravantinos, L. H. Margaritis and D. J. Stravopodis. Human bladder cancer cells undergo cisplatin-induced apoptosis that is associated with p53-dependent and p53-independent responses. *Int. J. Oncol.* **2009**, *35*, 401-416.
45. Z. Z. Wu, N. K. Sun, K. Y. Chien and C. C. K. Chao. Silencing of the SNARE protein NAPA sensitizes cancer cells to cisplatin by inducing ERK1/2 signaling, synoviolin ubiquitination and p53 accumulation. *Biochem. Pharmacol.* **2011**, *82*, 1630-1640.
46. T. Torigoe, H. Izumi, H. Ishiguchi, Y. Yoshida, M. Tanabe, T. Yoshida, T. Igarashi, I. Niina, T. Wakasugi, T. Imaizumi, Y. Momii, M. Kuwano and K. Kohno. Cisplatin resistance and transcription factors. *Curr. Med. Chem.: Anti-Cancer Agents* **2005**, *5*, 15-27.
47. C. St. Germain, N. Niknejad, L. Ma, K. Garbuio, T. Hai and J. Dimitroulakos. Cisplatin induces cytotoxicity through the mitogen-activated protein kinase pathways and activating transcription factor 3. *Neoplasia* **2010**, *12*, 527-538.

CHAPTER 3

CHARACTERIZATION OF THE DNA BINDING AND MAPK PROTEIN ACTIVATION ACTIVITIES OF PT(II) COMPLEXES CONTAINING 4,4′-DIALKOXY-2,2′-BIPYRIDINE LIGANDS

3.1 Abstract

The study of the anti-proliferative activities of our previously reported novel platinum(II) complexes containing 4,4′-dialkoxy-2,2′-bipyridine ligands were expanded to various lung, prostate, and breast cancer cell lines to examine differential responses to these potential cancer drugs. The EC_{50} values obtained from MTS assays demonstrate a generally improved cytotoxicity profile compared to cisplatin and carboplatin in all cell lines. One of the complexes, **Pt(II)-4C**, was studied further for its ability to interact with DNA and activation of important cell signaling pathways such as p53 and mitogen-activated protein kinase (MAPK) cascades.

UV-Vis analysis with calf thymus and gel electrophoresis with plasmid pBR322 DNA indicated that **Pt(II)-4C** can bind to DNA and cause unwinding of circular DNA. Moreover, results from inductively coupled plasma-atomic emission spectroscopy (ICP-AES) suggested that **Pt(II)-4C** can be taken up by A549 lung cancer cells and bind to intracellular DNA.

Measurement of protein expression by immunofluorescence microscopy, flow cytometric immunofluorescence, and western blotting show increased p53 expression in **Pt(II)-4C** treated A459 cells and co-treatment with the p53 inhibitor, PFTα, resulted in increased cell viability compared to **Pt(II)-4C** treatment alone. MAPK (JNK, ERK, and

p38) activation was also observed in A549 and DU145 (human prostate cancer) cells treated with **Pt(II)-4C**. Activation of MAPK was accompanied by phosphorylation of histone H2AX (γH2AX). Treatment of A549 and DU145 cells with **Pt(II)-4C** in the presence of MAPK inhibitors resulted in reduced levels of γH2AX. Furthermore, treatment of these two cell lines with **Pt(II)-4C** in the presence of the JNK and p38 inhibitors resulted in increased cell viability compared to **Pt(II)-4C** treatment alone. Treatment of A549 with **Pt(II)-4C** in the presence of the ERK inhibitor resulted in decreased cell viability compared to **Pt(II)-4C** treatment alone, but no effect was observed in DU145 cells. These results indicate that JNK and p38 may be involved in cell death signaling in response to **Pt(II)-4C** treatment.

3.2 Introduction

A chemotherapeutic drug that is commonly prescribed for the treatment of many cancers is cisplatin (CDDP), a square-planar Pt(II) compound. Together with its two analogues, carboplatin and oxaliplatin, platinum drugs constitute about 50% of all cancer chemotherapeutic regimens. However, treatment with these platinum drugs is accompanied by severe side effects such as nephrotoxicity, neuropathy, ototoxicity, and myelosuppression. Additionally, other drawbacks such as intrinsic or acquired resistance and limited activity against some major types of cancer have impeded the clinical utility of these drugs.[1–5] Motivated to overcome these drawbacks, we have previously reported on the synthesis of a series of platinum(II) [Pt(II)] complexes containing 4,4′-dialkoxy-2,2′-bipyridine ligands (with the dialkoxy having one to six carbons) and their anti-proliferative activity against the A549 lung cancer cell line (Chapter 2).[6] The improved anti-proliferative activity of these complexes compared to cisplatin warrant further

investigation of these compounds. Since only one of the complexes was tested in other cancer cells, it is necessary to expand the study of all the complexes in various cancer cell types to have a better indication of their effectiveness in different types of cancers. Furthermore, an understanding of the signaling pathways activated by these platinum complexes will provide the foundation necessary for developing strategies to utilize these compounds for the treatment of cancer. Thus, we seek to determine the signaling pathways activated within cancer cells in response to treatment by these novel platinum complexes.

The cytotoxic effect of cisplatin is mainly due to the formation of DNA adducts even though only a small percentage (5–10%) of the intracellular cisplatin concentration is found in the nucleus.[7] Cisplatin-induced DNA damage elicits various cellular responses such as cell cycle arrest, activation of repair mechanisms, stress responses, and cell death pathways. The two pathways that are of interest are the p53 and the mitogen-activated protein kinase (MAPK) cascades.

The p53 protein is a tumor suppressor that is involved in many processes including activation of DNA repair, cell cycle arrest, and initiation of apoptosis.[8] During normal cellular conditions, p53 has a short half-life and is kept at a low level by the Mdm2 ubiquitin ligase. However, the interaction of p53 with Mdm2 decreases when stimulated by stress signals, which allows for the accumulation and phosphorylation of p53.[8,9] Activated p53 can then interact with other proteins such as p21 (cell cycle protein) or Bax (apoptotic protein)[9] to culminate in various cellular outcomes such as cell survival and death.

Loss of p53 function can occur due to mutations in about 50% of all cancers.[10] The drug resistance of many cancers has been attributed to having mutant p53 and the differential p53 status has been taken advantage of for the development of treatment methods that are more specific by targeting p53.[11] Current data from the literature indicate that the role of p53 in cisplatin treated cells varies depending on the cell line and duration of treatment. In some reports, cisplatin-induced apoptosis is described as requiring functional p53; however, the opposite is reported by some authors indicating that cells with wild-type p53 are resistant to cisplatin treatment and sensitivity is achieved by inhibition of its expression.[7,9]

The MAPKs are proteins that are activated by various stimuli to regulate cellular processes such as proliferation, differentiation, movement, survival, and programmed cell death.[7,9] Three major MAPK members are extracellular signal-regulated kinases (ERK), c-Jun N-terminal kinases (JNK), and p38 kinases. Generally, ERK has a role in cell proliferation and development; however, JNK and p38 have roles in apoptotic signaling, inflammatory responses, and protective responses.[7] These proteins are activated through phosphorylation by upstream kinases and, in turn, phosphorylate downstream targets to activate them. ERK, JNK, and p38 have all been demonstrated to be activated by cisplatin; however, similar to p53, their roles also vary between different cell lines and duration of treatment. In some studies, in accordance with their roles, ERK activation protects cells from apoptosis, whereas, activation of JNK and p38 leads to apoptotic cell death; on the other hand, some studies demonstrated the reverse.[7,9,12,13]

Herein, the anti-proliferative activity of these complexes in various lung, prostate, and breast cancer cell lines are described. Additionally, **Pt(II)-4C** interaction with DNA and its effect on p53 and MAPK signaling are investigated.

3.3 Experimental

3.3.1 General

All general chemicals and reagents were purchased from common commercial vendors (Sigma-Aldrich, TCI, Alfa-Aesar, or Acros) unless otherwise noted. Pt(II) complexes were synthesized as described in Chapter 2. Minimum essential medium (MEM), fetal bovine serum (FBS), phosphate buffered saline (PBS), trypsin-EDTA, and penicillin-streptomycin were purchased from Life Technologies (Carlsbad, CA). The RPMI 1640 medium was purchased from ATCC (Manassas, VA). Cisplatin, carboplatin, HEPES, albumin from bovine serum (BSA), Tris-HCl, Trizma Base, and dimethyl sulfoxide (DMSO) were purchased from Sigma-Aldrich.

3.3.2 Cell culture

Human breast (HCC38, MCF-7, MDA-MB-231, SK-BR-3, T-47D, and ZR-75-1), lung (A549 and H520), and prostate (DU145 and PC-3) cancer cell lines were obtained from American Culture Type Collection (ATCC). The A549, HCC38, MCF-7, MDA-MB-231, SK-BR-3, T-47D, and ZR-75-1 cells were grown in MEM supplemented with 10% FBS, 25 mM HEPES buffer (pH 7.4), penicillin (100 U mL^{-1}) and streptomycin (100 μg mL^{-1}). The H520, DU145, and PC-3 cell lines were grown in RPMI-1640 supplemented with 10% FBS, 25 mM HEPES buffer (pH 7.4), penicillin (100 U mL^{-1}) and streptomycin (100 μg mL^{-1}). All cell lines were maintained at 37 °C in a humidified, 5% CO_2 atmosphere.

3.3.3 Cell viability assay

Cells were cultured at a density of 2–3.5 x 10^3 cells per well in flat bottomed 96-well plates in 100 μL of complete growth medium and incubated for 2 d to reach ~ 50% confluence. The cells were then treated with solvent or the appropriate drugs (CDDP stock was dissolved in 0.15 M NaCl, carboplatin stock was dissolved in 5% glucose, synthesized Pt(II) complexes were dissolved in DMSO) for 1 h, washed three times with 100 μL PBS, and incubated in 100 μL of fresh medium. After 2 d, the medium was replaced with 120 μL of medium containing CellTiter 96® Aq_{ueous} One Solution Reagent (MTS reagent) (Promega, Madison, WI). The cells were incubated at 37 °C for 4 h and the cell viability was determined by measuring the absorbance at 490 nm using a Tecan Infinite M1000 microplate reader. The 48 h treatment was done in a similar method, except the cells were not washed after treatment and the MTS reagent was immediately added. Viability of treated groups was calculated as a percent of control and graphed with GraphPad Prism.

The experiment was also done similarly for studies with p53 or MAPK inhibitors. The cells were pre-treated with pifithrin-α (PFTα) (Sigma-Aldrich #P4359) SB202190 (p38 inhibitor, Sigma-Aldrich #S7067), PD-098,059 (ERK inhibitor, Sigma-Aldrich #P215), or SP600125 (JNK inhibitor, Sigma-Aldrich #S5567) for the indicated time, followed by co-treatment with the indicated concentrations of **Pt(II)-4C**, and post-treatment with the inhibitors.

3.3.4 UV-Vis spectroscopy

The ability of **Pt(II)-4C** to bind DNA was determined analyzing its interaction with calf thymus DNA (CT-DNA) with UV-Vis spectroscopy. CT-DNA was purchased

from Life Technologies (#15633-019, 10 mg/mL in Dnase, Rnase free water) and the DNA concentration per nucleotide was determined from the UV absorbance at 260 nm using the molar extinction coefficient ε_{260} = 6600 $M^{-1}cm^{-1}$. CT-DNA (100 μM) was incubated with 0–140 μM of **Pt(II)-4C** (stock solution was dissolved in DMSO) in 10 mM Tris-HCl (pH 7.2) containing 10% DMSO for 1 or 24 h at 37 °C and the absorbance was measured with the NanoDrop ND-1000 UV-Vis Spectrophotometer (Thermo Scientific). **Pt(II)-4C** solutions of each concentration in the same buffer were used as blanks to eliminate the absorption of the **Pt(II)-4C** by itself. The study was also done by using a constant concentration of **Pt(II)-4C** (100 μM) and increasing the concentration of CT-DNA (0–100 μM). The same buffer system was used and samples with only CT-DNA at each concentration was used as blanks to eliminate the absorbance from the CT-DNA.

3.3.5 Agarose gel electrophoresis

A solution of pBR322 plasmid DNA (0.125 μg) (Life Technologies #15367-014, supplied at 0.25 μg/μl in 10 mM Tris-HCl (pH 7.4), 5 mM NaCl, 0.1 mM EDTA) was mixed with increasing concentrations (0–100 μM) of **Pt(II)-4C** and brought to 25 μL with TE buffer (Tris-EDTA) containing 25% DMSO. Cisplatin was used as a control. The samples were incubated at 37 °C in the dark for 24 h. After incubation, 5 μL of 6X DNA loading buffer (0.25% bromophenol blue, 0.25% Orange G, 30% glycerol) was added to each sample and 25 μL was electrophoresed through a 1% agarose gel immersed in 1X TBE buffer (2 mM EDTA, pH 8.0; 89 mM Tris; 89 mM Boric Acid) for 50 min at 100 V. Finally, the gel was stained with ethidium bromide (EB) (1 μg mL^{-1}) in the dark

for 30 min, followed by visualization on a Bio-Rad ChemiDoc XRS+ imaging system with a UV-Vis transilluminator.

3.3.6 Cellular uptake and intracellular DNA binding of platinum

Cells were seeded in 100 mm culture dishes and incubated at 37 °C until ~70-80% confluent. The cells were treated with the indicated concentrations of **Pt(II)-4C** for 4 h and harvested by trypsinization. The cells were washed twice with 10 mL of PBS, counted, and pelleted by centrifugation. For the cellular uptake study, the cell pellet was stored at -20 °C until analysis.

For intracellular DNA binding analysis, the cell pellet was resuspended in 500 µL of lysis buffer (100 mM Tris-HCl pH 8.0, 5 mM EDTA, 1% SDS, 0.5% Triton X-100, 200 mM NaCl, 100 µg mL^{-1} proteinase K). After 2 h of incubation at 56 °C, 4 µL of a 0.2 mg mL^{-1} RNAse A solution was added and the sample was incubated at room temperature for 15 min. The DNA was precipitated by addition of 2-propanol (500 µL), mixed by inversion, and stored overnight at -20 °C. The DNA was pelleted by centrifugation at 16 000 × g for 15 min at 4 °C. The pellet was washed with 70% ethanol and air dried by inverting the tube on a tissue for 10 min. The DNA was dissolved in 150 µL of nuclease-free water and the DNA concentration was determined with the NanoDrop ND-1000 Spectrophotometer. The samples were stored at -20 °C until analysis

For platinum analysis, 200 µL of high purity concentrated HNO_3 was added to the cell pellet and DNA samples, and the contents were transferred to borosilicate glass tubes. After heating at 80 °C for 2 h to digest the samples, they were diluted with ultra-pure water to a final concentration of 1% HNO_3. The samples were filtered with 0.45 µm

syringe filters and analyzed by inductively coupled plasma-atomic emission spectrometry (ICP-AES). Platinum standards (0-50 μM) were used as an external calibration curve to calculate the amount of platinum in the samples.

3.3.7 Western blot analysis

Cells were seeded in 100 mm dishes and grown to subconfluence. The cells were treated with increasing concentration of **Pt(II)-4C** for the indicated time, harvested, and collected. The cells were lysed by vigorously vortexing in 300 μL M-PER lysis buffer (Thermo Scientific # 78503) containing 2X phosphatase inhibitor cocktail (Pierce #88667), 2X protease inhibitor cocktail (Thermo Scientific # 78410), 1X EDTA (Thermo Scientific # 78410). The lysate was centrifuged at 14 000 × g for 15 min at 4 °C and supernatant was collected. The protein concentration was determined using the bicinchoninic acid (BCA) protein assay (Pierce # PI-23235) by following the manufacturer's instructions. The cell lysate was mixed with 1X LDS sample buffer (Life Technologies #B0007) and 1X DTT (Life Technologies #B0009), placed in boiling water for 5 min, and 30 μg of protein was separated on a Novex Bolt 4-12% Bis Tris Plus gel (Life Technologies # BG04125BOX) with Bolt MES SDS Running Buffer (Life Technologies # B0002). The protein was transferred onto a nitrocellulose membrane (iBlot® Transfer Stack, Life Technologies # IB301001) using the iBlot® Gel Transfer Device. The membrane was treated with SuperSignal Western Blot Enhancer Antigen Pretreatment Solution (Thermo Scientific # 46640) for 10 min, washed according to the manufacture's instruction, blocked with 5% bovine serum albumin (BSA) in 1X Tris-buffered saline containing 0.05% Tween-20 (TBST) buffer for 1 h at room temperature. After rinsing with TBST, the membrane was incubated with the appropriate primary

antibody (dilution in SuperSignal Western Blot Enhancer Primary Antibody Diluent (Thermo Scientific # 46640)) at 4 °C overnight. After washing with TBST, the membrane was incubated with the appropriate HRP-conjugated secondary antibody (diluted1:2000 in 5% BSA) for 1 h at room temperature. Protein bands were detected with Clarity Western ECL Substrate (Bio-Rad # 170-5061) and imaged on the Bio-Rad ChemiDoc XRS+.

SAPK/JNK Antibody (#9252), Phospho-SAPK/JNK (Thr183/Tyr185) Antibody (#9251), p38 MAPK Antibody (#9212), Phospho-p38 MAPK (Thr180/Tyr182) Antibody (#9211), p44/42 MAPK (Erk1/2) Antibody (#9102), Phospho-p44/42 MAPK (Erk1/2) (Thr202/Tyr204) Antibody (#9101) were purchased from Cell Signaling Technologies. B-Actin Antibody (C4) (#sc-47778) and p53 Antibody (DO-1) (#sc-126) were purchased from Santa Cruz Biotechnology.

3.3.8 Immunofluorescence microscopy

Cells (125,000) were seeded into 35 mm dishes containing #1.5 glass coverslips and incubated for 48 h at 37 °C. The cells were treated with the indicated concentration of **Pt(II)-4C** (or co-treated with the MAPK inhibitors) for the indicated time at 37 °C, washed 2X with PBS, and fixed with 4% formaldehyde for 15 min at room temperature. The cells were washed 3X with PBS, permeabilized with 0.2% Triton X for 5 min at room temperature, washed 3X with PBS, and blocked with 5% BSA in PBS for 1 h at 37 °C. After blocking, the cells were washed 2X with PBS and incubated with mouse anti-phospho-JNK (Santa Cruz Biotechnology #sc-6254), anti-phospho-ERK1/2 (Santa Cruz Biotechnology #sc-81492), anti-phospho-p38 (Santa Cruz Biotechnology #sc-7973), anti-phospho-Histone H2A.X (Ser139) (EMD Millipore #05-636), p53 Antibody (DO-1)

(Santa Cruz Biotechnology #sc-126) primary antibodies (1:50 dilution in 5% goat serum) at 4 °C overnight. The cells were washed 4X for 5 min each on a rocker, followed by incubation with Alexa-Fluor 488 goat anti-mouse secondary antibody (Life Technologies #A11029) [1:400 dilution in 5% goat serum (Santa Cruz Biotechnology #sc-2043)] at room temperature 30 min. The cells were washed 4X for 5 min each on a rocker, briefly rinsed with ultrapure H_2O, and mounted on glass slides with Prolong Gold Antifade Reagent with DAPI (Life Technologies #P36935). Images were taken with the Nikon A1R confocal laser scanning microscopy system (CLSM) mounted on a Nikon Eclipse Ti.

3.3.9 Flow cytometric immunofluorescence

Cells (100,000) were seeded in 60 mm dishes and grown for 3 d at 37 °C in a humidified, 5% CO_2 atmosphere. The cells were treated with the indicated concentration of **Pt(II)-4C** for the indicated time and harvested. The cells were fixed by addition of 16% formaldehyde to a final concentration of 4% and incubated at room temperature for 10 min. The cells were pelleted and the supernatant was discarded. The cells were permeabilized by resuspension in 500 μL of ice-cold methanol and incubated at 4 °C for 10 min. The samples were stored at -20 °C until staining. For staining, the cells were pelleted and washed 2X with 1% BSA in PBS. The cells were pelleted, resuspended in BD Stain Buffer (BS Biosciences #554656) containing the appropriate conjugated primary antibody [p38 MAPK (pT180/pY182) Alexa 488 (BD Biosciences #612594), JNK (pT183/pY185) PE N9-66 (BD Biosciences #562480), ERK1/2 (pT202/pY204) PerCP-Cy5.5 20A (BD Biosciences # 560115), p53 (pS37) Alexa 647 J159-641.79 (BD Biosciences #560280), the γH2AX antibody was purchased as a part of a Cell

Proliferation kit (BD Biosciences #562253)], and incubated at 4 °C overnight. After washing 2X with BD Stain Buffer, the cells were resuspended in PBS and analyzed on a Becton Dickinson FACS Calibur.

3.3.10 Statistical analysis

GraphPad Prism 5 was used to graph viability curves. ModFit version 3.0 was used for the flow cytometry analysis. Microsoft Office Excel was used to perform unpaired Student's t-test; values with $p < 0.05$ were considered significant. Student's t-tests were used to verify significant differences among the EC_{50} values.

3.4 Results and discussion

3.4.1 Cytotoxicity of Pt(II) complexes

The cellular response to a particular drug can vary between different types of cancers. In order to thoroughly examine the effectiveness of the dialkoxy-2,2′-bipyridyl Pt(II) complexes in different types of cancers, the anti-proliferative activities of all the complexes were determined in a lung (H520), two prostate (DU145 and PC-3), and six breast (HCC38, MCF-7, MDA-MB-231, SK-BR-3, T-47D, and ZR-75-1) cancer cell lines. The cells were treated with increasing concentrations of the complexes for 1 or 48 h and the viability was measured using an MTS colorimetric cell proliferation assay. The effective concentrations which resulted in 50% cell viability (EC_{50}) were obtained from the viability curves and tabulated in Tables 3-1–3-3. The novel Pt(II) complexes are generally more effective than cisplatin with EC_{50} values ranging from 1–80 μM, while the EC_{50} values of cisplatin are in the range of 20–900 μM. The EC_{50} values for the 1 h treatment with the two short chains complexes, **Pt(II)-1C** and **Pt(II)-2C**, were not obtainable in some cell lines (both complexes in H520 and MCF-7; **Pt(II)-1C** in PC-3

and MDA-MB-231 cells) with the highest concentration (100 μM) tested. Interestingly, the EC_{50} values tend to be higher in H520, MCF-7, and ZR-75-1, which all have wild type p53.[14,15]

Currently, cisplatin does not have a major role in the clinical treatment of breast cancers; however, some triple negative breast cancers (TNBC) are sensitive to platinum drugs.[16] Comparison of the EC_{50} values for complexes **Pt(II)-1C**–**Pt(II)-6C** and cisplatin demonstrate that in most cases the new complexes are more effective than cisplatin in the breast cancer cell lines tested. Moreover, the response is similar between cell lines with differential hormone receptors expression (HCC38 and MDA-MB-231 are TNBC).[17]

Table 3 – 1. EC_{50} (μM) of [Pt(II)Cl_2(4,4′-dialkoxy-2,2′-bipyridine)] complexes in H520, DU145 and PC-3 post 1 or 48 h treatment

	Lung cancer		Prostate cancer			
	H520		DU145		PC-3	
Compound	1 h	48 h	1 h	48 h	1 h	48 h
CDDP	200 ± 17	24 ± 2	400 ± 100	64 ± 8	200 ± 20	30 ± 1
Carboplatin	ND	ND	>1000	400 ± 100[a]	ND	ND
Pt(II)-1C	>100	30 ± 2	40 ± 10[a]	24 ± 2[a,b]	>100	40 ± 7
Pt(II)-2C	>100	21 ± 1	20 ± 5[a]	11 ± 4[a,b]	22 ± 5[a]	21 ± 7
Pt(II)-3C	40 ± 20 [a]	13 ± 5 [a]	6 ± 1[a]	4 ± 2[a,b]	5 ± 1[a]	5.1 ± 0.8[a]
Pt(II)-4C	20 ± 1 [a]	14 ± 6	12 ± 8[a]	5 ± 2[a,b]	11 ± 2[a]	7.4 ± 0.5[a]
Pt(II)-5C	23 ± 5 [a]	17 ± 3	8 ± 2[a]	6.0 ± 0.7[a,b]	7 ± 1[a]	7.3 ± 0.7[a]
Pt(II)-6C	>50	18 ± 1	2.1 ± 0.1[a]	1.9 ± 0.1[a,b]	2.24 ±0.03[a]	2.7 ± 0.1[a]

Values represent the mean ± SD of at least two independent experiments done in quadruplicates. ND = no data. [a] $P < 0.5$ compared to CDDP. [b] $P < 0.05$ compared to carboplatin.

Table 3 – 2. EC_{50} (μM) of [Pt(II)Cl_2(4,4′-dialkoxy-2,2′-bipyridine)] complexes in various human breast cancers post 1 h treatment

Compound	HCC38	MCF-7	MDA-MB-231	SK-BR-3	T-47D	ZR-75-1
CDDP	300 ± 30	900 ± 60	50 ± 4	420 ± 80	900 ± 100	260 ± 10
Carboplatin	ND	>1000	ND	ND	ND	ND
Pt(II)-1C	80 ± 20[a]	>100	>100	19 ± 5[a]	20 ± 1[a]	67 ± 27[a]
Pt(II)-2C	18 ± 4[a]	>100	30 ± 20	2.2 ± 0.2[a]	5 ± 2[a]	58 ± 15[a]
Pt(II)-3C	5 ± 2[a]	100 ± 0[a]	4 ± 2[a]	1.81 ± 0.03[a]	2.4 ± 0.1[a]	8.9 ± 0.4[a]
Pt(II)-4C	12 ± 6[a]	22 ± 2[a]	4 ± 3[a]	5 ± 4[a]	12 ± 7[a]	21 ± 2[a]
Pt(II)-5C	13 ± 5[a]	21 ± 5[a]	4 ± 2[a]	2.8 ± 0.8[a]	9 ± 3[a]	8 ± 3[a]
Pt(II)-6C	16 ± 5[a]	80 ± 30[a]	6 ± 3[a]	1.84 ± 0.03[a]	3.2 ± 0.8[a]	7 ± 2[a]

Values represent the mean ± SD of at least two independent experiments done in quadruplicates. ND = no data [a] $P < 0.5$ compared to CDDP. [b] $P < 0.05$ compared to carboplatin.

Table 3 – 3. EC_{50} (μM) of [Pt(II)Cl_2(4,4′-dialkoxy-2,2′-bipyridine)] complexes in various human breast cancers post 48 h treatment

Compound	HCC38	MCF-7	MDA-MB-231	SK-BR-3	T-47D	ZR-75-1
CDDP	30 ± 8	35 ± 1	21 ± 3	23 ± 6	35 ± 6	30 ± 8
Carboplatin	ND	800 ± 100[a]	ND	ND	ND	ND
Pt(II)-1C	57 ± 2[a]	>100	>100	23 ± 2	21 ± 1[a]	26 ± 1
Pt(II)-2C	20 ± 3	>100	20 ± 6	1.8 ± 0[a]	2.2 ± 0.4[a]	16.5 ± 0
Pt(II)-3C	4.7 ± 0.5[a]	19 ± 4[a,b]	2.2 ± 0.1[a]	1.73 ± 0.01[a]	1.9 ± 0.1[a]	5 ± 1[a]
Pt(II)-4C	7.3 ± 3	13 ± 1[a,b]	2.4 ± 0.6[a]	2.1 ± 0.2[a]	2.3 ± 0.4[a]	6.0 ± 0.9[a]
Pt(II)-5C	10 ± 2	15 ± 7[a,b]	4.1 ± 0.2[a]	2.4 ± 0.4[a]	3 ± 1[a]	6.6 ± 0.7[a]
Pt(II)-6C	14 ± 4	12 ± 4[a,b]	4 ± 1[a]	1.8 ± 0[a]	2.1 ± 0.2[a]	6.4 ± 0.4[a]

Values represent the mean ± SD of at least two independent experiments done in quadruplicates. ND = no data [a] $P < 0.5$ compared to CDDP. [b] $P < 0.05$ compared to carboplatin.

3.4.2 UV-Vis analysis of DNA binding

Absorption spectroscopy is one of the methods commonly used to examine the characteristics of metal complex interaction with DNA. The interactions of metal complexes with DNA can cause changes in the absorption spectra such as an increase (hyperchromism) or decrease (hypochromism) in absorbance, or a redshift (bathochromism) or blueshift (hypsochromism) of the wavelength. Hypochromism and redshift are usually observed for an intercalative binding of the compound to DNA. Damage to the DNA double helical structure such as breakage is usually identified by a hyperchromic shift in the absorbance spectra.[18] Various degrees of hyperchromic and hypochromic shifts have been described for different platinum complexes.[19–23] The absorbance spectra for one of the platinum complexes reported with coordination to 2,2′-bipyridine and substituted 1,10-phenanthroline ligands showed hypochromism.[22] Additionally, another complex similar to our compounds, but containing dicarboxylic acid substituents, also caused hypochromism in the absorbance spectra.[23] Thus, it is hypothesized that the dialkoxy-2,2′-bipyridyl Pt(II) complexes will also cause similar effects.

Due to having consistently low EC_{50} values in all of the cell lines tested, **Pt(II)-4C** was chosen for further studies. The UV-Vis analysis of the interaction of **Pt(II)-4C** with CT-DNA was first evaluated by incubation of the CT-DNA at a constant concentration (100 μM) with increasing concentrations of **Pt(II)-4C** for 1 or 24 h at 37 °C. Addition of **Pt(II)-4C** to CT-DNA for 1 h caused an increase in the DNA absorbance at 260 nm and, as illustrated in Figure 3-1 A, the increase in absorbance was concentration dependent. Further incubation of the DNA with **Pt(II)-4C** for 24 h did not

caused any dramatic changes to the absorption spectra (Figure 3-1 B). The experiment was repeated by keeping the **Pt(II)-4C** concentration constant (100 μM) and varying the concentrations of CT-DNA. The spectra for the 1 h incubation show an absorbance maximum for **Pt(II)-4C** (in the absence of DNA) around 250 nm and a broad absorption around 300 nm (Figure 3-2 A). Addition of 10 μM CT-DNA caused significant hyperchromism in the spectra and the **Pt(II)-4C** peak around 300 nm was shifted to 280 nm (blueshift). Further addition of CT-DNA caused slight increases in the absorbance of **Pt(II)-4C**. Results obtained for the 24 h incubation was similar to the 1 h incubation, except the characteristic absorption peaks of **Pt(II)-4C** in the absence of DNA was not observed as for the 1 h treatment period (Figure 3-2 B).

The hyperchromism observed for **Pt(II)-4C** interaction with CT-DNA is indicative of electrostatic attractions that may have caused separation of the DNA structure.[24] These results are in contrast to the hypochromism observed by Sun et al. for the structurally related Pt(II) complex containing dicarboxylic acid substituted 2,2′-bipyridyl.[23]

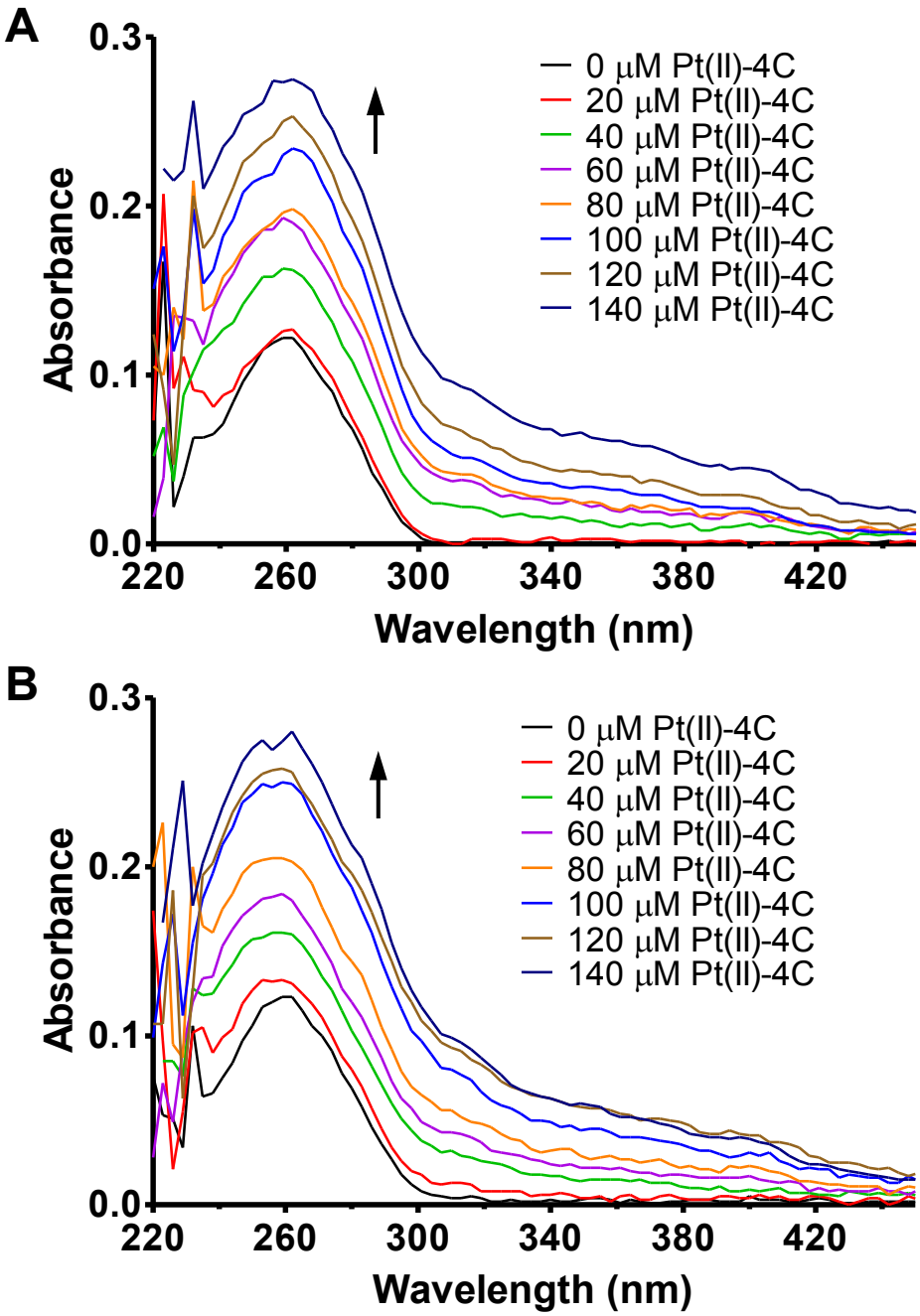

Figure 3 – 1. Absorption spectra of CT-DNA (100 μM) with increasing concentration of **Pt(II)-4C**. Samples were incubated at 37 °C for (A) 1 or (B) 48 h in 10 mM Tris-HCl (pH 7.2) containing 10% DMSO. **Pt(II)-4C** solutions of each concentration in the same buffer were used as blanks to eliminate the absorption of the **Pt(II)-4C** by itself. Spectra are representative of at least three independent experiments.

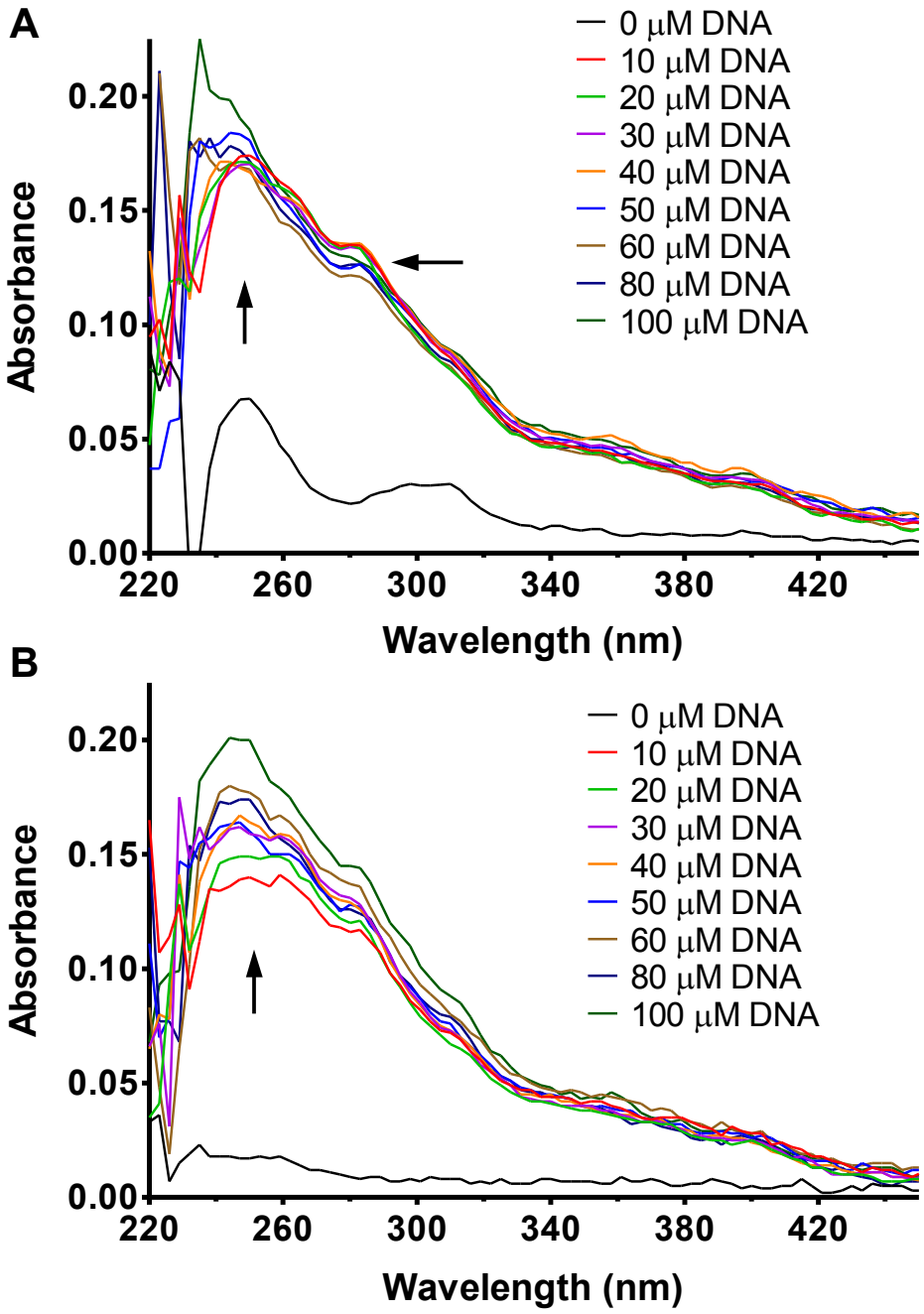

Figure 3 – 2. Absorption spectra of **Pt(II)-4C** (100 μM) with increasing concentration of CT-DNA. Samples were incubated at 37 °C for (A) 1 or (B) 48 h in 10 mM Tris-HCl (pH 7.2) containing 10% DMSO. Samples with only CT-DNA in the same buffer at each concentration were used as blanks to eliminate the absorbance from the CT-DNA. Spectra are representative of at least three independent experiments.

3.4.3 Gel electrophoretic analysis of DNA cleavage

Cleavage of circular plasmid DNA is another method used to determine the effects of a compound on DNA. Plasmid DNA cleavage generates different forms of DNA that have varying migration rates in gel electrophoresis. To utilize this characteristic, the interaction of **Pt(II)-4C** was further studied by examining its interaction with plasmid pBR322 DNA. Plasmid pBR322 can have three forms; Form I is the intact supercoiled structure, Form II results when one of the DNA strands is cleaved forming an opened circular structure, and Form III is the linear structure generated when both DNA strands are cleaved. Form I migrates the fastest in agarose gel electrophoresis, Form II migrates the slowest, and Form III migrates in between the two.[21–23]

The electrophoretic mobility shift of pBR322 incubated with increasing concentrations of **Pt(II)-4C** is shown in Figure 3-3. After incubation for 24 h at 37 °C, **Pt(II)-4C** did not affect the mobility of Form I at concentrations of 5 and 15 μM. At 25 μM of **Pt(II)-4C**, a slight decrease in the mobility of Form I was observed and this pattern was more evident at 50 μM with a slight increase in intensity for the Form II band. Treatment of pBR322 with 75 μM **Pt(II)-4C** resulted in three bands: a faint band in the Form I region, an increased Form II band, and a smeared band in between. This pattern is indicative of DNA cleavage by **Pt(II)-4C**. Cisplatin (100 μM) was used as a control. Cisplatin treatment resulted in two bands with decreased intensity and a different mobility pattern compared to DNA alone. Treatment with **Pt(II)-4C** resulted in different mobility patterns compared to cisplatin indicating that the interaction of **Pt(II)-4C** with DNA may be different than that of cisplatin.

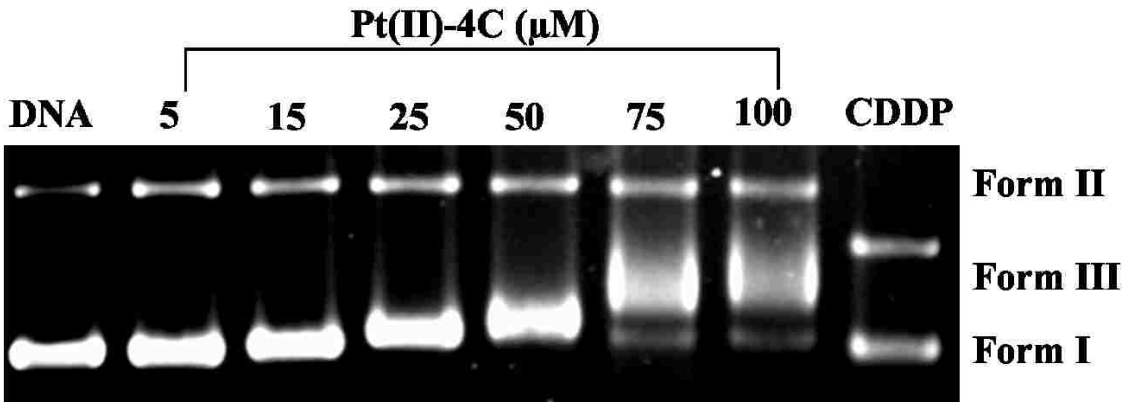

Figure 3 – 3. Gel electrophoretic analysis of the **Pt(II)-4C** complex interaction with DNA. Plasmid pBR322 DNA (0.125 μg) was incubated for 24 h at 37 °C with increasing concentrations of **Pt(II)-4C** in TE buffer (Tris-EDTA) containing 25% DMSO, subjected to electrophoresis in a 1% agarose gel, stained with ethidium bromide, and visualized with a UV-Vis transilluminator. Gel images are representative of at least two independent experiments.

3.4.4 Intracellular accumulation of **Pt(II)-4C**

Analysis of intracellular platinum concentrations were measured by ICP-AES to determine the extent of cellular uptake and DNA binding of **Pt(II)-4C** in A549 cells. A549 cells treated for 4 h with increasing concentrations of **Pt(II)-4C** had increasing accumulation of platinum in the cell (Figure 3-4 A), which was accompanied by a proportional increase in platinum bound to DNA (Figure 3-4 B). These results correlate well with the concentration dependent anti-proliferative effect of **Pt(II)-4C** in A549 cells (Chapter 2).[6]

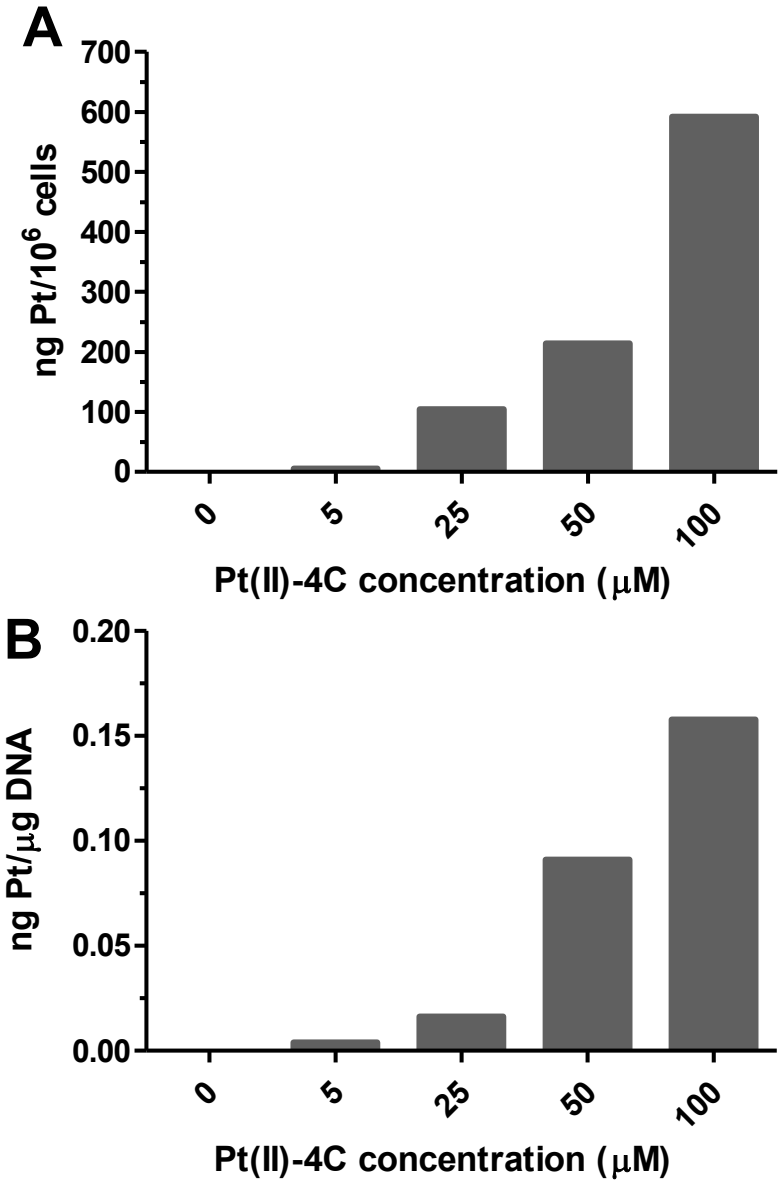

Figure 3 – 4. Cellular uptake of **Pt(II)-4C** in A549 human lung cancer cells. A549 cells were treated for 4 h with increasing concentrations of **Pt(II)-4C** and the amount of Pt (A) taken up by the cells or (B) bound to DNA was measured by ICP-AES. Values for the cell uptake are representative of two independent experiments and the values for Pt bound to DNA are from one trial.

3.4.5 **Pt(II)-4C** induced cell death in A549 cells is p53 dependent

The effects of **Pt(II)-4C** treatment on p53 signaling was examined in A549 cells to determine the role of p53 in **Pt(II)-4C** induced cell death. Immunofluorescence microscopy analysis of p53 expression in A549 cells treated with **Pt(II)-4C** showed increased p53 signal compared to control cells (Figure 3-5 A) with p53 localized in the nucleus. This result was confirmed by western blotting, in which A549 cells treated with increasing concentrations of **Pt(II)-4C** had increasing p53 expression (Figure 3-5 B). Additionally, measurement of phosphorylated p53 (p-p53) levels in A549 cells treated with **Pt(II)-4C** by flow cytometry showed an increased shift in p53 signal compared to control (Figure 4-5 C). The change of p-p53 expression calculated from the flow cytometry data indicated a 2–3 fold increase in activated p53 (Figure 4-5 D).

To determine the role of activated p53 in **Pt(II)-4C** induced cell death of A549 cells, p53 was inhibited by the chemical inhibitor PFTα. As shown in Figure 3-6, treatment of A549 cells with **Pt(II)-4C** in the presence of PFTα resulted in increased cell viability compared to cells treated with **Pt(II)-4C** alone. The partial reversal of **Pt(II)-4C** induced cell death by inhibition of p53 suggests that p53 is involved in the cell death signaling response to **Pt(II)-4C** treatment in A549. This result is consistent with reports of the role of p53 in regulating apoptosis.[9,25]

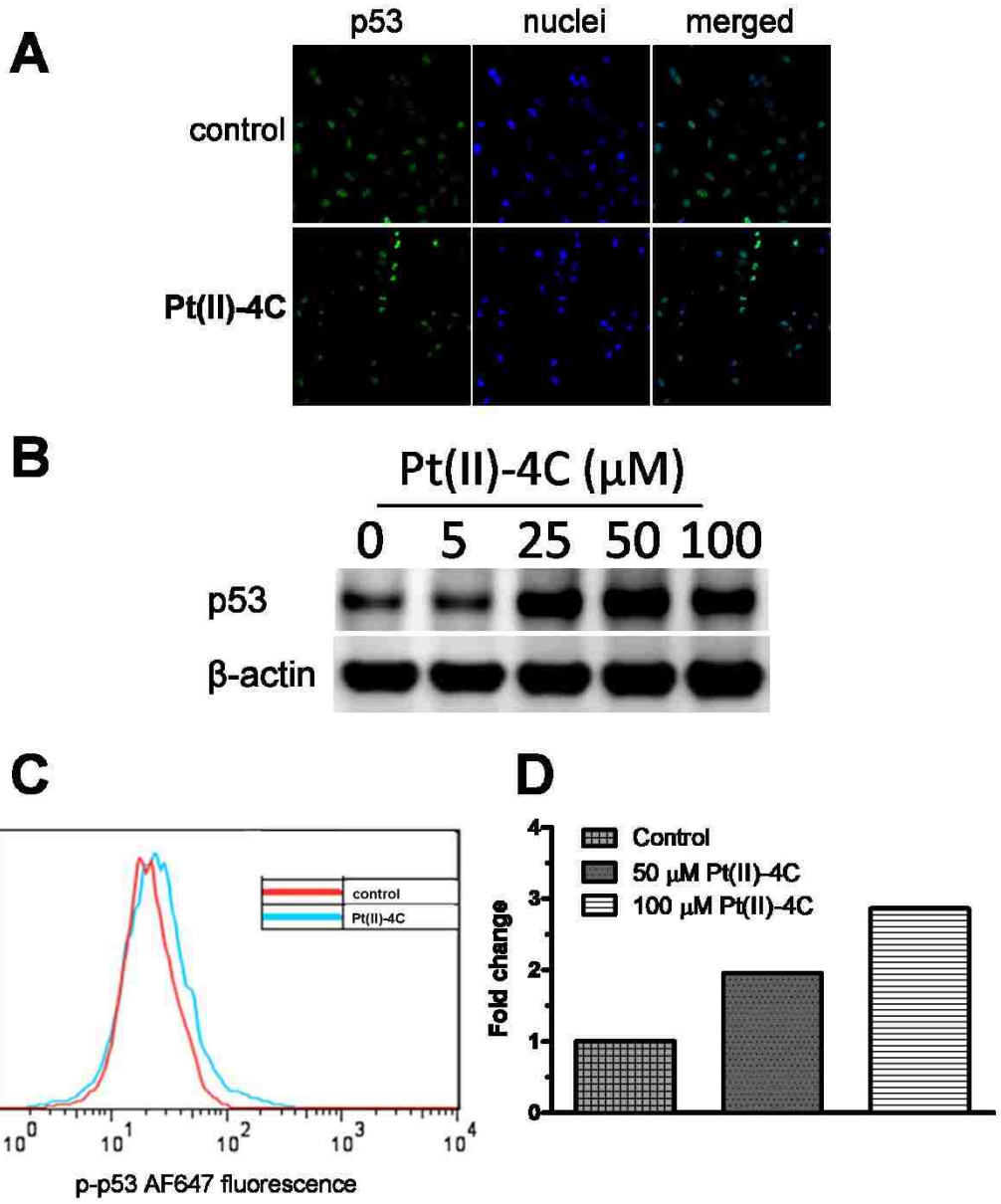

Figure 3 – 5. Expression of p53 in A549 cells. Expression of p53 was measured by (A) immunofluorescence microscopy of cells treated for 2 h with 100 uM of **Pt(II)-4C** (images are representative of two independent experiments done by taking images of at least three different fields) and (B) western blotting of cells treated for 3 h with increasing concentrations of **Pt(II)-4C** (representative of two independent experiments). (C) Flow cytometric analysis of phosphorylated p53 in cells treated for 6 h with 100 μM **Pt(II)-4C** (representative of three independent experiments). (D) Fold change (signal of treated cells/signal of control) in p-p53 fluorescence signal taken from the flow cytometry data.

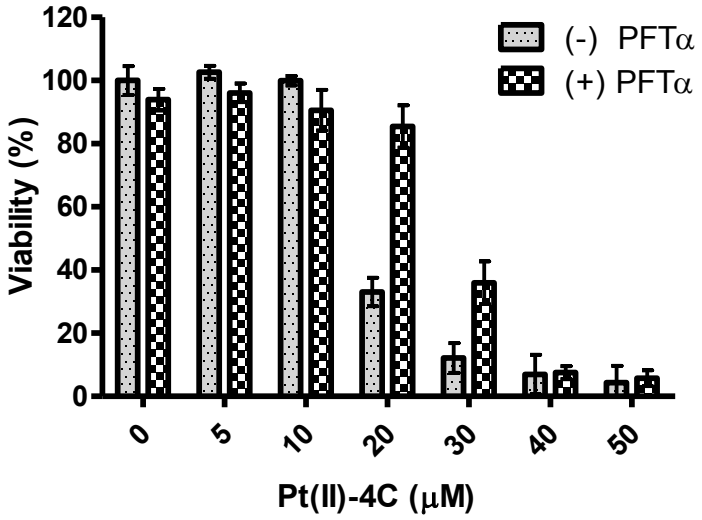

Figure 3 – 6. Effect of p53 inhibition on **Pt(II)-4C** induced cell death in A549 cells. A549 cells were pre-treated with 50 μM PFTα (p53 inhibitor) for 1h, co-treated with PFTα and increasing concentrations of **Pt(II)-4C** for 1 h, and the cell viability was measured by the MTS assay after 48 h of incubation with PFTα.

3.4.6 **Pt(II)-4C** induces activation of MAPK

The involvement of MAPK members in response to **Pt(II)-4C** was determined in A549 and DU145 cells. First, activation of JNK, p38, and ERK were analyzed using flow cytometry. The histogram of A549 and DU145 cells treated with 100 μM of **Pt(II)-4C** showed a right shift of phosphorylated p38 (Figure 3-7 A and E), JNK (Figure 3-7 B and F), and ERK (Figure 3-7 C and G) signals compared to control indicating activation of p38, JNK, and ERK. The fold change calculated from the flow data indicate increases of 4–25 times compared to control (Figure 3-7 D and H) with p-ERK being the highest. Additionally, a concentration dependent increase in MAPK members was observed.

Western blotting analysis of proteins from A549 (Figure 3-8 A) and DU145 (Figure 3-8 B) cells treated with increasing concentrations of **Pt(II)-4C** also showed a concentration dependent increase in p-JNK, p-p38, and p-ERK. The increase in phosphorylated proteins observed for A549 cells started at 25 μM, while this increase was observed at 5 μM in DU145 cells. These results correspond to the MTS data showing a lower EC_{50} value for DU145 cells.

Activation of MAPK in A549 and DU145 cells treated with **Pt(II)-4C** was further analyzed with immunofluorescence microscopy. Similar to the flow and western data, immunofluorescence images showed an increase in p-p38, p-JNK, and p-ERK signals in **Pt(II)-4C** treated A549 cells (Figure 3-9). Moreover, activated JNK and ERK appeared to be localized to the nucleus, while activated p38 localization was cytoplasmic. Similar results were obtained for DU145 cells (Figure 3-10).

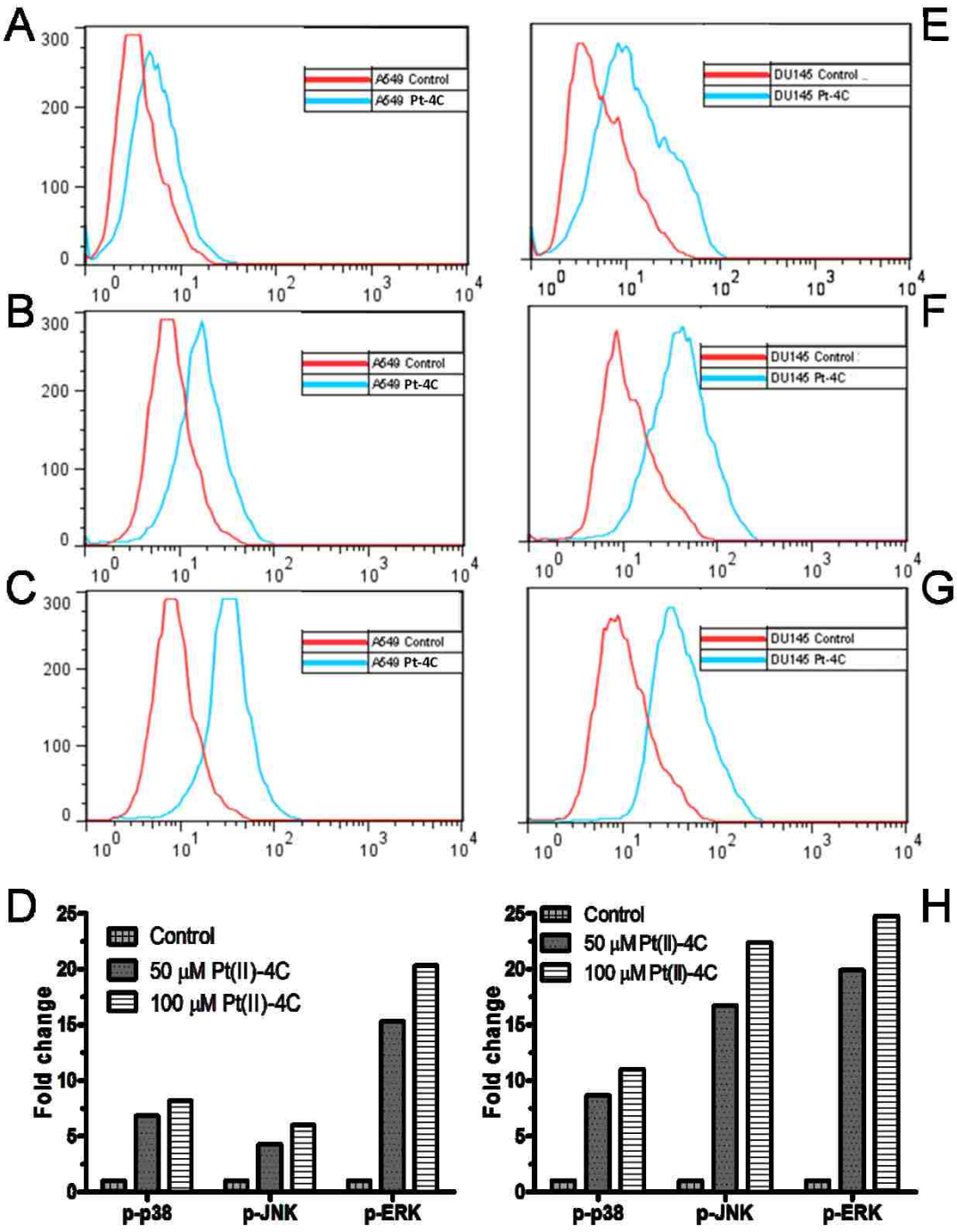

Figure 3 – 7. Flow cytometric immunofluorescence analysis of MAPK activation in A549 and DU145 cells. (A) p-p38, (B) p-JNK, and (C) p-ERK levels in A549 cells treated for 6 h with **Pt(II)-4C**. (E) p-p38, (F) p-JNK, and (G) p-ERK levels in DU145 cells treated for 1 h with **Pt(II)-4C**. Fold change for (D) A549 and (H) DU145 cells calculated by taking the ratio of the fluorescence signals of treated cells to control. Histograms are representative of three independent experiments done in triplicate.

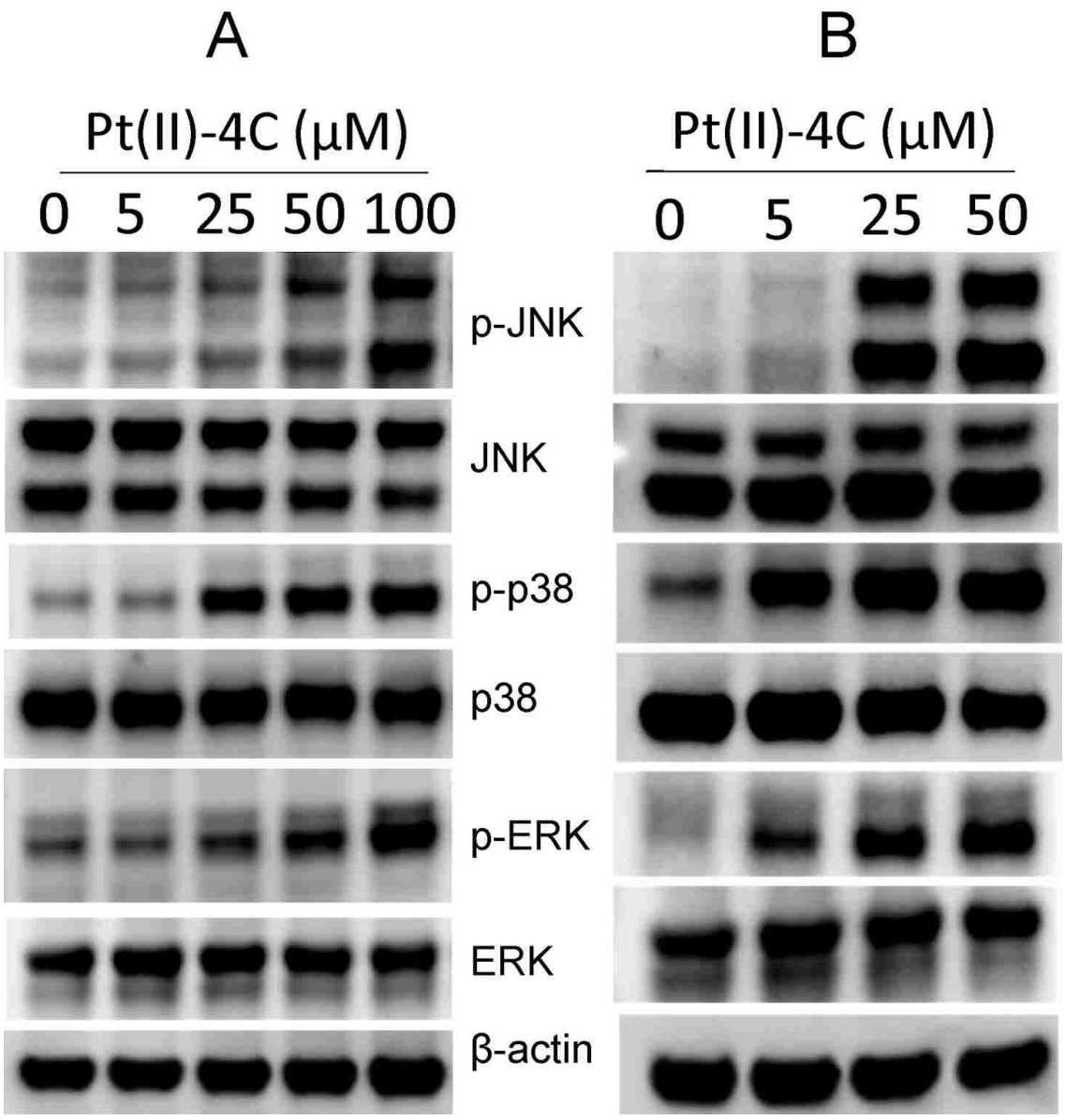

Figure 3 – 8. Western blot analysis of MAPK activation in A549 and DU145 cells. (A) A549 treated for 3 h with increasing concentrations of **Pt(II)-4C**. (B) DU145 treated for 1 h with increasing concentrations of **Pt(II)-4C**. Images are representative of at least two independent experiments.

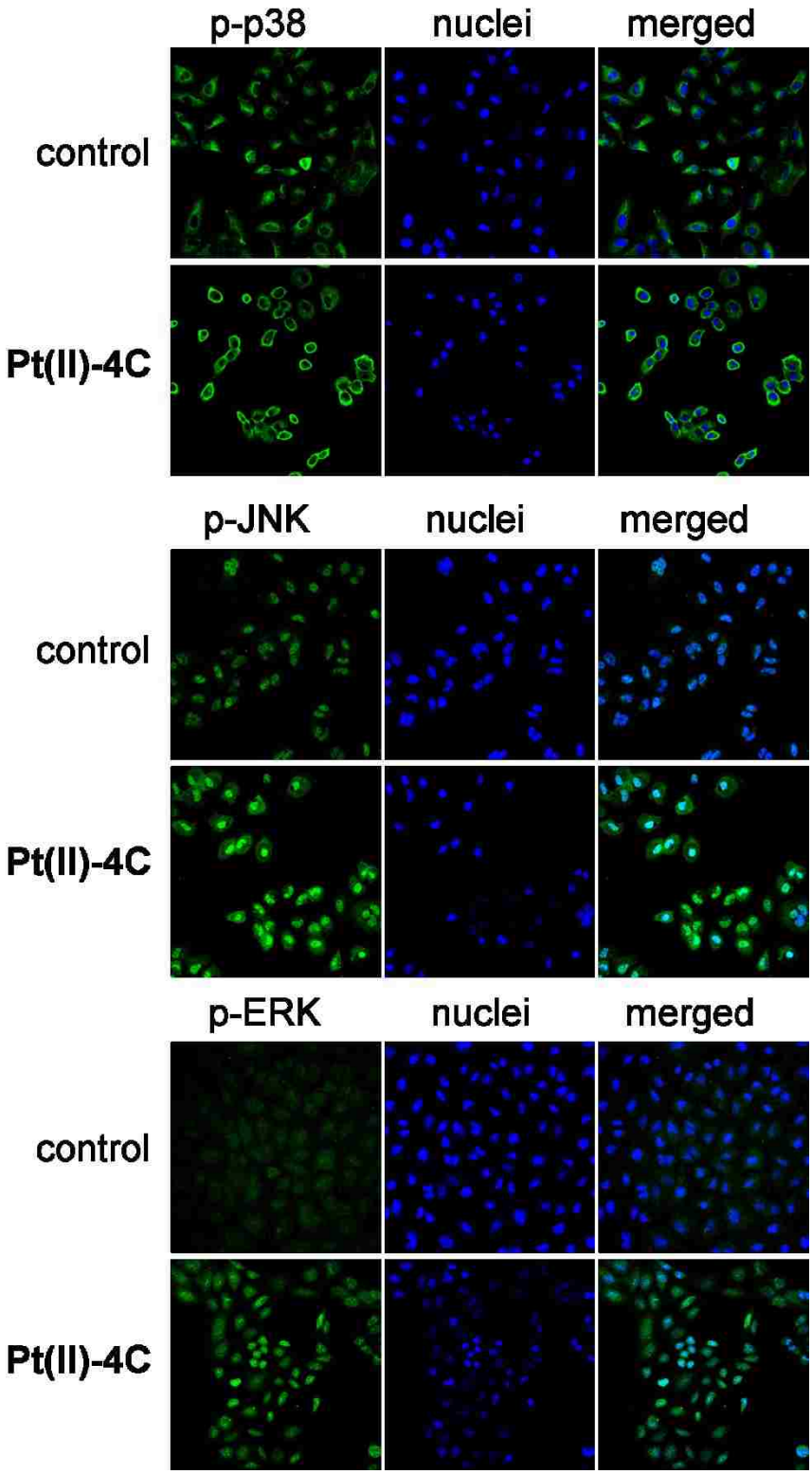

Figure 3 – 9. Immunofluorescence microscopy analysis of MAPK activation in A549 cells treated for 2 h with 100 μM **Pt(II)-4C**. Images are representative of two experiments done by taking images of at least three different fields.

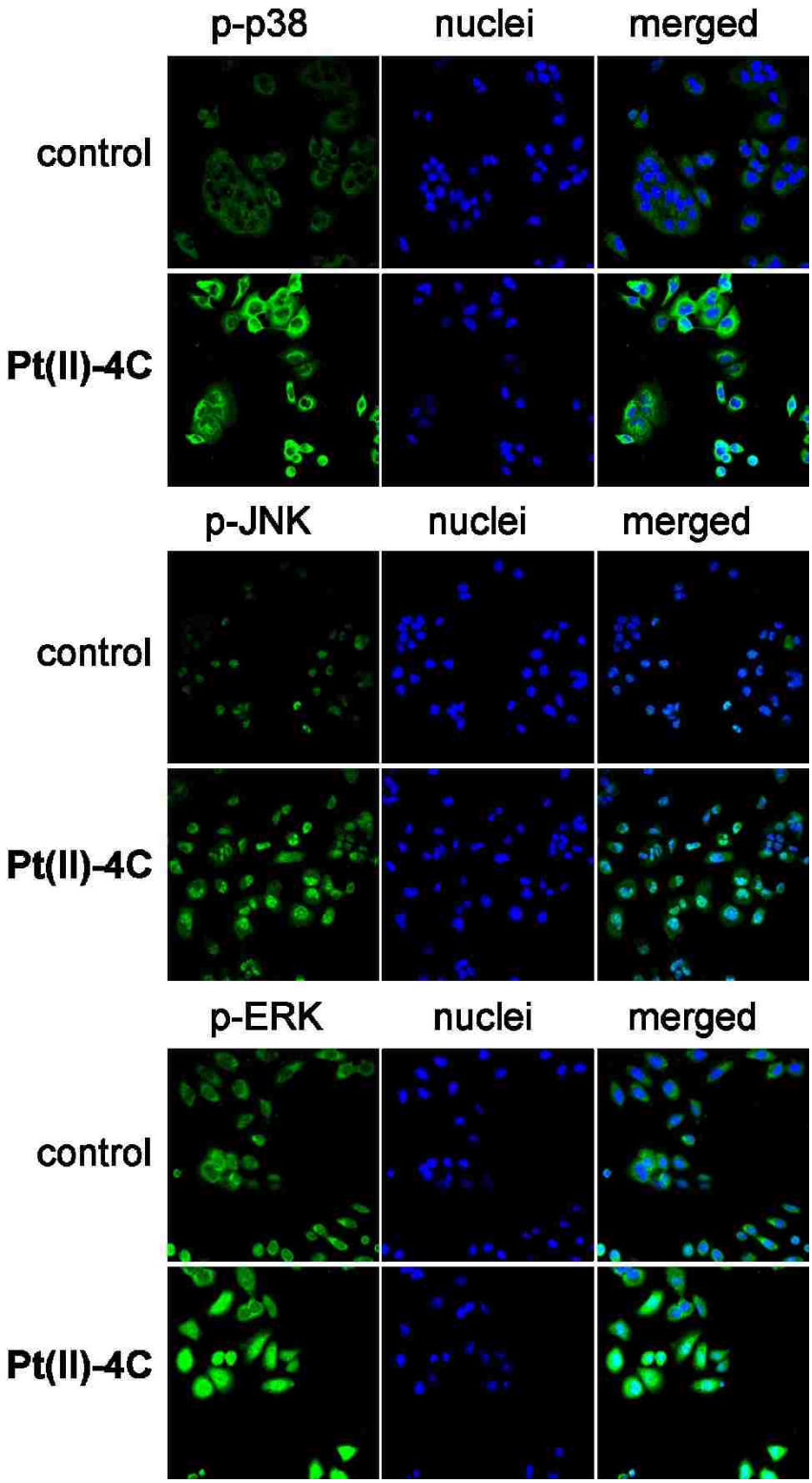

Figure 3 – 10. Immunofluorescence microscopy analysis of MAPK activation in DU145 cells treated for 1 h with 30 μM **Pt(II)-4C**. Images are representative of two experiments done by taking images of at least three different fields.

3.4.7 **Pt(II)-4C** induced activation of H2AX is dependent on MAPK

DNA double-strand breaks (DSBs) cause the activation of histone H2AX through its phosphorylation at Ser-139. Phosphorylated H2AX (γH2AX) is believed to play a role in DNA damage repair and regulation of apoptosis.[26] MAPK members have been associated with phosphorylation of H2AX.[27,28] Furthermore, phosphorylation of H2AX in cisplatin treated cells has been observed[29–32] and its phosphorylation by MAPK in cells treated with oxaliplatin has also been reported.[33]

Since **Pt(II)-4C** causes DNA damage and activates MAPK, it is possible that γH2AX will also be induced. As expected, immunofluorescence microscopy analysis showed an increased γH2AX fluorescence in A549 (Figure 3-10) and DU145 (Figure 3-11) cells treated with **Pt(II)-4C** compared to control (also confirmed by flow cytometry, Figure 3S-1 shown in the appendix). Co-treatment of A549 and DU145 cells with **Pt(II)-4C** and chemical inhibitors of p38 (SB202190), JNK (SP600125), and ERK (PD-098,059) resulted in decreased γH2AX fluorescence compared to **Pt(II)-4C** treatment alone. In A549 cells, inhibition of p38 and JNK resulted in decreased γH2AX fluorescence comparable to the control; however, the decreased γH2AX fluorescence resulting from the inhibition of ERK was not as dramatic (Figure 3-11). This was not observed for DU145 cells. These results indicate that **Pt(II)-4C** causes DSB and induces phosphorylation of H2AX in a MAPK dependent manner.

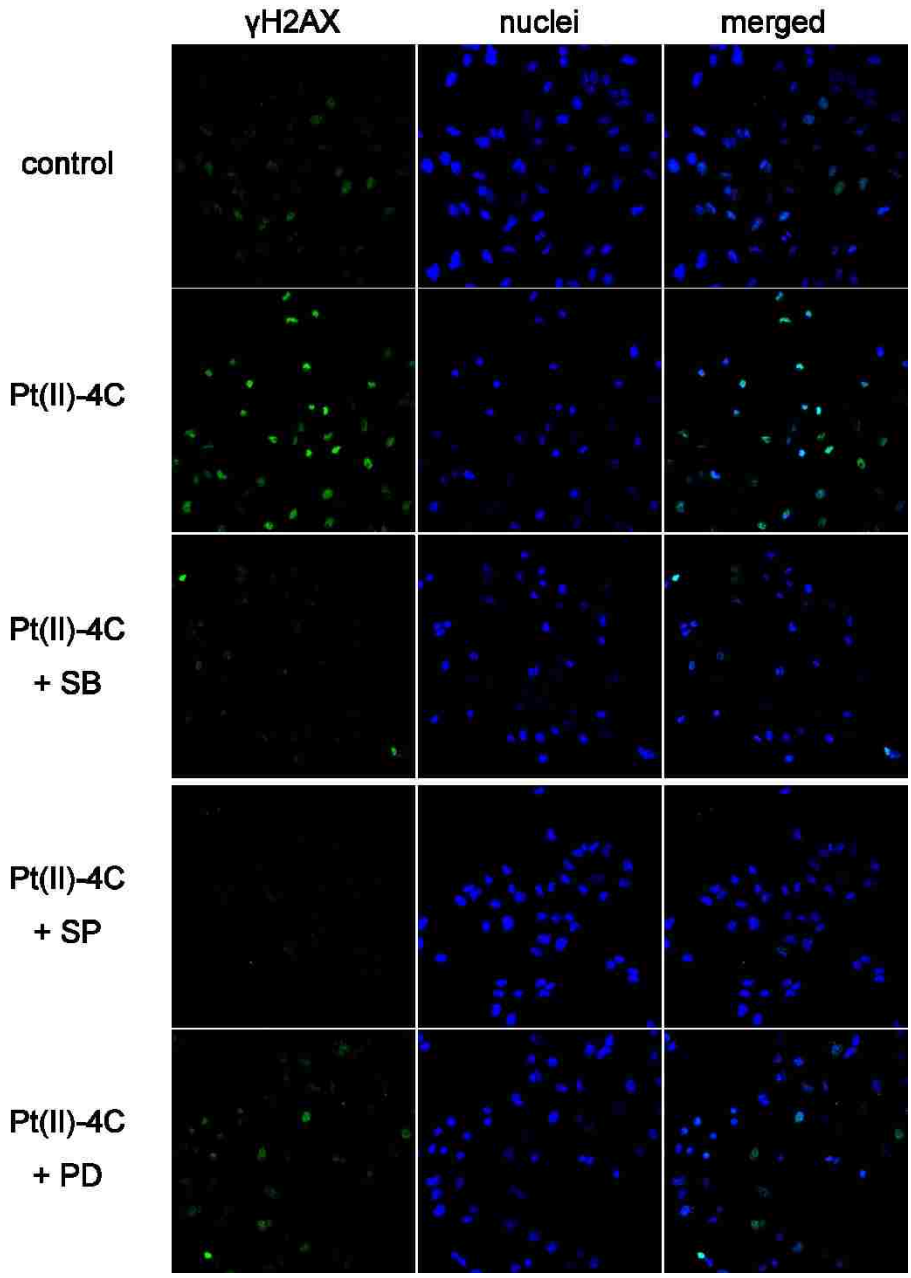

Figure 3 – 11. Effect of MAPK inhibitors on **Pt(II)-4C** induced H2AX phosphorylation in A549 cells. Cells were pre-treated with 10 μM of MAPK inhibitors (PD: ERK inhibitor, SB: p38 inhibitor, SP: JNK inhibitor) for 2 h, then co-treated with **Pt(II)-4C** (50 μM) for 2 h, and phosphorylated H2AX (γH2AX) was measured by immunofluorescence microscopy. Images are representative of two independent experiments.

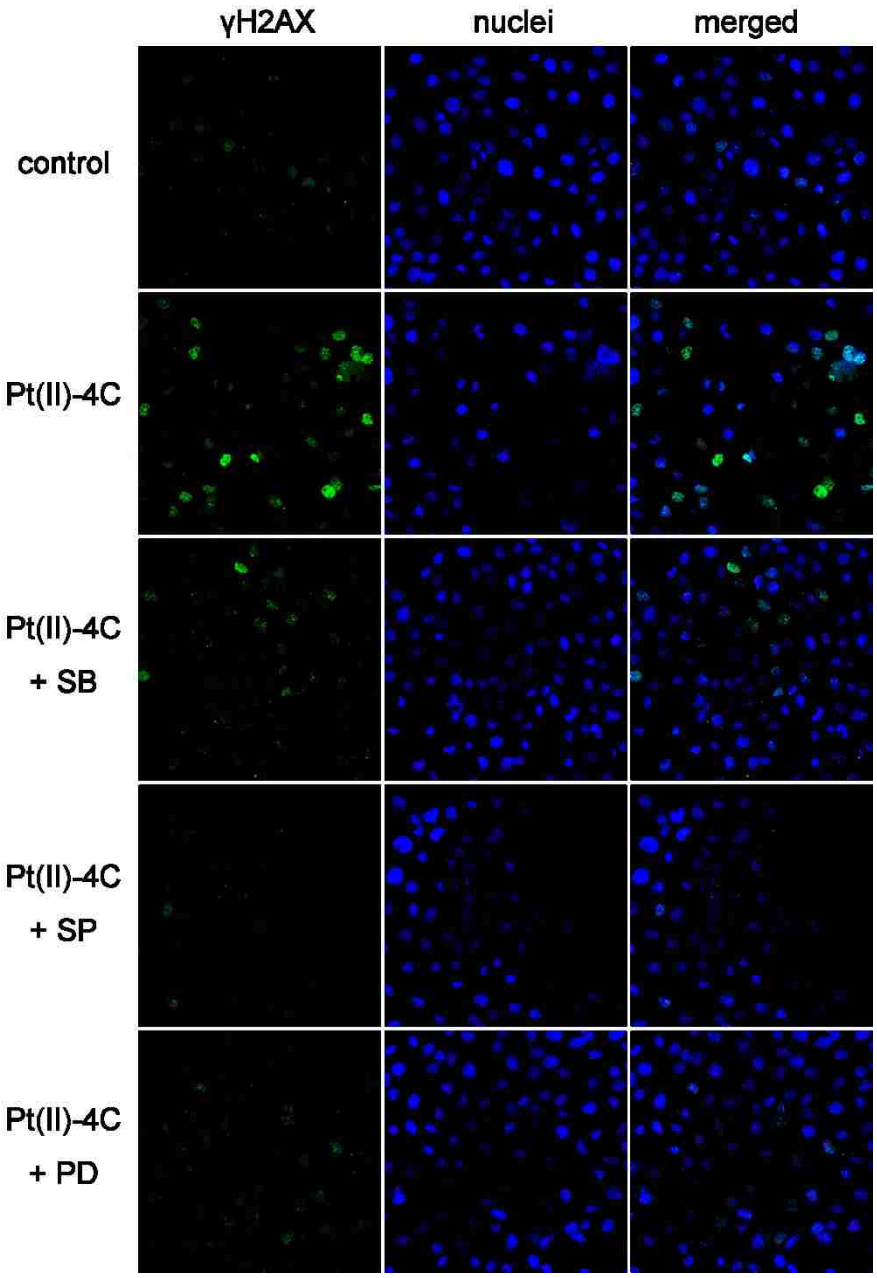

Figure 3 – 12. Effect of MAPK inhibitors on **Pt(II)-4C** induced H2AX phosphorylation in DU145 cells. Cells were pre-treated with 10 μM of MAPK inhibitors (PD: ERK inhibitor, SB: p38 inhibitor, SP: JNK inhibitor) for 24 h, then co-treated with **Pt(II)-4C** (30 μM) for 3 h, and phosphorylated H2AX (γH2AX) was measured by immunofluorescence microscopy. Images are from one experiment done by taking images of at least three different fields.

3.4.8 The effect on MAPK inhibitors on **Pt(II)-4C** induced cell death

To determine the role of MAPK in **Pt(II)-4C** induced cell death, the cell viability of A549 and DU145 cells treated with increasing concentrations of **Pt(II)-4C** in the absence or presence of the MAPK inhibitors was measured by the MTS assay. As shown in Figure 3-13 A, A549 cells treated with **Pt(II)-4C** in the presence of the ERK inhibitor had decreased cell viability compared to **Pt(II)-4C** treatment alone, while treatment in the presence of p38 and JNK inhibitors resulted in increased cell viability compared to **Pt(II)-4C** treatment alone. Similar results were observed for DU145 cells (Figure 3-13 B), except inhibition of ERK had no effect on the **Pt(II)-4C** induced cell death (comparable results were obtained even when the concentration of the inhibitors was increased, Figure 3S-2 shown in the appendix) . These results indicate that **Pt(II)-4C** induced cell death is dependent on functional p38 and JNK in both A549 and DU145 cells. Additionally, functional ERK protects A549 cells from **Pt(II)-4C** induced cell death. It is surprising that while **Pt(II)-4C** caused ERK activation in DU145 cells and its inhibition reduced the level of γH2AX formation, its inhibition did not affect **Pt(II)-4C** induced cell death. Perhaps its activation is not sufficient enough to overcome the effects of **Pt(II)-4C**.

The results obtained are consistent with the reported roles of ERK in protection against apoptosis, and p38 and JNK as apoptosis inducers.

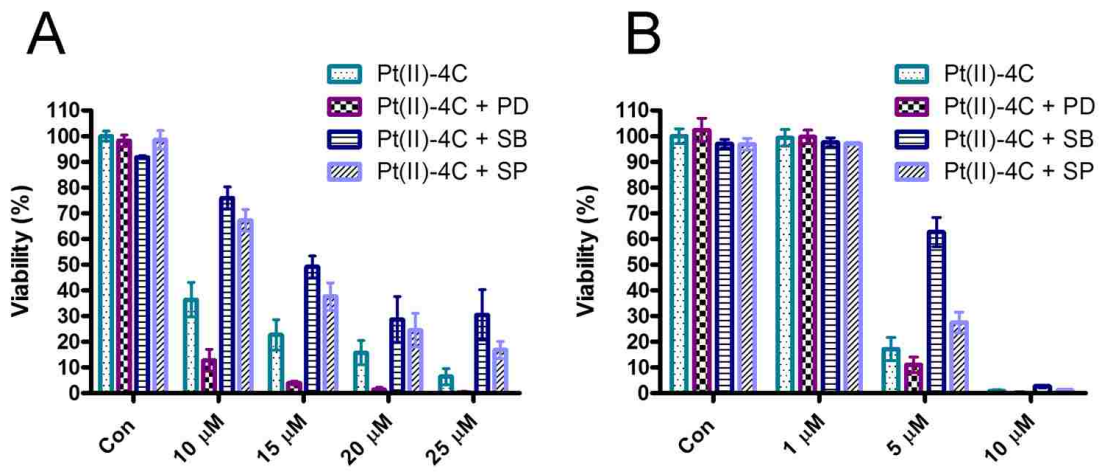

Figure 3 – 13. Effects of MAPK inhibitors on **Pt(II)-4C** induced cell death. (A) A549 treated with increasing concentrations of **Pt(II)-4C** in the absence and presence of 40 μM of MAPK inhibitors (PD: ERK inhibitor, SB: p38 inhibitor, SP: JNK inhibitor) for 48 h and (B) DU145 treated with increasing concentrations of **Pt(II)-4C** in the absence and presence of 10 μM of MAPK inhibitors for 48 h. Results are representative of at least three independent experiments done in quadruplicates.

3.5 Conclusions

The present work demonstrate that Pt(II) complexes containing 4,4′-dialkoxy-2,2′-bipyridyl ligands are more potent than cisplatin in various human breast, prostate, and lung cancers. One of the complexes, **Pt(II)-4C**, causes intracellular DNA strand breaks, activates p53 and MAPK signaling pathways, which may culminate in cell death. In A549 cells, p53 and the MAPK members, p38 and JNK, are responsible for inducing cell death in response to **Pt(II)-4C**, while ERK protects A549 from cell death. In DU145 cells, p38 and JNK are necessary for **Pt(II)-4C** induced cell death.

MAPK and p53 are two of the many pathways activated by cisplatin treatment. They are involved in a complex network of signaling cascades that regulate cell survival and death. For a more complete understanding of the effects of **Pt(II)-4C**, it would be

interesting to investigate the signaling of downstream target molecules of p53 and MAPKs such as proteins in the cell cycle, the repair pathway, and death pathways (apoptosis and autophagy) to determine the effects of **Pt(II)-4C**.

3.6 References

1. Harper, B. W.; Krause-Heuer, A. M.; Grant, M. P.; Manohar, M.; Garbutcheon-Singh, K. B.; Aldrich-Wright, J. R. Advances in Platinum Chemotherapeutic. *Chem. Eur. J.* **2010,** *16,* 7064-7077.
2. Casini, A.; Reedijk, J. Interactions of anticancer Pt compounds with proteins: an overlooked topic in medicinal inorganic chemistry? *Chem. Sci.* **2012,** *3,* 3135–3144.
3. Wexselblatt, E.; Gibson, D. What do we know about the reduction of Pt(IV) pro-drugs? *J. Inorg. Biochem.* **2012,** *117,* 220-229.
4. Wong, D. Y. Q.; Ang, W. H. Development of Platinum(IV) Complexes as Anticancer Prodrugs: The Story so Far. *COSMO* **2012,** *8,* 121-134.
5. Marques, M. P. M. Platinum and Palladium Polyamine Complexes as Anticancer Agents: The Structural Factor. *ISRN Spectroscopy* **2013,** *2013,* 1-29.
6. Vo, V.; Tanthmanatham, O.; Han, H.; Bhowmik, P. K.; Spangelo, B. L. Synthesis of [$PtCl_2$(4,4′-dialkoxy-2,2′-bipyridine)] complexes and their *in vitro* anticancer properties. *Metallomics* **2013,** *5,* 973-987.
7. Gómez-Ruiz, S.; Maksimović-Ivanić, D.; Mijatović, S.; Kaluđerović, G. N. On the discovery, biological effects, and use of Cisplatin and metallocenes in anticancer chemotherapy. *Bioinorg. Chem. Appl.* **2012,** *2012,* 140284.
8. Gudkov, A. V.; Komarova, E. A. Dangerous habits of a security guard: the two faces of p53 as a drug target. *Hum. Mol. Genet.* **2007,** *16,* 67-72.
9. Basu, A.; Krishnamurthy, S. Cellular Responses to Cisplatin-Induced DNA Damage. *J. Nucleic Acids* **2010,** *2010,* 201367.
10. Soussi, T.; Dehouche, K.; Beroud, C. p53 website and analysis of p53 gene mutations in human cancer: forging a link between epidemiology and carcinogenesis. *Hum. Mutat.* **2000,** *2,* 105–213.
11. Saha, M. N.; Qiu, L.; Chang, H. Targeting p53 by small molecules in hematological malignancies. *J. Hematol. Oncol.* **2013,** *6,* 23.

12. Germain, C. S.; Niknejad, N.; Ma, L.; Garbuio, K. . H. T.; Dimitroulakos, J. Cisplatin Induces Cytotoxicity through the Mitogen-Activated Protein Kinase Pathways and Activating Transcription Factor 3. *Neoplasia* **2010,** *12,* 527-538.

13. Guégan, J.-P.; Ezan, F.; Théret, N.; Langouët, S.; Baffet, G. MAPK signaling in cisplatin-induced death: predominant role of ERK1 over ERK2 in human hepatocellular carcinoma cells. *Carcinogenesis* **2013,** *34,* 38-47.

14. Tong, X.; Xie, D.; O'Kelly, J.; Miller, C. W.; Muller-Tidow, C.; Koeffler, H. P. Cyr61, a Member of CCN Family, Is a Tumor Suppressor in Non-Small Cell Lung Cancer. *J. Biol. Chem.* **2001,** *276,* 47709-47714.

15. Lacroix, M.; Toillon, R.-A.; Leclercq, G. p53 and breast cancer, an update. *Endocr. Relat. Cancer.* **2006,** *13,* 293-325.

16. Eckstein, N. Platinum resistance in breast and ovarian cancer cell lines. *J. Exp. Clin. Cancer Res.* **2011,** *30,* 91.

17. Kao, J.; Salari, K.; Bocanegra, M.; Choi, Y.-L.; Girard, L.; Gandhi, J.; Kwei, K. A.; Hernandez-Boussard, T.; Wang, P.; Gazdar, A. F.; Minna, J. D.; Pollack, J. R. Molecular Profiling of Breast Cancer Cell Lines Defines Relevant Tumor Models and Provides a Resource for Cancer Gene Discovery. *PLoS ONE* **2009,** *4,* e6146.

18. Parson, C.; Smith, V.; Krauss, C.; Banerjee, H. N.; Reilly, C.; Krause, J. A.; Wachira, J. M.; Giri, D.; Winstead, A.; Mandal, S. K. The Effect of Novel Rhenium Compounds on Lymphosarcoma, PC-3 Prostate and Myeloid Leukemia Cancer Cell Lines and an Investigation on the DNA Binding Properties of One of these Compounds through Electronic Spectroscopy. *J. Bioprocessing and Biotechniques* **2013,** *4,* 141.

19. Suntharalingam, K.; Mendoza, O.; Duarte, A. A.; Mann, D. J.; Vilar, R. A platinum complex that binds non-covalently to DNA and induces cell death via a different mechanism than cisplatin. *Metallomics* **2013,** *5,* 514-523.

20. Shahabadi, N.; Kashanian, S.; Fatahi, A. Identification of Binding Mode of a Platinum(II) Complex, $PtCl_2$(DIP), and Calf Thymus DNA. *Bioinorg. Chem. Appl.* **2011,** *2011*.

21. Kumari, N.; Maurya, B. K.; Koiri, R. K.; Coogan, M. P.; Mishra, L. Cytotoxic activity, cell imaging and photocleavage of DNA induced by a Pt(II) cyclophane bearing 1,2 diamino ethane as a terminal ligand. *Med. Chem. Comm.* **2011,** *2,* 1208-1216.

22. Coban, B.; Yildiz, U.; Sengul, A. Synthesis, characterization, and DNA binding of complexes $[Pt(bpy)(pip)]^{2+}$ and $[Pt(bpy)(hpip)]^{2+}$. *J. Biol. Inorg. Chem.* **2013,** *18,* 461–471.

23. Sun, Y.; Sun, D.; Yu, W.; Zhu, M.; Ding, F.; Liu, Y.; Gao, E.; Wang, S.; Xiong, G.; Dragutan, I.; Dragutan, V. Synthesis, characterization, interaction with DNA and cytotoxicity of Pd(II) and Pt(II) complexes containing pyridine carboxylic acid ligands. *Dalton Trans.* **2013,** *42,* 3957-3967.

24. Sirajuddin, M.; Ali, S.; Badshah, A. Drug-DNA interactions and their study by UV-Visible, fluorescence spectroscopies and cyclic voltammetry. *J. Photochem. Photobiol. B: Biol.* **2013,** *124,* 1–19.

25. Konstantakou, E.; Voutsinas, G.; Karkoulis, P.; Aravantinos, G.; Margaritis, L.; Stravopodis, D. Human bladder cancer cells undergo cisplatin-induced apoptosis that is associated with p53-dependent and p53-independent responses. *Int. J. Oncol.* **2009,** *35,* 401-416.

26. Lu, C.; Zhu, F.; Cho, Y.; Tang, F.; Zykova, T.; Ma, W.; Bode, A.; Dong, Z. Cell apoptosis: requirement of H2AX in DNA ladder formation, but not for the activation of caspase-3. *Mol. Cell.* **2006,** *23,* 121-132.

27. Sluss, H.; Davis, R. H2AX is a target of the JNK signaling pathway that is required for apoptotic DNA fragmentation. *Mol. Cell.* **2006,** *23,* 152-153.

28. Lu, C.; Shi, Y.; Wang, Z.; Song, Z.; Zhu, M.; Cai, Q.; Chen, T. Serum starvation induces H2AX phosphorylation to regulate apoptosis via p38 MAPK pathway. *FEBS Lett.* **2008,** *582,* 2703-2708.

29. Huang, X.; Okafuji, M.; Traganos, F.; Luther, E.; Holden, E.; Darzynkiewicz, Z. Assessment of histone H2AX phosphorylation induced by DNA topoisomerase I and II inhibitors topotecan and mitoxantrone and by the DNA cross-linking agent cisplatin. *Cytometry A.* **2004,** *58,* 99-110.

30. Meador, J. A.; Zhao, M.; Su, Y. N. G.; Geard, C. R.; Balajee, A. S. Histone H2AX is a critical factor for cellular protection against DNA alkylating agents. *Oncogene* **2008,** *27,* 5662–5671.

31. Pines, A.; Kelstrup, C.; Vrouwe, M.; Puigvert, J.; Typas, D.; Misovic, B.; de Groot, A.; von Stechow, L.; van de Water, B.; Danen, E.; Vrieling, H.; Mullenders, L.; Olsen, J. Global phosphoproteome profiling reveals unanticipated networks responsive to cisplatin treatment of embryonic stem cells. *Mol. Cell Biol.* **2011,** *31,* 4964-4977.

32. Barr, M.; Gray, S.; Hoffmann, A.; Hilger, R.; Thomale, J.; O'Flaherty, J. D.; Fennell, D. A.; Richard, D.; O'Leary, J. J.; O'Byrne, K. J. Generation and Characterisation of Cisplatin-Resistant Non-Small Cell Lung Cancer Cell Lines Displaying a Stem-Like Signature. *PLoS ONE* **2013,** *8,* e54193.

33. Chiu, S.-J.; Chao, J.-I.; Lee, Y.-J.; Hsu, T.-S. Regulation of gamma-H2AX and securin contribute to apoptosis by oxaliplatin via a p38 mitogen-activated protein kinase-dependent pathway in human colorectal cancer cells. *Toxicology Letters* **2008,** *179,* 63-70.

CHAPTER 4

SYNTHESIS AND CHARACTERIZATION OF PT(II) COMPLEXES CONTAINING 4,4′-DIOLIGOOXYETHYLENE-2,2′-BIPYRIDINE LIGANDS FOR CANCER TREATMENT

4.1 Abstract

Five [Pt(II)Cl_2(4,4′-dioligooxyethylene-2,2′-bipyridine)] complexes were synthesized and their anti-proliferative activities were determined in a panel of human breast, lung, and prostate cancer cell lines. While in some cases, the synthesized platinum complexes were less active than cisplatin, they were generally more effective than carboplatin. A549 and MCF-7 cells were the least sensitive to treatment, and the SK-BR-3 and T-47D lines were most sensitive.

Two of the complexes, **Pt(II)-4O,2C** and **Pt(II)-5O,1C**, have some water solubility, but their activities were inferior to the non-water soluble compounds. **Pt(II)-4O,2C** was further studied in A549 and DU145 for analysis of cell death induction due to its activity and solubility. A549 and DU145 cells treated with **Pt(II)-4O,2C** had an increase in phosphorylated H2AX, indicating that **Pt(II)-4O,2C** caused DNA damage. Furthermore, results from analysis of PI, Annexin V/PI, Hoechst/PI, and PARP cleavage indicated that **Pt(II)-4O,2C** induced apoptosis; however, some necrosis was also observed.

4.2 Introduction

Since the discovery of its anti-tumoral property in the 1960s, cisplatin (a Pt(II) complex) has facilitated worldwide interest in utilizing metal compounds for clinical

applications.[1,2] Currently, cisplatin and its two analogues (carboplatin and oxaliplatin) are approved worldwide for the treatment of various cancers. Additionally, five other Pt(II) complexes (lobaplatin, dicycloplatin, nedaplatin, miriplatin, and heptaplatin) are approved in selected countries.[2–8] While platinum drugs are used in about 50% of all cancer chemotherapeutic regimens as single agents or in combination with other types of treatment, complications such as intrinsic or acquired resistance and severe side effects have restricted their usefulness.[2,4,8] To minimize these inadequacies, many researchers are putting efforts toward the development of compounds with improved efficacies and lower toxic side effects.

Numerous metal compounds have now been developed as potential cancer drugs through methods such as replacing the platinum center with other metals (*i.e*. ruthenium, palladium, *etc.*), changing the leaving groups, altering the amine groups, oxidation of the platinum center, and incorporation into a delivery system.[1,7,9–11] With an aspiration to develop alternative cancer drugs, we have previously reported on the synthesis and anti-proliferative effects of some novel Pt(II) complexes in which the amine ligands are replaced with 4,4′-dialkoxy-2,2′-bipyryl ligands (Chapter 2).[12] As have been demonstrated, these complexes are much more effective than cisplatin and carboplatin when evaluated in the A549 human lung cancer cell line. Furthermore, one of the complexes, **Pt(II)-4C**, was also more effective than cisplatin in the DU145 prostate cancer line, the MCF-7 breast cancer line, and the MDA-MB-435 melanoma line. While the *in vitro* data gave promising results, our attempts to test the toxicity of **Pt(II)-4C** in mice revealed the challenges of solubilizing the compound. Due to the hydrophobic nature of the compound, it had low solubility in some common organic solvents and

virtually none in water. Thus, to improve these compounds, the dialkoxy substituents were modified to have increasing oxygen which will result in increasing hydrogen bonding and water solubility.

Herein, the synthesis of a series of [Pt(II)Cl_2(4,4′-dioligooxyethylene-2,2′-bipyridine)] complexes of the general formula of [Pt(II)Cl_2(4,4′-bis(RO)-2,2′-bipyridine)] (where R = $–(CH_2CH_2O)_n(CH_2)_mCH_3$, n = 1–4, m = 0–3) is presented and their anti-proliferative activities against a panel of human breast, lung, and prostate cancers in comparison to cisplatin are described.

4.3 Experimental

4.3.1 General

All starting materials and reagents for the synthetic procedures were purchased from the commercial vendors (Sigma-Aldrich, TCI, Alfa-Aesar, or Acros) unless otherwise noted. They were of high purity and were used without further purification unless noted in the procedure. The compound used for synthesis of the ligands, 2,2′-bipyridine-4,4′-diol, was synthesized as described in Chapter 2.[12,13] Minimum essential medium (MEM), fetal bovine serum (FBS), phosphate buffered saline (PBS), trypsin-EDTA, and penicillin-streptomycin were purchased from Life Technologies (Carlsbad, CA). The RPMI 1640 medium was purchased from ATCC (Manassas, VA). Cisplatin, carboplatin, HEPES, albumin from bovine serum (BSA), propidium iodide, Hoechst 33342, methanol, and dimethyl sulfoxide (DMSO) were purchased from Sigma-Aldrich. All reagents and enzymes used for flow cytometry were of analytical grade qualities and were purchased from Sigma-Aldrich, unless otherwise noted.

4.3.2 Chemical characterization instrumentation

All of the NMR spectra were obtained utilizing a Varian spectrometer at 298 K or the indicated temperature using deuterated dimethyl sulfoxide (DMSO-d_6) or chloroform ($CDCl_3$) as the solvents: ^{1}H NMR, 400 MHz; and ^{13}C NMR, 100 MHz. Either residual solvent or tetramethylsilane (TMS) were used as the internal chemical shift reference. Thermal transitions were determined by using a TA Instruments DSC 2010 differential scanning calorimeter in nitrogen at heating and cooling rates of 10 °C min^{-1}. The temperature axis of the DSC thermogram was calibrated with reference standards of high purity indium and tin before use. An amount of 2-3 mg of compound was used in this measurement. The T_{onset} and T_{max} temperatures of a melting endotherm of a compound were recorded from the DSC thermogram as Mp (T_{onset}-T_{max}). Elemental analysis (EA) was determined by NuMega Resonance Labs Inc. (San Diego, CA) using a Perkin Elmer PE2400-Series II with a CHNS/O analyzer.

4.3.3 Preparation of monoalkoxy glycol tosylate compounds

4.3.3.1 Procedure A

The tosylate was synthesized following the procedure of Keddie *et al.*[14] with a slight modification of the reaction condition. The desired glycol (1.1 equiv.) was dissolved in CH_2Cl_2 and cooled to 0 °C. After addition of KOH (4 equiv.), a solution of *p*-toluenesulfonyl chloride (1 equiv.) in CH_2Cl_2 was slowly added while maintaining the temperature at 0 °C. When all of the *p*-toluenesulfonyl chloride was added, the mixture was further stirred at 4 °C for 24 h. The resulting white suspension was filtered to remove salt and water was added to the filtrate. The product was isolated by extraction with CH_2Cl_2 and dried over Na_2SO_4. The solvent was removed using a rotary evaporator

resulting in a colorless oily liquid. The final product was dried *in vacuo* overnight at 50 °C.

4.3.3.2 Procedure B

The tosylate was synthesized following the procedure of Lenz *et al.*[15] with a slight modification of the reaction condition. The desired glycol (1.1 equiv.) was added to a solution of 7 M KOH (40-60 ml) and cooled to 0 °C. To the reaction flask, *p*-toluenesulfonyl chloride (1 equiv.) was slowly added and the mixture was stirred at 0 °C for 3 h. The product was isolated by extraction with CH_2Cl_2 and dried over Na_2SO_4. The solvent was removed using a rotary evaporator and the colorless oily liquid was washed with hexane. The final product was dried *in vacuo* overnight at 50 °C.

OTs-2O,1C. Yield: 73% (prepared by procedure A). ^{1}H NMR (298 K, 400 MHz, $CDCl_3$): δ (ppm) = 7.81 (d, J = 8.2 Hz, 2H), 7.34 (d, J = 7.8 Hz, 2H), 4.16 (t, J = 4.7 Hz, 2H), 3.58 (t, J = 4.8 Hz, 2H), 3.31 (s, 3H), 2.45 (s, 3H).

OTs-3O,2C. Yield: 81% (prepared by procedure B). ^{1}H NMR (298 K, 400 MHz, $CDCl_3$): δ (ppm) = 7.80 (d, J = 8.3 Hz, 2H), 7.34 (d, J = 8.0 Hz, 2H), 4.17 (t, J = 4.9 Hz, 2H), 3.70 (t, J = 4.9 Hz, 2H), 3.61 – 3.55 (m, 2H), 3.54 – 3.45 (m, 4H), 2.45 (s, 3H), 1.19 (t, J = 7.0 Hz, 3H).

OTs-4O,2C. Yield: 91% (prepared by procedure B). ^{1}H NMR (298 K, 400 MHz, $CDCl_3$): δ (ppm) = 7.78 (d, J = 7.9 Hz, 2H), 7.32 (d, J = 8.0 Hz, 2H), 4.14 (t, J = 4.8, 2H), 3.66 (t, J = 4.9, 2H), 3.61 – 3.52 (m, 8H), 3.49 (m, 2H), 2.42 (s, 3H), 1.18 (t, J = 7.0 Hz, 3H).

OTs-4O,4C. Yield: 76% (prepared by procedure B). ^{1}H NMR (298 K, 400 MHz, $CDCl_3$): δ (ppm) = 7.79 (d, J = 8.3 Hz, 2H), 7.33 (d, J = 8.1 Hz, 2H), 4.15 (t, J = 4.9 Hz,

2H), 3.68 (t, J = 4.9 Hz, 2H), 3.63 – 3.51 (m, 8H), 3.44 (t, J = 6.7 Hz, 2H), 2.44 (s, 3H), 1.60 – 1.49 (m, 2H), 1.41 – 1.27 (m, 2H), 0.90 (t, J = 7.4 Hz, 3H).

OTs-5O,1C. Yield: 86% (prepared by procedure B). ^{1}H NMR (298 K, 400 MHz, $CDCl_3$): δ (ppm) = 7.77 (d, J = 8.3 Hz, 2H), 7.32 (d, J = 8.0 Hz, 2H), 4.13 (t, J = 4.7 Hz, 2H), 3.66 (t, J = 4.9 Hz, 2H), 3.63 – 3.49 (m, 12H), 3.34 (s, 3H), 2.42 (s, 3H).

4.3.4 Preparation of 4,4′-dioligooxyethylene-2,2′-bipyridine

The appropriate tosylate (2.1 equiv.) was slowly added to a mixture of 2,2′-bipyridine-4,4′-diol (1 equiv.) and Cs_2CO_3 (2.3 equiv.) in DMF, and the suspension was heated to reflux for 48 h. The salt was removed by vacuum filtration and washed with CH_2Cl_2. A rotary evaporator was used to remove the solvents from the solution. The crude product was dissolved in CH_2Cl_2, filtered to remove any remaining salt, and washed with hexane. The product was further purified by recrystallization in the noted solvent or by extraction with CH_2Cl_2, dried over Na_2SO_4, and the solvent removed by a rotary evaporator. The final product was dried *in vacuo* for 48 h.

L-2O,1C. Yield: 77%, white crystals (by recrystallization in acetone-hexane). Mp 99-101 °C. ^{1}H NMR (298 K, 400 MHz, DMSO-d_6): δ (ppm) = 8.44 (d, J = 5.6 Hz, 1H), 7.88 (s, 1H), 7.00 (d, J = 5.5 Hz, 1H), 4.24 (d, J = 4.2 Hz, 2H), 3.67 (t, J = 4.2 Hz, 2H), 3.29 (s, 3H). ^{13}C NMR (298 K, 100 MHz, DMSO-d_6): δ (ppm) = 165.85, 157.27, 150.94, 111.55, 106.79, 70.44, 67.58, 58.63. Anal. Calcd for $C_{16}H_{20}N_2O_4$ (304.35 g mol^{-1}): C, 63.14; H, 6.62; N, 9.20%; found: C, 63.26; H, 6.85; N, 9.32%.

L-3O,2C. Yield: 79%, white solid. Mp 43–45 °C. ^{1}H NMR (298 K, 400 MHz, $CDCl_3$): δ (ppm) = 8.45 (d, J = 5.6 Hz, 1H), 7.97 (d, J = 2.6 Hz, 1H), 6.86 (dd, J = 5.7, 2.6 Hz, 1H), 4.30 (t, J = 4.8 Hz, 2H), 3.90 (t, J = 4.7 Hz, 2H), 3.72 (t, J = 4.7 Hz, 2H),

3.61 (t, J = 4.7 Hz, 2H), 3.58–3.46 (m, 2H), 1.21 (t, J = 7.0, 3H). ^{13}C NMR (298 K, 100 MHz, $CDCl_3$): δ (ppm) = 165.84, 157.81, 150.12, 111.47, 106.66, 71.00, 69.87, 69.39, 67.47, 66.71, 15.16. Anal. Calcd for $C_{22}H_{32}N_2O_6$ (420.50 g mol^{-1}): C, 62.87; H, 7.67; N, 6.66%; found: C, 61.87; H, 7.45; N, 6.75%. EA results showed a possibility of the hydrated form $C_{22}H_{32}N_2O_6 \bullet 0.5\ H_2O$. Anal. Calcd for $C_{22}H_{32}N_2O_6 \bullet 0.5\ H_2O$ (429.51 g mol^{-1}): C, 61.52; H, 7.74; N, 6.52%; found: C, 61.67; H, 7.45; N, 6.75%.

L-4O,2C. Yield: 83%, pale yellow oil. ^{1}H NMR (298 K, 400 MHz, $CDCl_3$): δ (ppm) = 8.44 (d, J = 5.6 Hz, 1H), 7.96 (d, J = 2.5 Hz, 1H), 6.85 (dd, J = 5.7, 2.6 Hz, 1H), 4.35–4.25 (m, 2H), 3.92–3.87 (m, 2H), 3.75–3.71 (m, 2H), 3.70–3.62 (m, 4H), 3.60–3.55 (m, 2H), 3.54–3.47 (m, 2H), 1.19 (t, J = 7.0 Hz, 3H). ^{13}C NMR (298 K, 100 MHz, $CDCl_3$): δ (ppm) = 165.85, 157.82, 150.12, 111.49, 106.63, 70.94, 70.75, 70.67, 69.82, 69.38, 67.48, 66.63, 15.17. Anal. Calcd for $C_{26}H_{40}N_2O_8$ (508.60 g mol^{-1}): C, 61.40; H, 7.93; N, 5.51%; found: C, 60.33; H, 8.63; N, 5.71%. EA results showed a possibility of the hydrated form $C_{26}H_{40}N_2O_8 \bullet 0.5\ H_2O$. Anal. Calcd for $C_{26}H_{40}N_2O_8 \bullet 0.5\ H_2O$ (517.61 g mol^{-1}): C, 60.33; H, 7.98; N, 5.41%; found: C, 60.33; H, 8.63; N, 5.71%.

L-4O,4C. Yield: 70%, pale yellow oil. ^{1}H NMR (298 K, 400 MHz, $CDCl_3$): δ (ppm) = 8.44 (d, J = 5.7 Hz, 1H), 7.96 (d, J = 2.6 Hz, 1H), 6.85 (dd, J = 5.6, 2.5 Hz, 1H), 4.29 (t, J = 4.7 Hz, 2H), 3.89 (t, J = 4.9 Hz, 2H), 3.75–3.54 (m, 8H), 3.44 (t, J = 6.7 Hz, 2H), 1.62–1.50 (m, 2H), 1.41–1.27 (m, 2H), 0.89 (t, J = 7.4 Hz, 3H). ^{13}C NMR (298 K, 100 MHz, $CDCl_3$): δ (ppm) = 165.87, 157.75, 150.09, 111.49, 106.69, 71.20, 70.94, 70.71, 70.67, 70.07, 69.36, 67.49, 31.71, 19.27, 13.93. Anal. Calcd for $C_{30}H_{48}N_2O_8$ (564.71 g mol^{-1}): C, 63.81; H, 8.57; N, 4.96%; found: C, 62.09; H, 8.87; N, 4.91%. EA results showed a possibility of the monohydrated form $C_{30}H_{48}N_2O_8 \bullet H_2O$. Anal. Calcd

for $C_{30}H_{48}N_2O_8 \bullet H_2O$ (582.73 g mol^{-1}): C, 61.83; H, 8.65; N, 4.81%; found: C, 62.09; H, 8.87; N, 4.91%.

L-5O,1C. Yield: 84%, pale yellow oil. ^{1}H NMR (298 K, 400 MHz, $CDCl_3$): δ (ppm) = 8.44 (d, J = 5.7 Hz, 1H), 7.96 (d, J = 2.5 Hz, 1H), 6.86 (dd, J = 5.6, 2.5 Hz, 1H), 4.29 (t, J = 4.8 Hz, 2H), 3.89 (t, J = 4.8 Hz, 2H), 3.77 – 3.59 (m, 10H), 3.57 – 3.49 (m, 2H), 3.36 (s, 3H). ^{13}C NMR (298 K, 100 MHz, $CDCl_3$): δ (ppm) = 165.96, 157.91, 150.23, 111.60, 106.76, 72.05, 71.03, 70.77, 70.76, 70.73, 70.63, 69.48, 67.59, 59.15. Anal. Calcd for $C_{28}H_{44}N_2O_{10}$ (568.66 g mol^{-1}): C, 59.14; H, 7.80; N, 4.99%; found: C, 58.75; H, 7.93; N, 5.31%.

4.3.5 Preparation of [Pt(II)Cl_2(4,4′-dioligooxyethylene-2,2′-bipyridine)] complexes

A concentrated solution of $K_2[PtCl_4]$ (1.0 equiv.) in H_2O (1–2 mL) was added to a solution of 4,4′-dioligooxyethylene-2,2′-bipyridine (1.0 equiv.) in acetone. The mixture was then heated to reflux for 24 h and the acetone was removed by using a rotary evaporator resulting in either a yellow suspension or a yellow wax-like solid. For reactions resulting in a yellow suspension, the crude product was collected by vacuum filtration and the final product was obtained by recrystallization in the noted solvent and dried *in vacuo* at 70 °C for 24 h. For reactions resulting in a yellow wax-like solid, the product was purified by extraction with CH_2Cl_2 and dried over Na_2SO_4. The solvent was removed using a rotary evaporator and the solid residue was washed with hexane. The final product was collected and dried *in vacuo* for 24 h.

Pt(II)-2O,1C. Yield: 86%, bright yellow solid (by recrystallization in $CHCl_3$). Mp 206–207 °C. ^{1}H NMR (298 K, 400 MHz, DMSO-d_6): δ (ppm) = 9.10 (d, J = 6.7 Hz, 1H), 8.21 (s, 1H), 7.39 (d, J = 6.6 Hz, 1H), 4.43 (t, J = 4.3 Hz, 2H), 3.74 (t, J = 4.2 Hz,

2H), 3.33 (s, 3H). ^{13}C NMR (298 K, 100 MHz, DMSO-d_6): δ (ppm) = 167.45, 158.46, 149.46, 113.55, 111.32, 70.13, 69.28, 58.64. Anal. Calcd for $C_{16}H_{20}Cl_2N_2O_4Pt$ (570.25 g mol^{-1}): C, 33.69; H, 3.53; N, 4.91%; found: C, 33.76; H, 3.70; N, 4.93%.

Pt(II)-3O,2C. Yield: 78%, bright yellow solid (by extraction, then recrystallization in isopropanol). Mp 126–130 °C. ^{1}H NMR (298 K, 400 MHz, $CDCl_3$): δ (ppm) = 8.86 (d, J = 6.8 Hz, 1H), 7.48 (d, J = 2.8 Hz, 1H), 6.85 (dd, J = 6.8, 2.7 Hz, 1H), 4.53–4.46 (m, 2H), 4.00–3.93 (m, 2H), 3.78–3.71 (m, 2H), 3.67– 3.59 (m, 2H), 3.57–3.50 (m, 2H), 1.21 (t, J = 7.0 Hz, 3H). ^{13}C NMR (298 K, 100 MHz, $CDCl_3$): δ (ppm) = 166.94, 157.77, 149.03, 113.20, 110.19, 70.94, 69.81, 69.24, 69.15, 66.71, 15.19. Anal. Calcd for $C_{22}H_{32}Cl_2N_2O_6Pt$ (686.47 g mol^{-1}): C, 38.49; H, 4.70; N, 4.08%; found: C, 38.26; H, 5.01; N, 4.10%.

Pt(II)-4O,2C. Yield: 72%, bright yellow solid (by extraction). Mp 94–98 °C. ^{1}H NMR (298 K, 400 MHz, $CDCl_3$): δ (ppm) = 8.84 (d, J = 6.8 Hz, 1H), 7.47 (d, J = 2.8 Hz, 1H), 6.86 (dd, J = 6.8, 2.7 Hz, 1H), 4.49 (t, J = 4.4 Hz, 2H), 3.95 (t, J = 4.5 Hz, 2H), 3.79–3.49 (m, 10H), 1.20 (t, J = 7.0 Hz, 3H). ^{13}C NMR (298 K, 100 MHz, $CDCl_3$): δ (ppm) = 166.93, 157.69, 148.99, 113.24, 110.21, 70.82, 70.69, 70.60, 69.79, 69.27, 69.13, 66.65, 15.18. Anal. Calcd for $C_{26}H_{40}Cl_2N_2O_8Pt$ (774.59 g mol^{-1}): C, 40.32; H, 5.21; N, 3.62%; found: C, 39.91; H, 5.61; N, 3.77.

Pt(II)-4O,4C. Yield: 93%, bright yellow solid (by extraction). Mp 109–114°C. ^{1}H NMR (298 K, 400 MHz, $CDCl_3$): δ (ppm) = 9.04 (d, J = 6.8 Hz, 1H), 7.42 (d, J = 2.8 Hz, 1H), 6.87 (dd, J = 6.8, 2.7 Hz, 1H), 4.39 (t, J = 4.5 Hz, 2H), 3.89 (t, J = 4.5 Hz, 2H), 3.70–3.48 (m, 8H), 3.38 (t, J = 6.7 Hz, 2H), 1.51–1.43 (m, 2H), 1.34–1.22 (m, 2H), 0.83 (t, J = 7.4 Hz, 3H). ^{13}C NMR (298 K, 100 MHz, $CDCl_3$): δ (ppm) = 166.64, 157.33,

148.13, 113.36, 110.18, 71.07, 70.62, 70.55, 70.48, 69.95, 69.12, 68.98, 31.60, 19.17, 13.86. Anal. Calcd for $C_{30}H_{48}Cl_2N_2O_8Pt$ (830.69 g mol^{-1}): C, 43.38; H, 5.82; N, 3.37%; found: C, 43.34; H, 6.30; N, 3.65%.

Pt(II)-5O,1C. Yield: 85%, wax-like yellow solid (by extraction). Mp 48–58 °C. ^{1}H NMR (298 K, 400 MHz, $CDCl_3$): δ (ppm) = 8.79 (d, J = 6.8 Hz, 1H), 7.48 (d, J = 2.8 Hz, 1H), 6.84 (d, J = 6.8 Hz, 1H), 4.48 (t, J = 4.5 Hz, 2H), 3.94 (t, J = 4.4 Hz, 2H), 3.77 – 3.59 (m, 10H), 3.56 – 3.49 (m, 2H), 3.35 (s, 3H). ^{13}C NMR (298 K, 100 MHz, $CDCl_3$): δ (ppm) = 167.06, 157.87, 149.11, 113.33, 110.36, 72.05, 70.94, 70.72 (3C overlapped), 70.64, 69.40, 69.25, 59.16. Anal. Calcd for $C_{28}H_{44}Cl_2N_2O_{10}Pt$ (834.65 g mol^{-1}): C, 40.29; H, 5.31; N, 3.36%; found: C, 40.50; H, 5.51; N, 3.64%.

4.3.6 Cell culture

Human breast (HCC38, MCF-7, MDA-MB-231, SK-BR-3, T-47D, and ZR-75-1), lung (A549 and H520), and prostate (DU145 and PC-3) cancer cell lines were obtained from American Culture Type Collection (ATCC). The A549, HCC38, MCF-7, MDA-MB-231, SK-BR-3, T-47D, and ZR-75-1 cells were grown in MEM supplemented with 10% FBS, 25 mM HEPES buffer (pH 7.4), penicillin (100 U mL^{-1}) and streptomycin (100 µg mL^{-1}). The H520, DU145, and PC-3 cell lines were grown in RPMI-1640 supplemented with 10% FBS, 25 mM HEPES buffer (pH 7.4), penicillin (100 U mL^{-1}) and streptomycin (100 µg mL^{-1}). All cell lines were maintained at 37 °C in a humidified, 5% CO_2 atmosphere.

4.3.7 Cell viability assay

Cells were cultured at a density of 2–3.5 x 10^3 cells per well in flat bottomed 96-well plates in 100 µL of complete growth medium and incubated for 2 d to reach ~ 50%

confluence. The cells were then treated with solvent or the appropriate drugs (CDDP stock was dissolved in 0.15 M NaCl, carboplatin stock was dissolved in 5% glucose, synthesized Pt(II) complexes were dissolved in DMSO) for 1 h, washed three times with 100 μL PBS, and incubated in 100 μL of fresh medium. After 2 d, the medium was replaced with 120 μL of medium containing CellTiter 96® Aq_{ueous} One Solution Reagent (MTS reagent) (Promega, Madison, WI). The cells were incubated at 37 °C for 4 h and the cell viability was determined by measuring the absorbance at 490 nm using a Tecan Infinite M1000 microplate reader. The 48 h treatment was done in a similar method, except the cells were not washed after treatment and the MTS reagent was immediately added. Viability of treated groups was calculated as a percent of control and graphed with GraphPad Prism.

4.3.8 Flow cytometry

4.3.8.1 Propidium iodide (PI) staining

Cells (~50-60% confluent in 60 mm dishes) were treated as indicated with the platinum compound. After the treatment duration, the floating cells were collected, and both attached and floating cells were washed 2X with PBS. The cells were resuspended in fresh medium and incubated as indicated. The cells were harvested (both the floating and attached cells were collected), counted, and pelleted. The cells were then washed two times with 5 mL PBS, fixed by resuspending in 0.1 mL of PBS and 1 mL of ice-cold 95% ethanol with gentle vortexing. Fixed cells were stored at 4 °C until analysis. For analysis, fixed cells were washed once with 1–2 mL of PBS and centrifuged at 500 × g for 5 minutes. The cell pellet was resuspended in 100 μL of a 1.0% Triton X-100 buffer solution, and 100 μL of a 1.0 mg mL^{-1} RNAse solution was added and allowed to stand at

room temperature for 10–15 min. While in the dark, 200 µL of a 100 µg mL^{-1} PI stain was added to make a final concentration of 50 µg mL^{-1} and gently vortexed. The cell mixture was incubated at room temperature for 30 min and flow cytometry acquisition was done on a Becton Dickinson FACS Calibur with the argon laser set at 488 nm on the linear Flow Channel 2 (FL-2) with Doublet Discriminatory Module (DDM) and threshold set on FL-2.

4.3.8.2 Annexin V-FITC/PI staining

Cells (~50–60% confluent in 60 mm dishes) were treated as indicated with the platinum compound. After the treatment duration, the floating cells were collected, and both attached and floating cells were washed 2X with PBS. The cells were resuspended in fresh medium and incubated as indicated. The cells were harvested (both the floating and attached cells were collected), counted, and pelleted. The cells were then washed two times with 5 mL of Ca^{2+} and Mg^{2+} free PBS. The pellets were then washed in 2.0 mL of 1X Annexin-V Binding buffer (BD Bioscience, San Jose, CA) and centrifuged at 500 × g for 5 min. The pellets were treated with Annexin-V-FITC conjugate (BD Bioscience, San Jose, CA) and incubated in the dark for 15 min. Just before acquisition, the volume of cells-conjugate mixture was adjusted by addition of 1X Annexin-V binding buffer. Acquisition to discriminate between apoptotic and necrotic cells was done by staining the cell-conjugate mixture with 10 µL of PI (50 µg mL^{-1}) solution (BD Bioscience, San Jose, CA). Acquisitions were done on a FACS Calibur Cytometer on the FL1 (Annexin) and FL3 (PI) channels with threshold and Duplet Discriminating Module (DDM) set at FL1. The level of shift in events distribution in the Annexin-V only and Annexin-V-PI populations in comparison to control is indicative of degree of effectiveness of the

treatment agents. A quantitative measure of these event shifts was accomplished by gating.

4.3.8.3 Flow cytometric immunofluorescence

Cells (200,000–250,000) were seeded in 60 mm dishes and incubated at 37 °C in a humidified, 5% CO_2 atmosphere for 2 d to reach ~50–60% confluence. The cells were treated with the platinum complexes as indicated, the floating cells were collected, and both attached and floating cells were washed 2X with PBS. The cells were resuspended in fresh medium and incubated as indicated. After incubation, both the floating and attached cells were collected and fixed by incubation in 4% formaldehyde for 10 min at room temperature. The fixed cells were pelleted and permeabilized by incubation in 500 µL of ice-cold methanol at 4 °C for 10 min. The samples were stored at -20 °C until analysis. For analysis, the cells were pelleted and washed 2X with 1% BSA in PBS. The cells were resuspended in BD Stain Buffer (BS Biosciences #554656) containing the appropriate conjugated primary antibody [PE Mouse Anti-Cleaved PARP (Asp214) and Alexa Fluor 647 Mouse Anti-H2AX (pS139) antibodies were purchased as a part of a Cell Proliferation Kit (BD Biosciences #562253)], and incubated at 4 °C overnight. After washing 2X with 1% BSA, the cells were resuspended in PBS and analyzed on a Becton Dickinson FACS Calibur.

4.3.9 Confocal microscopy

Cells (100,000–125,000) were seeded into 35 mm dishes and incubated for 48 h at 37 °C. The cells were treated as indicated, and while in the dark, the cells were washed twice with 1 mL PBS. After washing, 1 mL of a 2 µg mL^{-1} Hoechst 33342 and 10 µg mL^{-1} PI solution (in PBS) was added and the cells were incubated for 15 min at room

temperature. Images were acquired within 5 min with a Nikon A1R confocal laser scanning microscopy system (CLSM) mounted on a Nikon Eclipse Ti. At least three random areas on each dish were imaged.

4.3.10 Statistical analysis

GraphPad Prism was used to graph viability curves. ModFit version 3.0 was used for the flow cytometry analysis. Microsoft Office Excel was used to perform unpaired Student's t-test; values with $p < 0.05$ were considered significant. Student's t-tests were used to verify significant differences among the EC_{50} values.

4.4 Results and discussion

4.4.1 Synthesis and characterization

A method similar to the synthesis of the [Pt(II)Cl_2(4,4′-dialkoxy-2,2′-bipyridine)] complexes was used to synthesize the [Pt(II)Cl_2(4,4′-dioligooxyethylene-2,2′-bipyridine)] complexes (Scheme 4-1), except the ligands were synthesized using tosylate compounds as alkylating agents instead of alkylhalides. The tosylates were prepared from the desired glycols (containing increasing number of oxyethylene linkages and varying terminal carbon number) by following previously described procedures.[14,15] All of the tosylate compounds were colorless liquids and the yields were moderate to high (73–

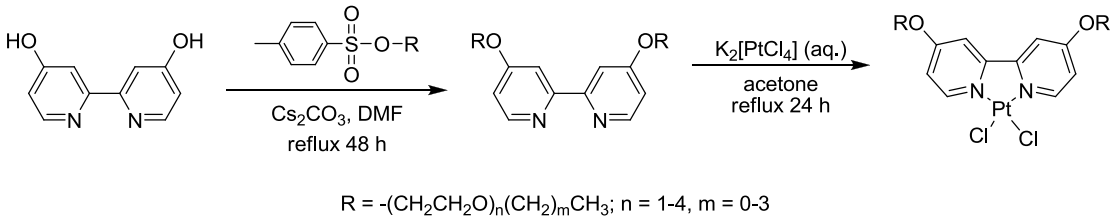

Scheme 4 – 1. Synthesis of [Pt(II)Cl_2(4,4′-dioligooxyethylene-2,2′-bipyridine)] complexes.

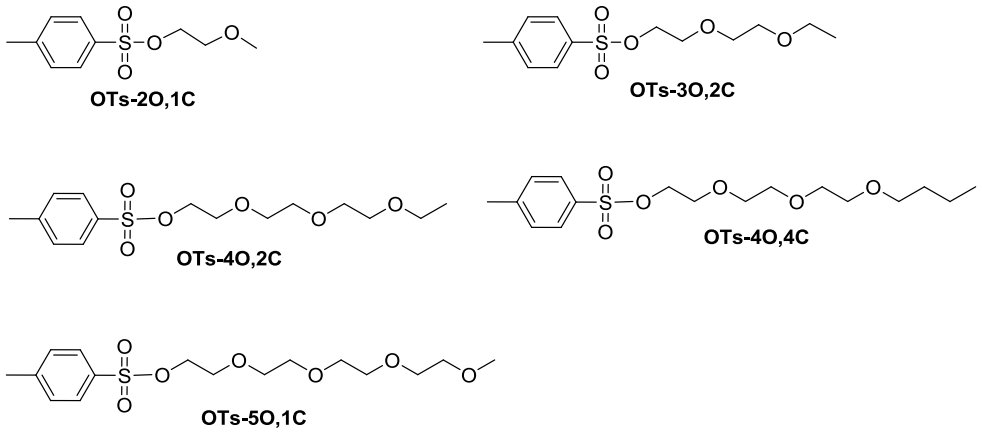

Figure 4 – 1. Structures of monoalkoxy glycol tosylate compounds.

91%). The structures of these tosylate compounds (Figure 4-1) were confirmed by proton NMR and used for the preparation of the ligands without further analysis.

The ligands were synthesized by reacting the respective tosylate compound with a mixture of 2,2′-bipyridine-4,4′-diol and Cs_2CO_3 in DMF on heating to reflux for 48 h. The yields for the ligands range from 70-84%. The platinum complexes were prepared by reacting the ligands with $K_2[PtCl_4]$ for 24 h on reflux. As was observed for the previously synthesized Pt(II) complexes, the formation of the product was monitored by the appearance of a yellow solid or solution. The structures of the synthesized platinum complexes are shown in Figure 4-2. The yields of the platinum complexes were in the range of 72–93%. All of the ligands and platinum complexes were characterized by ^{1}H and ^{13}C NMR spectroscopy, EA, and DSC measurements.

^{1}H and ^{13}C NMR spectra of the ligands and platinum complexes displayed the expected resonances. Formation of the ligand was marked by the disappearance of the tosylate characteristic aromatic peaks and appearance of the bipyridyl aromatic peaks in

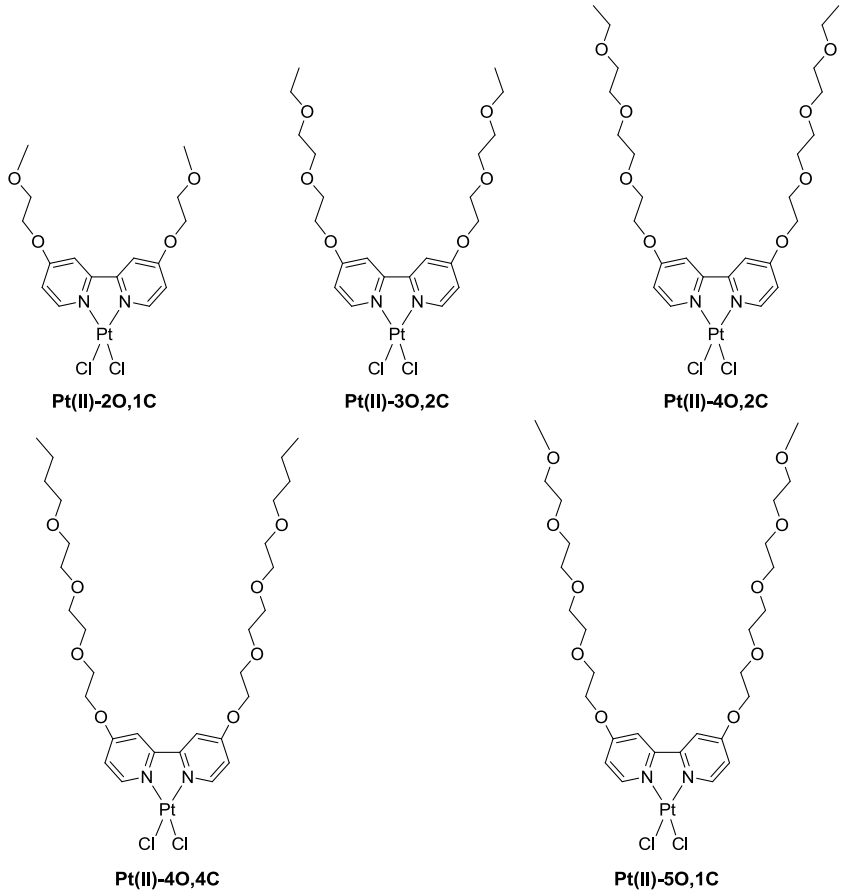

Figure 4 – 2. Chemical structures of the synthesized [Pt(II)Cl_2(4,4′-dioligooxyethylene-2,2′-bipyridine)] complexes.

the ^{1}H NMR spectra. Coordination of the ligands to the Pt was confirmed by observing the shifting of the bipyridyl aromatic peaks towards downfield.

Elemental analysis of the ligands, **L-2O,1C** and **L-5O,1C**, matched with that of the calculated values (within 0.5%); however, the carbon values for **L-3O,2C** and **L-4O,2C**, were 1% less than the calculated values. When considering the possibility of having hydration due to the many oxygen atoms in their structures, the EA results matched the calculated values for a hydrated form of **L-3O,2C** and **L-4O,2C** with 0.5 mol of H_2O. Further purification of **L-4O,2C** or re-synthesis did not improve the carbon

result. The carbon for **L-4O,4C** was also less than the calculated value; however, the EA result matched the calculated value for a monohydrated form of **L-4O,4C**. Elemental analysis of all the platinum complexes matched well with the calculated values (within 0.5%).

The melting point of the ligands decreased as the oxygen number increased. The DSC thermogram of **L-2O,1C** (contains two oxygens in each substituent) showed an endothermic transition at 99–100 °C, which is an indication of a melting transition. This melting transition was observed in the **L-3O,2C** (three oxygens in each substituent) DSC thermogram at 43–45 °C. **L-4O,2C**, **L-4O,4C**, and **L-5O,1C** were all liquid compounds and thus DSC analysis was not performed. Coordination to platinum caused an increase in the melting temperature and, similar to the ligands, the melting points of the platinum complexes decreased as the oxygen number increased. **Pt(II)-2O,1C** has the highest melting temperature with a sharp endothermic transition at 206–207 °C. **Pt(II)-5O,1C**, with the most oxygen in its structure, has a broad melting point at 48–58 °C. **Pt(II)-4O,2C** and **Pt(II)-4O,4C** have the same number of oxygen atoms, but **Pt(II)-4O,4C** has two more carbons on each end of the substituents than **Pt(II)-4O,2C**, which resulted in a higher melting temperature.

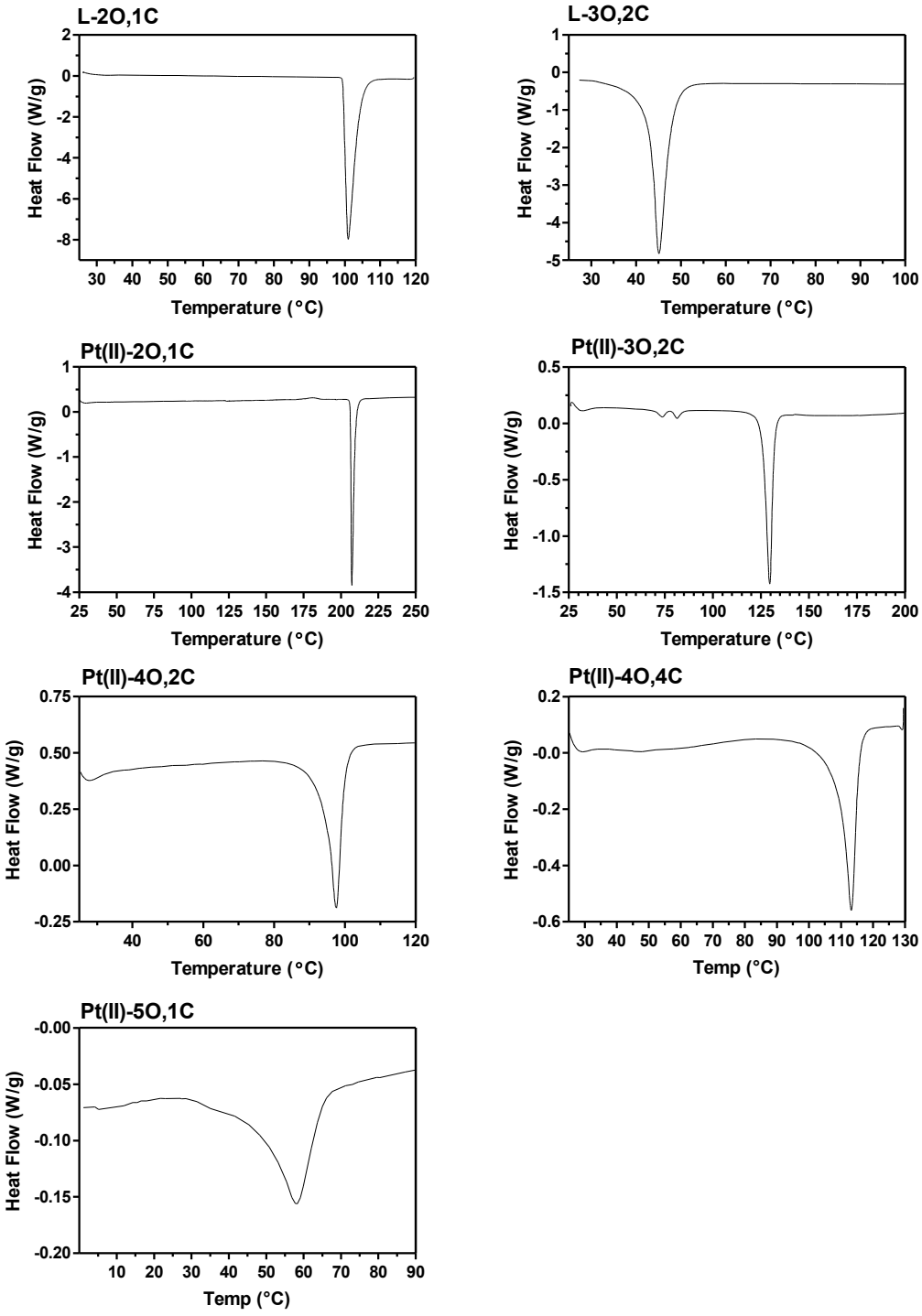

Figure 4 – 3. DSC thermograms of the [Pt(II)Cl_2(4,4′-dioligooxyethylene-2,2′-bipyridine)] complexes. The thermograms were obtained in the first heating cycles in nitrogen at heating and cooling rates of 10 °C/min.

The structure of **Pt(II)-2O,1C** is similar to **Pt(II)-4C**, except one of the carbons in each chain of the alkoxy substituent is replaced by an oxygen. Although the solubility of **Pt(II)-2O,1C** in common organic solvents is slightly improved, it was still poorly soluble in water. **Pt(II)-3O,2C**, which has an additional oxygen on each substituent by the addition of another oxyethylene linkage, is also poorly soluble in water. **Pt(II)-4O,4C** is also poorly soluble, but **Pt(II)-4O,2C** and **Pt(II)-5O,1C** both have some solubility in water (a 5 mM solution can be made).

4.4.2 Biological properties

4.4.2.1 *In vitro* cytotoxic activity

Three of the most commonly diagnosed cancers are breast, lung and prostate; thus, the anti-proliferative activities of the synthesized complexes were examined in human breast (HCC38, MCF-7, MDA-MB-231, SK-BR-3, T-47D, and ZR-75-1), lung (A549 and H520), and prostate (DU145 and PC-3) cancer cell lines using the MTS cell proliferation assay. The graphs of the results for a representative cell line from each type of cancer treated for 1 or 48 h with cisplatin, carboplatin, or the synthesized platinum complexes are shown in Figure 4-4 (DU145 cells), Figure 4-5 (MCF-7 cells), and Figure 4-6 (A549 cells). As shown in Figure 4-4, the viability of DU145 cells treated with the highest concentration of cisplatin (1 mM) was reduced by about 60%, while carboplatin had negligible effects. **Pt(II)-2O,1C** and **Pt(II)-3O,2C** were only tested up to a concentration of 100 μM due to limited solubility and had about the same effect as cisplatin at the concentrations tested. However, they were more effective than carboplatin. It is interesting to note that, with only a change of one carbon to an oxygen, the anti-proliferative activity of **Pt(II)-2O,1C** (EC_{50} for the 1 h treatment is 80 ± 20) is

greatly reduced compared to **Pt(II)-4C** (EC_{50} for the 1 h treatment is 12 ± 8, Chapters 2 and 3). While **Pt(II)-4O,2C** and **Pt(II)-5O,1C** have water solubility, **Pt(II)-4O,2C** had similar activity to cisplatin and **Pt(II)-5O,1C** was not as active. However, it is worth noting that **Pt(II)-4O,2C** is more effective than carboplatin. **Pt(II)-4O,4C** was the most effective; however, poor water solubility remains an issue. Similar results were observed for the 48 h treatment. All of the complexes were more effective than carboplatin, except **Pt(II)-5O,1C**, which had similar activity. Cisplatin was slightly more effective than **Pt(II)-2O,1C**, **Pt(II)-3O,2C**, and **Pt(II)-4O,2C**.

Similar results were obtained for A549 and MCF-7. It should be noted that, compared to DU145 cells, these cell lines are more resistant to cisplatin and all the other platinum complexes. The EC_{50} values obtained from the MTS data for all the tested cell lines are given in Tables 4-1 to 4-4. Comparison of the EC_{50} values indicates varying degrees of activity across the different cell lines. A549 and MCF-7 are the most resistant to treatment and SK-BR-3, ZR-75-1, and T-47D are generally more sensitive to the synthesized platinum complexes than to cisplatin for the 1 h treatment.

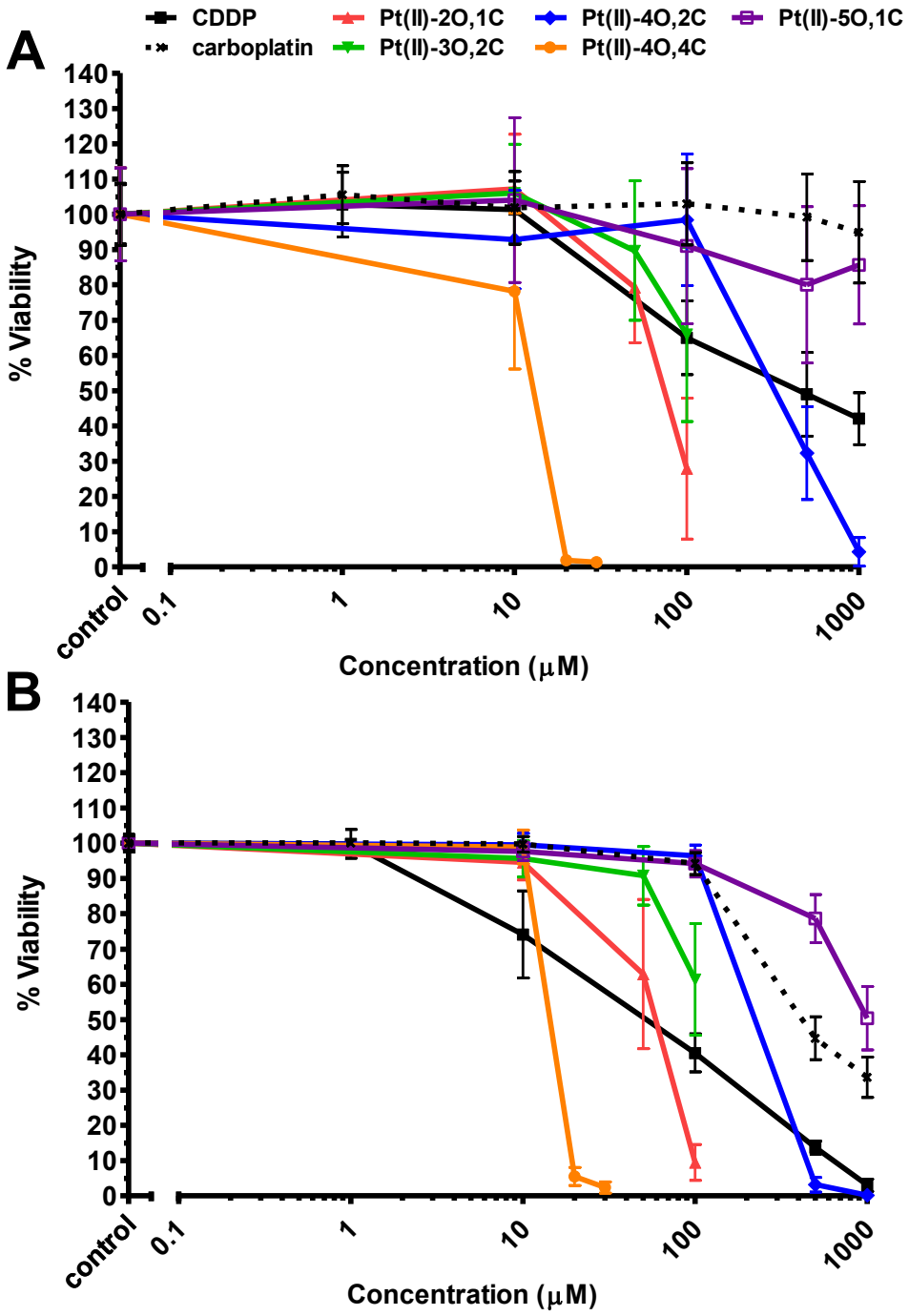

Figure 4 – 4. DU145 cell viability from MTS cell proliferation assays post (A) 1 h or (B) 48 h treatment.

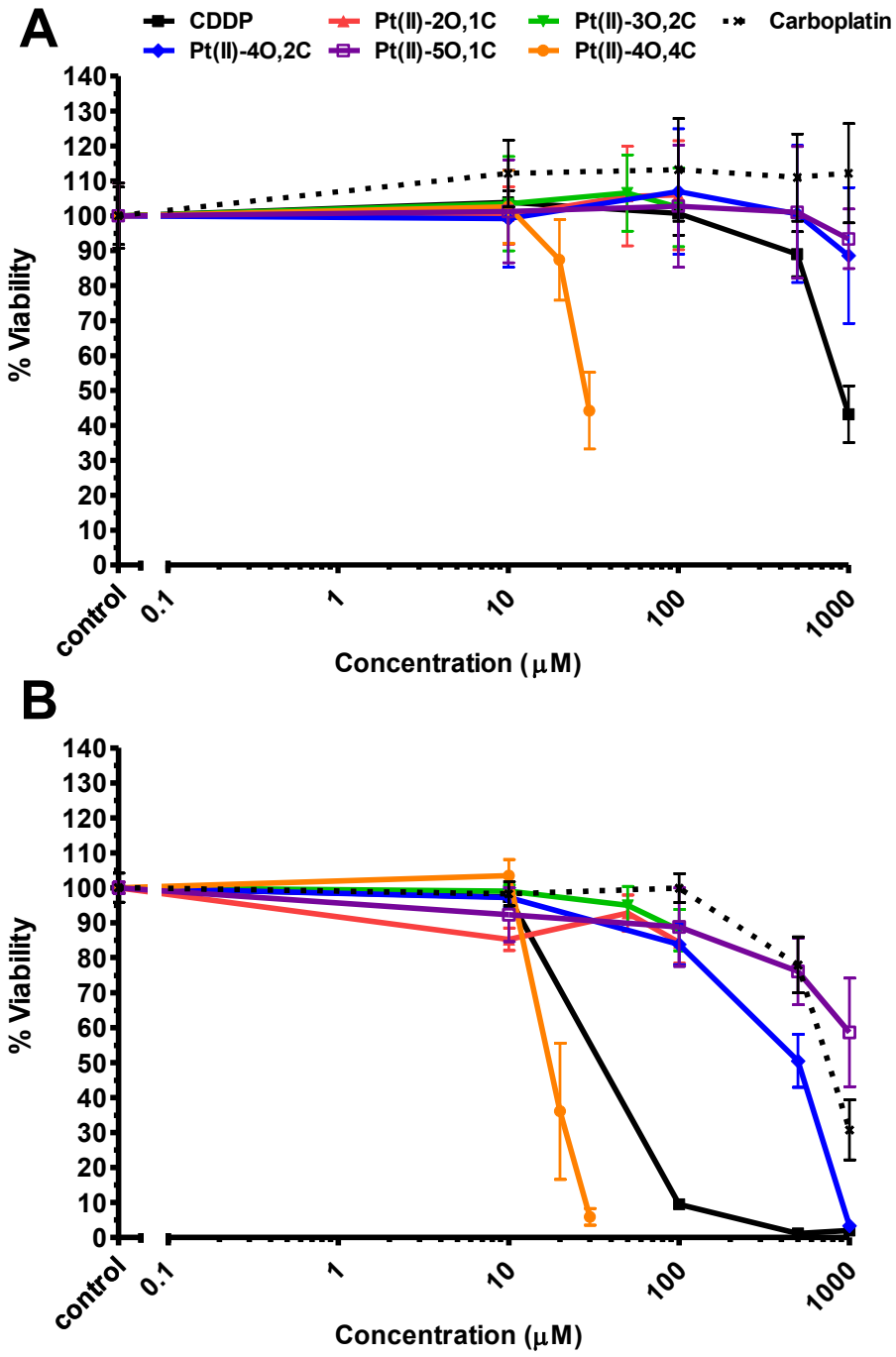

Figure 4 – 5. MCF-7 cell viability from MTS cell proliferation assays post (A) 1 h or (B) 48 h treatment.

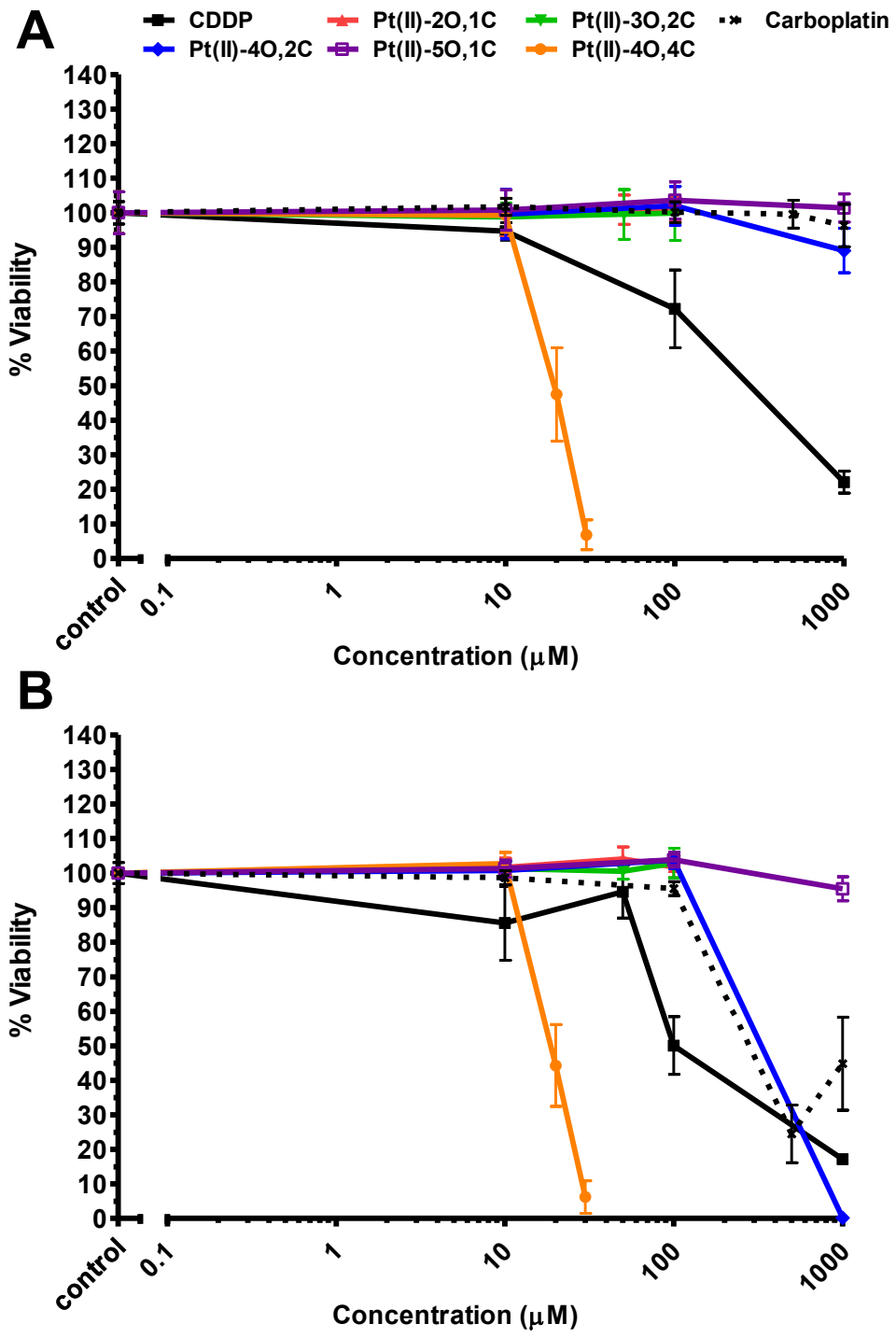

Figure 4 – 6. A549 cell viability from MTS cell proliferation assays post (A) 1 h or (B) 48 h treatment.

Table 4 – 1. EC_{50} (μM) of [Pt(II)Cl_2(4,4′-dioligooxyethylene-2,2′-bipyridine)] complexes in A549 and H520 post 1 or 48 h treatment

	Lung cancer			
	A549		H520	
	1 h	48 h	1 h	48 h
CDDP	900 ± 200	500 ± 100	200 ± 17	24 ± 2
Carboplatin	>1000	300 ± 30	ND	ND
Pt(II)-2O,1C	>100	>100	>100	36 ± 3[a]
Pt(II)-3O,2C	>100	>100	>100	60 ± 10
Pt(II)-4O,2C	>1000	330 ± 5	150 ± 100	197 ± 0[a]
Pt(II)-4O,4C	17 ± 4[a]	17 ± 3[a,b]	13.1 ± 0.9 [a]	12.1 ±0.5
Pt(II)-5O,1C	>1000	>1000	>1000	400 ± 100

Values represent the mean ± SD of at least two independent experiments done in quadruplicates. ND = no data. [a] $P < 0.5$ compared to CDDP. [b] $P < 0.05$ compared to carboplatin.

Table 4 – 2. EC_{50} (μM) of [Pt(II)Cl_2(4,4′-dioligooxyethylene-2,2′-bipyridine)] complexes in DU145 and PC-3 post 1 or 48 h treatment

	Prostate cancer			
	DU145		PC-3	
	1 h	48 h	1 h	48 h
CDDP	400 ± 100	64 ± 8	200 ± 20	30 ± 1
Carboplatin	>1000	400 ± 100[a]	ND	ND
Pt(II)-2O,1C	80 ± 20	60 ± 20[b]	90 ± 20[a]	70 ± 10[a]
Pt(II)-3O,2C	>100	100 ± 6[a,b]	>100	80 ± 8
Pt(II)-4O,2C	300 ± 60	250 ± 40[a,b]	300 ± 30[a]	310 ± 6[a]
Pt(II)-4O,4C	13 ± 2[a]	14.3 ± 0.2[a,b]	13 ± 1[a]	12 ± 1[a]
Pt(II)-5O,1C	>1000	800 ± 100	>1000	400 ± 70[a]

Values represent the mean ± SD of at least two independent experiments done in quadruplicates. ND = no data. [a] $P < 0.5$ compared to CDDP. [b] $P < 0.05$ compared to carboplatin.

Table 4 – 3. EC_{50} (μM) of [Pt(II)Cl_2(4,4′-dioligooxyethylene-2,2′-bipyridine)] complexes in various breast cancer cells post 1 h treatment

	HCC38	MCF-7	MDA-MB-231	SK-BR-3	T-47D	ZR-75-1
CDDP	300 ± 30	900 ± 100	50 ± 4	420 ± 80	900 ± 100	260 ± 10
Carboplatin	ND	>1000	ND	ND	ND	ND
Pt(II)-2O,1C	80 ± 6[a]	>100	>100	40 ± 10[a]	24 ± 6[a]	70 ± 20[a]
Pt(II)-3O,2C	>100	>100	>100	50 ± 20[a]	40 ± 9[a]	>100
Pt(II)-4O,2C	240 ± 30	>1000	210 ± 20[a]	240 ± 20[a]	190 ± 20[a]	345 ± 6[a]
Pt(II)-4O,4C	13 ± 1[a]	30 ± 2[a]	14.4 ± 0.4[a]	8 ± 6[a]	12.1 ±0.3[a]	19 ± 1[a]
Pt(II)-5O,1C	>1000	>1000	>1000	800 ± 200	1000 ± 30	>1000

Values represent the mean ± SD of at least two independent experiments done in quadruplicates. ND = no data. [a] $P < 0.5$ compared to CDDP. [b] $P < 0.05$ compared to carboplatin.

Table 4 – 4. EC_{50} (μM) of [Pt(II)Cl_2(4,4′-dioligooxyethylene-2,2′-bipyridine)] complexes in various breast cancer cells post 48 h treatment

	HCC38	MCF-7	MDA-MB-231	SK-BR-3	T-47D	ZR-75-1
CDDP	30 ± 8	34 ± 1	21 ± 3	23 ± 6	35 ± 6	30 ± 8
Carboplatin	ND	800 ± 100[a]	ND	ND	ND	ND
Pt(II)-2O,1C	70 ± 10[a]	>100	65 ± 3[a]	25 ± 5	25 ± 2	50 ± 20
Pt(II)-3O,2C	80 ± 20[a]	>100	>100	60 ± 10[a]	50 ± 8	90 ± 6[a]
Pt(II)-4O,2C	20 ± 6	500 ±100[a,b]	170 ± 7[a]	230 ± 70[a]	170 ± 10[a]	260 ± 50[a]
Pt(II)-4O,4C	12.5 ±0.4[a]	18 ± 4[a,b]	14.5 ±0.1[a]	8 ± 6[a]	12.2 ± 0.4[a]	18.2 ± 0.6
Pt(II)-5O,1C	100 ± 100	900 ± 100[a]	500 ± 90[a]	340 ± 20[a]	400 ± 50[a]	400 ± 100[a]

Values represent the mean ± SD of at least two independent experiments done in quadruplicates. ND = no data. [a] $P < 0.5$ compared to CDDP. [b] $P < 0.05$ compared to carboplatin.

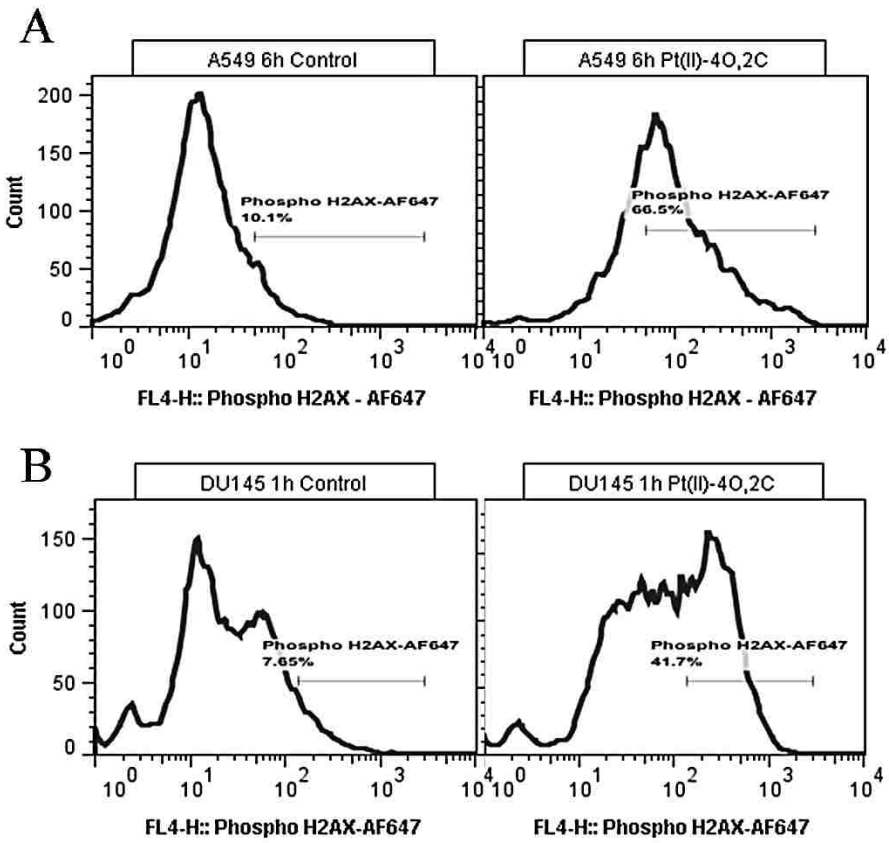

Figure 4 – 7. Pt(II)-4O,2C induced phosphorylation of H2AX in A549 and DU145 cells. (A) A549 cells were treated for 6 h with 1000 μM **Pt(II)-4O,2C** and analyzed 12 h post treatment, (B) DU145 cells were treated for 2 h with 250 μM **Pt(II)-4O,2C** and analyzed 7 h post treatment. Data are representative of three independent experiments.

4.4.2.2 Detection of DNA damage

The MTS results indicate that these dioligooxyethylene bipyridyl Pt(II) complexes have anti-proliferative effects in various cancer cells; thus, it is necessary to determine the type of cell death. Cisplatin treatment is often associated with apoptosis, a type of programmed cell death in which the cells go through various signaling cascades resulting in characteristic features such as externalization of phosphatidylserine to the membrane surface, activation of apoptotic proteins, membrane damage, cell shrinkage,

and chromatin condensation and fragmentation. These types of events can be measured by flow cytometry and fluorescence microscopy.

The cytotoxic effects of cisplatin result from the formation of DNA adducts, which stimulate multiple events such as cell cycle arrest, DNA damage repair, various stress response pathways, and death pathways. DNA damage by cisplatin induces phosphorylation of histone H2AX, which recognizes the damage and recruits proteins to repair the damage or to regulate the apoptotic pathway. Flow cytometry was used to analyze levels of phosphorylated H2AX (γH2AX) in A549 and DU145 cells treated with **Pt(II)-4O,2C**. Although the **Pt(II)-4O,4C** complex was the most effective, it was not selected for further analysis due to its low solubility when diluted in medium; thus, **Pt(II)-4C,2C** was selected due to its water solubility and comparable activity to cisplatin in some of the cell lines tested. As shown in Figure 4-7, treatment with **Pt(II)-4O,2C** resulted in an increase of phopho-H2AX in both A549 and DU145 cells. This indicates that **Pt(II)-4O,2C** may cause DNA damage in A549 and DU145 cells.

4.4.2.3 Evaluation of apoptosis

The increased level of γH2AX induced by **Pt(II)-4O,2C** is an indication of DNA damage; thus, the effects on the cell cycle was analyzed by measurement of PI fluorescence using flow cytometry. PI is a membrane impermeable molecule that can bind to DNA of cells with membrane damage, an event that occurs during late stage apoptosis or necrosis. Measurement of the PI fluorescence by the flow cytometer will give an indication of the DNA content in the cells. Different stages of the cell cycle are correlated with the amount of DNA in the cell and the PI fluorescence intensity is proportional to DNA content. A sub-G1 peak occurs when the cells have less DNA than

cells in the G1 phase, which has been attributed to cells undergoing apoptosis.

As shown in Figure 4-8, the flow histogram of the DNA contents in the different phases of the cell cycle did not show any significant changes in the cell cycle of both A549 and DU145 cells after treatment with **Pt(II)-4O,2C**, except for a small increase in the sub-G1 peak. This indicates that **Pt(II)-4O,2C** does not cause cell cycle arrest and may induce apoptosis in A549 and DU145 cells.

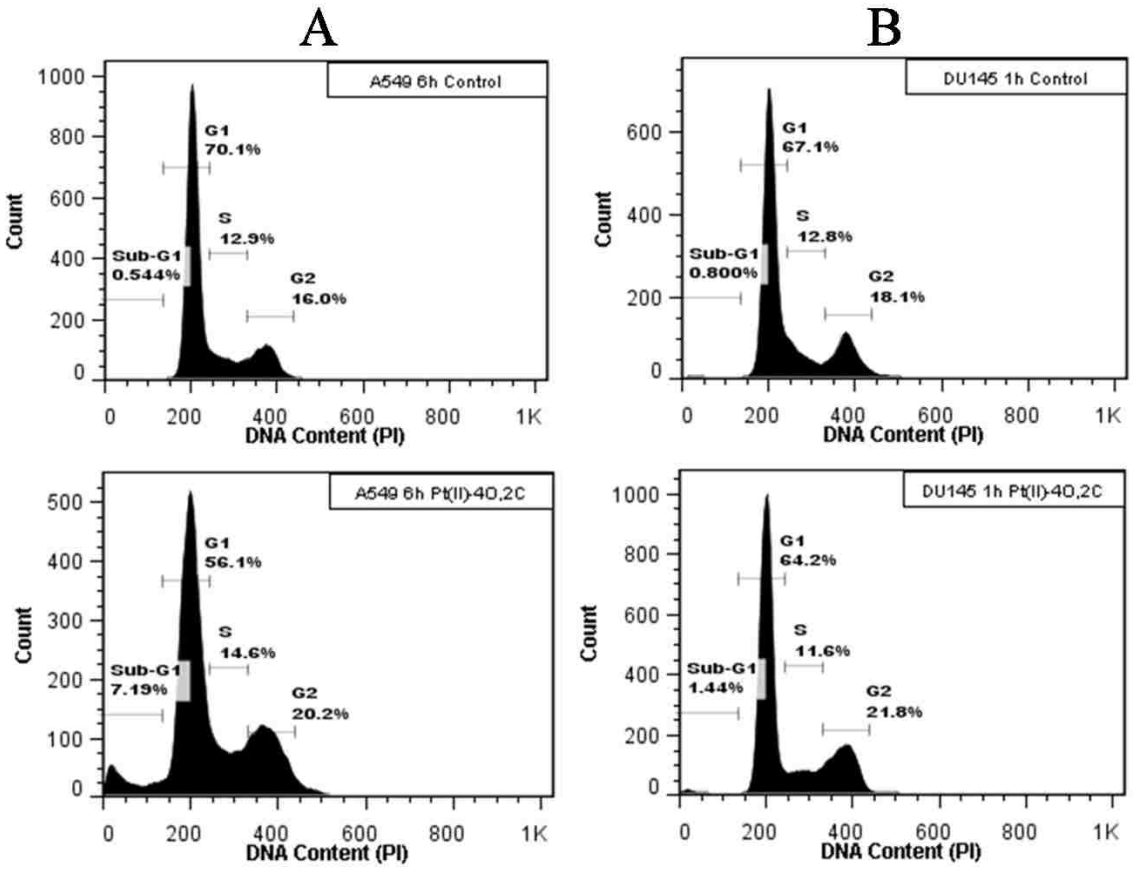

Figure 4 – 8. Cell cycle analysis of A549 and DU145 cells treated with **Pt(II)-4O,2C**. (A) A549 cells were treated for 6 h with 1000 µM of **Pt(II)-4O,2C** and analyzed 12 h post treatment, (B) DU145 cells were treated with 250 µM of **Pt(II)-4O,2C** for 1 h and analyzed 12 h post treatment. Data are representative of three independent experiments.

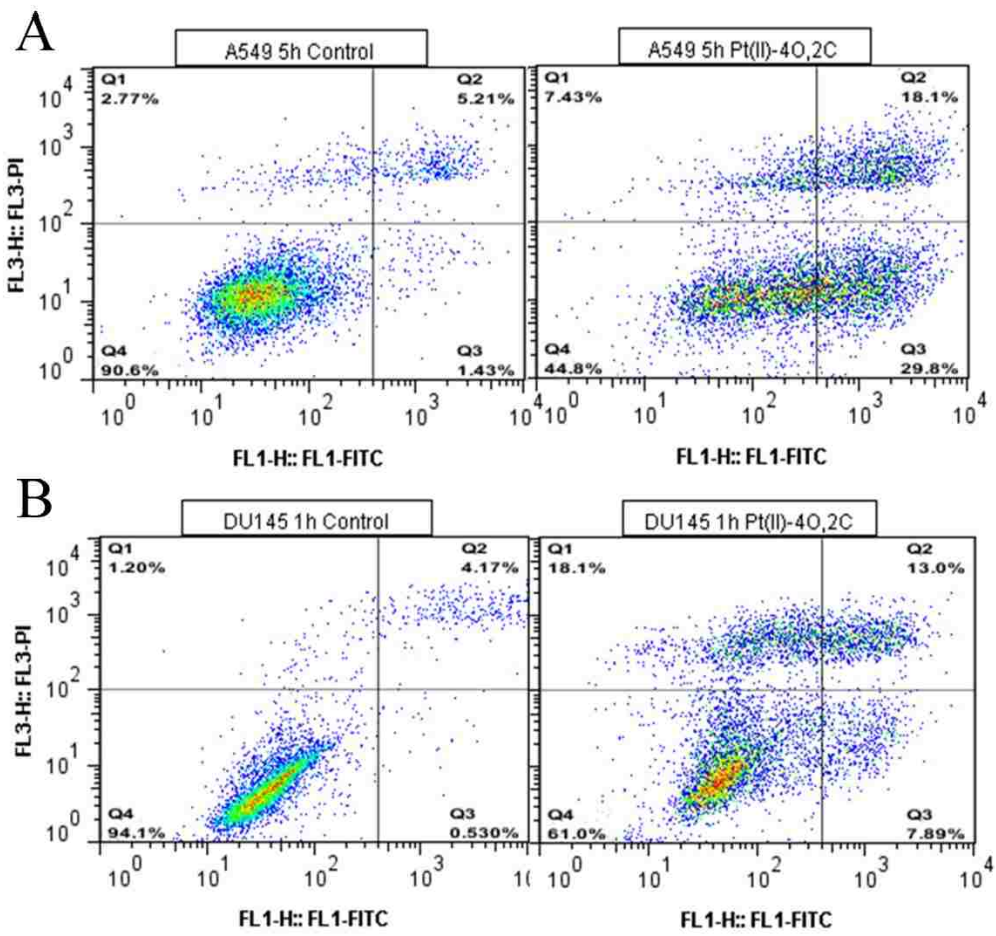

Figure 4 – 9. A549 and DU145 flow cytometry analysis of Annexin V/PI staining. (A) A549 cells were treated for 5 h with 1000 μM of **Pt(II)-4O,2C** and analyzed 12 h post treatment, (B) DU145 cells were analyzed after treatment with 250 μM of **Pt(II)-4O,2C** for 1 h. Q1 = PI+, represents necrotic cells; Q2 = Annexin V/PI+, representing late apoptotic/necrotic cells; Q3 = Annexin V+, representing early apoptotic cells; Q4 = AnnexinV/PI-, representing live cells. Data are representative of three independent experiments.

To confirm that **Pt(II)-4O,2C** induces apoptosis, flow cytometry was used to detect for signs of early apoptosis by analysis of Annexin V, which binds to exposed phosphatidylserine (occurs in early apoptosis). The flow scatter plot of A549 cells treated

with **Pt(II)-4O,2C** showed an increase in early apoptotic cells (Q3) and late apoptotic/necrotic cells (Q2), and a corresponding decrease in live cells (Q4) (Figure 4-9 A). Similar results were observed for DU145 cells, except, the plot of DU145 cells showed a 17% increase in necrotic cells (Q1) (Figure 4-9 A). These results indicate that **Pt(II)-4O,2C** induced DNA damage leads to apoptosis.

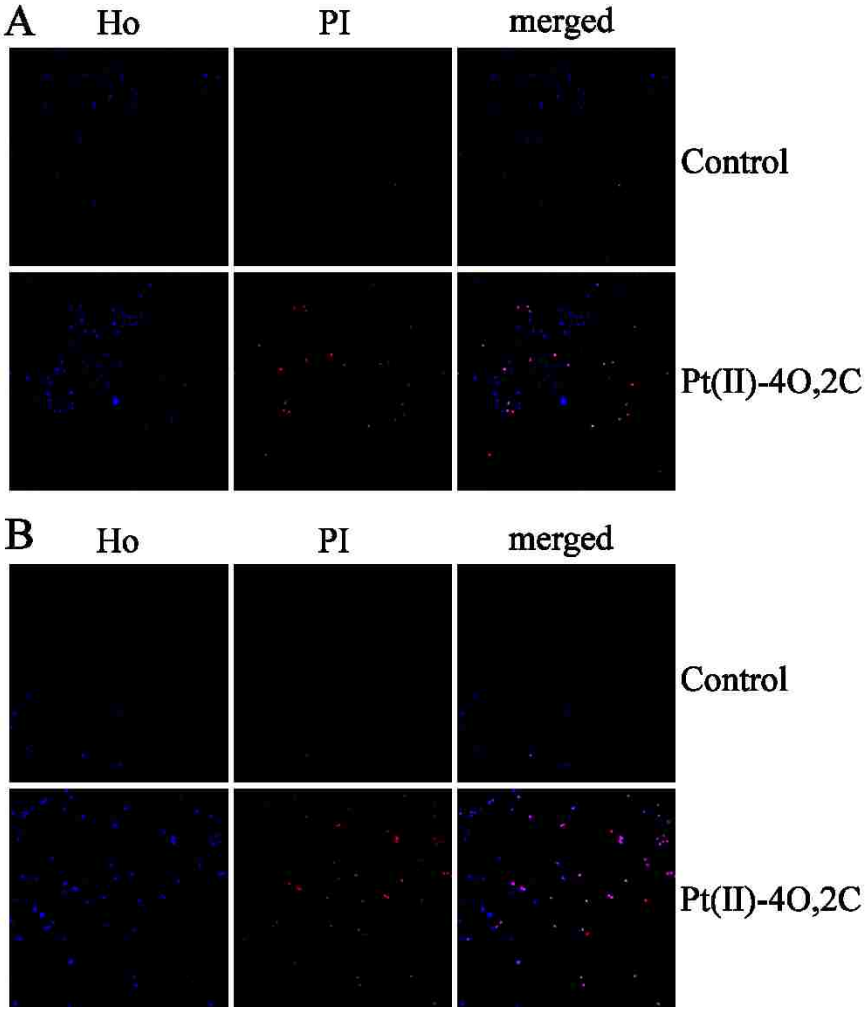

Figure 4 – 10. Microscopy analysis of PI and Ho uptake. (A) A549 were treated for 5 h with 1000 μM **Pt(II)-4O,2C** and (B) DU145 treated for 3.5 h with 250 μM **Pt(II)-4O,2C** were stained with Ho and PI and images were capture with a confocal microscope. Images are from one trial.

To further analyze for cell death, A549 and DU145 cells treated with **Pt(II)-4O,2C** were stained with Hoechst (Ho) and PI. Ho is membrane permeable and can stain both live cells and cells undergoing apoptosis; cells with intense bright fluorescence indicate apoptotic cells. PI, as mentioned earlier, is membrane impermeable and only stains cells with membrane damage. As shown in Figure 4-10, an increase of both Ho and PI positive cells were detected in A549 and DU145 cells treated with **Pt(II)-4O,2C**. Ho positive indicates cells undergoing apoptosis, while, PI positive indicates that the cells have membrane damage so they are either at late stage apoptosis or necrosis.

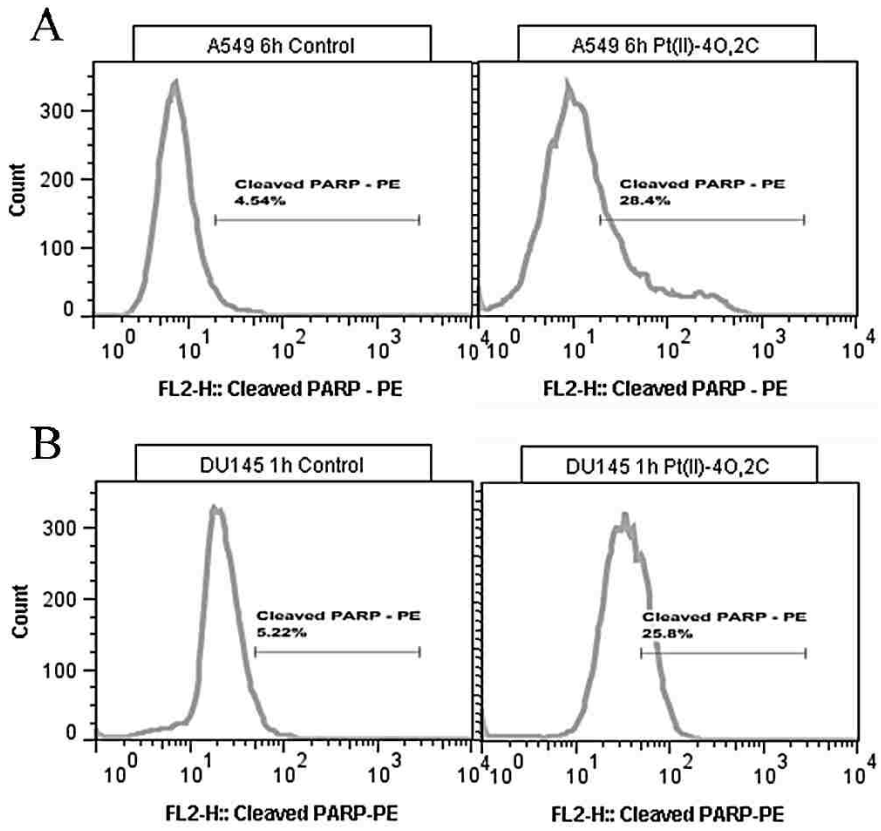

Figure 4 – 11. **Pt(II)-4O,2C** induced cleavage of PARP. (A) A549 were treated for 6 h with 1000 μM **Pt(II)-4O,2C** and analyzed 12 h treatment and (B) DU145 treated with 250 μM **Pt(II)-4O,2C** for 2 h analyzed 7 h post treatment. Data are representative of three independent experiments.

The last method used for analysis of apoptosis is measurement of cleaved-PARP by flow cytometry. PARP is a nuclear poly (ADP-ribose) polymerase that has been associated with DNA repair. During apoptosis, PARP is cleaved by caspase-3; thus, cleaved-PARP is an indication of apoptosis.[16] As shown in Figure 4-11, both A549 and DU145 cells treated with **Pt(II)-4O,2C** had increased levels of cleaved-PARP, suggesting that **Pt(II)-4O,2C** induced apoptosis in these two cell lines.

4.5 Conclusions

A series of Pt(II) complexes containing 4,4′-dioligooxyethylene-2,2′-bipyridyl ligands have been prepared and two of the complexes have some water solubility. Their anti-proliferative activities were investigated in a panel of human lung, breast, and prostate cancer cell lines. The results showed varying degrees of activity in the cell lines tested. In some cell lines, the synthesized complexes were as effective as cisplatin or less effective, while in others, the synthesized complexes were more potent than cisplatin. The breast cancer cell lines, SK-BR-3, T-47D, and ZR-75-1 were the most sensitive to the new platinum complexes, whereas, A549 and MCF-7 were most resistant, even to cisplatin. Results from confocal microscopy and flow cytometry, revealed that **Pt(II)-4O,2C** causes DNA damage in A549 and DU145 cancer cells and induced apoptosis.

It should be noted that there was no observable difference in the activity of **Pt(II)-4O,2C**, which is water soluble, whether the stock solution used was dissolved in DMSO or in 0.15 M NaCl. However, the activity of cisplatin was attenuated when the tested stock solution was made in DMSO instead of NaCl due to inactivation of cisplatin through displacement of the chloride leaving groups by DMSO (data not shown). This indicates that **Pt(II)-4O,2C** is more stable than cisplatin. Even though **Pt(II)-4O,2C** is

only as effective or less effective than cisplatin in some of the cell lines tested, it is still more effective than carboplatin in some cases; thus, it could still be potentially useful for clinical applications due to its increased solubility and stability which might result in less side effects.

4.6 References

1. Hannon; J., M. Metal-based anticancer drugs: From a past anchored in platinum chemistry to a post-genomic future of diverse chemistry and biology. *Pure Appl. Chem.* **2007,** *79,* 2243– 2261.
2. Harper, B. W.; Krause-Heuer, A. M.; Grant, M. P.; Manohar, M.; Garbutcheon-Singh, K. B.; Aldrich-Wright, J. R. Advances in Platinum Chemotherapeutic. *Chem. Eur. J.* **2010,** *16,* 7064-7077.
3. Florea, A. M.; Büsselberg, D. Cisplatin as an Anti-Tumor Drug: Cellular Mechanisms of Activity, Drug Resistance and Induced Side Effects. *Cancers* **2011,** *3,* 1351-1371.
4. Casini, A.; Reedijk, J. Interactions of anticancer Pt compounds with proteins: an overlooked topic in medicinal inorganic chemistry? *Chem. Sci.* **2012,** *3,* 3135–3144.
5. Kamimura, K.; Suda, T.; Tamura, Y.; Takamura, M.; Yokoo, T.; Igarashi, M.; Kawai, H.; Yamagiwa, S.; Nomoto, M.; Aoyagi, Y. Phase I study of miriplatin combined with transarterial chemotherapy using CDDP powder in patients with hepatocellular carcinoma. *BMC Gastroenterology* **2012,** *12,* 127.
6. Li, G.-q.; Chen, X.-g.; Wu, X.-p.; Xie, J.-d.; Liang, Y.-j.; Zhao, X.-q. C. W.-q.; Fu, L.-w. Effect of Dicycloplatin, a Novel Platinum Chemotherapeutical Drug, on Inhibiting Cell Growth and Inducing Cell Apoptosis. *PLoS ONE* **2012,** *7,* e48994.
7. Wang, X.; Guo, Z. Targeting and delivery of platinum-based anticancer drugs. *Chem. Soc. Rev.* **2013,** *42,* 202–224.
8. Wexselblatt, E.; Gibson, D. What do we know about the reduction of Pt(IV) pro-drugs? *J. Inorg. Biochem.* **2012,** *117,* 220-229.
9. Sun, Y.; Sun, D.; Yu, W.; Zhu, M.; Ding, F.; Liu, Y.; Gao, E.; Wang, S.; Xiong, G.; Dragutan, I.; Dragutan, V. Synthesis, characterization, interaction with DNA and cytotoxicity of Pd(II) and Pt(II) complexes containing pyridine carboxylic acid ligands. *Dalton Trans.* **2013,** *42,* 3957-3967.

10. Betanzos-Lara, S.; Novakova, O.; Deeth, R. J.; Pizarro, A. M.; Clarkson, G. J.; Liskova, B.; Brabec, V.; Sadler, P. J.; Habtemariam, A. Bipyrimidine ruthenium(II) arene complexes: structure, reactivity and cytotoxicity. *J. Biol. Inorg. Chem.* **2012,** *17,* 1033-1051.

11. Wheate, N. J.; Walker, S.; Craig, G. E.; Oun, R. The status of platinum anticancer drugs in the clinic and in clinical trials. *Dalton Trans.* **2010,** *39,* 8113– 8127.

12. Vo, V.; Tanthmanatham, O.; Han, H.; Bhowmik, P. K.; Spangelo, B. L. Synthesis of [$PtCl_2$(4,4′-dialkoxy-2,2′-bipyridine)] complexes and their in vitro anticancer properties. *Metallomics* **2013,** *5,* 973-987.

13. Hong, Y.-R.; Gorman, C. B. Synthetic Approaches to an Isostructural Series of Redox-Active, Metal Tris(bipyridine) Core Dendrimers. *J. Org. Chem.* **2003,** *68,* 9019-9025.

14. Keddie, D. J.; Grande, J. B.; Gonzaga, F.; Brook, M. A.; Dargaville, T. R. Amphiphilic silicone architectures via anaerobic thiol-ene chemistry. *Org. Lett.* **2011,** *13,* 6006-6009.

15. Lenz, R. W.; Furukawa, A.; Bhowmik, P. K.; Garay, R. O.; Majnusz, J. Synthesis and characterization of extended rod thermotropic polyesters with polyoxyethylene pendant substituents. *Polymer* **1991,** *32,* 1703-1712.

16. Boulares, A. H.; Yakovlev, A. G.; Ivanova, V.; Stoica, B. A.; Wang, G.; Iyer, S.; Smulson, M. Role of poly(ADP-ribose) polymerase (PARP) cleavage in apoptosis. Caspase 3-resistant PARP mutant increases rates of apoptosis in transfected cells. *J. Biol. Chem.* **1999,** *274,* 22932-22940.

CHAPTER 5

SYNTHESIS AND CHARACTERIZATION OF PT(IV) COMPLEXES CONTAINING 4,4′-DIALKOXY-2,2′-BIPYRIDINE LIGANDS FOR CANCER TREATMENT

5.1 Abstract

Seven [$Pt(IV)Cl_2(OAc)_2$(4,4′-dialkoxy-2,2′-bipyridine)] complexes have been synthesized and characterized by ^1H NMR, ^{13}C NMR spectroscopy, elemental analysis, and differential scanning calorimetry (DSC) measurements. The *in vitro* anti-proliferative activities of these Pt(IV) complexes were examined in a panel of human breast, prostate, and lung cancer cell lines. Comparison of the EC_{50} values showed varying degrees of activities in the 10 cell lines tested; however, the Pt(IV) complexes are generally more effective than cisplatin. A structure activity relationship was observed in which complexes with increasing carbon number on the alkoxy substituents had increasing anti-proliferative activity. These Pt(IV) complexes exhibited improved solubility in organic solvents compared to the Pt(II) precursors.

Analysis of the cell death pathways by confocal microscopy and various staining with flow cytometry showed an increase of phosphorylated H2AX in A549 and DU145 cells treated with **Pt(IV)-4C** and **Pt(IV)-5C.** This indicates that these complexes cause DNA damage leading to activation of apoptosis, although some necrosis might be involved.

5.2 Introduction

In 2012, there were 8.2 million cancer-related deaths and 14.1 million new cancer cases worldwide.[1] Furthermore, these values are projected to continue increasing to an

estimated 22.2 million new cases and 13.2 million cancer-related deaths by 2030.[2] Although new treatment techniques such as targeted therapy and immunotherapy are being explored,[3,4] the use of chemotherapeutic drugs has remained a mainstream.

In the 1960s, the accidental discovery of the anticancer activity of cisplatin (CDDP), a platinum(II) [Pt(II)] complex, opened up a new area of research on metal-based drug discovery.[5] Although numerous platinum complexes have been synthesized, only a few have been approved for clinical use. Along with cisplatin, two other Pt(II) complexes, carboplatin and oxaliplatin, are approved for use worldwide.[6] Additionally, five other Pt(II) complexes are used in China (lobaplatin and dicycloplatin), Japan (nedaplatin and miriplatin), and Korea (heptaplatin).[7–10] Currently, about 50% of cancer chemotherapeutic regimens consist of platinum-based drugs.[10,11] However, clinical application of these platinum drugs is hindered due to toxic side effects and intrinsic or acquired resistance.[12] Consequently, new strategies to improved platinum compounds are continually being introduced in hope of discovering compounds with greater efficacy and reduced toxicity.

While many researchers remain focused on improving Pt(II) complexes, some are expanding into the development of Pt(IV) complexes to act as prodrugs, which are activated by intracellular enzymatic reduction to Pt(II). The general structure of Pt(IV) complexes offers some advantages over their Pt(II) counterparts such as being more inert to substitution reactions owing to their low-spin d^6 electronic configuration and octahedral geometry; reduction of side effects and the potential for oral administration; and greater flexibility in strategies that improve solubility and target selectivity through modification of the additional axial ligands.[12–14] Additionally, Pt(IV) complexes could be

used to selectively target tumor cells since tumors are known to be hypoxic, which leads to a more reductive intracellular environment that favors the reduction of Pt(IV) to Pt(II).[12,15]

Along with cisplatin, several Pt(IV) complexes (cis-$[Pt(NH_3)_2Cl_4]$, trans-$[Pt(NH_3)_2Cl_4]$ and $[Pt(en)Cl_4]$) were described by Rosenberg *et al.*; however they were less effective than cisplatin.[14] Since then, iproplatin, tetraplatin, and satraplatin (Figure 5-1) are several other Pt(IV) complexes which have entered clinical trials.[10,13,14,16,17] Satraplatin, which can be administered orally, is the most successful example of Pt(IV) complexes, but failed Phase III clinical trials. However, it is still undergoing clinical trials in combination with other chemotherapeutic agents.[10]

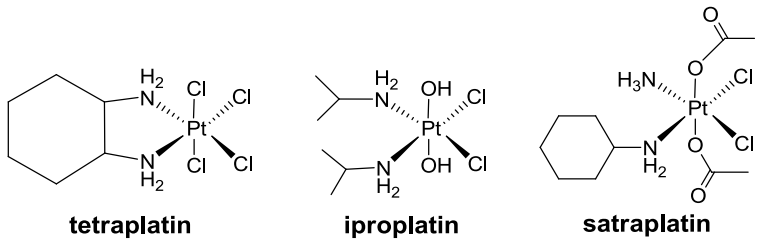

Figure 5 – 1. Structures of some platinum(IV) complexes that have entered clinical trials.

We have previously reported on the synthesis of a series of Pt(II) complexes containing 4,4′-dialkoxy-2,2′-bipyridine ligands (with the dialkoxy having one to six carbons) and their anti-proliferative activities against the A549 lung cancer cell line (Chapter 2).[18] The improved anti-proliferative activity of these complexes compared to cisplatin warrant further investigation of these compounds. However, these complexes have poor solubility in water and only moderate solubility in common organic solvents

and solubilizing agents. To increase solubility, the structures of these 4,4′-dialkoxy-2,2′-bipyridy Pt(II) complexes were modified by introducing increasing oxygen atoms into the dialkoxyl substituents. Although increased solubility was observed, the anti-proliferative activities of these complexes were decreased (by comparison of the EC_{50} values in Chapters 3 and 4). Thus, an alternative strategy to improve these [Pt(II)Cl_2(4,4′-dialkoxy-2,2′-bipyridine)] complexes was to convert them to Pt(IV) complexes owing to the attractive advantages of Pt(IV) complexes.

Herein, we describe the synthesis and characterization by ^{1}H NMR, ^{13}C NMR spectroscopy, elemental analysis, and differential scanning calorimetry (DSC) measurements of a series of [Pt(IV)$Cl_2(OAc)_2$(4,4′-dialkoxy-2,2′-bipyridine)] complexes. Additionally, the anti-proliferative activities of these complexes in a panel of human lung, prostate, and breast cancers will be discussed.

5.3 Experimental

5.3.1 General

All starting materials and reagents for the synthetic procedures were purchased from commercial vendors (Sigma-Aldrich, TCI, Alfa-Aesar, or Acros) unless otherwise noted. They were of high purity and were used without further purification unless noted in the procedure. [Pt(II)Cl_2(4,4′-dialkoxy-2,2′-bipyridine)] complexes were synthesized as described in Chapter 2.[18] Minimum essential medium (MEM), fetal bovine serum (FBS), phosphate buffered saline (PBS), trypsin-EDTA, and penicillin-streptomycin were purchased from Life Technologies (Carlsbad, CA). The RPMI 1640 medium was purchased from ATCC (Manassas, VA). CDDP, carboplatin, HEPES, albumin from bovine serum (BSA), propidium iodide, Hoechst 33342, methanol, and dimethyl

sulfoxide (DMSO) were purchased from Sigma-Aldrich. All reagents and enzymes used for flow cytometry were of analytical grade qualities and were purchased from Sigma-Aldrich, unless otherwise noted.

5.3.2 Chemical characterization instrumentation

All of the NMR spectra were obtained utilizing a Varian spectrometer at 298 K or the indicated temperature using deuterated DMSO (DMSO-d_6) or chloroform ($CDCl_3$) as the solvents: ^{1}H NMR, 400 MHz; and ^{13}C NMR, 100 MHz. Either residual solvent or tetramethylsilane (TMS) were used as the internal chemical shift reference. Thermal transitions were determined by using a TA Instruments DSC 2010 differential scanning calorimeter in nitrogen at heating and cooling rates of 10 °C min^{-1}. The temperature axis of the DSC thermogram was calibrated with reference standards of high purity indium and tin before use. An amount of 2–3 mg of the compounds was used for measurements. The T_{onset} and T_{max} temperatures of a melting endotherm of a compound were recorded from the DSC thermogram as Mp (T_{onset}–T_{max}). Elemental analysis was determined by NuMega Resonance Labs Inc. (San Diego, CA) by using a Perkin Elmer PE2400-Series II with a CHNS/O analyzer.

5.3.3 Preparation of [Pt(IV)$Cl_2$$(OAc)_2$(4,4′-dialkoxy-2,2′-bipyridine)] complexes

The Pt(IV) complexes were prepared from the corresponding Pt(II) complexes using a previously published procedure with slight modifications of the reaction condition.[19] [Pt(II)Cl_2(4,4′-dialkoxy-2,2′-bipyridine)] (1 equiv.) was suspended in 40 mL of glacial acetic acid (>99%) and H_2O_2 (30%, 33 equiv.) was added. The bright yellow suspension was protected from light and stirred at 298 K for 24 h to obtain a light yellow solution. The solvent was removed completely and 30 mL of acetic anhydride was added

to the pale yellow residue. A pale yellow suspension was obtained after stirring for 1–2 d at 298 K. The solvent was removed and ice-cold H_2O was added. The crude product (pale yellow solid) was collected by vacuum filtration. Unless otherwise noted, the product was purified by extraction with $CHCl_3$, dried over Na_2SO_4, removal of the solvent with a rotary evaporator, and then dried *in vacuo* at 80 °C.

[Pt(IV)Cl_2(OAc)$_2$(4,4′-dimethoxy-2,2′-bipyridine)] (Pt(IV)-1C). Yield: 87%, pale yellow powder (obtained by washing the crude product with water without further purification). Mp 249 °C (decomposed). ^{1}H NMR (298 K, 400 MHz, DMSO-d_6): δ (ppm) = 9.30 (d, 1H, J = 6.9 Hz), 8.37 (s, 1H), 7.58 (d, 1H, J = 7.0 Hz), 4.14 (s, 3H), 1.60 (s, 3H). ^{13}C NMR (298 K, 100 MHz, DMSO-d_6): δ (ppm) = 174.66, 170.03, 158.03, 149.74, 113.24, 111.20, 58.12, 22.38. Anal. Calcd for $C_{16}H_{18}Cl_2N_2O_6Pt$ (600.31 g mol^{-1}): C, 32.01; H, 3.02; N, 4.67%; found: C, 32.07; H, 3.11; N, 4.61%.

[Pt(IV)Cl_2(OAc)$_2$(4,4′-diethoxy-2,2′-bipyridine)] (Pt(IV)-2C). Yield: 90%, pale yellow powder. Mp 260 °C (decomposed). ^{1}H NMR (298 K, 400 MHz, DMSO-d_6): δ (ppm) = 9.27 (d, J = 6.9 Hz, 1H), 8.35 (d, J = 2.9 Hz, 1H), 7.54 (dd, J = 7.0, 2.8 Hz, 1H), 4.43 (q, J = 6.8 Hz, 2H), 1.59 (s, 3H), 1.44 (t, J = 6.5 Hz, 3H). ^{13}C NMR (298 K, 100 MHz, DMSO-d_6): δ (ppm) = 173.79, 168.41, 157.23, 148.83, 112.59, 110.47, 65.85, 21.54, 13.69. Anal. Calcd for $C_{18}H_{22}Cl_2N_2O_6Pt$ (628.37 g mol^{-1}): C, 34.41; H, 3.53; N, 4.46%; found: C, 34.58; H, 3.89; N, 4.59%.

[Pt(IV)Cl_2(OAc)$_2$(4,4′-dipropoxy-2,2′-bipyridine)] (Pt(IV)-3C). Yield: 64%, pale yellow powder. Mp 243 °C (decomposed). ^{1}H NMR (298 K, 400 MHz, DMSO-d_6): δ (ppm) = 9.27 (d, J = 7.0 Hz, 1H), 8.37 (d, J = 2.9 Hz, 1H), 7.55 (dd, J = 7.1, 2.9 Hz, 1H), 4.34 (t, J = 6.5 Hz, 2H), 1.90–1.81 (m, 2H), 1.60 (s, 3H), 1.05 (t, J = 7.4 Hz, 3H).

^{13}C NMR (298 K, 100 MHz, DMSO-d_6): δ (ppm) = 174.66, 169.42, 158.09, 149.69, 113.44, 111.38, 72.12, 22.39, 22.04, 10.62. Anal. Calcd for $C_{20}H_{26}Cl_2N_2O_6Pt$ (656.42 g mol^{-1}): C, 36.59; H, 3.99; N, 4.27%; found: C, 36.47; H, 4.08; N, 4.60%.

[Pt(IV)Cl$_2$(OAc)$_2$(4,4′-dibutoxy-2,2′-bipyridine)] (Pt(IV)-4C). Yield: 67%, pale yellow powder (further purified by recrystallization in $CHCl_3$-hexane). Mp 219 °C (decomposed). ^{1}H NMR (298 K, 400 MHz, DMSO-d_6): δ (ppm) = 9.25 (d, J = 7.0 Hz, 1H), 8.34 (d, J = 3.0 Hz, 1H), 7.54 (dd, J = 7.2, 2.8 Hz, 1H), 4.36 (t, J = 6.4 Hz, 2H), 1.83–1.76 (m, 2H), 1.58 (s, 3H), 1.53–1.44 (m, 2H), 0.96 (t, J = 7.5 Hz, 3H). ^{13}C NMR (298 K, 100 MHz, DMSO-d_6): δ (ppm) = 174.67, 169.43, 158.09, 149.69, 113.46, 111.40, 70.45, 30.64, 22.41, 18.99, 14.06. Anal. Calcd for $C_{22}H_{30}Cl_2N_2O_6Pt$ (684.47 g mol^{-1}): C, 38.60; H, 4.42; N, 4.09%; found: C, 38.48; H, 4.75; N, 4.10%.

[Pt(IV)Cl$_2$(OAc)$_2$(4,4′-dipentoxy-2,2′-bipyridine)] (Pt(IV)-5C). Yield: 92%, pale yellow powder. Mp 222 °C (decomposed). ^{1}H NMR (298 K, 400 MHz, $CDCl_3$): δ (ppm) = 9.57 (d, J = 6.9 Hz, 1H), 7.46 (d, J = 2.8 Hz, 1H), 7.16 (dd, J = 7.0, 2.7 Hz, 1H), 4.20 (t, J = 6.4 Hz, 2H), 1.91–1.84 (m, 2H), 1.82 (s, 3H), 1.54–1.34 (m, 4H), 0.96 (t, J = 7.1 Hz, 3H). ^{13}C NMR (298 K, 100 MHz, $CDCl_3$): δ (ppm) = 177.23, 169.18, 158.72, 150.21, 111.62, 110.01, 70.49, 28.46, 28.03, 22.90, 22.43, 14.05. Anal. Calcd for $C_{24}H_{34}Cl_2N_2O_6Pt$ (712.53 g mol^{-1}): C, 40.46; H, 4.81; N, 3.93%; found: C, 40.46; H, 5.12; N, 4.05%.

[Pt(IV)Cl$_2$(OAc)$_2$(4,4′-dihexyloxy-2,2′-bipyridine)] (Pt(IV)-6C). Yield: 74%, pale yellow powder (further purified by recrystallization in acetone-hexane). Mp 219 °C (decomposed). ^{1}H NMR (298 K, 400 MHz, $CDCl_3$): δ (ppm) = 9.58 (d, J = 6.9 Hz, 1H), 7.45 (d, J = 2.9 Hz, 1H), 7.15 (dd, J = 7.1, 2.9 Hz, 1H), 4.21 (t, J = 6.4 Hz, 2H), 1.92–

1.85 (m, 2H), 1.83 (s, 3H), 1.56–1.43 (m, 2H), 1.42–1.32 (m, 4H), 0.93 (t, J = 6.7 Hz, 3H). ^{13}C NMR (298 K, 100 MHz, $CDCl_3$): δ (ppm) = 177.12, 169.04, 158.54, 150.09, 111.44, 109.88, 77.32, 77.00, 76.69, 70.35, 31.33, 28.59, 25.46, 22.75, 22.50, 13.96. Anal. Calcd for $C_{26}H_{38}Cl_2N_2O_6Pt$ (740.58 g mol^{-1}): C, 42.17; H, 5.17; N, 3.78%; found: C, 42.08; H, 5.44; N, 3.80%.

[Pt(IV)Cl_2(OAc)$_2$(4,4′-dioctyloxy-2,2′-bipyridine)] (Pt(IV)-8C). Yield: 85%, pale yellow powder (further purified by recrystallization in acetone-hexane). Mp 203 °C (decomposed). ^{1}H NMR (298 K, 400 MHz, $CDCl_3$): δ (ppm) 9.57 (d, J = 6.9 Hz, 1H), 7.46 (d, J = 2.7 Hz, 1H), 7.15 (dd, J = 7.0, 2.7 Hz, 1H), 4.20 (t, J = 6.4 Hz, 2H), 1.93–1.84 (m, 2H), 1.82 (s, 3H), 1.54–1.43 (m, 2H), 1.43–1.25 (m, 8H), 0.90 (t, J= 6.6 Hz, 3H). ^{13}C NMR (298 K, 100 MHz, $CDCl_3$): δ (ppm) = 177.07, 169.04, 158.58, 150.07, 111.47, 109.86, 70.36, 31.73, 29.15, 29.11, 28.63, 25.78, 22.75, 22.61, 14.07. Anal. Calcd for $C_{30}H_{46}Cl_2N_2O_6Pt$ (796.69 g mol^{-1}): C, 45.23; H, 5.82; N, 3.52%; found: C, 45.07; H, 6.10; N, 3.55%.

5.3.4 Cell culture

Human breast (HCC38, MCF-7, MDA-MB-231, SK-BR-3, T-47D, and ZR-75-1), lung (A549 and H520), and prostate (DU145 and PC-3) cancer cell lines were obtained from American Culture Type Collection (ATCC). The HCC38, MCF-7, MDA-MB-231, SK-BR-3, T-47D, ZR-75-1, and A549 cells were grown in MEM supplemented with 10% FBS, 25 mM HEPES buffer (pH 7.4), penicillin (100 U mL^{-1}) and streptomycin (100 μg mL^{-1}). The H520, DU145, and PC-3 cell lines were grown in RPMI-1640 supplemented with 10% FBS, 25 mM HEPES buffer (pH 7.4), penicillin (100 U mL^{-1}) and streptomycin (100 μg mL^{-1}). All cell lines were maintained at 37 °C in a humidified, 5% CO_2

atmosphere.

5.3.5 Cell viability assay

Cells were cultured at a density of 2–3.5 x 10^3 cells per well in flat bottomed 96-well plates in 100 µL of complete growth medium and incubated for 2 d to reach ~ 50% confluence. The cells were then treated with solvent or the appropriate drugs (CDDP stock was dissolved in 0.15 M NaCl, carboplatin stock was dissolved in 5% glucose, synthesized Pt(IV) complexes were dissolved in DMSO) for 1 h, washed three times with 100 µL PBS, and incubated in 100 µL of fresh medium. After 2 d, the medium was replaced with 120 µL of medium containing CellTiter 96® Aq_{ueous} One Solution Reagent (MTS reagent) (Promega, Madison, WI). The cells were incubated at 37 °C for 4 h and the cell viability was determined by measuring the absorbance at 490 nm using a Tecan Infinite M1000 microplate reader. The 48 h treatment was done in a similar method, except the cells were not washed after treatment and the MTS reagent was immediately added. Viability of treated groups was calculated as a percent of control and graphed with GraphPad Prism.

5.3.6 Flow cytometry

5.3.6.1 Propidium iodide (PI) staining

Cells (~50–60% confluent in 60 mm dishes) were treated as indicated with the platinum compound. After the treatment duration, the floating cells were collected, and both attached and floating cells were washed 2X with PBS. The cells were resuspended in fresh medium and incubated as indicated. The cells were harvested (both the floating and attached cells were collected), counted, and pelleted. The cells were then washed two times with 5 mL PBS, fixed by resuspending in 0.1 mL of PBS and 1 mL of ice-cold 95%

ethanol with gentle vortexing. Fixed cells were stored at 4 °C until analysis. For analysis, fixed cells were washed once with 1–2 mL of PBS and centrifuged at 500 × g for 5 minutes. The cell pellet was resuspended in 100 μL of a 1.0% Triton X-100 buffer solution, and 100 μL of a 1.0 mg mL^{-1} RNAse solution was added and allowed to stand at room temperature for 10–15 min. While in the dark, 200 μL of a 100 μg mL^{-1} PI stain was added to make a final concentration of 50 μg mL^{-1} and gently vortexed. The cell mixture was incubated at room temperature for 30 min and flow cytometry acquisition was done on a Becton Dickinson FACS Calibur with the argon laser set at 488 nm on the linear Flow Channel 2 (FL-2) with Doublet Discriminatory Module (DDM) and threshold set on FL-2.

5.3.6.2 Annexin V-FITC/PI staining

Cells (~50–60% confluent in 60 mm dishes) were treated as indicated with the platinum compound. After the treatment duration, the floating cells were collected, and both attached and floating cells were washed 2X with PBS. The cells were resuspended in fresh medium and incubated as indicated. The cells were harvested (both the floating and attached cells were collected), counted, and pelleted. The cells were then washed two times with 5 mL of Ca^{2+} and Mg^{2+} free PBS. The pellets were then washed in 2.0 mL of 1X Annexin-V Binding buffer (BD Bioscience, San Jose, CA) and centrifuged at 500 × g for 5 min. The pellets were treated with Annexin-V-FITC conjugate (BD Bioscience, San Jose, CA) and incubated in the dark for 15 min. Just before acquisition, the volume of cells-conjugate mixture was adjusted by addition of 1X Annexin-V binding buffer. Acquisition to discriminate between apoptotic and necrotic cells was done by staining the cell-conjugate mixture with 10 μL of PI (50 μg mL^{-1}) solution (BD Bioscience, San Jose,

CA). Acquisitions were done on a FACS Calibur Cytometer on the FL1 (Annexin) and FL3 (PI) channels with threshold and Duplet Discriminating Module (DDM) set at FL1. The level of shift in events distribution in the Annexin-V only and Annexin-V-PI populations in comparison to control is indicative of degree of effectiveness of the treatment agents. A quantitative measure of these event shifts was accomplished by gating.

5.3.6.3 Flow cytometric immunofluorescence

Cells (200,000–250,000) were seeded in 60 mm dishes and incubated at 37 °C in a humidified, 5% CO_2 atmosphere for 2 d to reach ~50–60% confluence. The cells were treated with the platinum complexes as indicated, the floating cells were collected, and both attached and floating cells were washed 2X with PBS. The cells were resuspended in fresh medium and incubated as indicated. After incubation, both the floating and attached cells were collected and fixed by incubation in 4% formaldehyde for 10 min at room temperature. The fixed cells were pelleted and permeabilized by incubation in 500 μL of ice-cold methanol at 4 °C for 10 min. The samples were stored at -20 °C until analysis. For analysis, the cells were pelleted and washed 2X with 1% BSA in PBS. The cells were resuspended in BD Stain Buffer (BS Biosciences #554656) containing the appropriate conjugated primary antibody [PE Mouse Anti-Cleaved PARP (Asp214) and Alexa Fluor 647 Mouse Anti-H2AX (pS139) antibodies were purchased as a part of a Cell Proliferation Kit (BD Biosciences #562253)], and incubated at 4 °C overnight. After washing 2X with 1% BSA, the cells were resuspended in PBS and analyzed on a Becton Dickinson FACS Calibur.

5.3.7 Confocal microscopy

Cells (100,000–125,000) were seeded into 35 mm dishes and incubated for 48 h at 37 °C. The cells were treated as indicated, and while in the dark, the cells were washed 2X with 1 mL PBS. After washing, 1 mL of a 2 μg mL^{-1} Hoechst 33342 and 10 μg mL^{-1} PI solution (in PBS) was added and the cells were incubated for 15 min at room temperature. Images were acquired within 5 min with a Nikon A1R confocal laser scanning microscopy system (CLSM) mounted on a Nikon Eclipse Ti. At least three random areas on each dish were imaged.

5.3.8 Statistical analysis

GraphPad Prism was used to graph viability curves. ModFit version 3.0 was used for the flow cytometry analysis. Microsoft Office Excel was used to perform unpaired Student's t-test; values with $p < 0.05$ were considered significant. Student's t-tests were used to verify significant differences among the EC_{50} values.

5.4 Results and discussion

5.4.1 Synthesis and characterization

The activity of Pt(IV) complexes are believed to be due to activation by intracellular enzymatic reduction to Pt(II); thus, the reduction potential of the Pt(IV) compound is important. This is governed by the axial ligands; chlorido ligands are most easily reduced, followed by acetato ligands, and hydroxido ligands are the most difficult to reduce.[12] With this guideline taken into consideration and in combination with the fact that satraplatin, the most successful Pt(IV) to date, has acetato axial ligands, acetato axial ligands were selected for modification of the [Pt(II)Cl_2(4,4′-dialkoxy-2,2′-bipyridine)].

[Pt(II)Cl_2(4,4′-dialkoxy-2,2′-bipyridine)] complexes were synthesized as previously described (Chapter 2)[18] and used as precursors for the synthesis of the Pt(IV) complexes. Pt(IV) complexes of the formula [Pt(IV)$Cl_2(OAc)_2$(4,4′-bis(RO)-2,2′-bipyridine)] (where R = $–(CH_2)_{n–1}CH_3$, n = 2–6, 8) were synthesized with yields ranging from 64–92% by following the procedure (Scheme 5-1) of Mackay *et al.*[19] with slight modification of the reaction condition. The Pt(II) precursors were first converted to unsymmetrical Pt(IV) complexes containing a mixture of OH and OAc axial ligands by an oxidation reaction with H_2O_2 in acetic acid. The progress of the reaction was visually monitored by the disappearance of the insoluble bright yellow solid of the Pt(II) compounds into a light yellow solution. After removal of the solvent, the [Pt(IV)Cl_2(OAc)(OH)(4,4′-bis(RO)-2,2′-bipyridine)] complexes were then reacted with acetic anhydride to form the desired [Pt(IV)$Cl_2(OAc)_2$(4,4′-bis(RO)-2,2′-bipyridine)] complexes. This step in the reaction was visually monitored by the appearance of a pale yellow suspension. Seven complexes were successfully synthesized and their chemical structures are shown in Figure 5-2; these Pt(IV) complexes have not been reported in the literature.

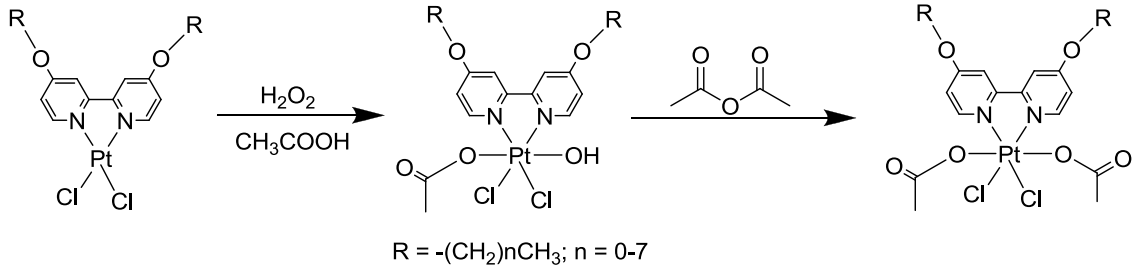

R = -(CH_2)nCH_3; n = 0-7

Scheme 5 – 1. Synthetic route for the preparation of [Pt(IV)$Cl_2(OAc)_2$(4,4′-bis(RO)-2,2′-bipyridine)] complexes.

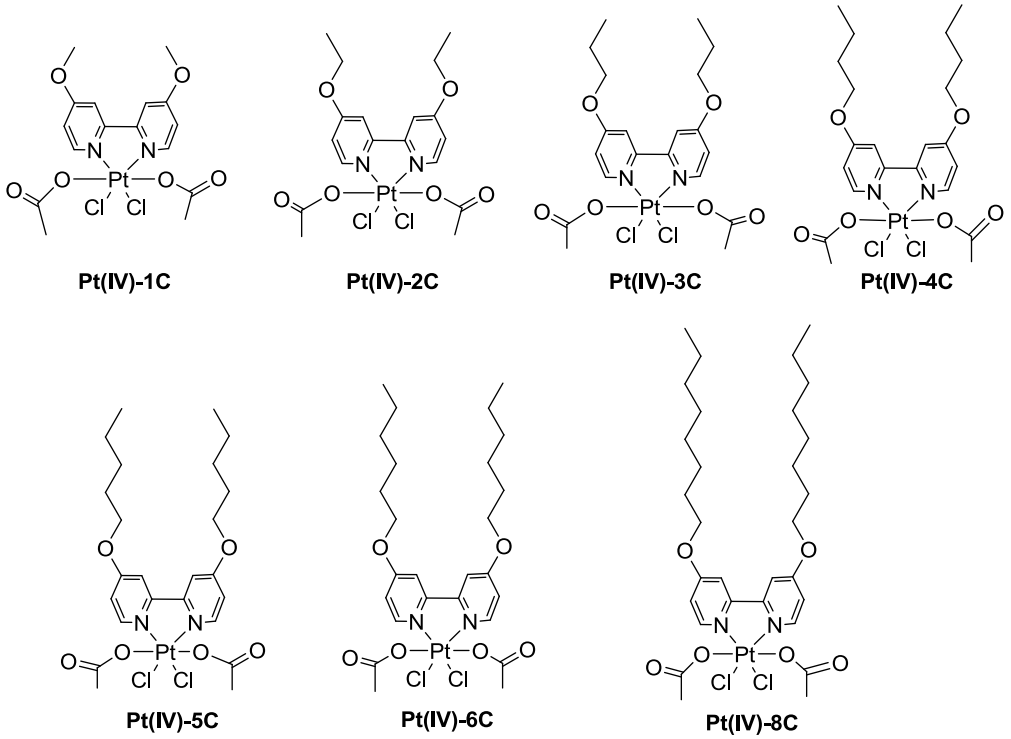

Figure 5 – 2. Chemical structures of the synthesized [Pt(IV)$Cl_2(OAc)_2$(4,4′-dialkoxy-2,2′-bipyridine)] complexes.

All of the compounds were characterized by ^{1}H and ^{13}C NMR spectroscopy, elemental analysis, and DSC measurements. Elemental analyses of the complexes were in excellent agreement (within 0.5%) with the expected values; thus, validating the molecular formulae of these compounds. To compare the NMR chemical shifts of the Pt(IV) complexes to that of the Pt(II) complexes, the Pt(IV) samples were prepared in the same deuterated solvent as the corresponding Pt(II) precursors. The ^{1}H and ^{13}C NMR spectra of **Pt(IV)-1C**–**Pt(IV)-4C** were recorded in DMSO-d_6, whereas those of **Pt(IV)-5C**–**Pt(IV)-8C** were recorded in $CDCl_3$. The spectra of all of the complexes displayed the expected proton and carbon resonances; the ^{1}H NMR chemical shifts of the Pt(II) and Pt(IV) complexes are depicted in Figure 5-3. The appearance of a singlet peak between 1.6–1.8 ppm in the ^{1}H spectra (peak e) and two additional peaks in the ^{13}C spectra

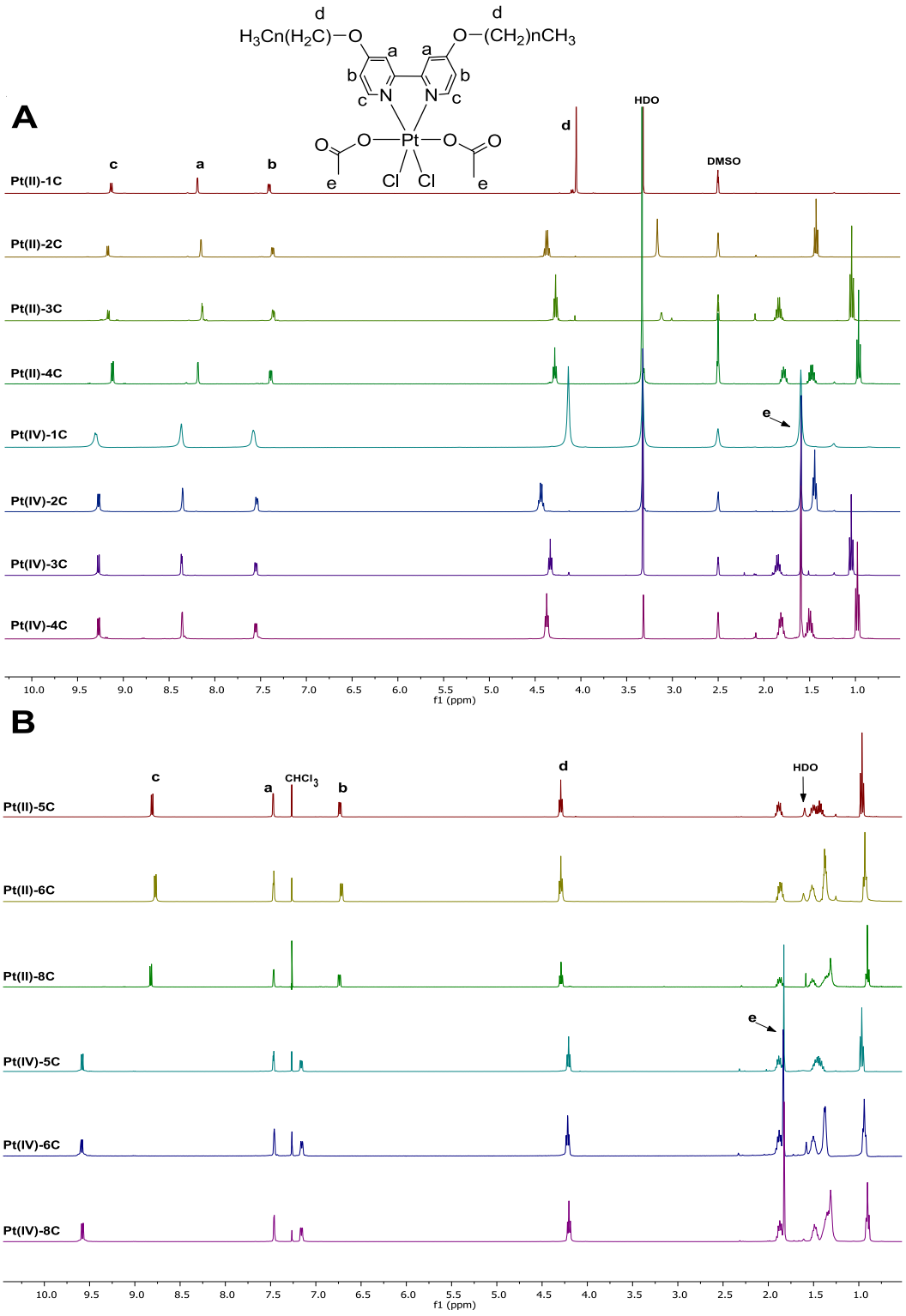

Figure 5 – 3. ^{1}H NMR spectra of Pt(II) and Pt(IV) complexes recorded in (A) DMSO-d_6 or (B) $CDCl_3$ at room temperature.

indicate the presence of the diacetato ligands attached to the Pt center. While the chemical shifts of the protons in the alkyl region remained relatively the same between the Pt(II) and Pt(IV) complexes, the chemical shifts of the aromatic protons (peaks a–c) and the methylene protons next to the oxygen attached to the bipyridine ring (peak d) are slightly shifted. All of the aromatic proton peaks (Figure 5-3 A, peaks a–c) and the methylene protons peak (Figure 5-3 A, peak d) of the Pt(IV) complexes in DMSO-d_6 are shifted downfield compared to Pt(II); however, the methylene proton signal (Figure 5-3 B, peak d) of the Pt(IV) complexes recorded in $CDCl_3$ is slightly shifted upfield and only the peaks corresponding to the protons at the 6,6′ (peak c) and 5,5′ (peak b) positions are shifted downfield. Similar to the proton signals, carbon signals of the Pt(IV) complexes are shifted to varying degrees compared to Pt(II) complexes (the chemical shifts of the Pt(II) complexes are given in the experimental section of Chapter 2 and the shifts for the Pt(IV) complexes are given in the experimental section of this chapter).

The thermal characteristics of the synthesized Pt(IV) compounds were studied by using DSC analysis. As depicted in the DSC thermogram (Figure 5-4), the thermal transitions of all the synthesized Pt(IV) complexes had a similar trend, but there are slight variations. Although all of the complexes had an exothermic peak indicating decomposition, the T_{onset}–T_{max} ranges for the decomposition temperatures of **Pt(IV)-1C**–**Pt(IV)-4C** were lower than the melting ranges of the Pt(II) counterparts and the ranges for **Pt(IV)-5C**–**Pt(IV)-8C** were higher than the melting ranges of the Pt(II) (Table 5-1). All of the Pt(IV) complexes also had an endotherm at varying temperatures after decomposition. Additionally, the DSC thermogram of **Pt(IV)-1C** displayed an endotherm about 10 °C before the T_{onset} of decomposition, and **Pt(IV)-5C** and **Pt(IV)-8C** each had

an endotherm immediately before T_{onset} of decomposition. **Pt(IV)-6C** also had a broad low energy endotherm between 150–160 °C. The endotherms occurring before the decomposition temperature may be due to crystal-to-crystal transitions. Since the compounds decompose, only one heating cycle was done instead of performing both heating and cooling cycles.

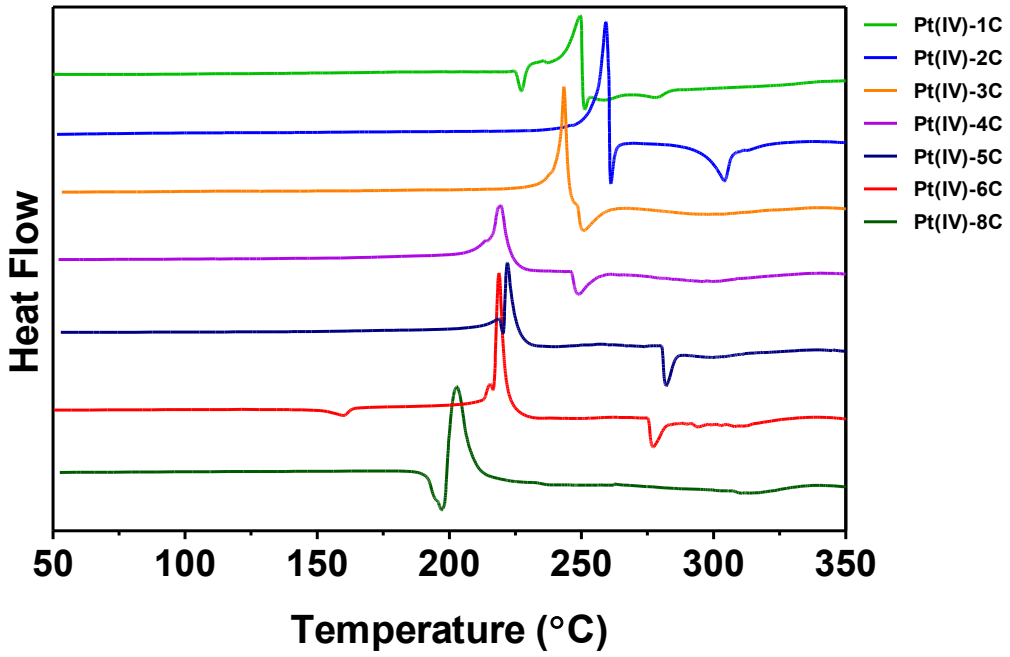

Figure 5 – 4. DSC thermograms of [Pt(IV)$Cl_2(OAc)_2$(4,4′-bis(RO)-2,2′-bipyridine)] complexes obtained in the first heating cycles in nitrogen at a heating rate of 10 °C/min.

Table 5 – 1. T_{onset}–T_{max} (°C) of the Pt(II) melting temperatures *vs.* the Pt(IV) decomposition temperatures

Complex	**Pt-1C**	**Pt-2C**	**Pt-3C**	**Pt-4C**	**Pt-5C**	**Pt-6C**	**Pt-8C**
Pt(II)	311–316	318–322	269–272	229–230	173–175	176–179	169–172
Pt(IV)	239–249	256–259	242–243	215–219	220–222	217–219	197–203

Coordination of the axial ligands to the Pt center improved the solubility of the complexes in common organic solvents. DMSO solutions of the Pt(IV) complexes with concentrations of 10 mM or higher were obtainable, whereas, the Pt(II) can only be made at the highest concentration of 5 mM. The solubility of **Pt(IV)-8C** was markedly improved compared to **Pt(II)-8C**, which was not evaluated for anti-proliferative activities due to poor solubility in DMSO and other common organic solvents that could be used for *in vitro* testing.

5.4.2 Biological properties

5.4.2.1 *In vitro* cytotoxic activity

The anti-proliferative activities of all the Pt(IV) complexes were determined in two lung (H520), two prostate (DU145 and PC-3), and six breast (HCC38, MCF-7, MDA-MB-231, SK-BR-3, T-47D, and ZR-75-1) cancer cell lines. The cells were treated with increasing concentrations of cisplatin, carboplatin, or the Pt(IV) complexes for 1 or 48 h and the viability was measured using an MTS colorimetric cell proliferation assay. The graphs of the results for DU145 (Figure 5-5), A549 (Figure 5-6), and MCF-7 (Figure 5-7) are shown to represent each type of cancer.

For the 1 h treatment in DU145 cells (Figure 5-5 A), cisplatin caused a concentration dependent decrease in cell viability (a 60% reduction by the highest concentration of 1 mM) and carboplatin had no effect even up to 1 mM. The two complexes with short alkoxy substituents, **Pt(IV)-1C** (one carbon) and **Pt(IV)-2C** (two carbons), also did not have any effects at the concentrations tested (up to 100 μM for **Pt(IV)-1C** and 50 μM for **Pt(IV)-2C**). Complexes **Pt(IV)-3C–Pt(IV)-8C** all caused a concentration dependent decrease in DU145 cell viability and were more effective than

cisplatin. **Pt(IV)-3C** was the least effective among the five active compounds, followed by **Pt(IV)-4C**, with **Pt(IV)-5C–Pt(IV)-8C** having similar activities. When the treatment time was extended to 48 h (Figure 5-5 B), the activities of all the platinum compounds were increased. However, all of the Pt(IV) complexes were still more effective than cisplatin except for **Pt(IV)-1C**, which was more effective than carboplatin.

Similar trends were observed for A549 (Figure 5-6) and MCF-7 (Figure 5-7) cells, except these cells were not as sensitive to treatment with the platinum complexes as DU145 cells. Also, **Pt(IV)-3C** and **Pt(IV)-4C** did not have any effects on A549 and MCF-7 cells at the concentrations tested for the 1 h treatment, and **Pt(IV)-1C** and **Pt(IV)-2C** had no effects for the 48 h treatment. The dramatic increased activities of **Pt(IV)-3C** and **Pt(IV)-4C** for the 48 h treatment compared to the 1 h treatment is an indication that the anti-proliferative activities of the platinum complexes are not due to a surfactant effect since interactions of the hydrophobic alkyl chain with the cell membrane would result in a faster response.

It should be noted that while the solubility of these Pt(IV) complexes in organic solvents are increased compared to their Pt(II) precursors, they were still poorly soluble in water; thus, **Pt(IV)-1C**–**Pt(IV)-3C** were limited to a highest concentration of 100 μM. Interestingly, **Pt(IV)-4C** precipitates out of solution at concentrations of 30 μM or higher when the stock DMSO solution was diluted in the culture medium; thus, testing of **Pt(IV)4C** was limited to 25 μM. **Pt(IV)-8C** gave similar results regardless of whether the stock solution was made in DMSO or ethanol, which suggests that the chloride leaving groups were not displaced by DMSO and indicates that the **Pt(IV)-8C** structure is stable.

The effective concentration that resulted in 50% cell viability (EC_{50}) for all the cell lines tested are given in Tables 5-2–5-5. Comparison of the EC_{50} values indicate that the Pt(IV) complexes are generally more effective than cisplatin. A549 and MCF-7 are the most resistant cell lines, while SK-BR-3 and T-47D are the most sensitive. Similar to Pt(II) complexes (Chapters 2 and 3), the activity of the Pt(IV) complexes increases as the carbon number on the alkoxy substituent increases. Pt(IV) complexes with short carbon chains (1–3 carbons) are not as effective as their Pt(II) precursors and Pt(IV) complexes with long carbon chains (5–8) are more effective than their Pt(II) precursors. **Pt(II)-4C** and **Pt(IV)-4C** (four carbon chain) have similar activities.

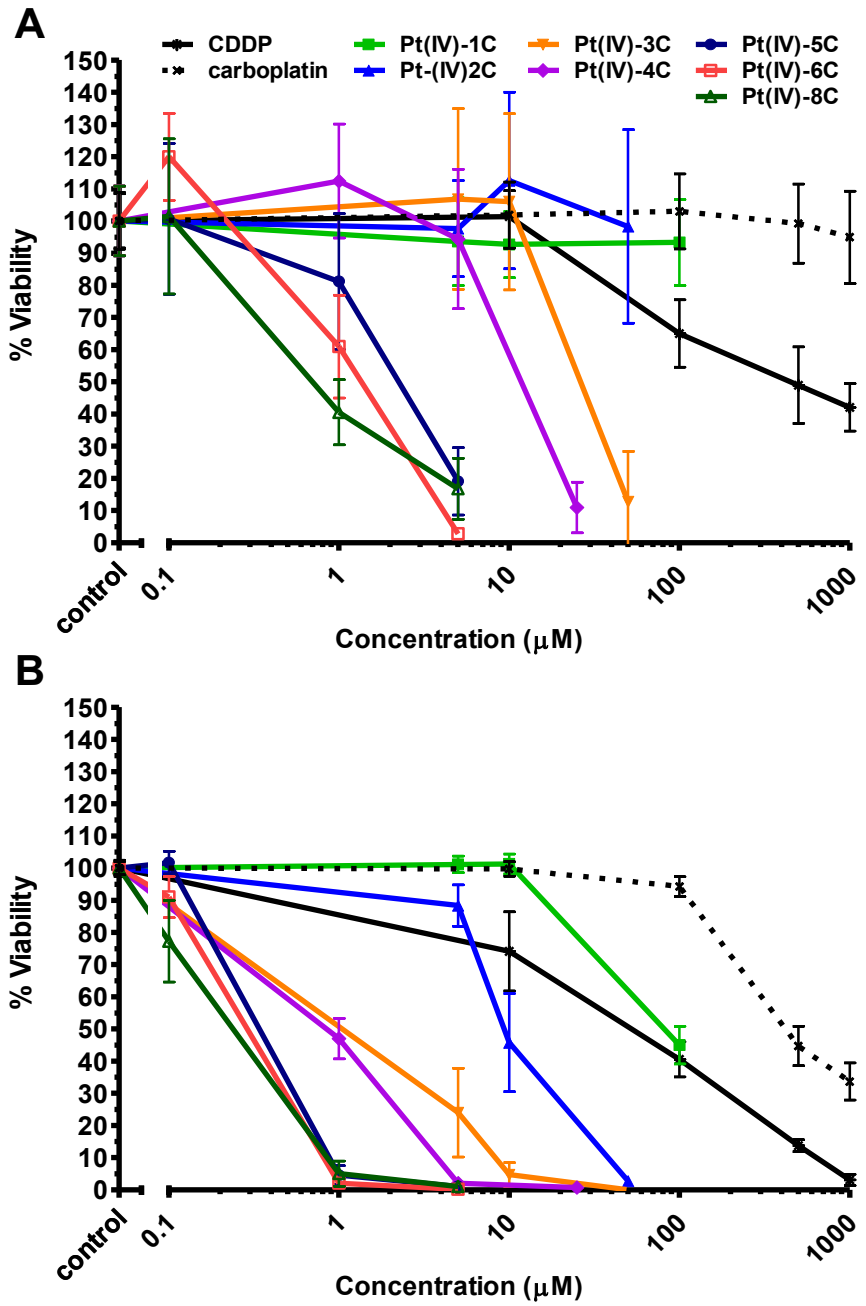

Figure 5 – 5. Cytotoxic activity of the synthesized [Pt(IV)$Cl_2(OAc)_2$(4,4′-dialkoxy-2,2′-bipyridine)] complexes vs. CDDP and carboplatin against DU145 cells. Cells were treated with CDDP or the platinum analogs at various concentrations for (A) 1 h or (B) 48 h and the viability was determined using the MTS assay. Data points represent mean ± SD of at least two independent experiments done in quadruplicates.

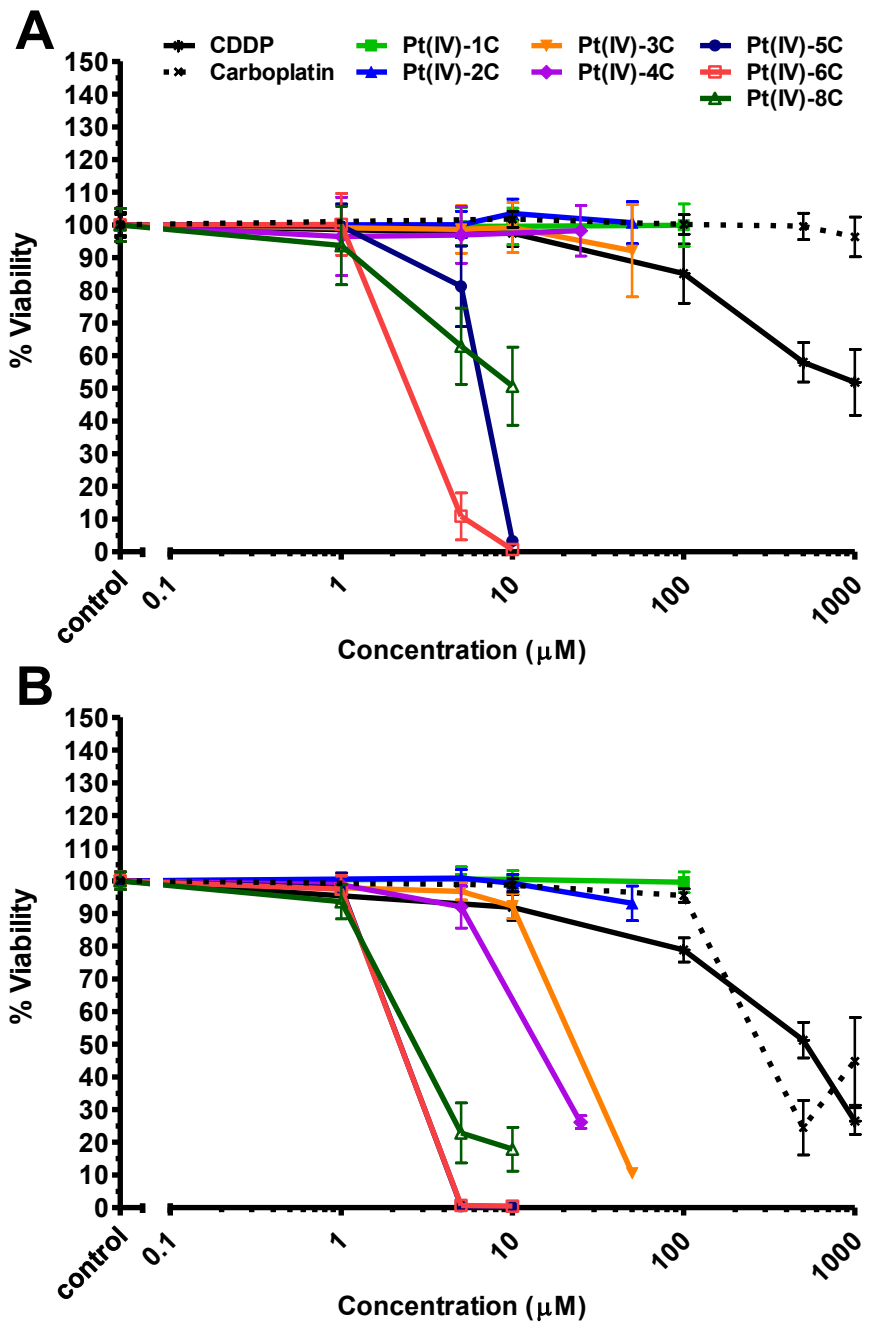

Figure 5 – 6. Cytotoxic activity of the synthesized [Pt(IV)$Cl_2(OAc)_2$(4,4′-dialkoxy-2,2′-bipyridine)] complexes *vs*. CDDP and carboplatin against A549 cells. Cells were treated with CDDP or the platinum analogs at various concentrations for (A) 1 h or (B) 48 h and the viability was determined using the MTS assay. Data points represent mean ± SD of at least two independent experiments done in quadruplicates.

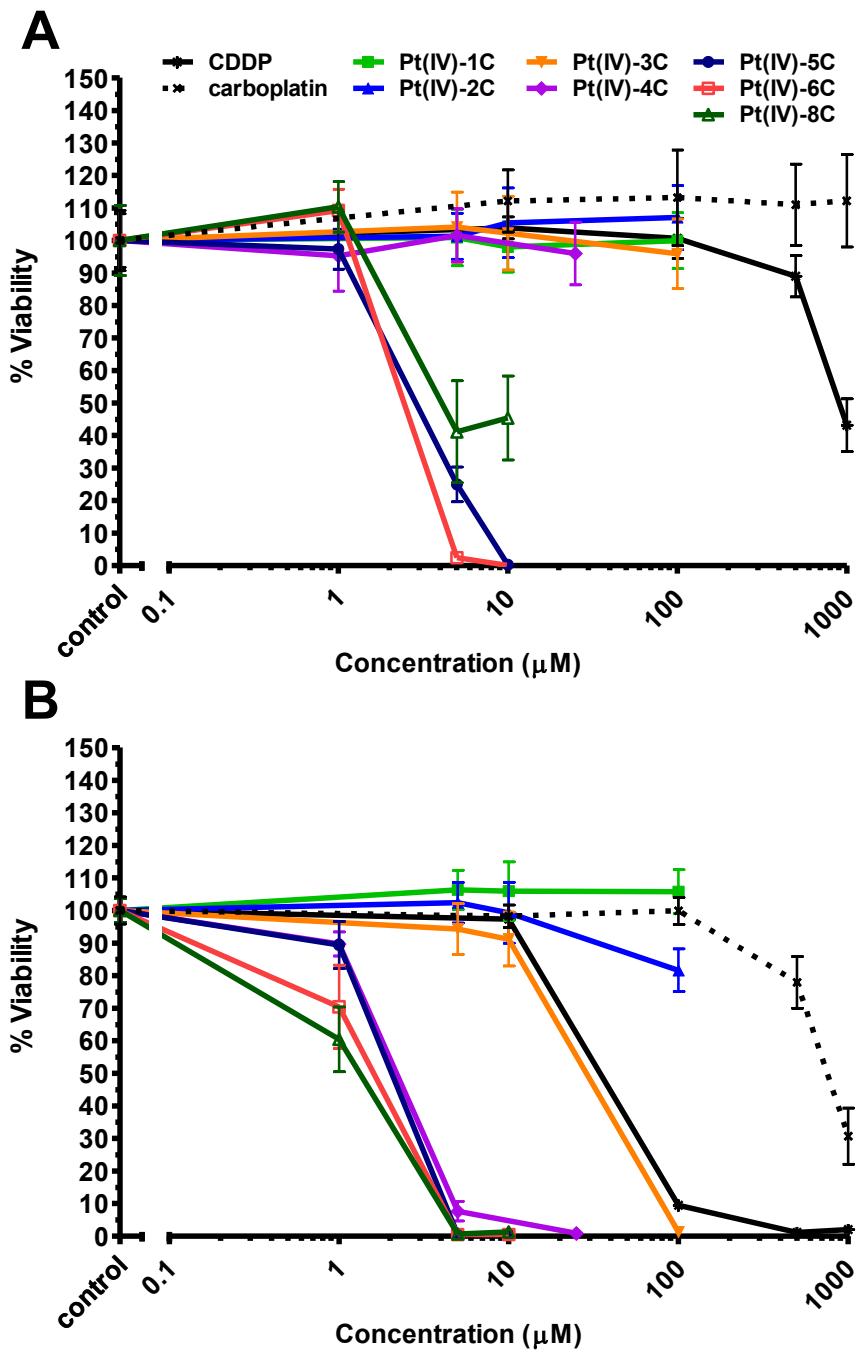

Figure 5 – 7. Cytotoxic activity of the synthesized [Pt(IV)$Cl_2(OAc)_2$(4,4′-dialkoxy-2,2′-bipyridine)] complexes *vs*. CDDP and carboplatin against MCF-7 cells. Cells were treated with CDDP or the platinum analogs at various concentrations for (A) 1 h or (B) 48 h and the viability was determined using the MTS assay. Data points represent mean ± SD of at least two independent experiments done in quadruplicates.

Table 5 – 2. EC_{50} (μM) of [Pt(IV)Cl_2($OAc)_2$(4,4′-dialkoxy-2,2′-bipyridine)] complexes in A549 and H520 post 1 or 48 h treatment

	Lung cancer			
	A549		H520	
	1 h	48 h	1 h	48 h
CDDP	900 ± 200	500 ± 100	200 ± 17	24 ± 2
Carboplatin	>1000	300 ± 30	ND	ND
Pt(IV)-1C	>100	>100	>100	>100
Pt(IV)-2C	>50	>50	>100	61 ± 2[a]
Pt(IV)-3C	>50	23 ± 1[a,b]	80 ± 20[a]	8 ± 6[a]
Pt(IV)-4C	>25	14 ± 1[a,b]	13 ± 5[a]	2.2 ± 0.1[a]
Pt(IV)-5C	6.6 ± 0.3[a]	2.2 ± 0.1[a,b]	3 ± 1[a]	1.0 ± 0.3[a]
Pt(IV)-6C	2.5 ± 0.2[a]	2.2 ± 0.1[a,b]	2.1 ± 0.2[a]	1.0 ± 0.4[a]
Pt(IV)-8C	7.0 ± 0.4[a]	3.0 ± 0.5[a,b]	7 ± 5[a]	1.2 ± 0.6[a]

Values represent the mean ± SD of at least two independent experiments done in quadruplicates. ND = no data. [a] $P < 0.5$ compared to CDDP. [b] $P < 0.05$ compared to carboplatin.

Table 5 – 3. EC_{50} (μM) of [Pt(IV)Cl_2($OAc)_2$(4,4′-dialkoxy-2,2′-bipyridine)] complexes in DU145 and PC-3 post 1 or 48 h treatment

	Prostate cancer			
	DU145		PC-3	
	1 h	48 h	1 h	48 h
CDDP	400 ± 100	64 ± 8	200 ± 20	30 ± 1
Carboplatin	>1000	400 ± 100[a]	ND	ND
Pt(IV)-1C	>100	80 ± 20[b]	>100	>100
Pt(IV)-2C	>50	10 ± 4[a,b]	>50	20 ± 2[a]
Pt(IV)-3C	24 ± 7[a]	1 ± 1[a,b]	23.0 ± 0.3[a]	1.1 ± 0.4[a]
Pt(IV)-4C	8 ± 7[a]	0.9 ± 0.2[a,b]	5 ± 3[a]	1.1 ± 0.4[a]
Pt(IV)-5C	1 ± 1[a]	0.34 ± 0.02[a,b]	1.7 ± 0.2[a]	0.5 ± 0.2[a]
Pt(IV)-6C	1.3 ± 0.2[a]	0.5 ± 0.3[a,b]	2.0 ± 0.3[a]	0.33 ± 0.04[a]
Pt(IV)-8C	0.7 ± 0.3[a]	0.2 ± 0.1[a,b]	1.2 ± 0.5[a]	0.11 ± 0.02[a]

Values represent the mean ± SD of at least two independent experiments done in quadruplicates. ND = no data. [a] $P < 0.5$ compared to CDDP. [b] $P < 0.05$ compared to carboplatin.

Table 5 – 4. EC_{50} (μM) of [Pt(IV)Cl_2($OAc)_2$(4,4′-dialkoxy-2,2′-bipyridine)] complexes in various breast cancer cells post 1 h treatment

	HCC38	MCF-7	MDA-MB-231	SK-BR-3	T-47D	ZR-75-1
CDDP	300 ± 30	900 ± 100	50 ± 4	420 ± 80	900 ± 100	260 ± 10
Carboplatin	ND	>1000	ND	ND	ND	ND
Pt(IV)-1C	>100	>100	>100	>100	>100	>100
Pt(IV)-2C	93 ± 10[a]	>100	>100	40 ± 10[a]	46 ± 8[a]	>50
Pt(IV)-3C	26 ± 6[a]	>100	34 ± 7[a]	19 ± 2[a]	24 ± 3[a]	24 ± 3[a]
Pt(IV)-4C	17 ± 3[a]	>25	2.8 ± 0.1[a]	4.0 ± 0.7[a]	10 ± 1[a]	2.9±0.3[a]
Pt(IV)-5C	3 ± 1[a]	2.9 ± 0.13[a]	1.8 ± 0.1[a]	1.3 ± 0.6[a]	2.3 ± 0.3[a]	1.6 ± 0.1[a]
Pt(IV)-6C	2.3 ± 0.2[a]	2.4 ± 0.1[a]	1.1 ± 0.2[a]	0.36±0.02[a]	2.1 ± 0.4[a]	1.1 ± 0.4[a]
Pt(IV)-8C	3.0 ± 0.6[a]	4 ± 1[a]	2.1 ± 0.2[a]	0.33±0.05[a]	1.5 ± 0.5[a]	3.0 ± 1[a]

Values represent the mean ± SD of at least two independent experiments done in quadruplicates. ND = no data. [a] $P < 0.5$ compared to CDDP. [b] $P < 0.05$ compared to carboplatin.

Table 5 – 5. EC_{50} (μM) of [Pt(IV)Cl_2($OAc)_2$(4,4′-dialkoxy-2,2′-bipyridine)] complexes in various breast cancer cells post 48 h treatment

	HCC38	MCF-7	MDA-MB-231	SK-BR-3	T-47D	ZR-75-1
CDDP	30 ± 8	34 ± 1	21 ± 3	23 ± 6	35 ± 6	30 ± 8
Carboplatin	ND	800 ± 100[a]	ND	ND	ND	ND
Pt(IV)-1C	>100	>100	>100	80 ± 20[a]	32.0 ± 0.5	>100
Pt(IV)-2C	30 ± 9	>100	28 ± 7	8.3 ± 0.7[a]	0.95 ± 0.03[a]	17 ± 7
Pt(IV)-3C	8 ± 1[a]	29 ± 2[a,b]	6.1 ± 0.4[a]	0.9 ± 0.1[a]	0.59 ± 0.01[a]	1.21±0.04[a]
Pt(IV)-4C	2.1±0.2[a]	2.2 ±0.1[a,b]	1.0 ± 0.2[a]	0.44±0.02[a]	0.33 ± 0.07[a]	0.7 ± 0.2[a]
Pt(IV)-5C	2.1±0.3[a]	2.0 ± 0.1[a,b]	0.26±0.01[a]	0.30±0.03[a]	0.25±0[a]	0.55±0.07[a]
Pt(IV)-6C	1.8±0.5[a]	1.6 ± 0.2[a,b]	0.31±0.04[a]	0.21±0.03[a]	0.24 ± 0.01[a]	0.55±0.04[a]
Pt(IV)-8C	1.6±0.3[a]	1.3 ± 0.3[a,b]	0.9 ± 0.3[a]	0.22±0.03[a]	0.25 ± 0[a]	1.3 ± 0.1[a]

Values represent the mean ± SD of at least two independent experiments done in quadruplicates. ND = no data. [a] $P < 0.5$ compared to CDDP. [b] $P < 0.05$ compared to carboplatin.

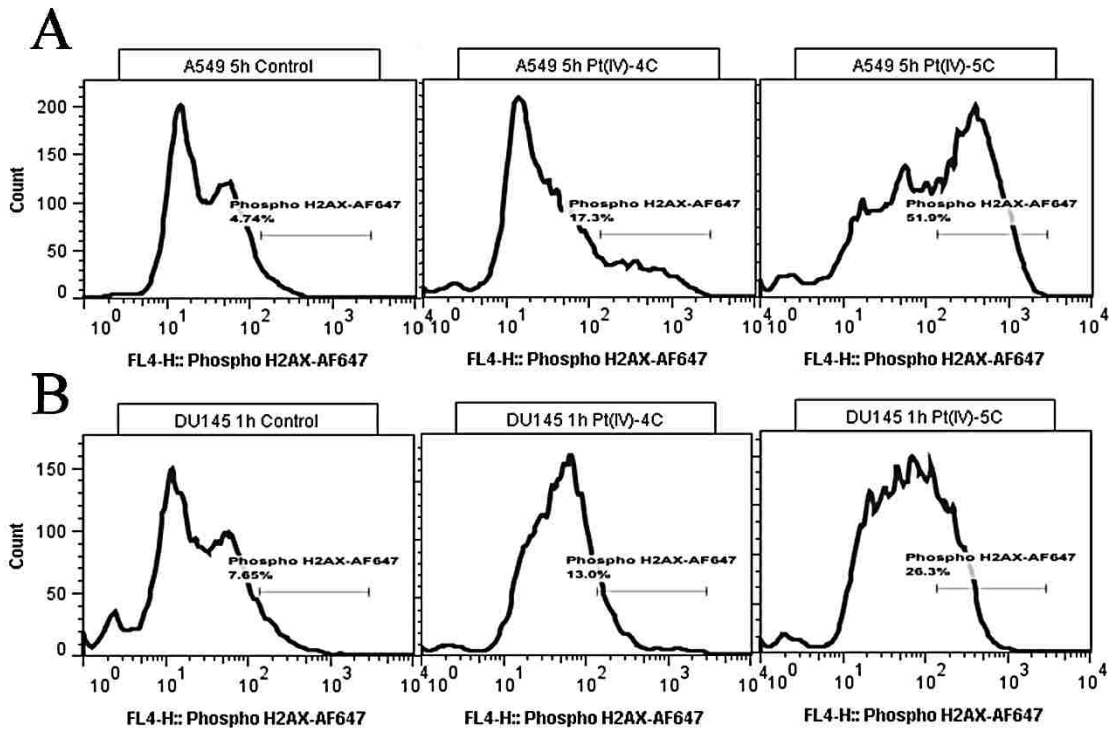

Figure 5 – 8. Pt(IV) complexes induced phosphorylation of H2AX in A549 and DU145 cells. (A) A549 cells were treated for 6 h with 25 μM **Pt(IV)-4C** or 7.5 μM **Pt(IV)-5C** and analyzed 12 h post treatment, (B) DU145 cells were treated for 2 h with 10 μM **Pt(IV)-4C** or 2.5 μM **Pt(IV)-5C** and analyzed 7 h post treatment. Data are representative of three independent experiments.

5.4.2.2 Detection of DNA damage

Cisplatin is known to bind DNA and form adducts, which induces cell cycle arrest, DNA damage repair, various stress response pathways, and death pathways. DNA damage by cisplatin has been shown to induce phosphorylation of histone H2AX, which is believed to be involved in recognition and repair of damaged DNA, and regulation of the apoptotic pathway. Flow cytometry was used to analyze levels of phosphorylated H2AX (γH2AX) in A549 and DU145 cells treated with **Pt(IV)-4C** and **Pt(IV)-5C**.

Representative histograms for each cell line are shown in Figure 5-8. As shown, treatment with **Pt(IV)-4C** and **Pt(IV)-5C** resulted in an increase of γH2AX in both A549 and DU145 cells. The increase in γH2AX caused by **Pt(IV)-4C** treatment was not as high as **Pt(IV)-5C**. Nonetheless, these results indicate that treatment with **Pt(IV)-4C** and **Pt(IV)-5C** caused DNA damage in A549 and DU145 cells.

5.4.2.3 Evaluation of apoptosis

Cisplatin induced DNA damage has been associated with cell cycle arrest and induction of apoptosis. Since treatment with **Pt(IV)-4C** and **Pt(IV)-5C** caused an increase in γH2AX in A549 and DU145 cells, their effects on the cell cycle was examined. Flow cytometric analysis of propidium iodide provides information on DNA content, which is correlated with the stages in the cell cycle. Additionally, appearance of a sub-G1 peak is an indication of apoptosis. A549 cells treated with **Pt(IV)-4C** and **Pt(IV)-5C** had a decreased percentage of cells in the G1 phase and a corresponding increase in the sub-G1 peak, while the S and G2 phases remained relatively similar to the control (Figure 5-9 A). Treatment of DU145 cells with **Pt(IV)-4C** and **Pt(IV)-5C** did not affect the cell cycle and a sub-G1 peak was not detected (Figure 5-9 B). A sub-G1 peak was not detected even when the treatment time was extended to 2 and 4 h; perhaps these treatment duration are not enough to cause fragmentation and leakage of the DNA content to produce a sub-G1 peak. Alternatively, the difference between the response of A549 and DU145 may be due to differences in p53 status; A549 has wild type p53, while DU145 has mutant p53. It is possible that lack of apoptotic features in DU145 cells is the result of not having functional p53 to signal the apoptotic pathway.

The sub-G1 peak is a measurement of cells with less DNA than cells in the G1 phase, which is attributed to leakage of DNA content from cells undergoing late apoptosis or necrosis. Since the sub-G1 peak is not a clear indication of apoptosis, flow cytometric analysis of Annexin V and PI double staining was performed. Annexin V binds to exposed phosphatidylserine on the membrane surface, which is an event that occurs in early apoptosis. Co-staining with PI, a membrane impermeable dye, allows for differentiation between cells with intact membrane and cells with membrane damage, which occurs in late stage apoptosis or necrosis. As shown in Figure 5-10, A549 and DU145 cells treated with **Pt(IV)-4C** and **Pt(IV)-5C** had decreased AnnexinV/PI negative cells (Q4, live cells) and a corresponding increase in Annexin V positive (Q3, early apoptotic cells) and Annexin V/PI positive cells (Q2, late apoptotic/necrotic cells). These changes were higher in **Pt(IV)-5C** treated cells than **Pt(IV)-4C** treated cells. A549 cells treated with **Pt(IV)-5C** also had an increase in PI positive cells (Q1, necrotic cells) (Figure 5-10 A). DU145 had higher increases of Annexin V/PI positive cells than Annexin V positive cells suggesting that they may be in late stage apoptosis or necrosis (Figure 5-10 B). Together, these results indicate that **Pt(IV)-4C** and **Pt(IV)-5C** induce apoptosis in A549 and DU145 cells, although some necrosis was also observed.

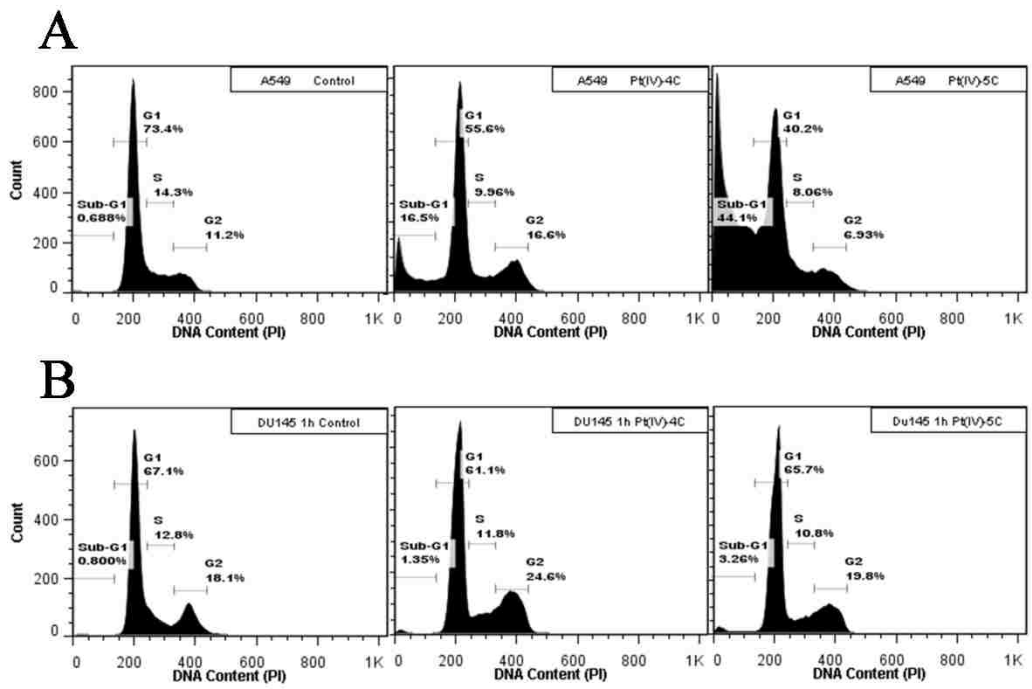

Figure 5 – 9. Cell cycle analysis of A549 and DU145 cells treated with **Pt(IV)-4C** and **Pt(IV)-5C**. (A) A549 cells were treated for 5 h with 25 μM **Pt(IV)-4C** or 7.5 μM **Pt(IV)-5C** and analyzed 12 h post treatment, (B) DU145 cells were treated for 1 h with 10 μM **Pt(IV)-4C** or 2.5 μM **Pt(IV)-5C** and analyzed 12 h post treatment. Data are representative of three independent experiments.

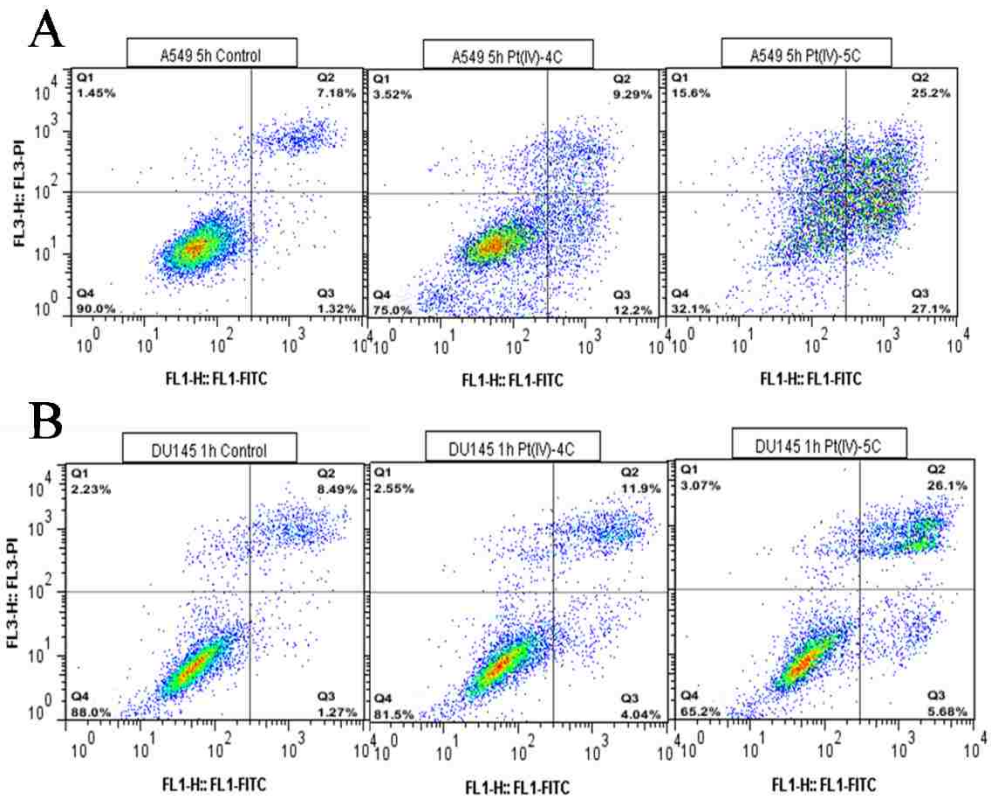

Figure 5 – 10. Flow cytometry analysis of Annexin V/PI staining in A549 and DU145 treated with **Pt(IV)-4C** and **Pt(IV)-5C**. (A) A549 cells were treated for 5 h with 25 μM **Pt(IV)-4C** or 10 μM **Pt(IV)-5C** and analyzed 12 h post treatment, (B) DU145 cells were treated for 1 h with 10 μM **Pt(IV)-4C** or 2.5 μM **Pt(IV)-5C** analyzed 12 h post treatment. Q1 = PI+, represents necrotic cells; Q2 = Annexin V/PI+, representing late apoptotic/necrotic cells; Q3 = Annexin V+, representing early apoptotic cells; Q4 = AnnexinV/PI-, representing live cells. Data are representative of three independent experiments.

Analysis of hoechst (Ho) and PI staining by confocal microscopy was performed to detect cell death. PI stains cells with membrane damage; whereas, Ho stains both live and apoptotic cells, but apoptotic cells will have more intense Ho fluorescence. A549 cells treated with **Pt(IV)-4C** and **Pt(IV)-5C** had increased Ho fluorescence compared to control (Figure 5-11). There was no difference between the PI fluorescence of **Pt(IV)-5C**

treated cells compared to the control, but **Pt(IV)-4C** treated cells had increased PI positive cells. Similar results were obtained for DU145 cells, except **Pt(IV)-5C** treated cells had more PI positive staining than Ho staining compared to the control (Figure 5-12). Additionally, unlike A549, the PI positive cells in **Pt(IV)-4C** treated cells were higher than **Pt(IV)-5C** treated cells. The increase in PI staining suggests that the cells have membrane damage, which indicates that the cells were either at late stage apoptosis or were undergoing necrosis. These results correspond to the flow results indicating that **Pt(IV)-4C** and **Pt(IV)-5C** induce apoptosis and possibly some necrosis.

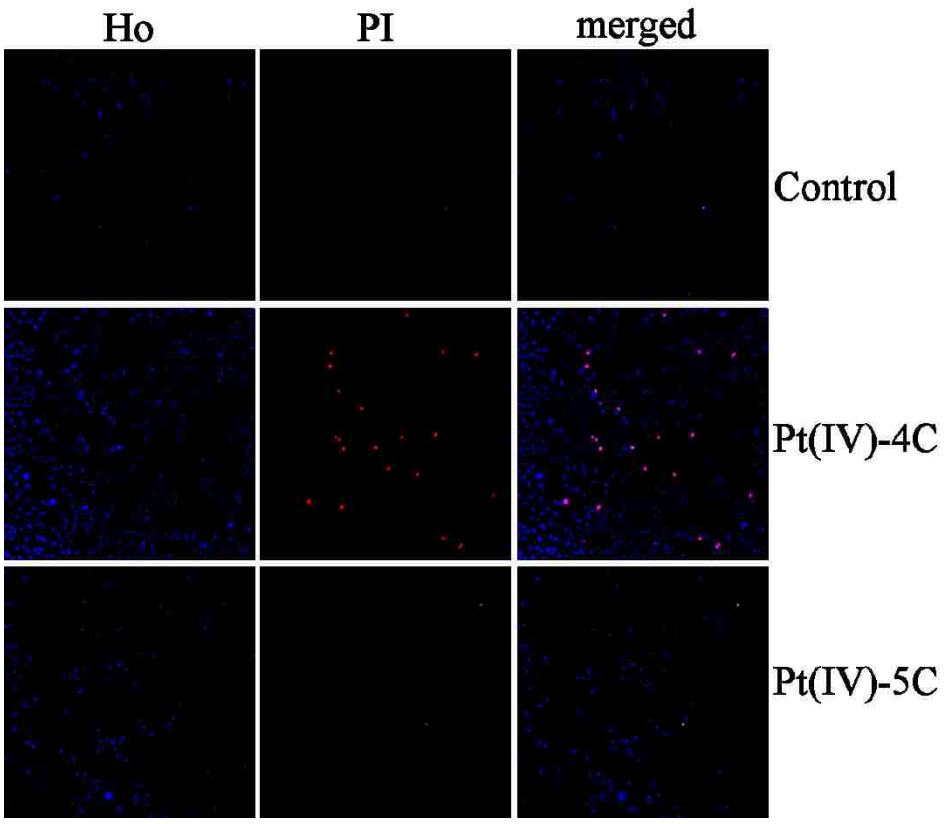

Figure 5 – 11. Confocal microscopy analysis of PI and Ho uptake in A549 cells treated with **Pt(IV)-4C** and **Pt(IV)-5C**. A549 cells treated for 5 h with 25 μM **Pt(IV)-4C** or 7.5 μM **Pt(IV)-5C** were stained with Ho and PI and images were capture with a confocal microscope. Images are from one trial.

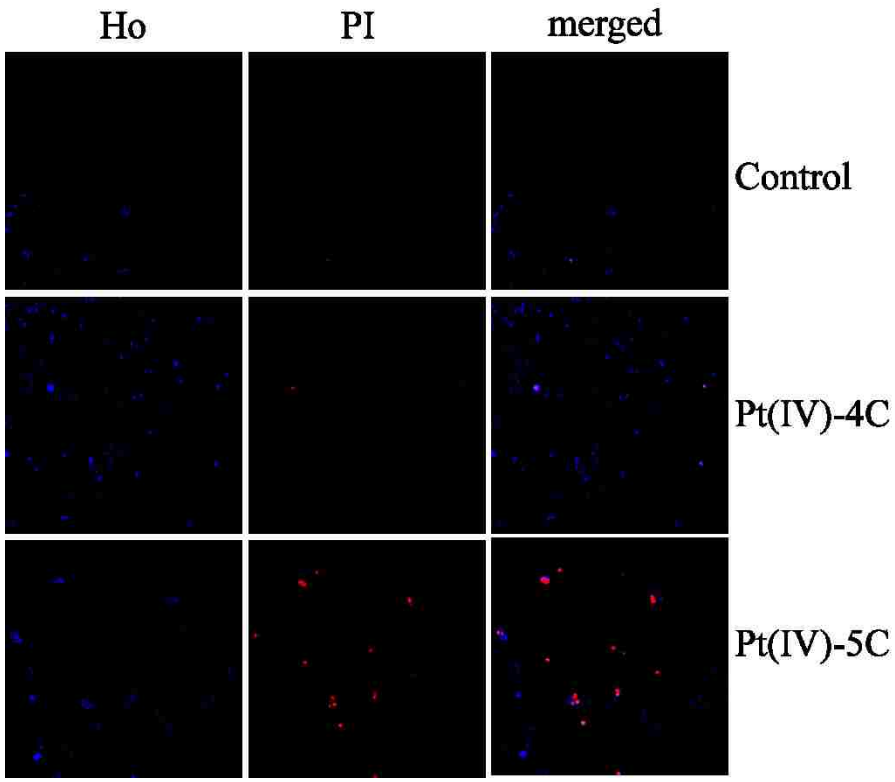

Figure 5 – 12. Confocal microscopy analysis of PI and Ho uptake in DU145 cells treated with **Pt(IV)-4C** and **Pt(IV)-5C**. DU145 cells treated for 3.5 h with 10 μM **Pt(IV)-4C** or 2.5 μM **Pt(IV)-5C** were stained with Ho and PI and images were capture with a confocal microscope. Images are from one trial.

Finally, detection of cleaved-PARP by flow cytometry was used as an indication of apoptosis. PARP is a nuclear poly (ADP-ribose) polymerase that has been associated with DNA repair. During apoptosis, PARP is cleaved by caspase-3.[20] As shown in Figure 5-13, both A549 and DU145 cells treated with **Pt(IV)-4C** and **Pt(IV)-5C** had increased levels of cleaved-PARP, suggesting that **Pt(IV)-4C** and **Pt(IV)-5C** induced caspase-3 mediated apoptosis in these two cell lines. The fold increase of cleaved-PARP in A549 (~7 fold for both compounds) were higher than DU145 (~2 fold for both compounds). Similar to the flow data with PI staining, the differences between A549 and DU145 may be due to treatment time or p53 status.

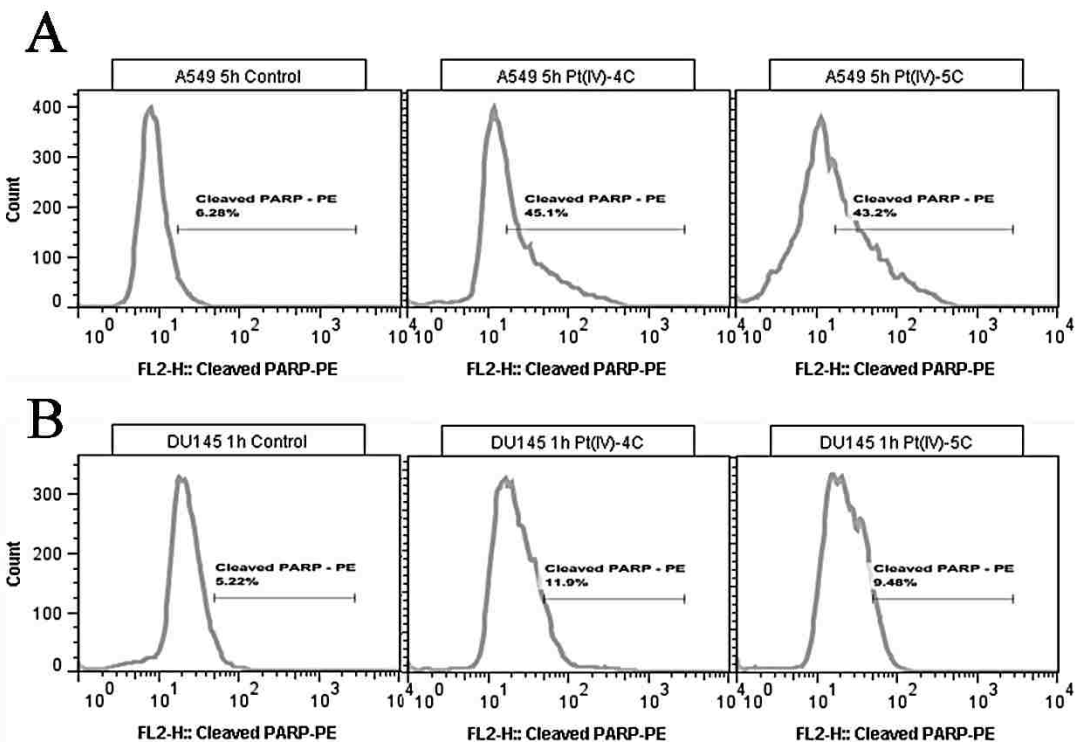

Figure 5 – 13. Pt(IV)-4C and **Pt(IV)-5C** induced cleavage of PARP. (A) A549 cells were treated for 5 h with 25 μM **Pt(IV)-4C** or 7.5 μM **Pt(IV)-5C** and analyzed 12 h post treatment, (B) DU145 cells were treated for 2 h with 10 μM **Pt(IV)-4C** or 2.5 μM **Pt(IV)-5C** analyzed 7 h post treatment. Data are representative of three independent experiments.

5.5 Conclusions

We have synthesized a series of Pt(IV) derivatives with diacetato axial ligands from our recently reported Pt(II) complexes containing 4,4′-dialkoxy-2,2′-bipyridyl ligands. Solubility of these Pt(IV) complexes in DMSO was increased compared to the Pt(II) precursor. *In vitro* testing of these Pt(IV) complexes in a panel of human lung, breast, and prostate cancer cell lines suggested that these Pt(IV) complexes are generally more effective than cisplatin. Similar to the Pt(II) precursors, a structure activity relationship was observed in which the compounds had increasing anti-proliferative activities with increasing carbon chain length of the dialkoxy substituents. The activities

of **Pt(IV)-5C**–**Pt(IV)-8C** were similar, but in some cases **Pt(IV)-8C** was less active. **Pt(IV)-1C**–**Pt(IV)-3C** were less active than the Pt(II) counterparts and **Pt(IV)-4C** had similar activity to **Pt(II)-4C**. **Pt(IV)-5C** and **Pt(IV)-6C** were more active than their Pt(II) counterparts in both the 1 h and the 48h treatment. **Pt(II)-8C** could not be tested due to poor solubility, but the increased solubility of Pt(IV) complexes allowed for the testing of **Pt(IV)-8C**, which had activity in both the 1 h and the 48 h treatment.

Analysis of cell death using confocal microscopy and flow cytometry staining with various dyes and antibodies demonstrated that **Pt(IV)-4C** and **Pt(IV)-5C** induced DNA damage in A549 and DU145 cells, which led to activation of apoptosis with some necrotic response.

These findings demonstrate that the Pt(IV) complexes have the potential to be used as anticancer drugs.

5.6 References

1. Ferlay, J.; Soerjomataram, I.; Ervik, M.; Dikshit, R.; Eser, S.; Mathers, C.; Rebelo, M.; Parkin, D. M.; Forman, D.; Bray, F. GLOBOCAN 2012 v1.0, Cancer Incidence and Mortality Worldwide: IARC CancerBase No. 11 [Internet]. Lyon, France: International Agency for Research on Cancer; 2013. http://globocan.iarc.fr (accessed March 9, 2014).
2. Bray, F.; Jemal, A.; Grey, N.; Ferlay, J.; Forman, D. Global cancer transitions according to the Human Development Index (2008–2030): a population-based study. *Lancet Oncol.* **2012,** *13,* 790-801.
3. Urruticoechea, A.; Alemany, R.; Balart, J.; Villanueva, A.; Viñals, F.; Capellá, G. Recent advances in cancer therapy: an overview. *Curr. Pharm. Des.* **2010,** *16,* 3-10.
4. Biemar, F.; Foti, M. Global progress against cancer—challenges and opportunities. *Cancer Biol. Med.* **2013,** *10,* 183-186.
5. Fricker, S. Metal based drugs: from serendipity to design. *Dalton Trans.* **2007,** *43,* 4903-4917.
6. Harper, B. W.; Krause-Heuer, A. M.; Grant, M. P.; Manohar, M.; Garbutcheon-Singh, K. B.; Aldrich-Wright, J. R. Advances in Platinum Chemotherapeutic. *Chem. Eur. J.* **2010,** *16,* 7064-7077.
7. Kamimura, K.; Suda, T.; Tamura, Y.; Takamura, M.; Yokoo, T.; Igarashi, M.; Kawai, H.; Yamagiwa, S.; Nomoto, M.; Aoyagi, Y. Phase I study of miriplatin combined with transarterial chemotherapy using CDDP powder in patients with hepatocellular carcinoma. *BMC Gastroenterology* **2012,** *12,* 127.
8. Li, G.-q.; Chen, X.-g.; Wu, X.-p.; Xie, J.-d.; Liang, Y.-j.; Zhao, X.-q. C. W.-q.; Fu, L.-w. Effect of Dicycloplatin, a Novel Platinum Chemotherapeutical Drug, on Inhibiting Cell Growth and Inducing Cell Apoptosis. *PLoS ONE* **2012,** *7,* e48994.
9. Wang, X.; Guo, Z. Targeting and delivery of platinum-based anticancer drugs. *Chem. Soc. Rev.* **2013,** *42,* 202–224.
10. Wheate, N. J.; Walker, S.; Craig, G. E.; Oun, R. The status of platinum anticancer drugs in the clinic and in clinical trials. *Dalton Trans.* **2010,** *39,* 8113– 8127.
11. Casini, A.; Reedijk, J. Interactions of anticancer Pt compounds with proteins: an overlooked topic in medicinal inorganic chemistry? *Chem. Sci.* **2012,** *3,* 3135–3144.

12. Graf, N.; Lippard, S. J. Redox activation of metal-based prodrugs as a strategy for drug delivery. *Adv. Drug Deliv. Rev.* **2012,** *64,* 993–1004.
13. Wexselblatt, E.; Gibson, D. What do we know about the reduction of Pt(IV) pro-drugs? *J. Inorg. Biochem.* **2012,** *117,* 220-229.
14. Wong, D. Y. Q.; Ang, W. H. Development of Platinum(IV) Complexes as Anticancer Prodrugs: The Story so Far. *COSMO* **2012,** *8,* 121-134.
15. Bharti, S. K.; Singh, S. K. Recent Developments in the Field of Anticancer Metallopharmaceuticals. *Int. J. PharmTech Res.* **2009**, *1*, 1406-1420.
16. Marques, M. P. M. Platinum and Palladium Polyamine Complexes as Anticancer Agents: The Structural Factor. *ISRN Spectroscopy* **2013,** *2013,* 1-29.
17. Muhammad, N.; Guo, Z. Metal-based anticancer chemotherapeutic agents. *Curr. Opin. Chem. Biol.* **2014,** *19,* 144-153.
18. Vo, V.; Tanthmanatham, O.; Han, H.; Bhowmik, P. K.; Spangelo, B. L. Synthesis of [$PtCl_2$(4,4′-dialkoxy-2,2′-bipyridine)] complexes and their *in vitro* anticancer properties. *Metallomics* **2013,** *5,* 973-987.
19. Mackay, F. S.; Farrer, N. J.; Salassa, L.; Tai, H.-C.; Deeth, R. J.; Moggach, S. A.; Wood, P. A.; Parsons, S.; Sadler, P. J. Synthesis, characterisation and photochemistry of Pt^{IV} pyridyl azido acetato complexes. *Dalton Trans.* **2009,** *13,* 2315-2325.
20. Boulares, A. H.; Yakovlev, A. G.; Ivanova, V.; Stoica, B. A.; Wang, G.; Iyer, S.; Smulson, M. Role of poly(ADP-ribose) polymerase (PARP) cleavage in apoptosis. Caspase 3-resistant PARP mutant increases rates of apoptosis in transfected cells. *J. Biol. Chem.* **1999,** *274,* 22932-22940.

CHAPTER 6

CONCLUSIONS AND FUTURE DIRECTIONS

6.1 Conclusions

Platinum-based drugs are currently used worldwide for the treatment of various cancers; however, severe side effects and intrinsic or acquired resistance have hindered their clinical utility. Motivated to develop platinum drugs with improved efficacy and lower toxicity, three series of platinum(II) and platinum(IV) complexes containing 4,4′-disubstituted-2,2′-bipyridine ligands have been synthesized and investigated for possible anti-tumoral activity.

The first series that was prepared consisted of seven [Pt(II)Cl_2(4,4′-dialkoxy-2,2′-bipyridine)] complexes of the general formula of [Pt(II)Cl_2(4,4′-bis(RO)-2,2′-bipyridine)] (where R = $–(CH_2)_{n–1}CH_3$, n = 2–6, 8), five of which are novel compounds. The anti-proliferative activities of these complexes were examined in a panel of 10 human cancer cell lines from lung, prostate, and breast origin. Although the effects of these [Pt(II)Cl_2(4,4′-dialkoxy-2,2′-bipyridine)] complexes varies between the different cell lines, it can be generalized that all of the novel complexes are more effective than cisplatin and carboplatin in the cell lines tested. The superior activity of these novel platinum complexes are more evident in the short 1 h treatment than in the extended 48 h treatment, suggesting that these novel platinum complexes may reach intracellular targets faster than cisplatin.

The EC_{50} values for two of the complexes, **Pt(II)-1C** and **Pt(II)-2C**, could not be determined in some cell lines due to their poor solubility which prevented testing at

concentrations above 100 μM. However, comparison of the effects at the concentrations tested revealed a correlation between structure and activity; the anti-proliferative activity of the complexes increases as the carbon number on the alkoxy substituents increases from one (**Pt(II)-1C**) to four (**Pt(II)-4C**) carbons. **Pt(II)-5C** (5 carbons) and **Pt(II)-6C** (6 carbons) generally have similar activity to **Pt(II)-4C**. **Pt(II)-8C**, which has eight carbons on the alkoxy substituents, was not tested due to poor solubility.

Pt(II)-4C was selected for further investigation due to having consistently low EC_{50} values in all of the cell lines tested. Examination of **Pt(II)-4C** interaction with DNA by UV-Vis analysis with calf thymus DNA, gel electrophoresis with plasmid pBR322 DNA, and ICP-AES measurement of platinum in **Pt(II)-4C** cells revealed that **Pt(II)-4C** is able to induce DNA damage. Results from western blotting, flow cytometric immunofluorescence, and immunofluorescence microscopy indicate induction of apoptosis and activation of p53, histone H2AX (γH2AX), and MAPK members (JNK, ERK, and p38). Treatment of cells with **Pt(II)-4C** in the presence of MAPK inhibitors resulted in decreased γH2AX compared to cells treated with **Pt(II)-4C** alone suggesting that activation of H2AX is dependent on MAPKs. Furthermore, cells treated with **Pt(II)-4C** in the presence of p53, JNK, or p38 inhibitors had increased cell viability compared to cells treated with **Pt(II)-4C** alone. These results indicate that p53, JNK, and p38 are involved in activation of the apoptotic pathway in response to **Pt(II)-4C**. Moreover, **Pt(II)-4C** induced apoptosis may be regulated by γH2AX in a JNK and p38 dependent manner.

The *in vitro* data indicate that these complexes have potential clinical utility, thus, **Pt(II)-4C** toxicity was tested in mice. Mice injected with **Pt(II)-4C** at a dose of 12.5 mg

kg^{-1} d^{-1} for 3 d survived the study period of 7 d post injection and did not show any abnormal signs. This result indicates that **Pt(II)-4C** is not toxic in animal models at the tested dose; thus, further *in vivo* studies are warranted. However, *in vivo* investigation of **Pt(II)-4C** is complicated by its low solubility in common organic solvents and solubilizing agents.

To improve the solubility of [Pt(II)Cl_2(4,4′-dialkoxy-2,2′-bipyridine)] complexes, the second series of Pt(II) complexes were developed by modification of the dialkoxy substituents to have increasing oxygen which will result in increasing hydrogen bonding and water solubility. This series consist of five [Pt(II)Cl_2(4,4′-dioligooxyethylene-2,2′-bipyridine)] complexes of the general formula of [Pt(II)Cl_2(4,4′-bis(RO)-2,2′-bipyridine)] (where R = $–(CH_2CH_2O)_n(CH_2)_mCH_3$, n = 1–4, m = 0–3). The anti-proliferative activities of these complexes were also examined in a panel of 10 human cancer cell lines from lung, prostate, and breast origin. The results showed varying degrees of activity in the cell lines tested. In some cell lines, the synthesized complexes were as effective as cisplatin or less effective, while in others, the synthesized complexes were more effective than cisplatin. Although these complexes have improved solubility in organic solvents and two have some solubility in water; their anti-proliferative activity is greatly diminished compared to the dialkoxy series.

The third series was then prepared by oxidation of the Pt(II) dialkoxy series to Pt(IV), which resulted in seven [Pt(IV)$Cl_2(OAc)_2$(4,4′-dialkoxy-2,2′-bipyridine)] complexes. The solubility of these Pt(IV) complexes in organic solvents were improved, but they still have poor solubility in water. The anti-proliferative activities of these complexes were also examined in the same panel of cancer cell lines. Similar to the Pt(II)

precursors, these Pt(IV) complexes are generally more effective than cisplatin. **Pt(IV)-1C**–**Pt(IV)-3C** were less active than the Pt(II) counterparts and **Pt(IV)-4C** had similar activity to **Pt(II)-4C**. **Pt(IV)-5C** and **Pt(IV)-6C** were more active than their Pt(II) counterparts in both the 1 h and the 48h treatment. **Pt(II)-8C** could not be tested due to poor solubility, but the increased solubility of Pt(IV) complexes allowed for the testing of **Pt(IV)-8C**, which had high anti-proliferative activity for both the 1 h and the 48 h treatments.

Analysis of cell death revealed that **Pt(IV)-4C** and **Pt(IV)-5C** induced DNA damage in A549 and DU145 cells, which led to activation of apoptosis with some necrotic response. These findings demonstrate that the Pt(IV) complexes have the potential to be used as anticancer drugs and warrant further investigation.

6.2 Future directions

The two Pt(II) series described were prepared by utilizing the 4,4′ positions on the 2,2′-bipyridyl ligand. Other series can be made by changing the functional group at these positions. A few compounds with —COOR and phosphate groups at the 4,4′ positions have been prepared, but their anti-proliferative activities have not been thoroughly investigated. Examination of their anti-proliferative activities may provide useful information on the structure-activity relationship.

New platinum complexes are continuously being made through modifications of existing compounds by employing methods to alter the leaving groups and/or the non-leaving groups.[1] The structure of the 2,2′-bipyridyl ligand offers many opportunities for functionalization to create new compounds. However, it would be interesting to explore the effects of replacing the chloride leaving groups with other types of leaving groups on

the activity of the 2,2′-bipyridyl platinum complexes. Compounds in which the chloride leaving groups were replaced by a pyrophosphate group have been shown to have better or comparable activity to cisplatin and having a different mechanism of action than DNA binding.[2,3] These compounds were also demonstrated to be effective in cisplatin resistance cancer cells. This would be an interesting option to modify the disubstituted-2,2′-bipyridyl platinum(II) and platinum(IV) complexes. Alternatively, modification of the axial ligands of the Pt(IV) complexes may result in improvements.[4]

In addition to the synthesis of new compounds, further investigation of the three synthesized series should be done. Some of the results presented are only from one or two trials; thus they need to be repeated to confirm the results. Also, a major concern with cisplatin is intrinsic or acquired resistance; thus, these complexes should be tested in cisplatin resistant cells.

Cisplatin induced DNA damage activates many signaling pathways. Although activation of p53 and MAPKs by **Pt(II)-4C** have been demonstrated, it is not exactly clear how they are involved. Thus, their upstream and downstream signaling should be examined. Additionally, the use of a chemical inhibitor may not provide accurate information since they can interact with other biological molecules. Consequently, results obtained with the p53 and MAPK inhibitors should be confirmed with knockout experiments.

Since the Pt(IV) complexes are also highly effective and various data indicate that they induce apoptosis, the p53 and MAPK experiments done for the **Pt(II)-4C** should be repeated with **Pt(IV)-4C** or **Pt(IV)-5C**. Although the Pt(II)-dioligooxyethylene series are not as effective as the other two series, **Pt(II)-4O,2C** should be examined further since it

is water soluble and had comparable activity to cisplatin in some of the tested cell lines. Perhaps combination treatment with phytochemicals[4–6] or photochemical internalization-mediated delivery may increase the effectiveness of these complexes.[7,9] Lastly, instead of directly modifying the complexes to improve solubility, it might be beneficial to explore delivery methods such as incorporation into a macromolecular delivery system.[10–12]

6.3 References

1. Wilson, J. J.; Lippard, S. J. Synthetic Methods for the Preparation of Platinum Anticancer Complexes. *Chem. Rev.* **2014,** *114,* 4470−4495.
2. Bose, R. N.; Maurmann, L.; Mishur, R. J.; Yasui, L.; Gupta, S.; Grayburn, W. S.; Hofstetter, H.; Salley, T. Non-DNA-binding platinum anticancer agents: Cytotoxic activities of platinum-phosphato complexes towards human ovarian cancer cells. *Proc. Natl. Acad. Sci. U. S. A.* **2008,** *105,* 18314-18319.
3. Moghaddas, S.; Majmudar, P.; Marin, R.; Dezvareh, H.; Qi, C.; Soans, E.; Bose, R. N. Phosphaplatins, next generation platinum antitumor agents: A paradigm shift in designing and defining molecular targets. *Inorganica Chimica Acta* **2012,** *393,* 173-181.
4. Zheng, Y.-R.; Suntharalingam, K.; Johnstone, T. C.; Yoo, H.; Lin, W.; Brooks, J. G.; Lippard, S. J. Pt(IV) Prodrugs Designed to Bind Non-Covalently to Human Serum Albumin for Drug Delivery. *J. Am. Chem. Soc.* **2014,** *136,* 879.
5. Yeruva, L.; Hall, C.; Elegbede, J. A.; Carper, S. W. Perillyl alcohol and methyl jasmonate sensitize cancer cells to cisplatin. *Anticancer Drugs* **2010,** *21,* 1-9.
6. Al Moundhri, M. S.; Al-Salam, S.; Al Mahrouqee, A.; Beegam, S.; Ali, B. H. The Effect of Curcumin on Oxaliplatin and Cisplatin Neurotoxicity in Rats: Some Behavioral, Biochemical, and Histopathological Studies. *J. Med. Toxicol.* **2013,** *9,* 25-33.
7. Zhao, J.-l.; Zhao, J.; Jiao, H.-j. Synergistic Growth-Suppressive Effects of Quercetin and Cisplatin on HepG2 Human Hepatocellular Carcinoma Cells. *Appl. Biochem. Biotechnol.* **2014,** *172,* 784–791.
8. Prasmickaite, L.; Høgset, A.; Selbo, P.; Engesæter, B.; Hellum, M.; Berg, K. Photochemical disruption of endocytic vesicles before delivery of drugs: a new strategy for cancer therapy. *Br. J. Cancer* **2002,** *86,* 652 – 657.
9. Mathews, M.; Vo, V.; Shih, E.; Zamora, G.; Sun, C.; Madsen, S.; Hirschberg, H. Photochemical internalization-mediated delivery of chemotherapeutic agents in human breast tumor cell lines. *J. Environ. Pathol. Toxicol. Oncol.* **2012,** *31,* 49-59.

10. Harper, B. W.; Krause-Heuer, A. M.; Grant, M. P.; Manohar, M.; Garbutcheon-Singh, K. B.; Aldrich-Wright, J. R. Advances in Platinum Chemotherapeutic. *Chem. Eur. J.* **2010,** *16,* 7064-7077.

11. Wong, D. Y. Q.; Ang, W. H. Development of Platinum(IV) Complexes as Anticancer Prodrugs: The Story so Far. *COSMO* **2012,** *8,* 121-134.

12. Butler, J. S.; Sadler, P. J. Targeted delivery of platinum-based anticancer complexes. *Curr. Opin. Chem. Biol.* **2013,** *17,* 175-188.

APPENDIX 1

SUPPORTING INFORMATION FOR CHAPTER 2

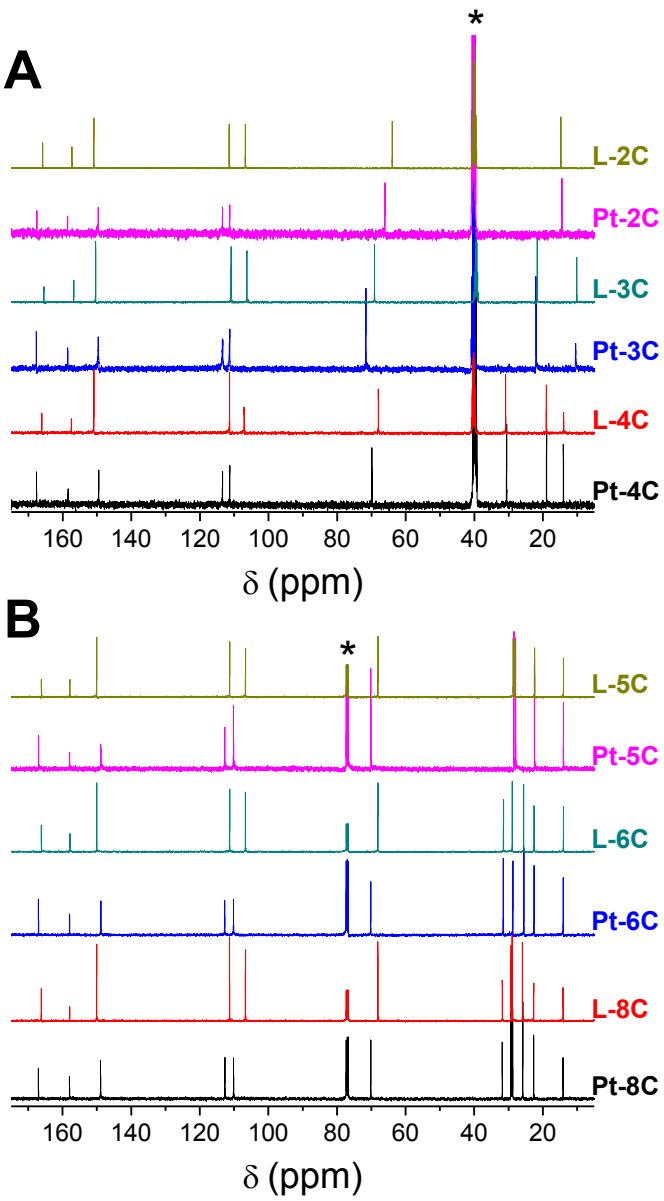

Figure 2S – 1. ^{13}C NMR spectra of ligands and Pt(II)-complexes recorded in A) DMSO-d_6 and B) $CDCl_3$ at temperatures indicated in the experimental section (* solvent peak).

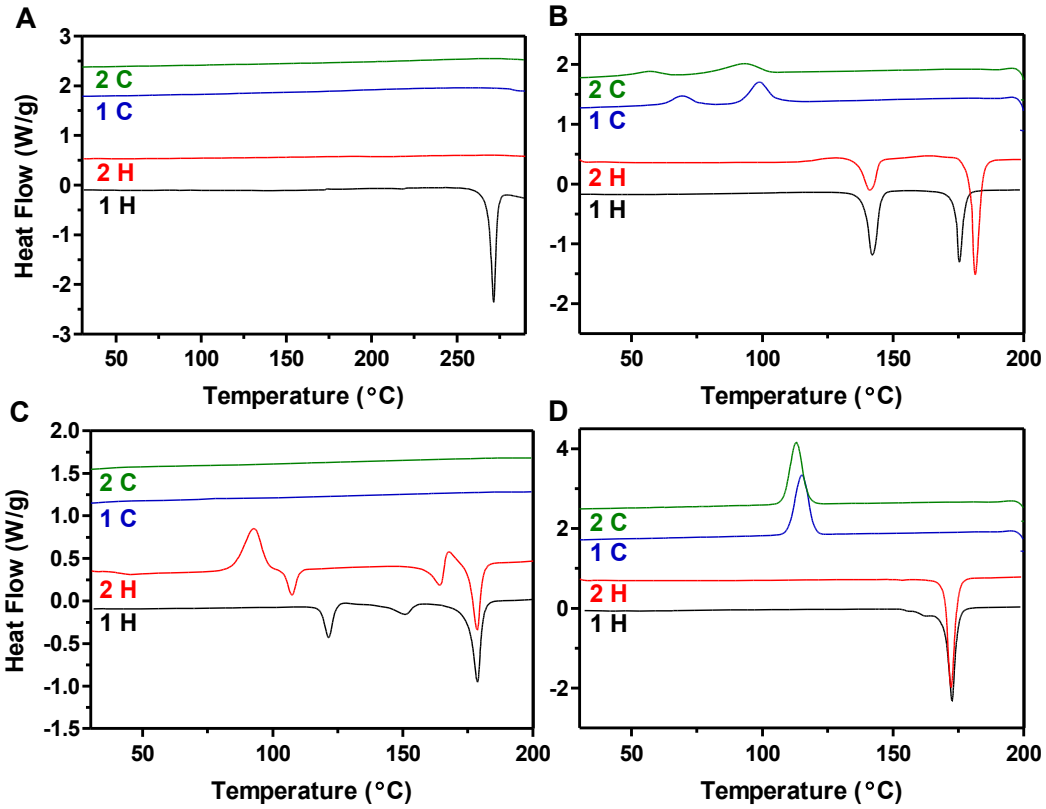

Figure 2S – 2. DSC thermograms of A) **Pt-3C**, B) **Pt-5C**, C) **Pt-6C**, and D) **Pt-8C** obtained in nitrogen at heating and cooling rates of 10 °C/min.

APPENDIX 2

SUPPORTING INFORMATION FOR CHAPTER 3

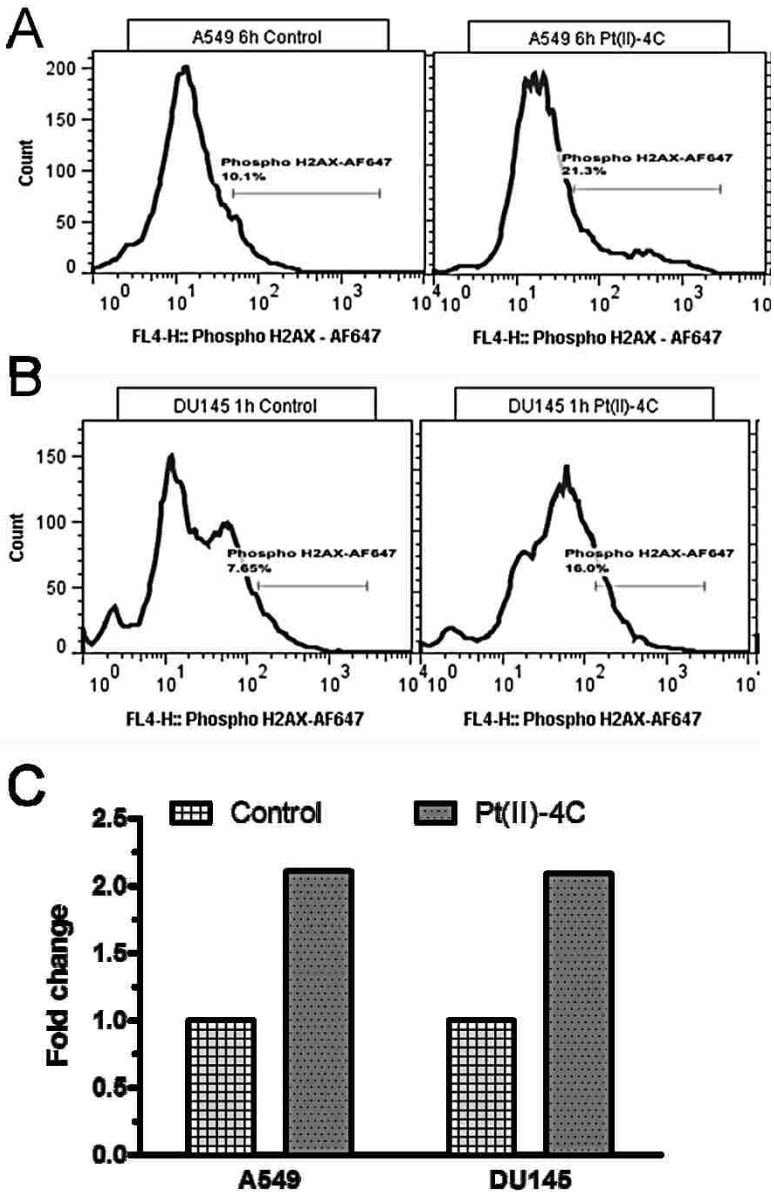

Figure 3S – 1. Flow cytometric analysis of γH2AX. (A) A549 cells treated for 6 h with 25 μM **Pt(II)-4C**, (B) DU145 cells treated for 1 h with 25 μM **Pt(II)-4C**, and (D) fold change in the fluorescence signals compared to control. Histograms are representative of three experiments.

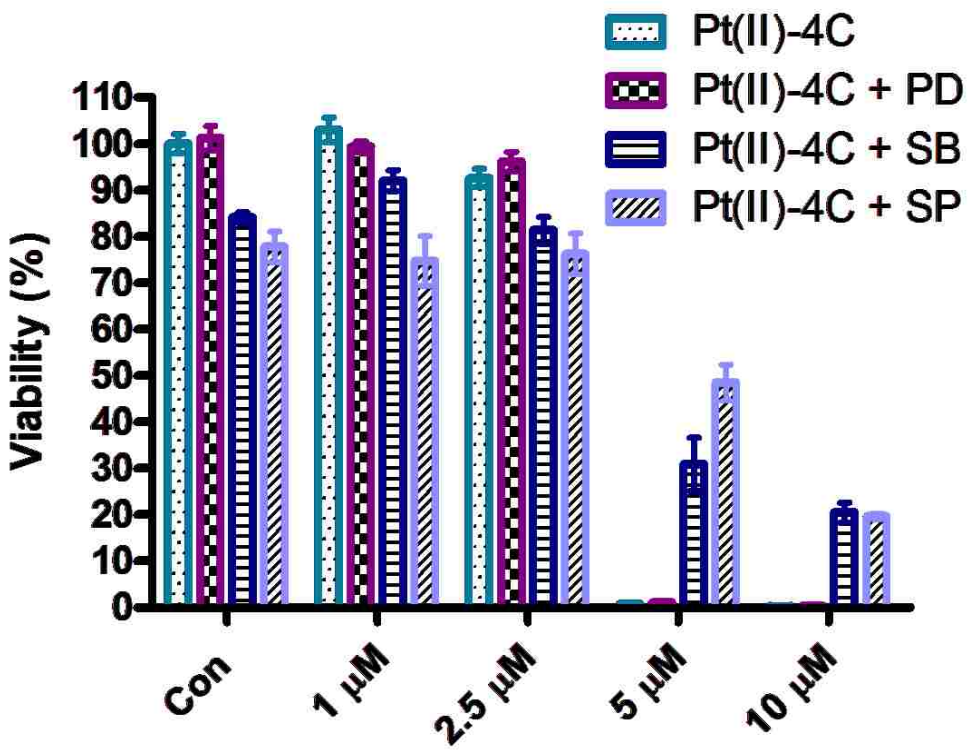

Figure 3S – 2. Effects of MAPK inhibitors on **Pt(II)-4C** induced cell death in DU145 cells. The cells were treated with increasing concentrations of **Pt(II)-4C** in the absence and presence of 50 μM of MAPK inhibitors (PD: ERK inhibitor, SB: p38 inhibitor, SP: JNK inhibitor) for 48 h. Results are representative of two independent experiments done in quadruplicates.

APPENDIX 3

SUPPORTING INFORMATION FOR CHAPTER 4

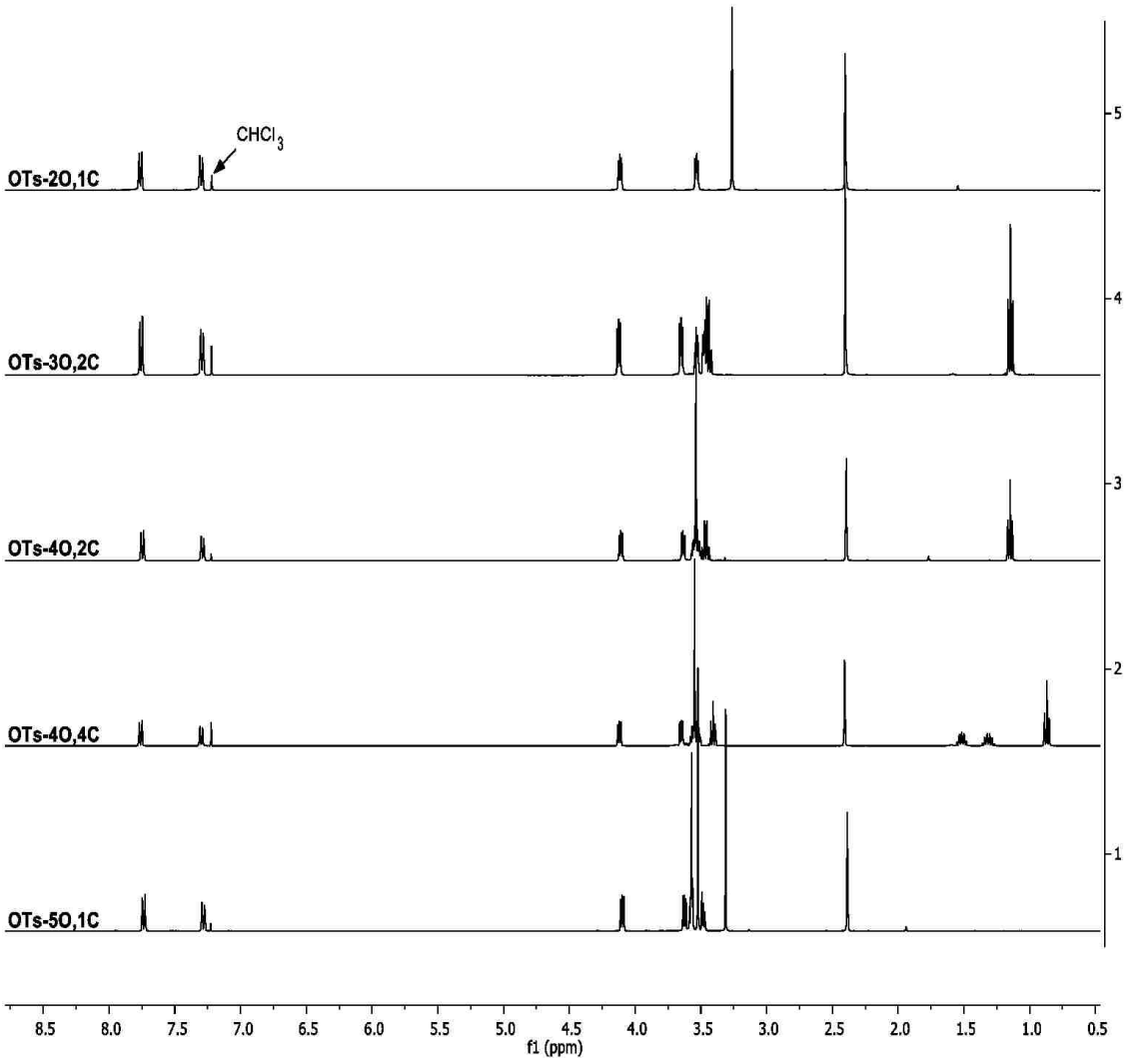

Figure 4S – 1. ^{1}H NMR of tosylate compounds recorded in $CDCl_3$ at room temperature.

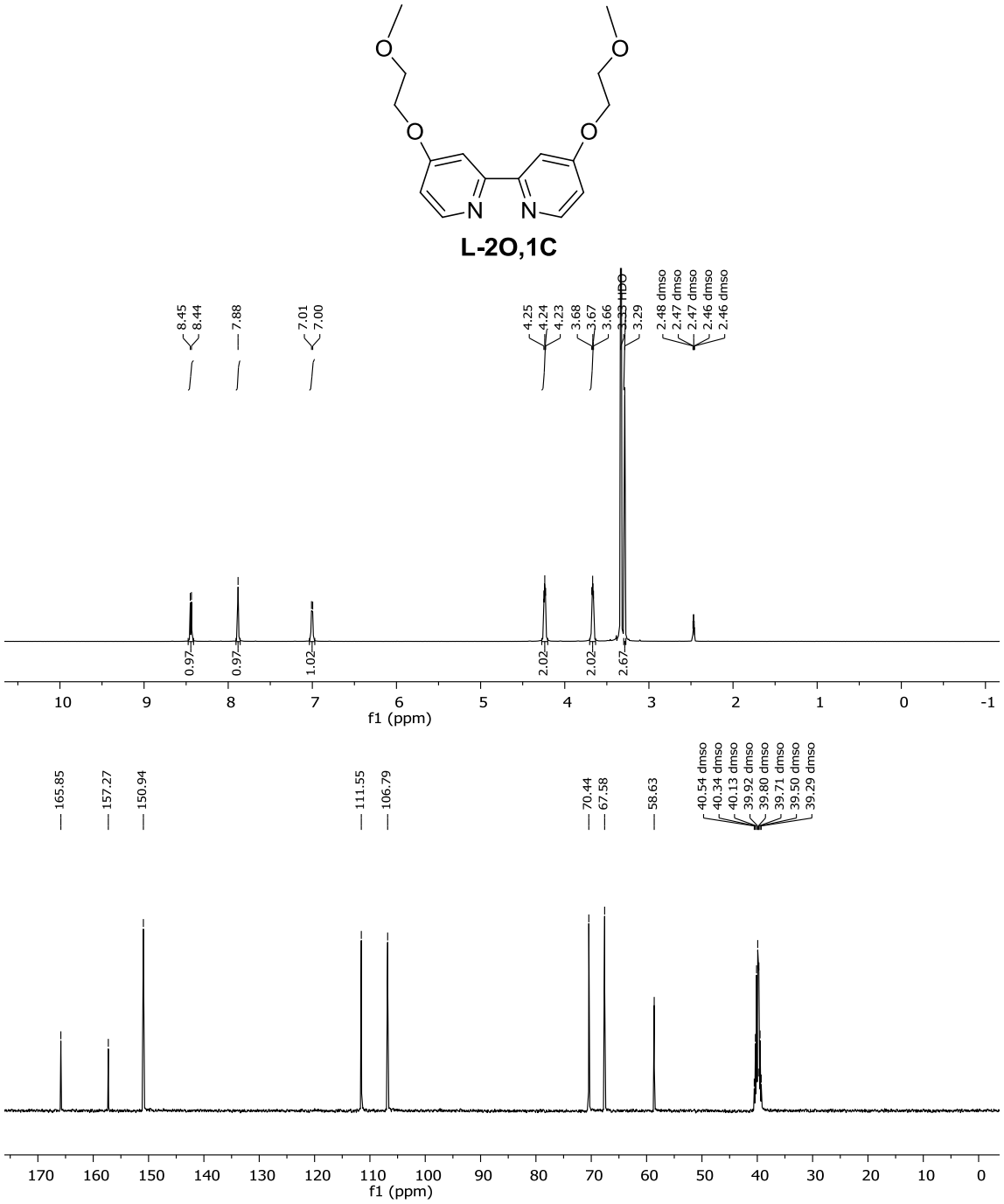

Figure 4S –2. ^{1}H (top) and ^{13}C (bottom) NMR spectra of compound **L-2O,1C** recorded in DMSO-d_6 at room temperature.

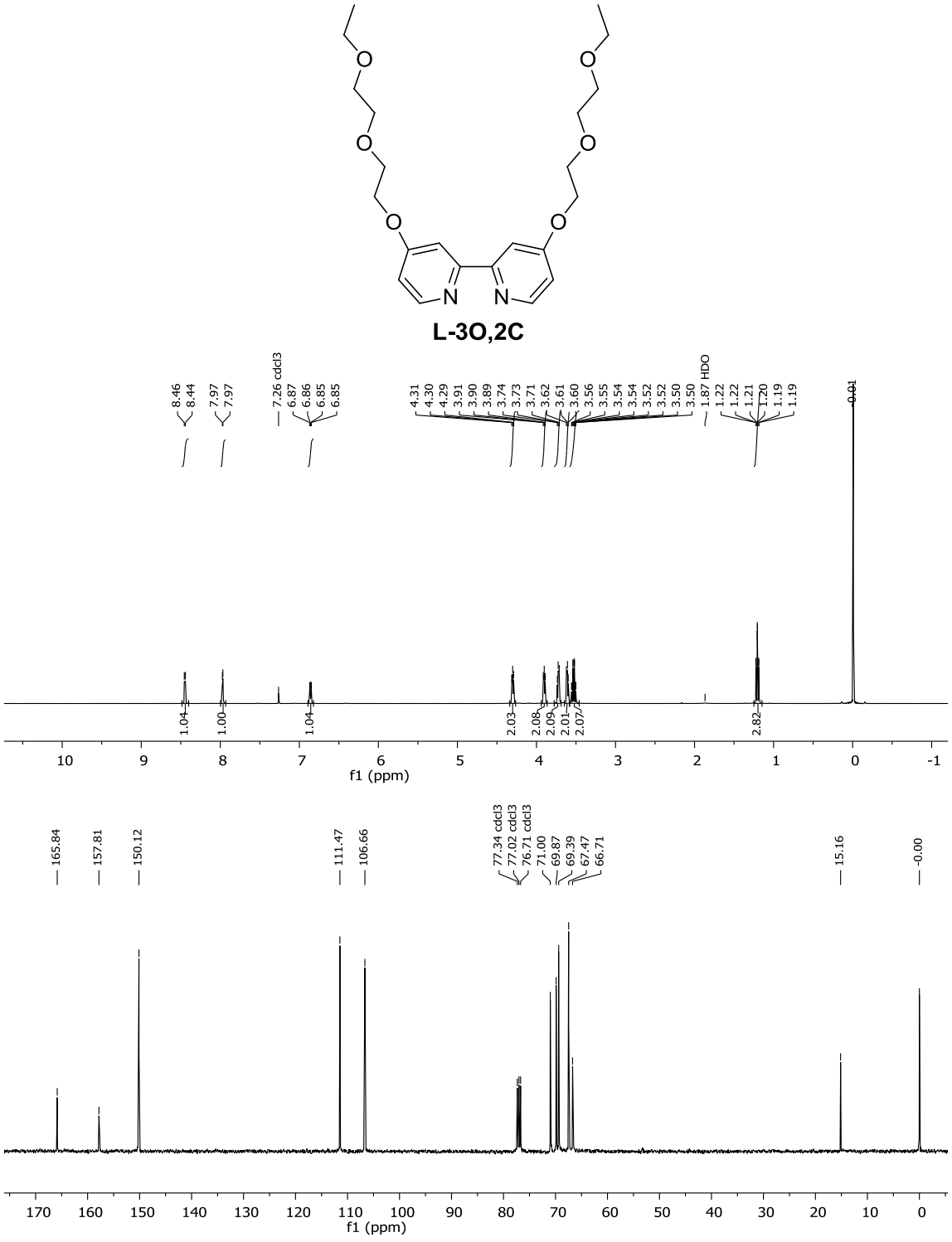

Figure 4S –3. ^{1}H (top) and ^{13}C (bottom) NMR spectra of compound **L-3O,2C** recorded in $CDCl_3$ at room temperature.

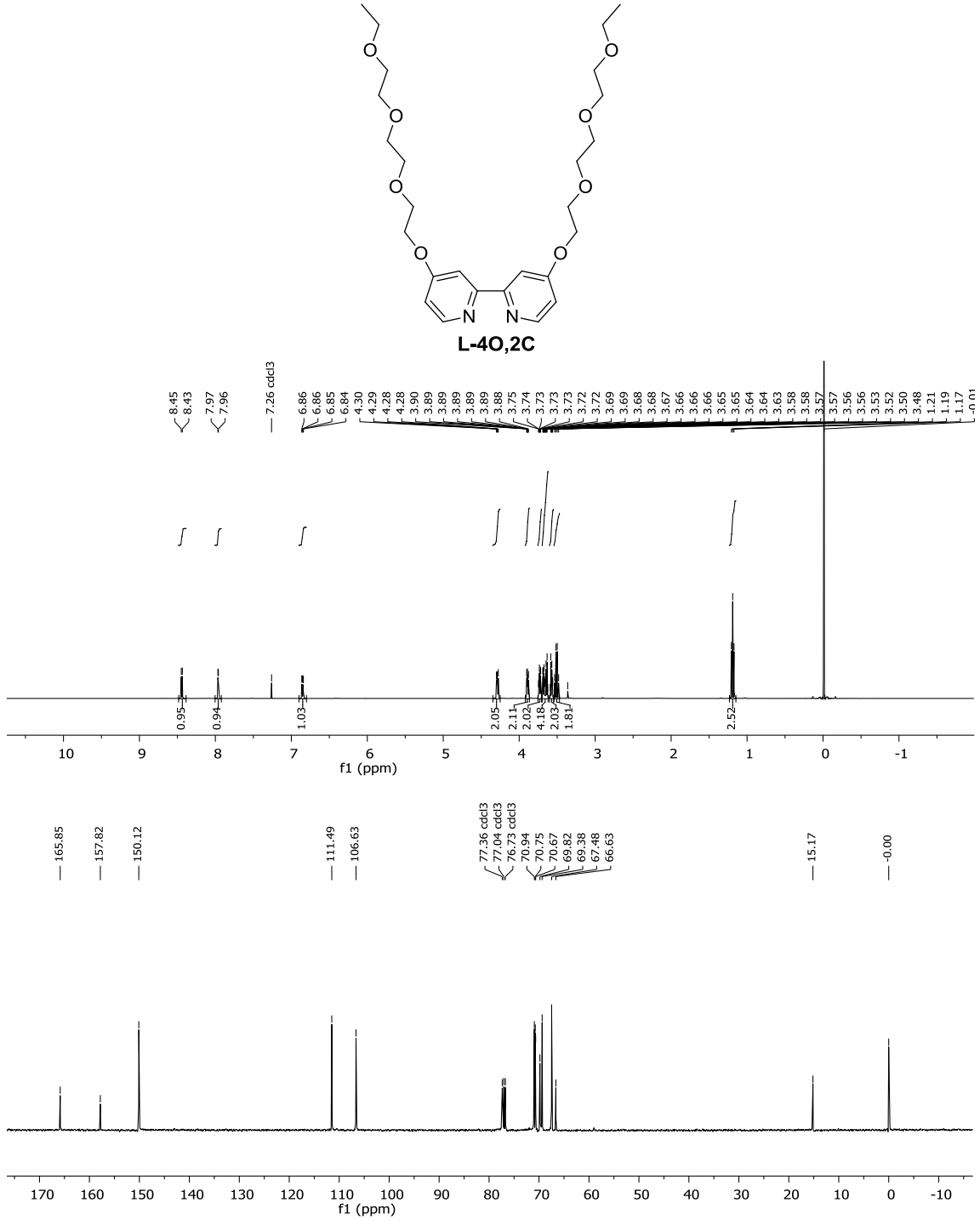

Figure 4S –4. ^{1}H (top) and ^{13}C (bottom) NMR spectra of compound **L-4O,2C** recorded in $CDCl_3$ at room temperature.

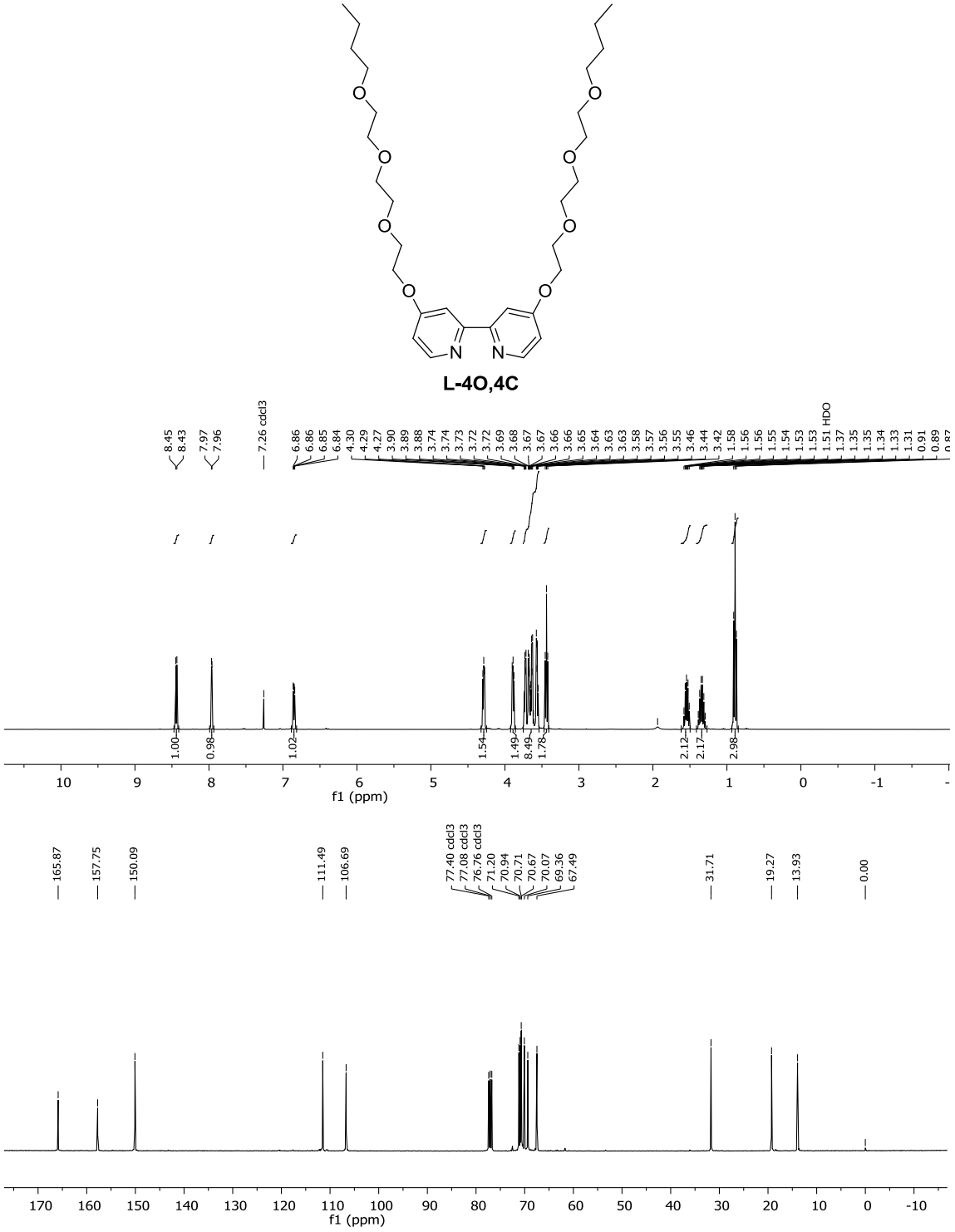

Figure 4S –5. ^{1}H (top) and ^{13}C (bottom) NMR spectra of compound **L-4O,4C** recorded in $CDCl_3$ at room temperature.

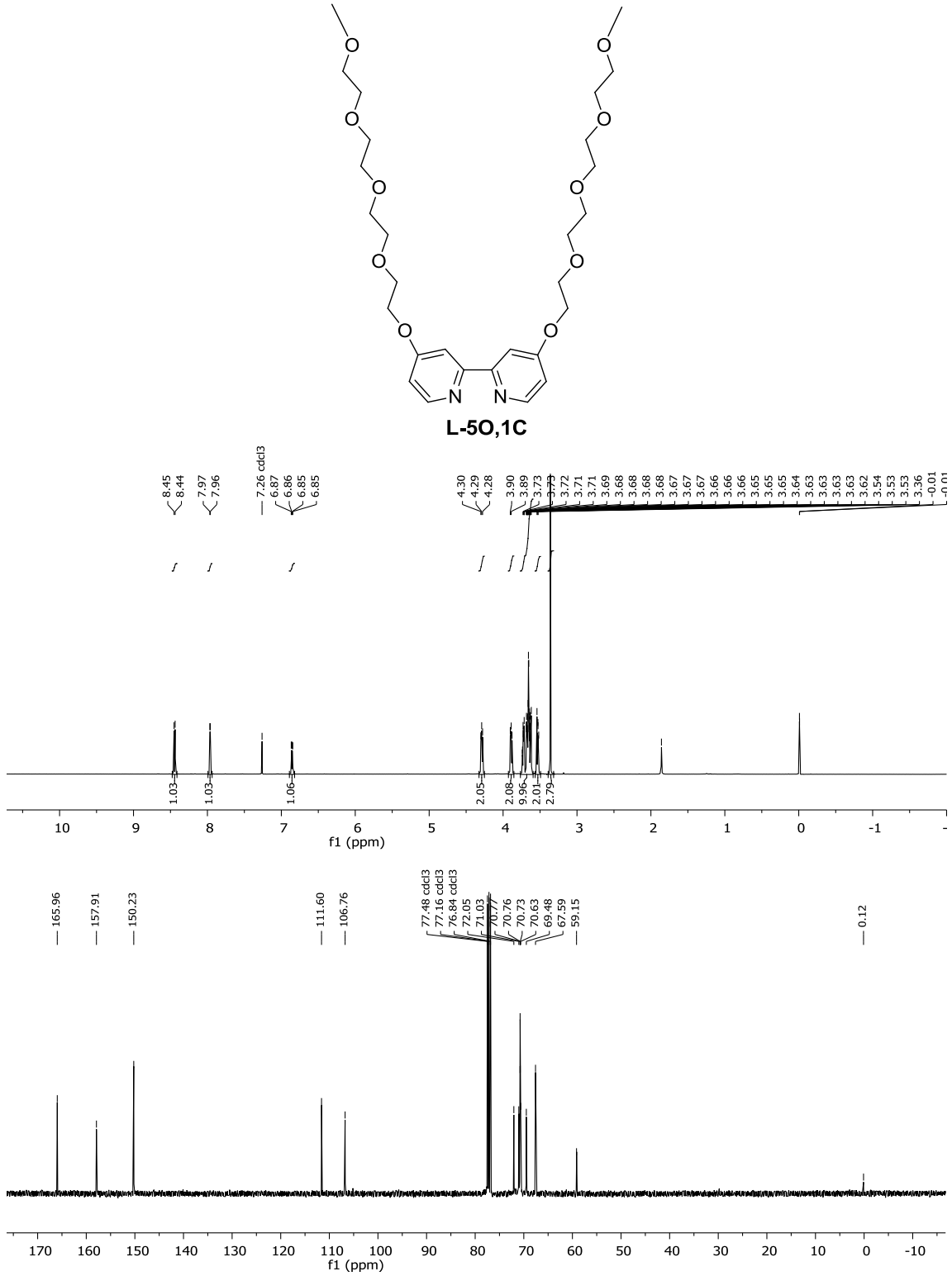

Figure 4S –6. ^{1}H (top) and ^{13}C (bottom) NMR spectra of compound **L-5O,1C** recorded in $CDCl_3$ at room temperature.

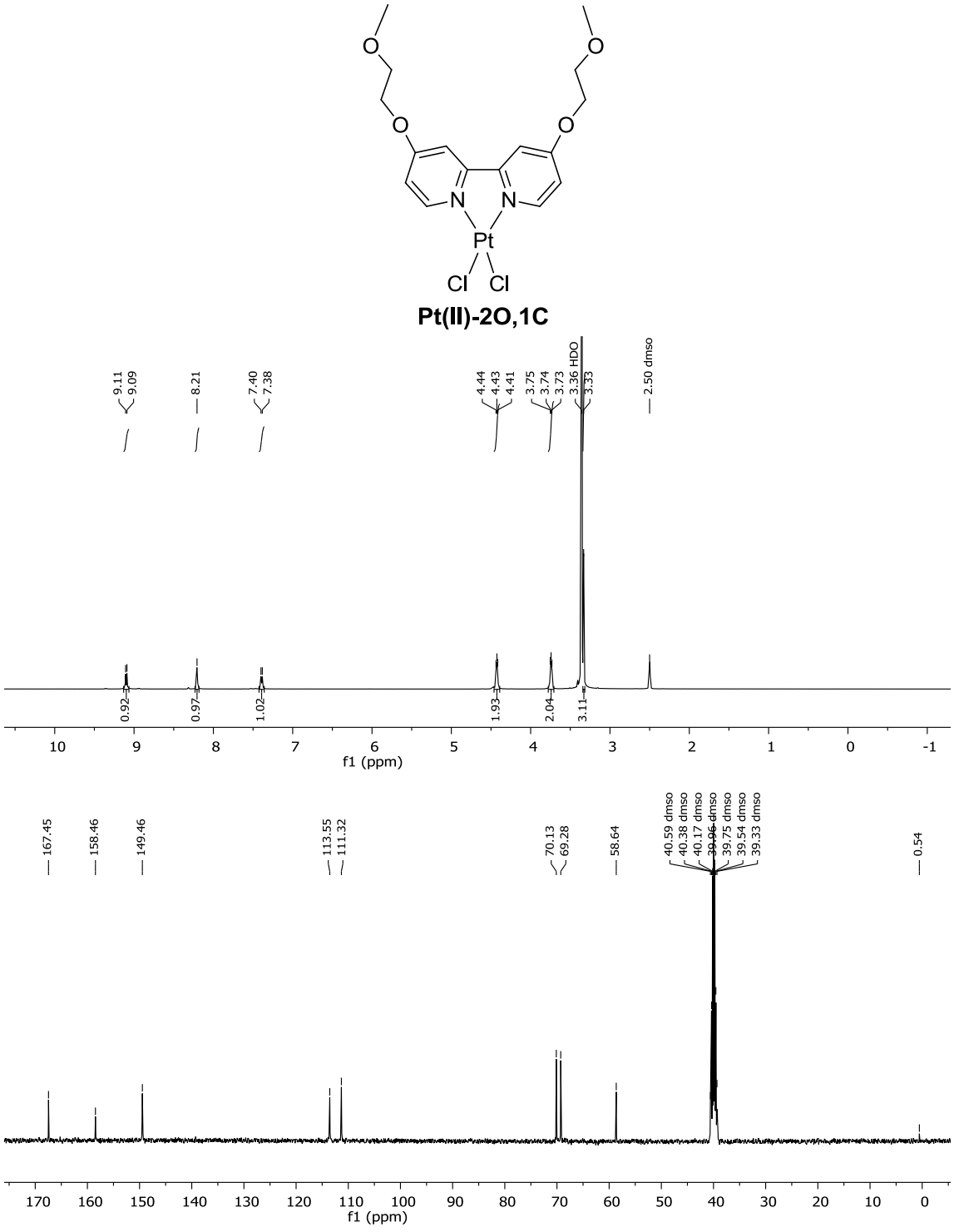

Figure 4S –7. ^{1}H (top) and ^{13}C (bottom) NMR spectra of compound **Pt(II)-2O,1C** recorded in DMSO-d_6 at room temperature.

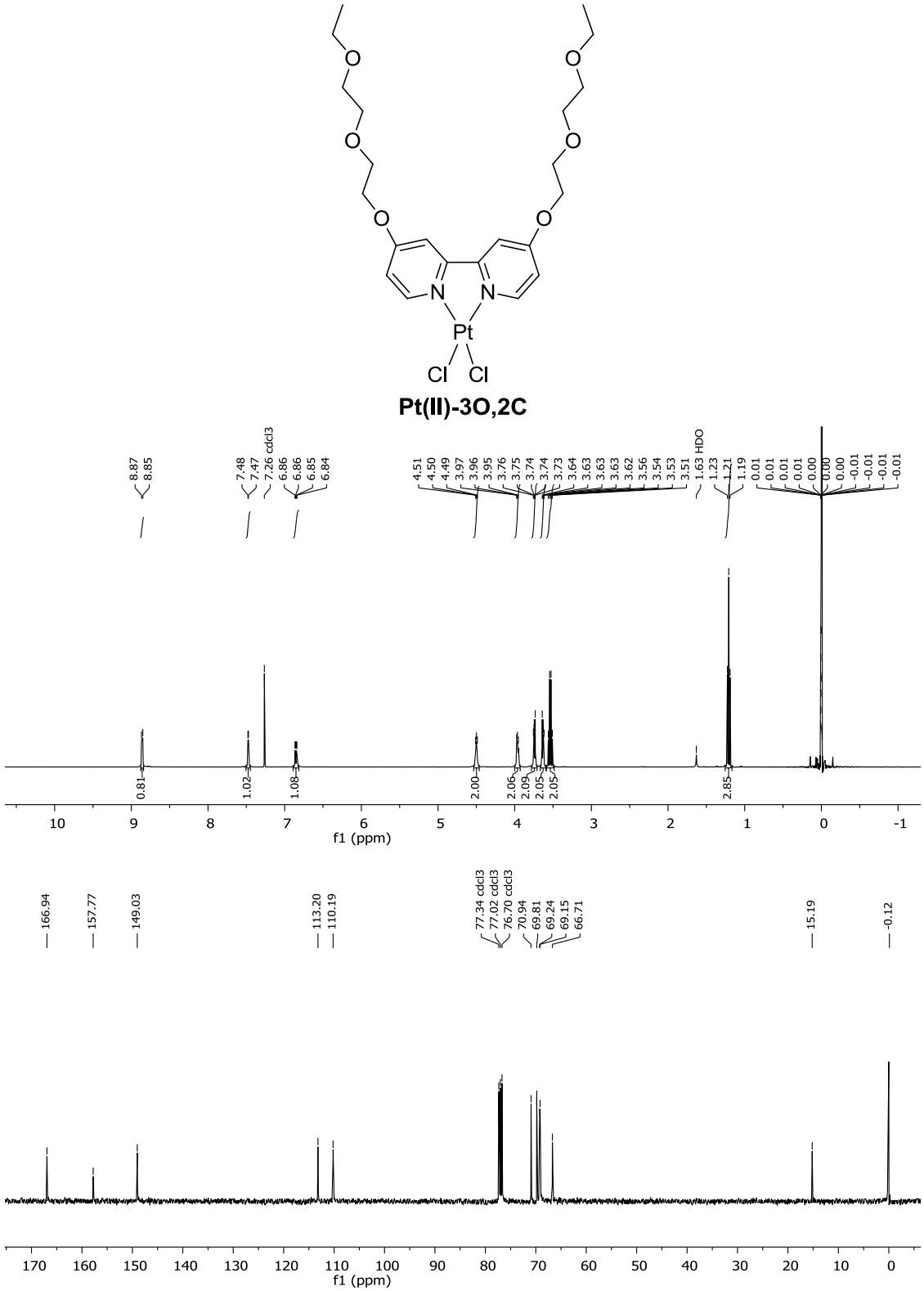

Figure 4S –8. ^{1}H (top) and ^{13}C (bottom) NMR spectra of compound **Pt(II)-3O,2C** recorded in $CDCl_3$ at room temperature.

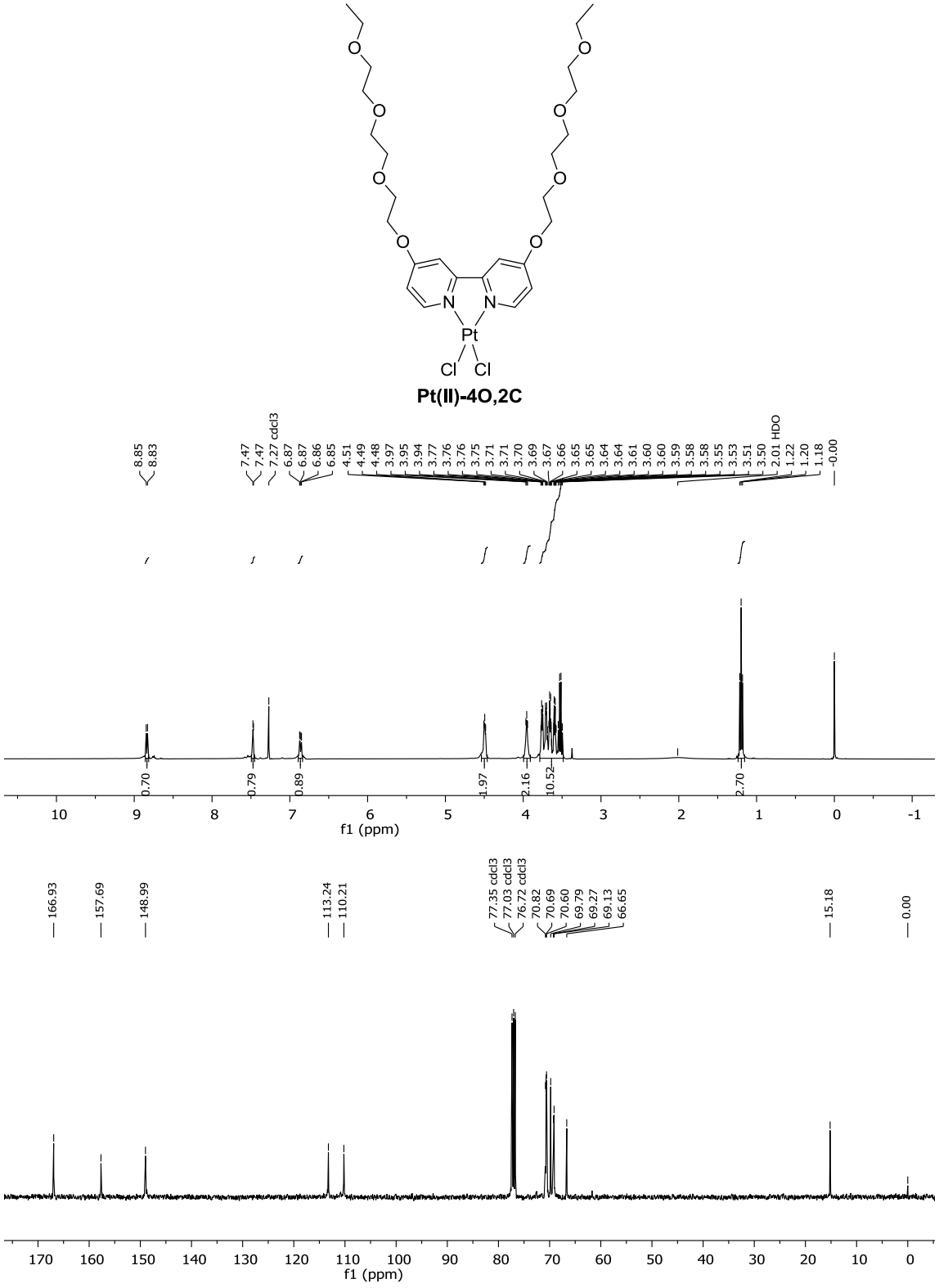

Figure 4S –9. ^{1}H (top) and ^{13}C (bottom) NMR spectra of compound **Pt(II)-4O,2C** recorded in $CDCl_3$ at room temperature.

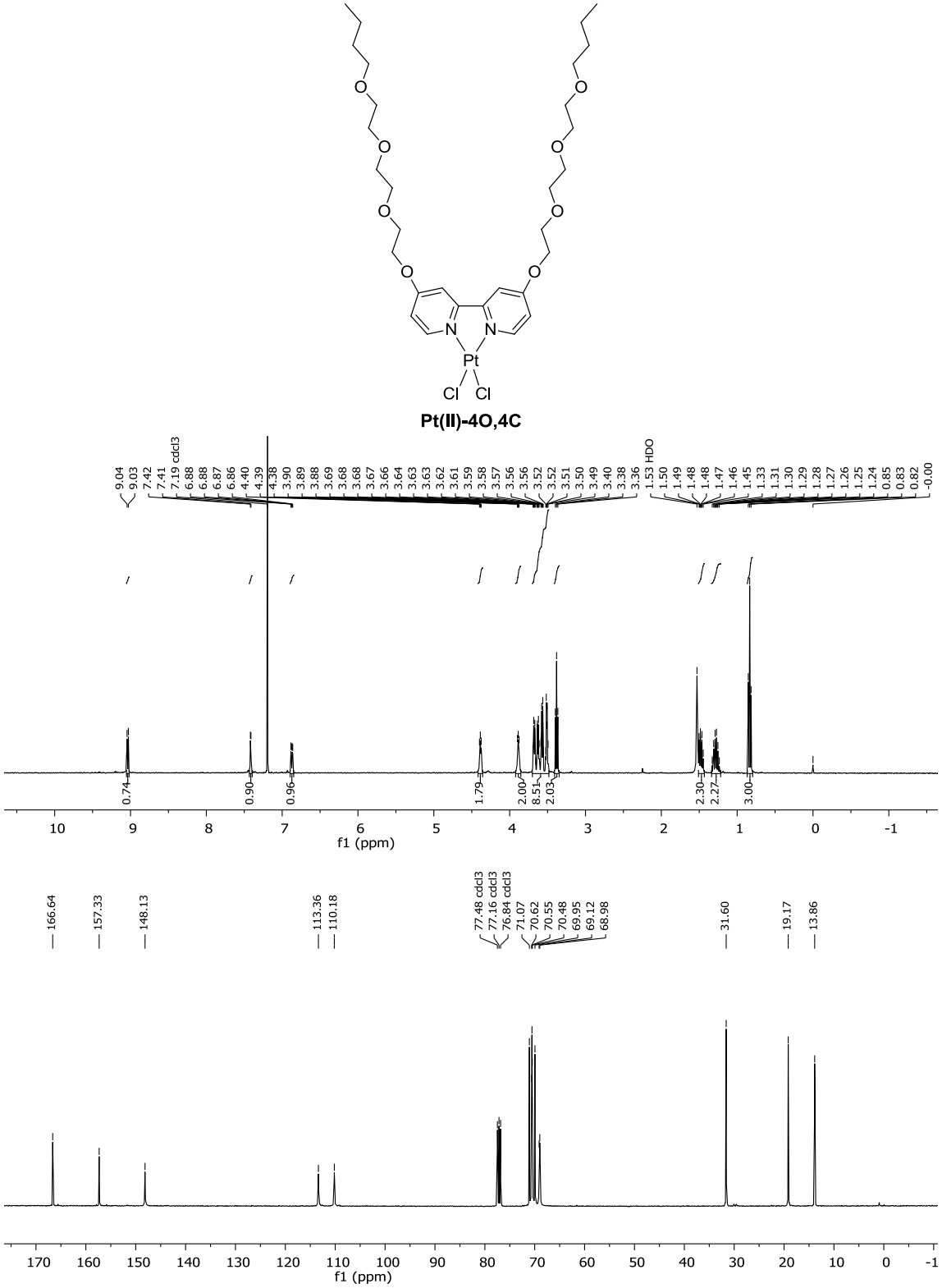

Figure 4S –10. ^{1}H (top) and ^{13}C (bottom) NMR spectra of compound **Pt(II)-4O,4C** recorded in $CDCl_3$ at room temperature.

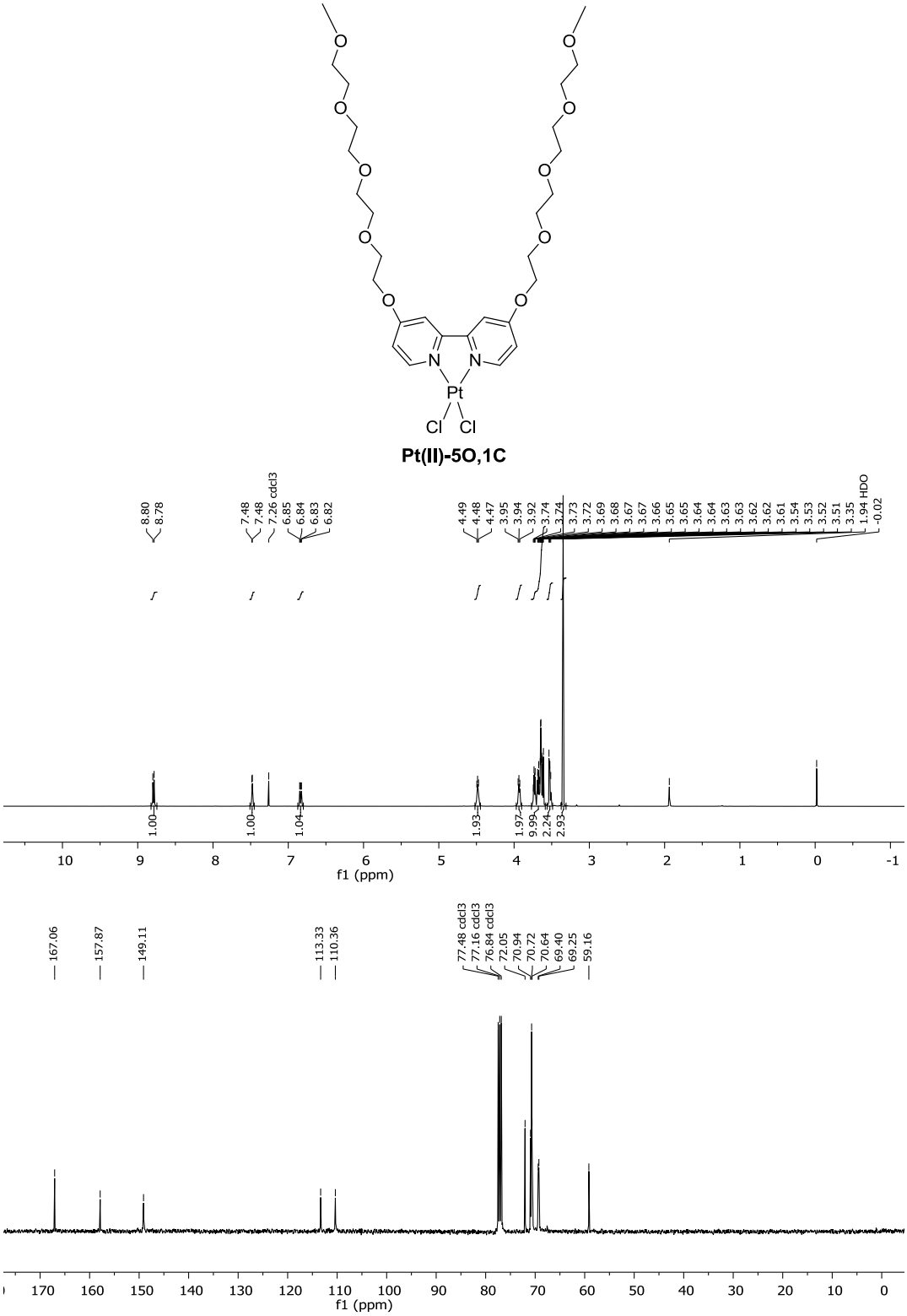

Figure 4S –11. ^{1}H (top) and ^{13}C (bottom) NMR spectra of compound **Pt(II)-5O,1C** recorded in $CDCl_3$ at room temperature.

APPENDIX 4

SUPPORTING INFORMATION FOR CHAPTER 5

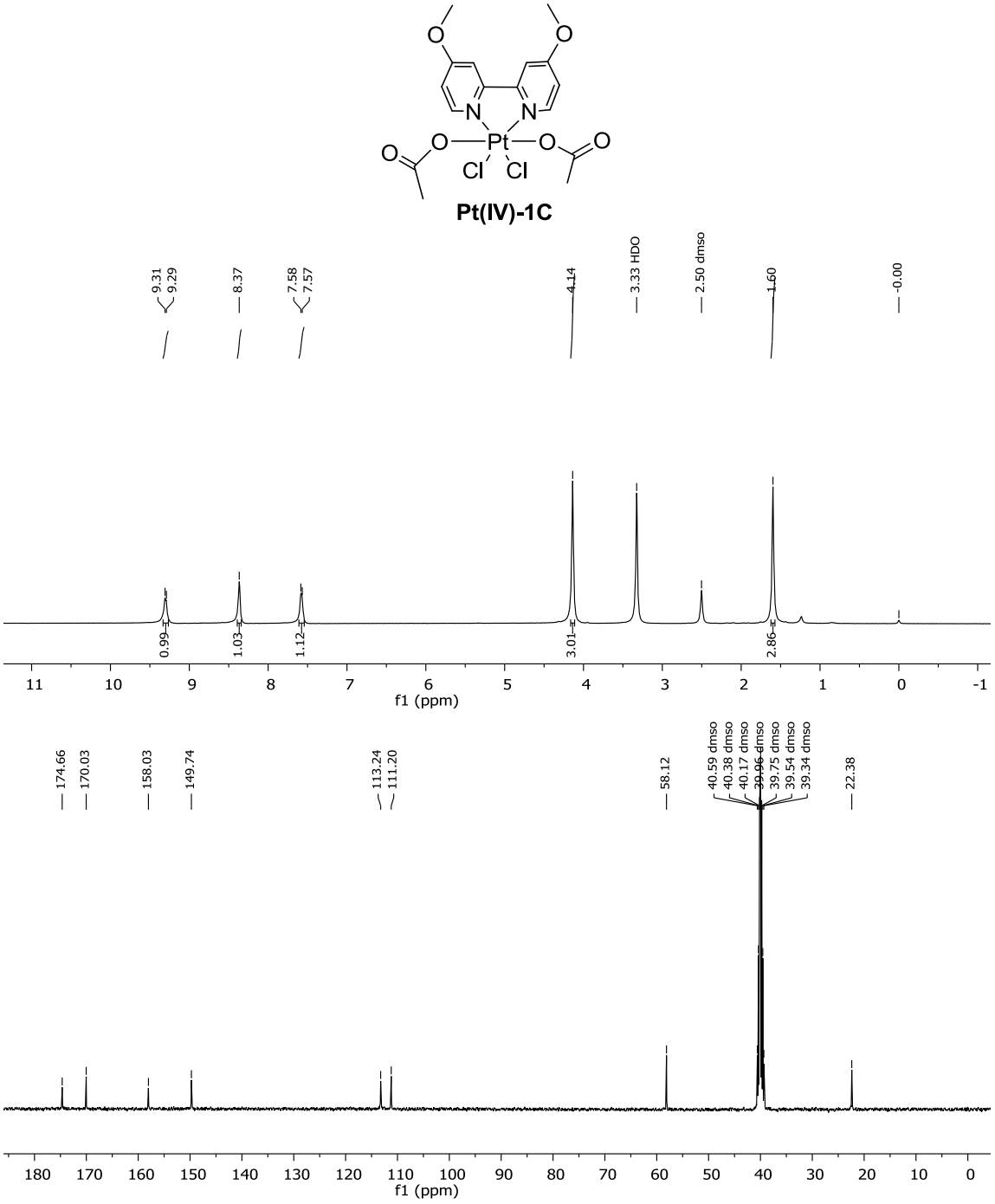

Figure 5S –1. ^{1}H (top) and ^{13}C (bottom) NMR spectra of compound **Pt(IV)-1C** recorded in DMSO-d_6 at room temperature.

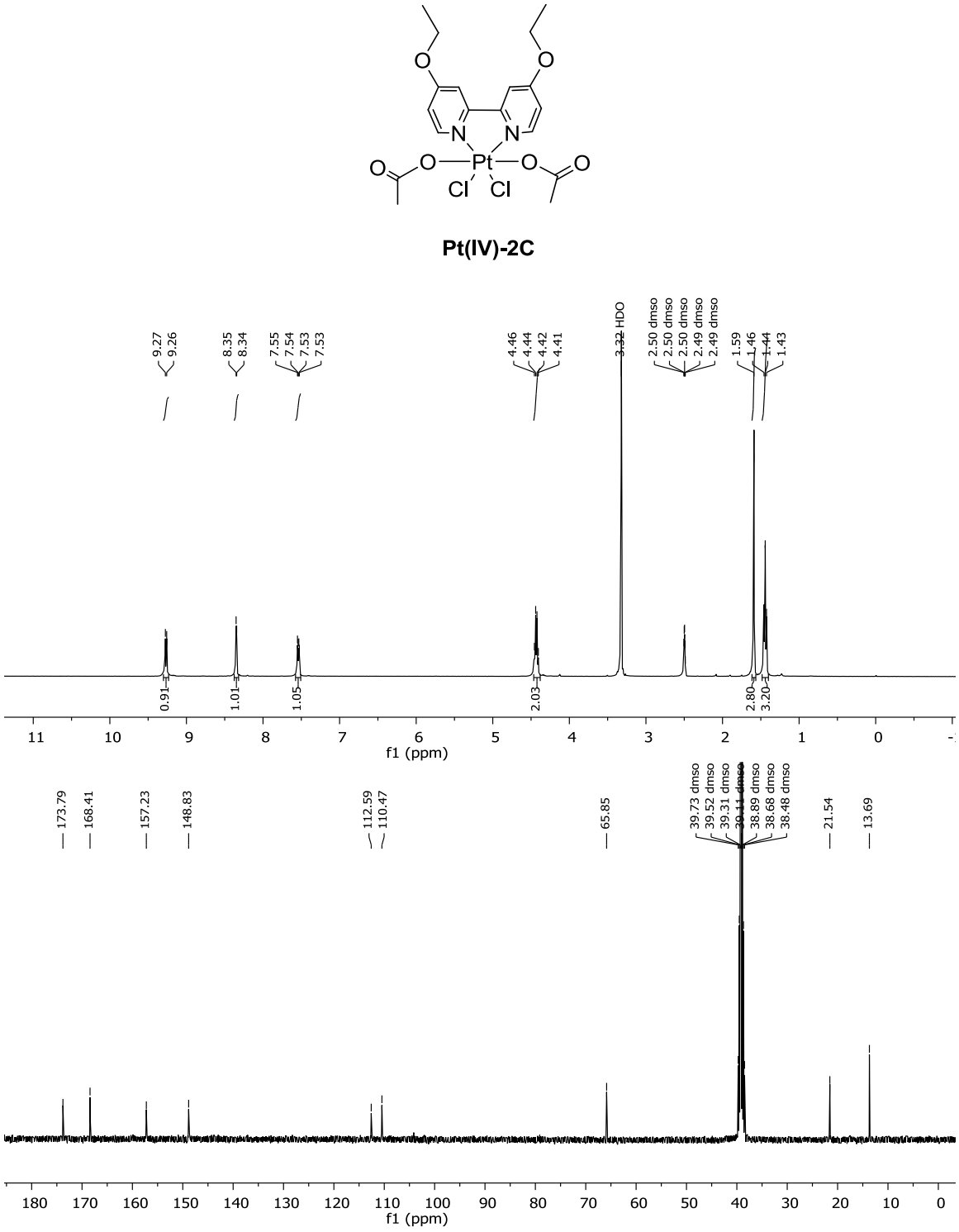

Figure 5S –2. ^{1}H (top) and ^{13}C (bottom) NMR spectra of compound **Pt(IV)-2C** recorded in DMSO-d_6 at room temperature.

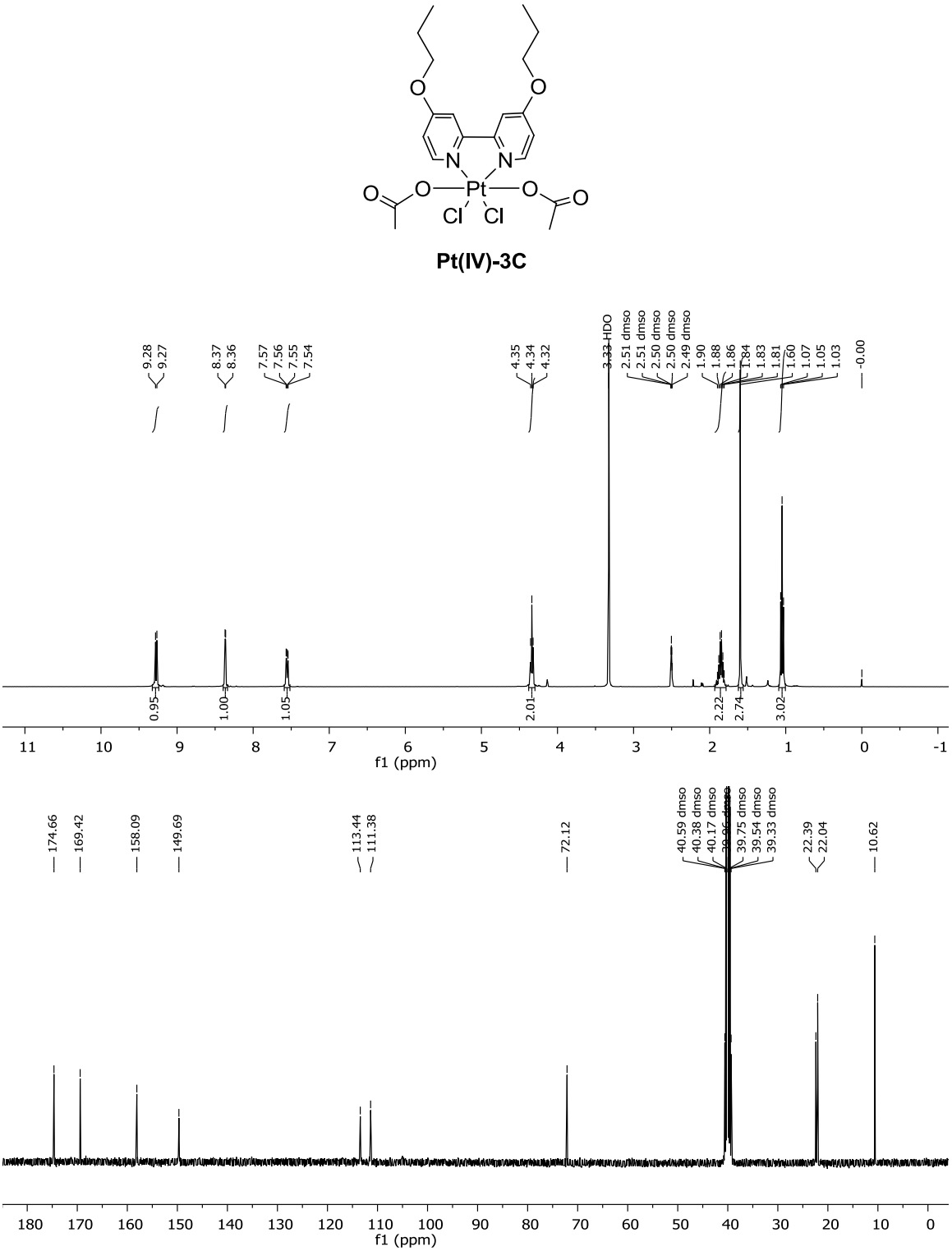

Figure 5S – 3. ^{1}H (top) and ^{13}C (bottom) NMR spectra of compound **Pt(IV)-3C** recorded in DMSO-d_6 at room temperature.

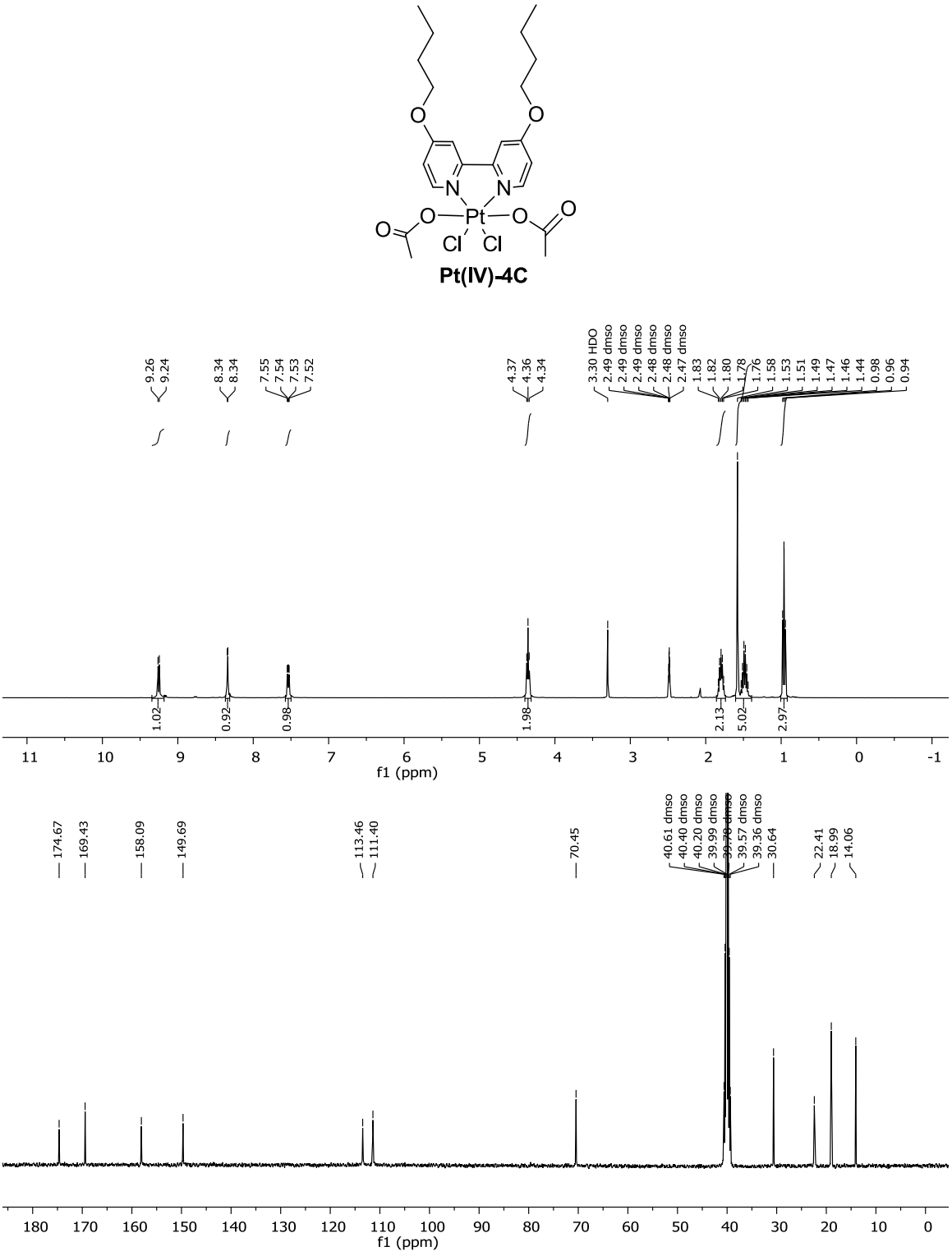

Figure 5S – 4. ^{1}H (top) and ^{13}C (bottom) NMR spectra of compound **Pt(IV)-4C** recorded in DMSO-d_6 at room temperature.

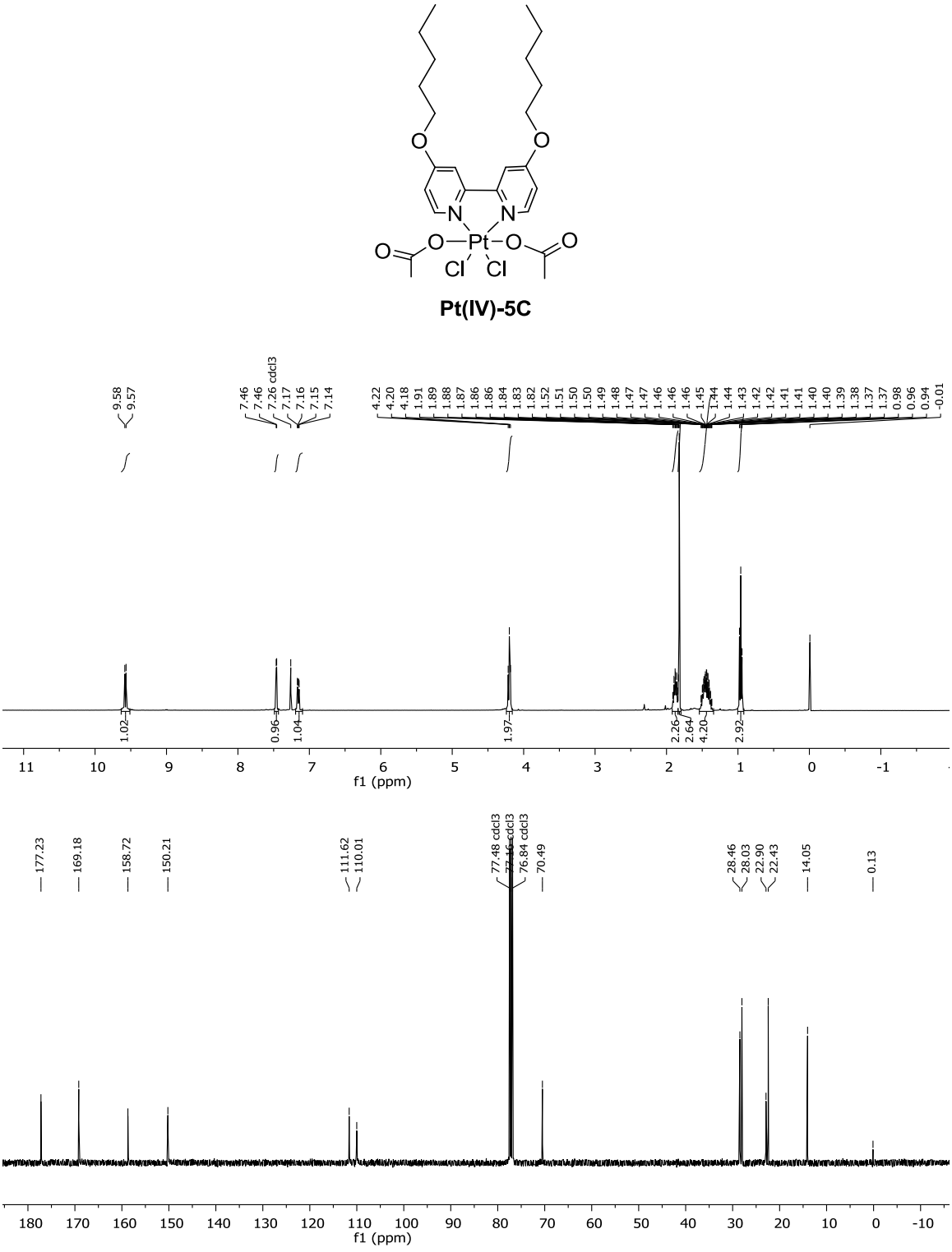

Figure 5S – 5. ^{1}H (top) and ^{13}C (bottom) NMR spectra of compound **Pt(IV)-5C** recorded in $CDCl_3$ at room temperature.

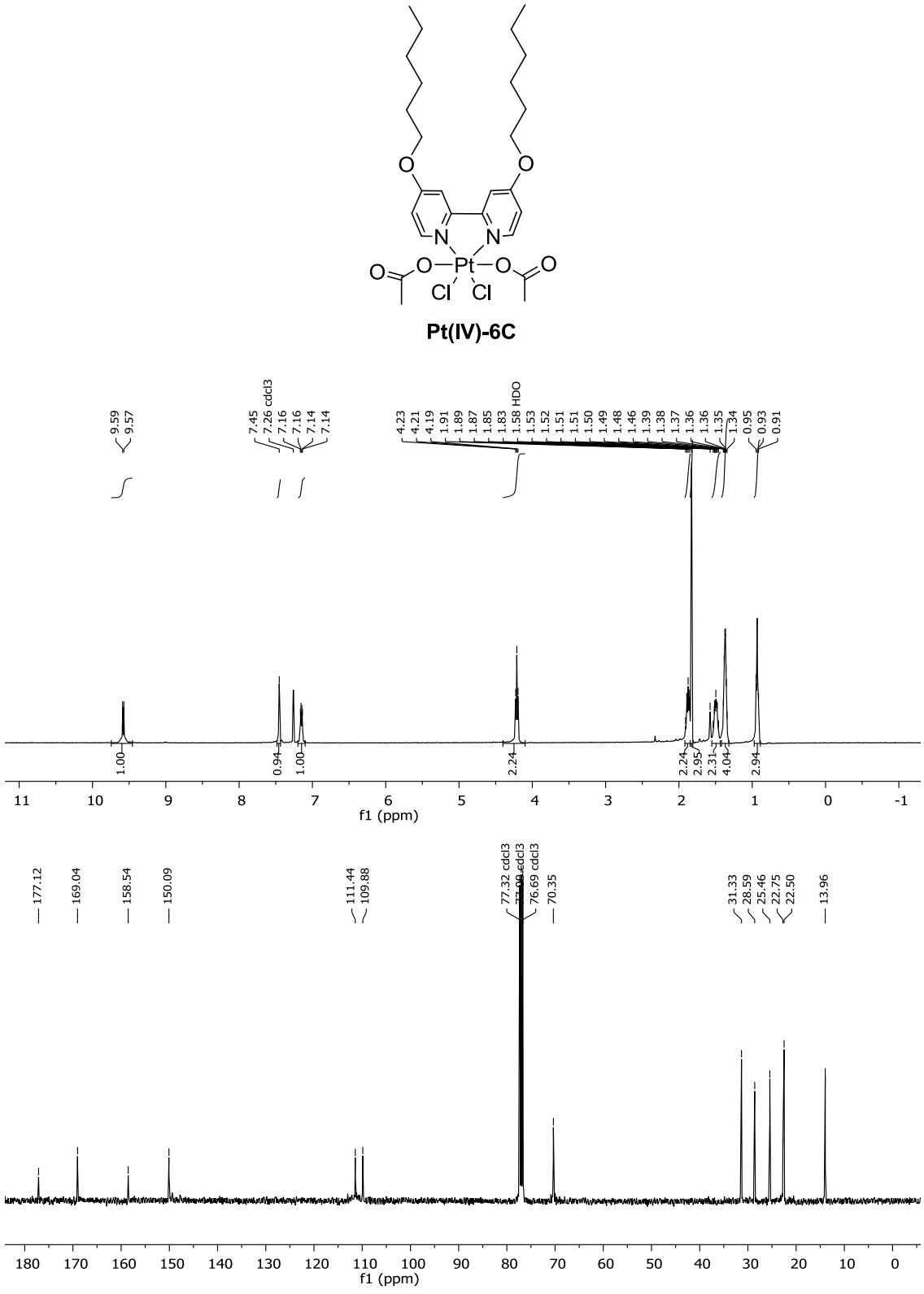

Figure 5S – 6. ^{1}H (top) and ^{13}C (bottom) NMR spectra of compound **Pt(IV)-6C** recorded in $CDCl_3$ at room temperature.

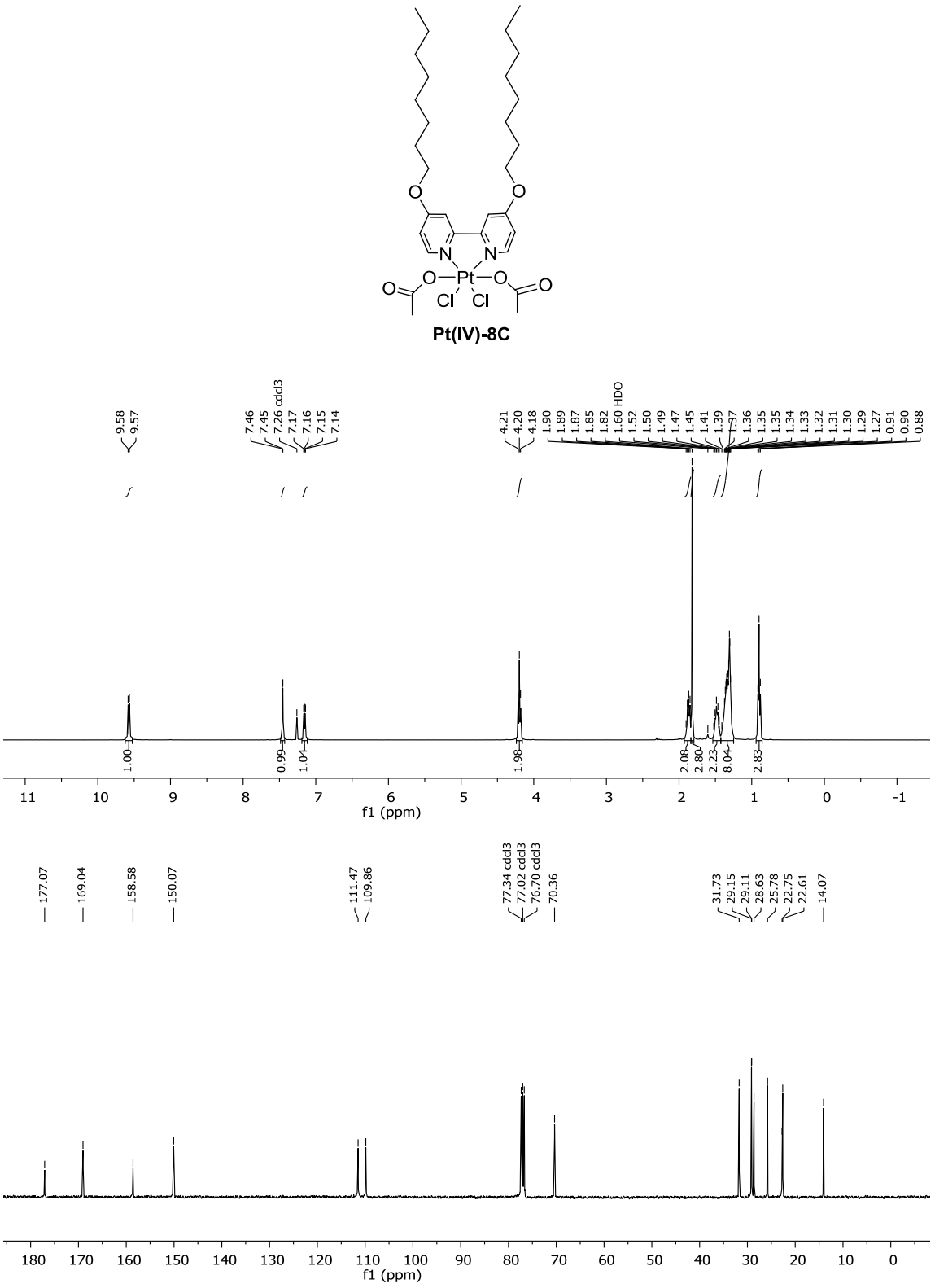

Figure 5S – 7. ^{1}H (top) and ^{13}C (bottom) NMR spectra of compound **Pt(IV)-8C** recorded in $CDCl_3$ at room temperature.

VITA

Graduate College
University of Nevada, Las Vegas

Van Vo

Degrees:

Bachelor of Science, Biochemistry, 2005
University of Nevada, Las Vegas

Master of Science, Biochemistry, 2007
University of Nevada, Las Vegas

Special Honors and Awards:

1. Chemistry Department Outstanding Graduate Student Award (2014)
2. UNLV Graduate & Professional Student Research Forum Award (2014)
3. ACS Southern Nevada Chapter Travel Award (2014)
4. Donna Weistrop and David B. Shaffer Scholarship (2013–2014)
5. Travel Award from the Dean of the College of Sciences (2013)
6. UNLV Graduate and Professional Student Association Research Grant (2013)
7. UNLV Graduate & Professional Student Research Forum Award (2013)
8. UNLV Graduate and Professional Student Association Research Grant (2012)
9. Chemistry Department Outstanding Teaching Assistant Award (2012)
10. UNLV Graduate & Professional Student Research Forum Award (2012)
11. Patricia Sastaunak Scholarship (2011–2012)
12. UNLV Graduate and Professional Student Association Travel Award (2011)
13. ACS Southern Nevada Chapter Research Award (2010)

Patent:

1. Spangelo BL, **Vo V**, Bhowmik PK, Tanthmanatham O, Han H, inventors; The Board of Regents of the Nevada System of Higher Education on behalf of the University of Nevada, Las Vegas, assignee. Pt(IV) complexes containing 4,4′-disubstituted-2,2′-bipyridyl and their use in cancer therapy. United States patent application (Attorney Docket No. 38785-0016P01).
2. Spangelo BL, **Vo V**, Bhowmik PK, Tanthmanatham O, Han H, inventors; The Board of Regents of the Nevada System of Higher Education on behalf of the University of Nevada, Las Vegas, assignee. Synthetic procedure and cancer treatment with cisplatin derivatives. United States patent US 8,703,756 B2 (4/22/2014).

Publications:

1. **Vo V**, Tanthmanatham O, Han H, Bhowmik PK, Spangelo BL. Synthesis of [$PtCl_2$(4,4′-dialkoxy-2,2′-bipyridine)] complexes and their *in vitro* anticancer properties. *Metallomics*, 2013; 5: 973-987.

2. Mathews MS, Blickenstaff JW, Shih EC, Zamora G, **Vo V**, Sun CH, Hirschberg H, Madsen SJ. Photochemical internalization of bleomycin for glioma treatment. *J Biomed Opt*. 2012; 17(5): 058001.
3. Mathews MS, **Vo V**, Shih EC, Zamora G, Sun CH, Madsen SJ, Hirschberg H. Photochemical internalization-mediated delivery of chemotherapeutic agents in human breast tumor cell lines. *J Environ Pathol Toxicol Oncol*. 2012; 31(1): 49-59.
4. **Vo V**, Kabuloglu-Karayusuf ZG, Carper SW, Bennett BL, Evilia C. Novel 4,4'-diether-2,2'-bipyridine cisplatin analogues are more effective than cisplatin at inducing apoptosis in cancer cell lines. *Bioorg Med Chem*. 2010; 18(3): 1163-70.
5. Madsen SJ, Mathews MS, Angell-Petersen E, Sun CH, **Vo V**, Sanchez R, Hirschberg H. Motexafin gadolinium enhances the efficacy of aminolevulinic acid mediated-photodynamic therapy in human glioma spheroids. *J Neurooncol*. 2009; 91(2): 141-149.
6. Mathews MS, Angell-Petersen E, Sanchez R, Sun CH, **Vo V**, Hirschberg H, Madsen SJ. The effects of ultra low fluence rate single and repetitive photodynamic therapy on glioma spheroids. *Lasers Surg Med*. 2009; 41(8): 578-84.

Abstracts/Oral and Poster Presentations

1. **Vo V**. Syntheis and characterization of cisplatin derivatives for cancer treatment. UNLV Foundation Board Meeting, Las Vegas, NV, May 2014.
2. **Vo V**, Han H, Bhowmik PK, Spangelo BL. Activation of mitogen-activated protein kinases (MAPKs) in DU145 human prostate cancer by a novel [$PtCl_2$(4,4′-dialkoxy-2,2′-bipyridine)] complex. UNLV Graduate & Professional Student Research Forum, Las Vegas, NV, March 2014.
3. **Vo V**, Han H, Bhowmik PK, Spangelo BL. The role of mitogen-activated protein kinases (MAPKs) in human prostate cancer cell death induced by [$PtCl_2$(4,4′-dialkoxy-2,2′-bipyridine)] complexes. 6th International Conference on Drug Discovery and Therapy, Dubai, United Arab Emirates, February 2014.
4. **Vo V**, Tanthmanatham O, Han H, Bhowmik PK, Spangelo BL. Synthesis of (4,4′-bis[oligo(oxyethylene)]-2,2′-bipyridine)$PtCl_2$ complexes and their in vitro effects in human lung cancer cells. American Association for the Advancement of Science, Pacific Division 94th Annual Meeting, Las Vegas, NV, June 2013.
5. **Vo V**, Han H, Bhowmik PK, Spangelo BL. Novel (4,4′-dialkoxy-2,2′-bipyridine)Pt(II)Cl_2 complexes induce apoptosis in breast cancer cells. American Association for the Advancement of Science, Pacific Division 94th Annual Meeting, Las Vegas, NV, June 2013.
6. **Vo V**, Tanthmanatham O, Han H, Bhowmik PK, Spangelo BL. The synthesis of novel cisplatin analogues and their in vitro cytotoxic effects in cancer cells. Nevada Biotechnology & Bioscience Consortium Luncheon, Las Vegas, NV, April 2013.

7. **Vo V,** Tanthmanatham O, Han H, Bhowmik PK, Spangelo BL. The *in vitro* cytotoxic effects of cisplatin analogues in cancer and normal cells. UNLV Graduate & Professional Student Research Forum, Las Vegas, NV, March 2013.
8. **Vo V,** Tanthmanatham O, Han H, Bhowmik PK, Spangelo BL. Cytotoxic effects of novel cisplatin analogues in human A549 lung cancer cells. UNLV's STEM Summit (January 2013) and ACS Southern Nevada Section Poster Competition (December 2012), Las Vegas, NV.
9. Main MJ, **Vo V**, Tanthmanatham O, Han H, Bhowmik PK, Spangelo BL. A novel Pt-containing drug synergizes with acetylsalicylic acid to prevent human A549 lung cancer cell proliferation; a new role for an old drug? INBRE Undergraduate Research Opportunity Program Summer 2012 Symposium, Las Vegas, NV, August 2012.
10. **Vo V,** Tanthmanatham O, Han H, Bhowmik PK, Spangelo BL. Cytotoxic effects of novel cisplatin analogues in human A549 lung cancer cells. UNLV Graduate & Professional Student Research Forum, Las Vegas, NV, March 2012.
11. **Vo V,** Tanthmanatham O, Han H, Bhowmik PK, Spangelo BL. Synthesis of novel cisplatin analogues with superior efficacy in A549 lung cancer cells apoptotic responses. 2012 3rd Cancer Targets & Therapeutics Conference, Las Vegas, NV, February 2012.
12. **Vo V,** Tanthmanatham O, Han H, Bhowmik PK, Spangelo BL. Synthesis and cytotoxicity of cisplatin analogs against oncogenic cells. American Chemical Society 242nd National Meeting, Denver, CO, August 2011.
13. **Vo V**. Synthesis and characterization of cisplatin analogues with cytotoxicity for oncogenic cells. The Southern Nevada Section of the American Chemical Society guest speaker. Las Vegas, NV. October 2010.
14. Madsen SJ, **Vo V**, Hirschberg H. PCI-mediated delivery of chemotherapeutic agents in human breast cancer cells. International Photodynamic Association, Seattle, USA, June 2009.
15. Madsen SJ, **Vo V**, Angell-Petersen E, Blickenstaff JW, Hirschberg H. Photochemical internalization enhances the efficacy of bleomycin in malignant glioma cells. BiOS'09, International Symposium on Biomedical Optics, San Jose, USA, January 2009.
16. Blickenstaff JW, **Vo V**, Hirschberg H, Madsen SJ, Photochemical delivery of bleomycin in malignant glioma cells. Fifty-third Annual Meeting of the Health Physics Society, Pittsburgh, USA, June 2008
17. Steen JM, **Vo V**, Angell-Petersen E, Blickenstaff JW, Zhou YH, Hirschberg H. Photochemical-mediated delivery of macromolecules for the treatment of malignant gliomas. BIT Life Sciences 1st Annual World Cancer Congress, Shanghai, China, June 2008.
18. Grigg D, Grover B, Bennett B, **Vo V**, Hall C, Kabuloglu-Karayusuf ZG, Carper SW, Sehdev V, Gilmore S, Lai JCK, Bhushan A. 4,4′-Disubstituted-2,2′-bipyridine Pt(II) Complexes: Synthesis and efficacy of novel cisplatin analogs against cancer cell lines. Joint 63rd Northwest / 21st Rocky Mountain Regional Meeting, Park City, UT, June 2008.

19. Blinkenstaff JW, **Vo V**, Hirschberg H, Madsen SJ. Photochemical delivery of bleomycin in malignant glioma cells. Interdisciplinary Research Scholarship Day. Las Vegas, NV, April 2008.
20. Bennett B, **Vo V**, Kabuloglu-Karayusuf ZG, Carper SW, Sehdev V, Gilmore S, Lai JCK, Bhushan A. 4,4′-Disubstituted-2,2′-bipyridine Pt(II) Complexes: Cisplatin Analogues of Increased Cytotoxicity. Idaho Academy of Science 50th Anniversary Meeting, Boise, ID, March 2008.
21. Carper SW, Hall C, Adebayo J, **Vo V**, Meacham SL. Boric acid induces apoptosis in prostate cancer cell line DU-145 via a caspase three dependent mechanism. Experimental Biology 06, San Francisco, CA, April 2006.

Dissertation Title:

Synthesis and Characterization of Novel Platinum(II) and Platinum(IV) Complexes Containing 4,4′-Disubstituted-2,2′-bipyridine Ligands for the Treatment of Cancer

Dissertation Examination Committee:

Co-Chair, Pradip K. Bhowmik, Ph.D.
Co-Chair, Bryan L. Spangelo, Ph.D.
Committee Member, Ronald K. Gary, Ph.D.
Committee Member, Vernon F. Hodge, Ph.D.
Graduate Faculty Representative, Steen Madsen, Ph.D.